

DETERMINATION OF ORGANOLEAD SALTS IN BIOLOGICAL TISSUE

© Donald Scott Forsyth

Department of Agricultural Chemistry and Physics

Faculty of Agriculture

McGill University, Montreal.

October, 1985.

A thesis submitted to the Faculty of Graduate Studies and
Research in partial fulfillment of the requirements for the
degree of Ph.D.

Suggested short title:

DETERMINATION OF ORGANOLEAD SALTS

ABSTRACT

Ph.D.

Donald Forsyth

Agricultural Chemistry
and Physics.

DETERMINATION OF ORGANOLEAD SALTS IN BIOLOGICAL TISSUE

Ionic trialkyl- and dialkyllead species (R_3Pb^+ , R_2Pb^{2+}) were extracted after complexation with diphenylthiocarbazone (dithizone) from enzymatically hydrolyzed tissue, butylated by Grignard reaction and then quantified by gas chromatography (GC)-atomic absorption spectrometry (AAS). The extraction procedure was tested at trace levels (3-4 ppb as Pb) using four domestic chicken (Gallus domesticus) tissues as models for environmental avian tissues. Trialkyllead recoveries generally exceeded dialkyllead recoveries. An automated GC-AAS system equipped with a quartz T-tube furnace was developed and optimized for organolead detection. The GC-AAS system performance was enhanced by the mediation of organolead atomization by hydrogen radicals formed in the quartz furnace. The determined detection limits (5-7 pg Pb) are the lowest reported for GC-AAS instrumentation. In binding studies, ethyllead species exhibited more interaction with egg homogenate/yolk than methyllead species. Egg homogenate/yolk retained more ionic alkyllead than egg albumin. Trimethyllead (Me_3Pb^+) was found to be ubiquitous in environmental samples of three avian species, supporting the possibility of environmental methylation of Pb(II).

RÉSUMÉ

Ph.D.

Donald Scott Forsyth

Chimie et Physique Agricoles

DETERMINATION DES SELS ORGANOPLOMB DANS LES TISSUS BIOLOGIQUES

Les espèces ioniques dialkylplomb et trialkylplomb (R_2Pb^{2+} , R_3Pb^+) ont été extraites, après complexation avec la diphenyldithiocarbazone (dithizone), de tissus traités enzymatiquement; ensuite elles ont été butylées en employant la réaction de Grignard et finalement quantifiées par chromatographie en phase gazeuse (CG) couplée à la spectrométrie d'absorption atomique (SAA). La procédure d'extraction a été évaluée au niveau de traces (3-4 ppb de Pb) en utilisant quatre tissus de poulet domestique (Gallus domesticus) comme modèles de tissus avicoles environnementaux. Généralement les recouvrements de trialkylplomb excèdent ceux des dialkylplomb. Un système automatisé CG-SAA, équipé d'une fournaise faite d'un tube de quartz en T, a été développé et optimisé pour la détection des composés organoplomb. La performance du système CG-SAA a été accrue par l'intervention de radicaux hydrogènes formés dans la fournaise de quartz lors de l'atomisation des composés organoplomb. La limite de détection (5-7 pg de Pb) est la plus basse jamais rapportée pour ce type d'instrument. Dans les études de liaison, les espèces ethylplomb montrent plus d'interaction avec l'homogénat de jaune d'oeuf que les espèces methylplomb. L'homogénat de jaune d'oeuf retient plus d'espèces ioniques d'alkylplomb que le blanc d'oeuf. L'espèce trimethylplomb a été trouvée dans tous les échantillons environnementaux provenant de trois espèces avicoles; ce qui supporte la possibilité de méthylation environnementale du Pb(II).

ACKNOWLEDGMENTS

The author sincerely appreciates Dr. W.D. Marshall for his suggestions, guidance and endless patience throughout the course of this study.

I also thank Dr. M.A. Fanous for consultation on statistical analysis, Mr. Robert Simpson for kindly translating the abstract into French and the Plant Science Department for the use of a flame burner equipped atomic absorption spectrometer.

Many thanks to my fellow graduate students and summer undergraduates of the department for their aid and friendship and all other friends and acquaintances who made my years at Macdonald College fun and rewarding.

I gratefully acknowledge the financial support provided by the Natural Sciences and Engineering Research Council of Canada, Fonds F.C.A.C. pour l'aide et le soutien à la recherche and the J.W. McConnell Foundation during this study.

Special thanks to my wife Sheila, for her love, understanding, help and support throughout this work. Finally, I thank God for His grace and power which have comforted and sustained me.

Table of Contents

Abstract.....	iii
Resumé.....	iv
Acknowledgments.....	v
List of Tables.....	xi
List of Figures.....	xiii

1. General Introduction.....	1
------------------------------	---

2. Literature Review.....	3
---------------------------	---

2.1 Environmental Sources of Organoleads.....	3
---	---

2.1.1 Automotive Industry.....	3
--------------------------------	---

2.1.2 Bioalkylation.....	5
--------------------------	---

2.2 Environmental Decomposition of Organoleads.....	7
---	---

2.3 Toxicology.....	9
---------------------	---

2.3.1 Acute Toxicity.....	9
---------------------------	---

2.3.2 Subacute/Chronic Toxicity.....	11
--------------------------------------	----

2.3.3 Mutagenic, Carcinogenic and Teratogenic Effects.....	11
--	----

2.3.4 Toxicokinetics.....	13
---------------------------	----

2.3.4.1 Absorption.....	13
-------------------------	----

2.3.4.2 Metabolism.....	13
-------------------------	----

2.3.4.3 Body Organ Distribution.....	14
--------------------------------------	----

2.3.4.4 Biological Half-life.....	14
-----------------------------------	----

2.3.4.5 Excretion.....	16
------------------------	----

2.3.5 Toxic Mechanisms.....	16
-----------------------------	----

2.3.5.1 Effects on Membranes.....	16
2.3.5.2 Biochemical Effects.....	17
3. Organolead Standards Synthesis.....	19
3.1 Introduction.....	19
3.2 Materials and Methods.....	20
3.2.1 Triethyllead Chloride $[(CH_3CH_2)_3PbCl]$ Synthesis.....	21
3.2.2 Trimethyllead Chloride $[(CH_3)_3PbCl]$ Synthesis.....	22
3.2.3 Diethyllead Dichloride $[(CH_3CH_2)_2PbCl_2]$ Synthesis.....	22
3.2.4 Dimethyllead Dichloride $[(CH_3)_2PbCl_2]$ Synthesis.....	22
3.2.5 Ethyl or Methylbutyllead Compounds Synthesis.....	23
3.2.6 Compound Characterization.....	24
3.2.6.1 Thin-Layer Chromatography.....	24
3.2.6.2 Infrared (IR) Spectroscopy.....	24
3.2.6.3 Nuclear Magnetic Resonance (NMR) Spectroscopy.....	24
3.2.6.4 Elemental Analysis (C, H, Cl).....	25
3.2.6.5 Gas Chromatography.....	25
3.2.6.6 Lead Content.....	25
3.3 Results and Discussion.....	26
4. Extraction Methodology.....	35
4.1 Introduction.....	35
4.2 Materials and Methods.....	37
4.2.1 Enzyme Hydrolysis.....	37
4.2.2 Extraction Methodology.....	39
4.2.3 Butylation.....	40

4.3 Results and Discussion.....	43
4.3.1 Enzyme Hydrolysis.....	43
4.3.2 Extraction Recovery.....	46
5. Analytical Instrumentation.....	50
5.1 Introduction.....	50
5.1.1 Instrumentation Optimization and Characterization.....	53
5.1.2 Atomization Processes.....	55
5.2 Materials and Methods.....	57
5.2.1 GC-AAS System.....	57
5.2.1.1 Quartz T-tube furnace.....	59
5.2.1.2 GC-AAS Interface.....	62
5.2.1.3 Timed Gas Purge Circuit.....	62
5.2.2 Optimization and Characterization of GC-AAS System.....	64
5.2.3 Atomic Processes.....	66
5.2.3.1 Volatilization of Deposited Lead in Furnace.....	66
5.2.3.2 Lead Volatilization from Quartz Insert.....	67
5.2.3.3 Gas Mixtures at Two Furnace Temperatures.....	68
5.3 Results and Discussion.....	69
5.3.1 GC-AAS System.....	69
5.3.2 Optimization and Characterization of GC-AAS System.....	72
5.3.3 Atomization Processes.....	86
6. Organolead Egg Interaction.....	96
6.1 Introduction.....	96
6.2 Materials and Methods.....	97

6.2.1 Analytical Methods.....	97
6.2.2 Organolead Egg Interaction Studies.....	99
6.3 Results and Discussion.....	100
7. Environmental Sample Analysis.....	106
7.1 Introduction.....	106
7.2 Materials and Methods.....	108
7.3 Results and Discussion.....	113
8. Claims of Original Work.....	127
9. Recommendations for Future Work.....	129
10. Appendices.....	130
Appendix A. GC-ECD analysis of alkyllead compounds.....	131
Appendix B. Alkylphenyllead synthesis.....	145
Appendix C. Complexation of organoleads with ammonium pyrrolidine dithiocarbamate (APDC).....	160
Appendix D. Calculations of amino nitrogen.....	164
Appendix E. Calculations for organolead recoveries from biological tissue.....	166
Appendix F. High pressure liquid chromatography-atomic absorption spectroscopy.....	168
Appendix G. Effects of parameters on GC-AAS system sensitivity and analyte peak shape.....	175
Appendix H. GC column resolution of $\text{Me}_2\text{Bu}_2\text{Pb}$ and Et_3BuPb	179

Appendix I. Analysis of variance and t-tests of linear regression	
equations.....	180
Appendix J. Analysis of variance.....	181
Appendix K. Analysis of variance.....	182
Appendix L. Environmental sample collection data.....	183
Appendix M. Transalkylation reaction.....	185
Appendix N. Calculations of alkylbutyllead levels in environmental	
samples.....	187
Appendix O. Analysis of variance	190
Appendix P. Paired-observation t-test between ionic alkyllead	
(as alkylbutyllead) concentrations of immature and mature	
gull tissues.....	191
Appendix Q. Analysis of Canadian gasolines for alkyllead content.....	192
Appendix R. Paired-observation t-test between ionic alkyllead	
(as alkylbutyllead) concentrations of male and female mallard	
ducks.....	194
11. Literature Cited.....	195

List of Tables

1. Organolead air concentrations.....	4
2. LD ₅₀ values for various lead compounds.....	10
3. Tissue distribution of organolead compounds.....	15
4. Lead content of synthesized organolead standards.....	33
5. Recovery procedures and mean recoveries of ionic alkyllead compounds from biological tissue.....	42
6. Extent of tissue hydrolysis after 24 h enzymatic digestion relative to acid hydrolysis.....	44
7. Detection limit and precision of instrumentation used for organolead analysis.....	51
8. Limits of detection (LOD).....	83
9. GC-AAS system reproducibility.....	85
10. Volatilization and atomization of lead in furnace with air to H ₂ switching.....	89
11. Volatilization and atomization of lead in furnace with N ₂ to H ₂ switching.....	90
12. Effect of egg components on alkyllead recoveries.....	102
13. Effect of analyte on alkyllead recoveries from egg components.....	105
14. Concentrations of organolead compounds in environmental samples.....	107
15. Absolute retention times and retention indices of mixed methylethylleads (based on retention times) relative to alkylbutyllead standards.....	111
16. Ionic alkyllead levels (as alkylbutyllead) in herring gull liver and kidney samples from various Great Lakes colonies.....	114

17. Effect on gull tissue ionic alkyllead levels (as alkylbutyllead) by sampling site.....	115
18. Ionic alkyllead (as alkylbutyllead) levels in domestic chickens.....	117
19. Correlations between alkyllead concentrations of gull tissue from combined birds and lake sediment lead levels.....	119
20. Correlations between alkyllead concentrations of gull tissue from mature birds.....	120
21. Correlations between alkyllead concentrations of gull tissue from immature birds.....	121
22. Ionic alkyllead (as alkylbutyllead) levels in herring gull whole egg homogenate from Great Lakes colonies.....	123
23. Correlations between trimethyllead concentrations of gull egg homogenate and other tissues.....	124
24. Ionic alkyllead (as alkylbutyllead) levels in separate tissues from mallard ducks.....	125
A1. Absolute retention times and retention indices (based on retention times) of alkylphenylleads relative to a homologous series of n-bromoalkanes..	139
A2. Linear regression analysis of calibration curves for alkylphenylleads.....	141
A3. Mean recoveries of ionic alkylleads from water, buffer and whole egg homogenate using different extraction procedures.....	142
A4. Distillation conditions for R_xPh_4-xPb compounds.....	149

List of Figures

1. Chromatographic, elemental and spectroscopic analyses of trimethyllead compounds.....	27
2. Chromatographic, elemental and spectroscopic analyses of dimethyllead compounds.....	28
3. Chromatographic, elemental and spectroscopic analyses of triethyllead compounds.....	29
4. Chromatographic, elemental and spectroscopic analyses of diethyllead compounds.....	30
5. Amino nitrogen released from various tissues during enzymatic hydrolysis.....	45
6. Block diagram of GC-QTAAS system.....	58
7. Exploded view of GC-AAS interface.....	60
8. Exploded view of quartz T-tube furnace.....	61
9. Variable time delay gas purge circuit.....	63
10. System response to changes in transfer line distance from upper tube....	73
11. System response to changes in GC column flow rate.....	74
12. System response to changes in furnace makeup gas flow rate.....	75
13. System response to different furnace makeup gases.....	78
14. System response to changes in furnace temperature.....	79
15. Response linearity at 217 nm and 283.3 nm.....	81
16. Typical GC-AAS chromatograms.....	84
17. System response during air → H ₂ and N ₂ → H ₂ gas switching	88
18. Weight loss of lead coated quartz inserts under air or H ₂	92

19. System response to various air/H ₂ or N ₂ /H ₂ mixtures at 900°C and 600°C..	94
20. Environmental sampling sites in the Great Lakes region.....	109
21. GC-AAS chromatograms of male mallard sample at 217 and 283.3 nm.....	112
A1. Amino nitrogen released from egg homogenate during enzymatic hydrolysis.....	132
A2. Exploded view of splitless injector.....	136
A3. GC-ECD response to changes in operating parameters.....	138
A4. GC-ECD chromatograms of alkylphenylleads.....	144
A5. Controlled atmosphere glove box.....	147
A6. GC-ECD chromatograms of transalkylation reaction products.....	153
A7. GC-AAS chromatograms of alkylphenyllead standards.....	154
A8. Elemental and spectral analyses of Et ₃ PhPb.....	155
A9. Elemental and spectral analyses of Me ₃ PhPb.....	156
A10. Elemental and spectral analyses of Me ₂ Ph ₂ Pb.....	157
A11. Elemental and spectral analyses of Et ₂ Ph ₂ Pb.....	158
A12. Mass spectra of Et ₃ PbPDC and Et ₂ Pb(PDC) ₂	161
A13. Mass spectra of Me ₃ PbPDC and Me ₂ Pb(PDC) ₂	162
A14. Mass spectra of Pb(PDC) ₂	163
A15. HPLC-AAS system.....	169
A16. Exploded view of quartz T-tube furnace.....	170
A17. Exploded view of HPLC-AAS interface.....	172
A18. HPLC-AAS system response to Et ₃ PbCl.....	173
A19. GC-AAS chromatograms of transalkylation reaction.....	186
A20. GC-AAS chromatograms of some Canadian leaded gasolines.....	193

1. GENERAL INTRODUCTION

Organolead compounds have been used as antiknock additives in gasoline since 1923 and constitute the largest industrial usage of organometallic compounds. By 1970, over 5 million tons of lead (as tetraethyllead) have been used in automobiles in the northern hemisphere (equivalent to 120 pounds of lead per square mile) (Venugopal and Luckey 1978).

Tetraalkyllead compounds, R_4Pb , enter the environment by emissions from automobiles and related industry and possibly from environmental alkylation of inorganic lead. Organolead compounds are considered much more toxic than inorganic lead. Tetraalkylleads decompose in the environment and animals to ionic trialkyl- (R_3PbX), dialkyllead (R_2PbX_2) compounds, and eventually to inorganic lead. The ionic organolead species, particularly trialkyllead (R_3Pb^+), are believed to be the active agents involved in almost all toxic effects of tetraalkyllead compounds. Organolead compounds exhibit some mutagenic and carcinogenic effects, whereas teratogenic effects have not been conclusively found.

The future of organolead compounds as gasoline antiknock additives remains unclear. The American Government appears committed to reducing the current level of 0.29 g Pb per liter to 0.026 g per liter by 1988 (Ember 1984). Environment Canada is expected to lower the present limit of 0.77 g Pb per liter to 0.29 g Pb per liter by 1987 (Environment Canada 1985). However, strong lobbying by the chemical companies involved in organolead synthesis and the fact that some domestic and many imported late model cars operate with leaded gasoline may pressure modifications to these regulations. A legislated reduction in the quantities of organolead additives permissible in gasolines

may not result in a corresponding reduction in environmental levels of methyllead compounds as environmental methylation of inorganic lead already present in aquatic systems cannot be dismissed.

Investigations of the environmental fate of organolead compounds have been hampered by the lack of suitable methodology for determining ionic alkyllead species in biological tissue. The present study was undertaken to develop methodology and instrumentation that would permit environmental monitoring of ionic alkyllead compounds in biological tissues even in regions where levels of organolead compounds are relatively low. The binding of organolead species to components of egg homogenate was examined. Evidence for environmental alkylation was sought by analysis of environmental samples from different regions of the Great Lakes.

2. LITERATURE REVIEW

2.1 Environmental Sources of Organoleads

2.1.1 Automotive Industry

World wide organolead production is approximately 300,000 metric tons per year (Grandjean 1983). It has been estimated that 61% (64.5 tons) of the total lead emissions from Canadian manufacturing industries in 1970 occurred from the synthesis of gasoline additives (Jaworski 1979). The amounts of organolead compounds were not reported.

Losses of organolead compounds during gasoline handling and from automotive fuel systems have been estimated to be 1.3% (Huntzicker et al. 1975). Organolead additives can pass through the automotive engine unchanged into the environment. (Huntzicker et al. 1975). Estimates of unconverted tetraalkyllead compounds range from 1.8-3.8% (Reamer et al. 1978, Huntzicker et al. 1975).

The release of vapourous tetraalkyllead from car exhaust varies with driving conditions; cold starts (10-20°C) 1000-5000 $\mu\text{g m}^{-3}$, idling (warm motor) 50-1000 $\mu\text{g m}^{-3}$, and when driving at constant speed (warm motor) 5-100 $\mu\text{g m}^{-3}$ (Laveskog 1971). Reamer et al. (1978) found, using a gas chromatography (GC)-microwave plasma detector (MPD) system, that vapourous tetraalkyllead released from a system vehicle exhaust when tested cold was about twice that of the same vehicle when running at normal operating temperature. A summary of organolead concentrations in air is presented in Table 1.

The highest organolead levels occurred in underground parking garages.

Table 1. Organolead air concentrations

Location	R _g Pb (ng m ⁻³)	% Organic Pb of Total Pb	Reference
Baltimore tunnel	74-100 ⁱ	0.4-0.7	Reamer et al. (1978)
U.S. No. 1 Highway	42-75	3.5-5.2	
Stockholm, Sweden busy street	47-77	-	Nielsen et al. (1981)
Lancaster, rural	0.5-230	3.2-9.2	Birch et al. (1980)
Central London, U.K.	94±64 ⁱⁱ	6.2±2.4	
Antwerp, Belgium			De Jonghe and Adams (1980)
Downtown	76-262	12.4-20.8	
Residential	8-20	2.5-11.6	
Gasoline Station	192-213	23.9-24.3	
Tunnel	99-112	1.7-5.7	
London Area, U.K.			Harrison et al. (1974)
Gasoline Station	590	9.7	
Tunnel	20	0.1	
Street	60	1.5	
Frankfurt, West Germany			Rohbock et al. (1980)
Gasoline Station	45±34	7.1±3.7	
Residential	24±29	7.8±9.9	
Highway	8±4	0.7±0.4	
Underground Parking Garage	678±253	27.9±9.9	
Underground Parking Garage	1900-2200	15-18	Purdue et al. (1973)
6 U.S. Cities	200-300	4-14	
College Street, Toronto, Canada	14	2.2	Radzuik et al. (1979)

ⁱ-range ⁱⁱ-mean± one standard deviation (SD)

Numerous startups of cold automobile engines, evaporation and accumulation of organolead vapour in an enclosed area would cause these elevated levels. Urban areas tend to have higher organolead air concentrations than suburban or rural areas because of slower denser traffic flow. Air in the vicinity of gasoline stations has a high organolead concentration because of spillage, storage tank venting, and evaporation losses during gasoline filling operations (Table 1).

2.1.2 Bioalkylation

There is at present no conclusive evidence as to the environmental occurrence and importance of bioalkylation of lead. Sirota and Uthe (1977) found relatively high ratios of tetraalkyllead to total lead in certain fishery products indicating possible methylation in sediment or fish tissue. Harrison and Laxen (1978a) found unusually high tetraalkyllead to total lead percentages in air which had passed over a coastal/estuarine mud flat region. Natural environmental methylation of lead was proposed as the cause.

Laboratory studies support the possibility of environmental alkylation, but the actual mechanism(s) involved remain(s) unclear. Tetramethyllead (Me_4Pb) has been isolated from the headspace over incubated natural lake sediments under anaerobic conditions. The addition of lead nitrate, lead chloride or trimethyllead acetate (Me_3PbOAc) enhanced the Me_4Pb production (Wong et al. 1975). Purified bacterial isolates from lake sediment were found to transform Me_3PbOAc but not Pb(II) salts into Me_4Pb (Wong et al. 1975). Schmidt and Huber (1976) found that Pb(II) (as Pb(OAc)_2) was converted to Me_4Pb by microorganisms under anaerobic conditions. Pure Aeromonas cultures were shown to change Me_3PbOAc to Me_4Pb , with 15-20% of the total Me_4Pb produced by chemical disproportionation. (Chau and Wong 1978).

Other studies however, have found no evidence to support bioalkylation of Me_3PbOAc (Craig 1980, Reisinger et al. 1981, Jarvie et al. 1975) or Pb(II) salts (Jarvie et al. 1983, Reisinger et al. 1981) and generally suggest chemical alkylation (Jarvie et al. 1975, Reisinger et al. 1981) possibly sulfide mediated, of the Pb(IV) salts but not for Pb(II) salts.

Possible mechanisms for Pb(II) methylation in water include nucleophilic displacement of X^- in PbX_2 by CH_3^- to produce $\text{Me}_2\text{Pb(II)}$ which could then disproportionate to Me_4Pb and Pb^0 (Ahmad et al. 1980). However, Pb(II) alkyls have extreme hydrolytic instability (Shapiro and Frey 1968). Electrophilic attack by CH_3^+ on PbX_2 was initially presumed unlikely as well since the oxidative addition intermediate $(\text{MePbX}_2)^+$ was assumed unstable. However, recent work (Ahmad et al. 1980, Jarvie and Whitmore 1981) has shown that aqueous Pb(II) salts can be alkylated to Me_4Pb (Ahmad et al. 1980) or to ionic methyllead compounds in the presence of carbonium ion reagents. With the presence of methyl iodide in the environment (Lovelock and Maggs 1973) this could represent an important pathway for organolead into the environment.

Methylcobalamin, a methyl corrinoid compound synthesized by anaerobic bacteria has been implicated as the primary route for methylation and mobilization of mercury from bottom sediments in polluted waters (Summers and Silver 1978) presumably by acting as a carbanion donor (Wood and Wang 1983). The possible involvement of methylcobalamin in alkylation of Pb(II) or Pb(IV) salts has also been investigated. Pb(IV) and Pb(II) salts have been shown to demethylate methylcobalamin (Thayer 1978, 1983); a very small percentage of the volatile products (0.5%) was identified as Me_4Pb . However, neither Reisinger et al. (1981) or Jarvie et al. (1975) were able to find any evidence of methylation of either Pb(II) or Pb(IV) salts in the presence of

methylcobalamin.

Although available laboratory evidence supports the possibility of Pb(IV) and even Pb(II) environmental alkylation, it remains unclear whether biological or chemical alkylation is the predominant process involved.

2.2 Environmental Decomposition of Organoleads

Tetraalkyllead compounds decompose after entry into the environment to trialkyl-, dialkyl- and inorganic lead species. Some of the organic lead released from car exhaust is alkyllead salts caused by pyrolytic decomposition of tetraalkyllead additives in the presence of halogenated scavengers in gasoline. Rifkin and Walcutt (1956) found that approximately 18% of the organic lead sampled in the exhaust was in the form of trialkyl- and dialkyllead salts. Triethyllead bromide was formed when Et_4Pb containing gasoline (with dibromoethane) was autoclaved (Widmaier 1953, cited by Grandjean and Nielsen 1979).

Some trialkyl- and dialkyllead species may result from the atmospheric decomposition of tetraalkyllead compounds. Tetramethyllead and Et_4Pb have photolytic decay rates of $8\% \text{ h}^{-1}$ and $26\% \text{ h}^{-1}$ respectively under conditions approximating bright summer sunlight. Winter or cloudy conditions would lower the decay rates. In the dark, the decomposition rates of Me_4Pb and Et_4Pb were $0.2\% \text{ h}^{-1}$ and $0.7\% \text{ h}^{-1}$ respectively (Harrison and Laxen 1978b). The known existence of $\text{R}_3\text{Pb}^\cdot$ radicals (Booth et al. 1976) and formation of R_3PbBr when R_4Pb was photolyzed in the presence of an alkyl bromide (Cooper et al. 1973) indicate that R_4Pb is split into alkyl- and trialkyllead radicals which could react with other species in the atmosphere or decompose further.

Tetraalkyllead compounds also reacted with ozone, OH radicals and atomic oxygen enhancing the overall decay rates of Me_4Pb and Et_4Pb in an irradiated moderately polluted atmosphere (Harrison and Laxen 1978b). No reaction products were identified, but the formation of some alkyllead salt or related compound (e.g. organolead peroxide) was likely.

Tetraalkyllead compounds decompose in aqueous systems, forming primarily R_3Pb^+ species. Grove (1980) and Noden (1980) reported that Me_4Pb and Et_4Pb solutions in contact with water decomposed to R_3Pb^+ , with much lower amounts of R_2Pb^{2+} and Pb^{2+} also present. Jarvie et al. (1981) determined that an aqueous solution of Et_4Pb in the dark was relatively stable with 2% decomposition to Et_3Pb^+ in 77 days. Metallic cations enhanced decomposition. Aqueous solutions of Me_4Pb reacted more rapidly with 16% decomposition after 22 days, producing Me_3Pb^+ .

The rate of photolysis of aqueous solutions of tetraalkylleads appears dependent on light intensity. Grove (1980) found that diffused sunlight did not accelerate decomposition whereas Jarvie et al. (1981) reported 99% decomposition of Et_4Pb after 15 days and 59% decomposition of Me_4Pb after 22 days exposure to direct sunlight. Decomposition produced R_3Pb^+ species.

Alkyllead ions are more stable than tetraalkyllead compounds in aqueous systems. Trimethyllead and Et_3Pb^+ showed virtually no decomposition when kept in the dark for up to 6 months (Jarvie et al. 1981). Metallic ions did not promote decomposition of these alkyllead salts.

Photolysis of aqueous R_3Pb^+ solutions occurred with Me_3Pb^+ (4% loss) and Et_3Pb^+ (99% loss) decomposition over 15 days in direct sunlight resulting in primarily inorganic lead and some Et_2Pb^{2+} . Grove (1980), however, found that diffused sunlight had little effect on R_3Pb^+ decomposition. Dialkyllead ions in aqueous solutions disproportionated to Pb^{2+} and R_3Pb^+ , with 10% and 6% losses of Me_2Pb^{2+} and Et_2Pb^{2+} respectively over 30 days. Photolysis of Et_2Pb^{2+} and Me_2Pb^{2+} was minimal, with 25% and 5% losses respectively over 40 days (Jarvie et al. 1981).

Tetraalkylleads decompose rapidly in the environment forming ionic alkyllead and inorganic lead species. The ionic alkyllead species persist longer than the tetraalkyllead compounds under comparable conditions and could accumulate in aquatic systems.

2.3 Toxicology

2.3.1 Acute Toxicity

Although organolead compounds may constitute only a small portion of the total lead intake of an organism, they may markedly increase toxicity (Table 2).

Acute poisoning with tetraalkyl or trialkyllead compounds in rats results in hyperexcitability, tremors, periodic convulsions and aggressive behaviour (Springman et al. 1963, Schroeder et al. 1972, Cremer and Callaway 1961). Schroeder et al. (1972) described three stages of organolead poisoning: (1) initial lethargy, irritability and ataxia, (2) violent reaction to noise and aggressive behaviour, (3) convulsions, thrashing and finally death. Humans exposed to near lethal concentrations of tetraethyllead have exhibited similar

Table 2. LD₅₀ values for various lead compounds

Compound	Route ¹	Animal	LD ₅₀ (mg/kg)	Reference
Et ₄ Pb	i.g.	Rat	14.2	Schroeder et al. (1972).
	i.v.	Rat	15.4	Cremer (1959)
	i.p.	Mouse	30.3	Hayakawa (1972)
Et ₃ PbCl	i.p.	Rat	11.2	Cremer (1959)
	i.p.	Mouse	12.8	Hayakawa (1972)
Et ₂ PbCl ₂	i.g.	Rat	120	Springman et al. (1963)
Et ₂ Pb(OAc) ₂	oral	Mouse	130	Jaworski (1978)
Me ₄ Pb	i.v.	Rat	109.3	Cremer and Callaway (1961)
	i.p.	Mouse	14.3	Hayakawa (1972)
Me ₃ PbCl	i.p.	Rat	25.5	Cremer and Callaway (1961)
	i.p.	Mouse	9.4	Hayakawa (1972)
Me ₂ Pb(OAc) ₂	oral	Mouse	120	Jaworski (1979)
PbCl ₂	oral	Guinea pig	2000	Venugopal and Luckey (1978)
Pb(OAc) ₂	i.p.	Rat	150	

¹- i.g.-intra gastric, i.p.-intra peritoneal, i.v.-intravenous

symptoms (Sanders 1964, Beattie et al. 1972). There is presently no effective treatment for acute organolead poisoning (Grandjean and Nielsen 1979).

The symptoms of acute toxicity indicate involvement of the central nervous system. High dosage levels of tetraethyllead and tetramethyllead have been found to produce lesions in various regions of the brain of rats (Davis et al. 1963, Schepers 1964) and dogs (Davis et al. 1963). Tetramethyllead caused more neural damage and affected more areas of the nervous system than did tetraethyllead (Schepers 1964).

2.3.2 Subacute/Chronic Toxicity

Few studies of this type are reported in the literature although the general population is constantly exposed to subacute levels of organolead compounds. Schepers (1964) reported some occurrences of swollen and friable liver, fatty thymus tissue and brain lesions in rats given daily subacute dosages of tetraethyllead and tetramethyllead for 147 days. Heywood et al. (1978, 1979) did not find any treatment related histological changes in tissue from Rhesus monkeys administered either tetraethyllead or tetramethyllead for up to six months.

2.3.3 Mutagenic, Carcinogenic and Teratogenic Effects

Tetraethyllead (0.1 mM) has been shown to induce giant multinucleate cells of the unicellular flagellate Poterochromonas stipitata (Roderer 1976). Triethyllead was 250 times more effective than colchicine, a well known cytokinetic inhibitor, for the inhibition of cytokinesis of the flagellate Poterochromonas malhamensis leading to giant multinucleate cells (Roderer 1979).

Triethyllead and trimethyllead were reported to cause changes in the number of dividing cells and to increase spindle fiber disturbances in the mitotic spindle of onion shoots (Allium sepa) (Ahlberg et al. 1972). Tetraethyllead has also been reported to increase the incidence of lymphomas in female mice (Epstein and Mantel 1968).

Organolead compounds can interfere with reproductive processes. Odenbro and Kihlstrom (1977) found that female mice treated orally with triethyllead chloride displayed decreased frequencies of pregnancy at dosages of 3.0 and 2.2 mg kg⁻¹ body weight. Females given 1.5 mg kg⁻¹ showed a decreased frequency of implanted ova although there was no difference in the percentage of viable embryos.

Oral doses of tetraethyllead, tetramethyllead and trimethyllead administered to female rats during organogenesis resulted in resorbed fetuses. Incomplete ossification and growth retardation occurred only at dosage levels which caused distinct signs of maternal intoxication (McClain and Becker 1972).

Neshkov (1971, cited by Grandjean and Nielsen 1979) found abnormal spermatogenesis among male workers exposed to leaded gasoline. Symptoms included reduced ejaculate volume, lowered spermatozoa count and immobile spermatozoa. However, no direct teratogenic effects have been found in experimental studies using rats (McClain and Becker 1972, Kennedy et al. 1975) or mice (Kennedy et al. 1975).

Thus, organolead compounds appear to possess some mutagenic and carcinogenic effects whereas teratogenic effects have not been demonstrated conclusively.

2.3.4 Toxicokinetics

2.3.4.1 Absorption Tetraalkyllead compounds, because of their lipophilic nature tend to penetrate skin and membrane barriers. Rabbits absorb appreciable quantities of pure tetraethyllead applied to bare skin in approximately one hour. Three daily 30 min dermal exposures to 10^5 Et_4Pb in gasoline caused paralysis and death. The absorption of tetraethyllead increased with application area and exposure time (Kehoe and Thamann 1931). The absorption of tetramethyllead through the skin appears to be slower than tetraethyllead (Davis et al. 1963).

Pulmonary absorption of tetraalkylleads is estimated to be about 80% (Grandjean and Nielsen 1979). Presumably, absorption through the gastrointestinal system would be extensive as well.

2.3.4.2 Metabolism Tetraalkylleads appear to be rapidly converted to trialkyllead ions (R_3Pb^+) in mammals. This has been shown in laboratory studies with mice (Hayakawa 1972), rats (Cremer and Callaway 1961, Cremer 1959, Bolanowska 1968) and rabbits (Hayakawa 1972). In the case of a fatal human poisoning with tetraethyllead, Et_3Pb^+ was found to be the predominate lead compound present (Bolanowska et al. 1967).

Casida et al. (1971) found that there was sequential dealkylation of tetra and trialkyllead compounds, at least to dialkyllead compounds. It was concluded that organolead dealkylation involved hydroxylation at the 1-position leading in the release of 1-alkene from n-alkyl moieties and ketones and alcohols from sec-alkyl moieties. Dealkylation of tetraalkyllead has been demonstrated by in vitro studies of liver homogenates of rat (Bolanowska and Wisniewska-knypl 1971, Cremer 1959, 1961) and rabbit (Bolanowska and

Wisniewska-knypl 1971). Rat and rabbit kidney and brain tissue homogenates also dealkylate Et_4Pb to Et_3Pb^+ although at a much lower rate than liver (Bolanowska and Wisniewska-knypl 1971). Liver microsomes of rat (Cremer 1959) and rabbit (Casida et al. 1971) were the active liver component.

Although sequential dealkylation of tetra and trialkyllead compounds may proceed to dialkyllead compounds (Casida et al. 1971), Hayakawa (1972) and Bolanowska (1968) suggested that Et_4Pb was converted to Et_3Pb^+ and inorganic lead directly although neither study directly analyzed for dialkyllead compounds.

2.3.4.3 Body Organ Distribution Distribution of the trialkyllead metabolites has been examined by various researchers (Table 3). Although the highest levels of Et_3Pb^+ or Me_3Pb^+ are generally found in the liver, followed by kidney, brain and blood, variations occurred from interspecies differences, administered organolead compound and from the time between administration and sacrifice (Hayakawa 1972).

2.3.4.4 Biological Half-life The conversion rate of Et_4Pb to Et_3Pb^+ is quite rapid; a value of $60 \mu\text{g Et}_3\text{Pb}^+ \text{ g}^{-1} \text{ wet wt rat liver h}^{-1}$ was reported (Cremer 1959). In rats, Me_4Pb appeared to be metabolized more slowly than Et_4Pb (Cremer and Callaway 1961, Hayakawa 1972) whereas in mice the opposite occurred (Hayakawa 1972).

The triethyllead concentration remained virtually constant in the liver, kidney and brain tissue of rats for at least 16 days after a single injection of Et_4Pb , whereas the blood levels dropped steadily (Bolanowska 1968). The biological half-life of Me_3Pb^+ in blood was 15 days and 40 days in the liver

Table 3. Tissue distribution of organolead compounds

Animal	Time [†] (hours)	Compound	Organolead Levels (µg/g wet wt)				Reference
			-----Organ----- Liver Kidney Brain Blood				
Human	30	Et ₃ Pb ⁺	18.5	17.5	14.0	-	Bolanowska et al. (1967)
Rat	24	Me ₃ Pb ⁺	10.2	1.9	-	22.0	Cremer and Callaway (1961)
Mouse	24	Me ₃ Pb ⁺	23.8	24.4	5.0	3.5	Hayakawa (1972)
Rat	"	"	9.7	2.9	0.3	8.7	"
Mouse	"	Et ₃ Pb ⁺	23.6	10.4	5.1	1.5	"
Rat	"	"	21.2	6.8	0.8	2.4	"

¹ - time after administration

and kidney of rats (Hayakawa 1972). There was little decrease in the brain levels over the observation period. Triethyllead however, had a biological half-life of 3-5 days in blood, 15 days in liver and kidney and approximately 7-8 days in brain.

2.3.4.5 Excretion Although Me_4Pb and Et_4Pb could be excreted via several routes, only faecal and urinary excretion have been studied. Other possible routes include exhalation and perspiration. Elevated urinary lead output occurred in a human after ingestion of a lethal dose of Et_4Pb (Bolanowska et al. 1967). Trimethyllead was found in the urine of printers one month after discontinuation of exposure to leaded gasoline (Hayakawa 1972).

Rabbits when exposed to Me_4Pb or Et_4Pb excreted Me_3Pb^+ or Et_3Pb^+ respectively in the urine (Hayakawa 1972). Bolanowska (1968) found Et_3Pb^+ in the urine and faeces of rats exposed to Et_4Pb . The excretion rate never exceeded 1% of the dose, with approximately twice as much Et_3Pb^+ being excreted in the faeces than in the urine after 12 days post injection.

2.3.5 Toxic Mechanisms

2.3.5.1 Effects on Membranes Trialkyllead compounds are amphiphilic (contain both a lipophilic and hydrophilic component) and can be expected to concentrate along water-lipid boundaries, such as cell or organelle membranes.

Triethyllead appeared to act as an anion carrier across the mitochondrial membrane, causing an exchange of external Cl^- ions for intramitochondrial OH^- ions (Aldridge et al. 1977). Bjerrum (1978, cited by Grandjean and Nielsen 1979) found that Et_3Pb^+ or Me_3Pb^+ induced Cl^- ion transport (which was directly proportional to the added organolead salt concentration) across human

erythrocyte membranes.

2.3.5.2 Biochemical Effects The action of trialkyllead compounds on membranes causes a variety of biochemical effects. Energy consumption, as indicated by increased ATP hydrolysis and oxygen uptake occurred as a result of an induced Cl^- and OH^- ion exchange across mitochondrial membranes (Aldridge et al. 1977, Aldridge 1978). Organolead salts can also uncouple oxidative phosphorylation (Cremer 1962, Aldridge et al. 1962). Exposure to trimethyl or triethyllead alters the glycolytic pathway. A reduction of oxygen consumption and accumulation of lactic acid was found in vitro (Cremer 1961, 1962, Cremer and Callaway 1961) and in vivo for brain samples (Cremer 1959, 1961). Although brain slices were more sensitive than liver, mitochondrial preparations from each tissue were equally sensitive to the applied organolead salt (Cremer 1962).

Tributyllead acetate inhibited high affinity uptake and stimulated the release of putative neurotransmitters (eg. dopamine, glutamate) in mouse brain homogenate (Bondy et al. 1979). Interference with neurotransmitters could result in the observed acute poisoning symptoms (ie. tremors, hyperexcitability and irritability). Triethyllead inhibited serum cholinesterase in vitro (Galzigna et al. 1969) while Et_4Pb was found to alter drug metabolizing enzyme activities in rats (Ahotupa et al. 1979).

Acute and subacute studies with triethyllead administered to young rat pups resulted in a reduction of brain myelin and myelin protein synthesis (Konat et al. 1976, Konat and Clausen 1974). These effects were considered to have resulted from interference with some posttranslational processes involved in supplying myelin membrane proteins (Konat et al. 1979, Konat and Clausen

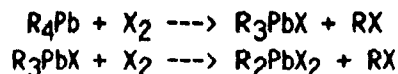
1980). These results suggest that young infants in areas of high leaded gasoline consumption may be at greater health risk than the general population.

3. ORGANOLEAD STANDARDS SYNTHESIS

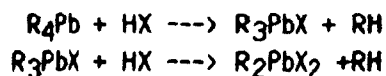
3.1 Introduction

Organolead salt compounds are generally not available commercially, necessitating their synthesis for environmental studies. Laboratory scale synthesis of triorganolead (R_3PbX) and diorganolead (R_2PbX_2) salts uses R_4Pb compounds (available commercially) as starting material, since few direct syntheses from lead metal or inorganic lead salts are known (Shapiro and Frey 1968).

The most common method of synthesis of organolead salts is the reaction of a tetraorganolead with a halogen:



or halogen acid:

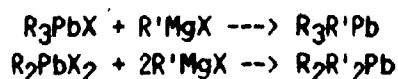


(Shapiro and Frey 1968).

The reaction proceeds in a stepwise manner to cleave one or more lead-carbon bonds. The degree of halogenation can be controlled by (a) reagent used, (b) solvent, and (c) reaction temperature. Halogens react more vigorously than halogen acids, therefore a reaction with a halogen must be run at low temperatures (-80°C) to form R_3PbX and at -10°C to allow the reaction to proceed to R_2PbX_2 (Gilman and Robinson 1930). Halogen acid allows the reaction to be more readily stopped at the R_3PbX stage (Leeper et al. 1954). The reaction solvents can be chosen to enhance the selection of the halogenation reactions. Non-polar solvents (hexane, heptane) precipitate R_3PbX salts and

prevent further reaction (Calingaert et al. 1945, Shapiro and Frey 1968). More polar solvents (chloroform, toluene) allow the initial reaction product R_3PbX to remain soluble, and the reaction to proceed to R_2PbX_2 . Careful monitoring of the reaction by thin-layer chromatography is necessary to prevent excessive PbX_2 formation.

Alkylphenyllead standards used with initial gas chromatography (GC)-electron capture detection (ECD) studies (Appendix A) were prepared from lead(II) and organolead halides (Appendix B). The use of n-butyl derivatives of the organolead halides with the GC-AAS system, required the synthesis of unsymmetrical R_4Pb standards which are most commonly prepared by reacting an organolead halide with a Grignard reagent:



Alkyl derivatives of organolead halides are readily synthesized in this manner. Trialkyllead (Estes et al. 1982, Chau et al. 1983, 1984) and dialkyllead salts (Chau et al. 1983, 1984) reacted quantitatively with n-butyl Grignard reagent.

The purity of all synthesized organolead standards was determined by chromatographic, elemental and spectroscopic analyses.

3.2 Materials and Methods

All solvents used unless otherwise noted were distilled in glass pesticide grade (Caledon Laboratories Ltd.). ACS reagent grade reagents were used unless otherwise designated. Double distilled water was prepared using an all glass distillation system (Corning AG1-B) and the distillate stored in glass

containers.

3.2.1 Triethyllead Chloride $[(CH_3CH_2)_3PbCl]$ Synthesis

Approximately 4 mL of tetraethyllead (ICN K and K Fine Chemicals Lab.) was added to hexane (150 mL) in a 300 mL three-necked round bottom flask. Anhydrous hydrogen chloride (Matheson Specialty Gases Ltd.) was introduced into the solution through a sintered glass gas diffuser under a nitrogen atmosphere. A water cooled Liebig condenser with an attached calcium chloride moisture trap was connected to the center glass joint of the flask. The reaction solution was mixed with a teflon covered magnetic stirrer for 30 minutes and then tested to ensure excess acidity. The hexane was removed under vacuum (rotary evaporator at ambient temperature) and the residue solubilized in warm acetone.

The liquor was filtered (Whatman No. 1), diluted with hexane to the point of crystal formation, and then placed in a freezer overnight. The resulting crystals were recovered by decanting the supernatant and washing several times with cold hexane. Residual solvent was removed by drying under a stream of nitrogen.

Thin-layer chromatography (Section 3.2.6.1) of the crude product indicated some diethyllead dichloride present. A purification procedure adapted from Bolanowska (1968) was used. The product was dissolved in ethyl acetate (75 mL) and extracted four times with 30% (w/v) NaCl (25 mL). The organic layer was then dried with anhydrous sodium sulfate and reduced in volume under a stream of nitrogen at ambient temperature. Hexane was added to the point of crystal formation and the mixture was then placed in a freezer overnight.

3.2.2 Trimethyllead Chloride $[(CH_3)_3PbCl]$ Synthesis

Trimethyllead chloride was synthesized from tetramethyllead (80% tetramethyllead in toluene, Dupont Canada Ltd.) using essentially the same procedure described for Et_3PbCl .

3.2.3 Diethyllead Dichloride $[(CH_3CH_2)_2PbCl_2]$ Synthesis

Diethyllead dichloride was purchased from Alfa Products, Ventron Corp. Thin-layer chromatography indicated that the product contained a considerable level of triethyllead chloride and lead(II) chloride impurities. Accordingly, the product was washed three times with diethyl ether (20 mL), and then dissolved in hot methanol. The liquor was filtered, and reduced in volume under a stream of nitrogen at $70^\circ C$. The concentrated solution was cooled and diethyl ether added to the point of crystal formation. The recovered product contained some triethyllead chloride which was removed by initially washing the product four times with diethyl ether (50 mL) and then hot benzene (50 mL). The product was then dissolved in hot methanol, filtered, and the solvent volume reduced under vacuum. Diethyl ether was added to the point of crystal formation and the mixture then placed in a freezer overnight. The crystals were washed four times with hot diethyl ether (50 mL) and then dried under a stream of nitrogen.

3.2.4 Dimethyllead Dichloride $[(CH_3)_2PbCl_2]$ Synthesis

Tetramethyllead solution (about 4 mL) was added to reagent grade chloroform (50 mL) in a 100 mL three-necked round bottom flask. Chlorine gas (Medigaz Ltée.) was slowly bubbled into the solution under a nitrogen atmosphere. A Liebig condenser with attached calcium chloride drying tube was

used as described previously (Section 3.2.1). The reaction mixture was maintained at -20°C with a crushed ice-acetone bath (cooled with small amounts of liquid air). The reaction was monitored by thin-layer chromatography and stopped after 15 minutes when lead(II) chloride was detected.

The solvent was removed under vacuum, and the product washed three times with hot benzene (25 mL) to remove Me_3PbCl . The remaining material was dissolved in hot methanol, filtered and reduced in volume under a stream of nitrogen at 70°C . Diethyl ether was added to the point of saturation and the mixture then placed in a freezer overnight. The crystals were washed four times with hot diethyl ether (25 mL) and then dried under a stream of nitrogen.

3.2.5 Ethyl or Methylbutyllead Compounds Syntheses

Organolead halide (10–25 mg) was added to a dry 15 mL graduated screw-cap centrifuge tube. Tetrahydrofuran (2 mL, HPLC anhydrous grade, Caledon Laboratories Ltd.) and 500 μL n-butyl magnesium chloride (BuMgCl) (2.5 M, Alfa Products, Ventron Corp.) were added under nitrogen. The mixture was initially vortexed (Vortex-Genie, Fisher Sci. Co.) for one minute (until all the organolead halide was dissolved) and then magnetically stirred for 10 min.

The reaction mixture was then cooled in an ice bath, isooctane (3 mL) added, vortexed, rechilled, and the excess Grignard destroyed by the dropwise addition of double distilled water (1 mL). The mixture volume was then made up to 13 mL with double distilled water, mechanically shaken for 5 min, and the organic layer removed. Two additional extractions with isooctane (3 mL) were performed. Centrifugation (1550 rpm, Precision Clinical Centrifuge, Precision Sci. Co.) after each extraction hastened phase separation. The pooled organic

extract was centrifuged 5 min (1550 rpm), dried with anhydrous sodium sulfate and transferred to a 50 mL volumetric flask (with three washings of isooctane (3 mL)).

3.2.6 Compound Characterization

3.2.6.1 Thin-Layer Chromatography Purity was monitored by thin-layer chromatography (TLC). Eastman Kodak 6061 gel plates (0.2 mm, Eastman Kodak Co.) were activated at 120°C for 30 min prior to use. An optimum separation was achieved using acetone:hexane:propionic acid as eluent (3:7:0.2 v/v/v). Relative mobilities (R_f) were as follows: Me_3PbCl (0.71), Et_3PbCl (0.88), Me_2PbCl_2 (0.32), Et_2PbCl_2 (0.55) and PbCl_2 (0.00).

Products were visualized by fluorescence quench and confirmed by overspraying with 0.1% (w/v) dithizone in chloroform (Pb(II) , pink; R_2PbCl_2 , salmon; R_3PbCl , yellow).

3.2.6.2 Infrared (IR) Spectroscopy The organolead halides were prepared as solid dispersions in IR grade potassium bromide (KBr) (BDH Chemicals) using a commercial KBr disk press (Perkin-Elmer Corp.). Spectra were recorded from 4000 to 625 cm^{-1} on a Model 257 Perkin-Elmer Spectrophotometer (Perkin-Elmer Corp.). The performance of the instrument was checked by polystyrene film standard.

3.2.6.3 Nuclear Magnetic Resonance (NMR) Spectroscopy Trialkyl- and dialkyllead salt samples were dissolved in 99.8% deuterium oxide (Stohler Isotope Chemicals) with 1% sodium salt of 2,2 dimethyl-2-silapentane-5-sulphonic acid (DSS) as the internal reference compound. Triethyllead chloride was also examined in deuterated chloroform (CDCl_3) with tetramethylsilane as the zero reference. Spectra were recorded

over a 600 Hz sweep width on a Varian EM360 NMR Spectrometer (Varian Associates Inc.) at ambient temperature.

3.2.6.4 Elemental Analysis (C,H,Cl) Samples were analyzed for carbon, hydrogen and chlorine content by Agriculture Canada, Research Branch, C.B.R.I. Technological Services Unit, Ottawa.

3.2.6.5 Gas Chromatography The butylated ethyl or methyllead standards were diluted in isooctane and then analyzed with the GC-AAS system under conditions described in Section 5.3.2. Each standard was injected twice with lead peak areas measured by a recording integrator (Hewlett Packard Model 3390A).

3.2.6.6 Lead Content The lead content of each derivatized alkyllead compound was determined by flame atomic absorption spectrometry using a procedure adapted from Robinson (1961) and Messman and Rains (1981). Four samples of each standard were diluted with methyl iso-butyl ketone (MIBK). A Jarrell Ash Model 850 AAS (Fisher Sci. Co.) equipped with an air acetylene flame burner and deuterium background corrector was used. The 283.3 nm lead resonance line was selected to minimize interference from the organic solvent. The AAS was operated in accordance to manufacturer's instructions. Samples and standard (Me_3PbCl in MIBK) solutions were aspirated long enough to obtain four time averaged (4 s) readings. Pure solvent (MIBK) was aspirated between samples. Standards were aspirated in order of increasing concentration to avoid possible "memory" effect. The lead content of each organolead standard was determined from linear regression equations.

3.3 Results and Discussion

Elemental analysis results (Figs. 1 to 4) generally agreed with the theoretical elemental percentages. Similar deviations from expected values have been reported (Calingaert et al. 1945, Davies and Puddephatt 1967). The Me_2PbCl_2 standard had a higher chlorine and lower carbon content than expected, possibly caused by PbCl_2 contamination. The standard was therefore dissolved in hot methanol, filtered and recrystallized prior to further usage.

The infrared (IR) spectra were interpreted from and in close agreement with reported alkyllead IR spectra (Clark et al. 1968, Amberger and Honigschmid-Grossich 1965). The IR spectra do not show lead-carbon or lead-halide absorption bands as they occur below 625 cm^{-1} .

The methyllead salt spectra (Figs. 1B and 2B) contained only methyl group absorption bands. Symmetric and asymmetric methyl group stretching caused absorption bands in the $2900\text{--}3020\text{ cm}^{-1}$ region, whereas asymmetric and symmetric bending produced absorption bands at $\sim 1390\text{ cm}^{-1}$ and in the $1140\text{--}1170\text{ cm}^{-1}$ region respectively. Absorption bands in the $750\text{--}850\text{ cm}^{-1}$ region were caused by the methyl group rocking mode.

The ethyllead salt IR spectra (Figs. 3B and 4B) contained methyl group, methylene group and carbon-carbon bond absorption bands. Symmetric and asymmetric methyl and methylene group stretching produced absorption bands in the $2840\text{--}2980\text{ cm}^{-1}$ region. The methylene group wagging mode caused an absorption band in the $1200\text{--}1250\text{ cm}^{-1}$ region. Carbon-carbon bond stretching occurred in the $950\text{--}1040\text{ cm}^{-1}$ region. Absorption bands caused by methyl and methylene group rocking modes occurred at 945 cm^{-1} and in the $680\text{--}720\text{ cm}^{-1}$ region respectively.

Figure 1. Chromatographic, elemental and spectroscopic analyses of trimethyllead compounds: (A) GC-AAS chromatogram of Me_3BuPb ; (B) IR spectrum of Me_3PbCl ; (C) NMR spectrum of Me_3PbCl .

Elemental Analysis

Calculated: 12.52% C 3.15% H 12.32% Cl

Found: 12.53% C 2.56% H 12.34% Cl

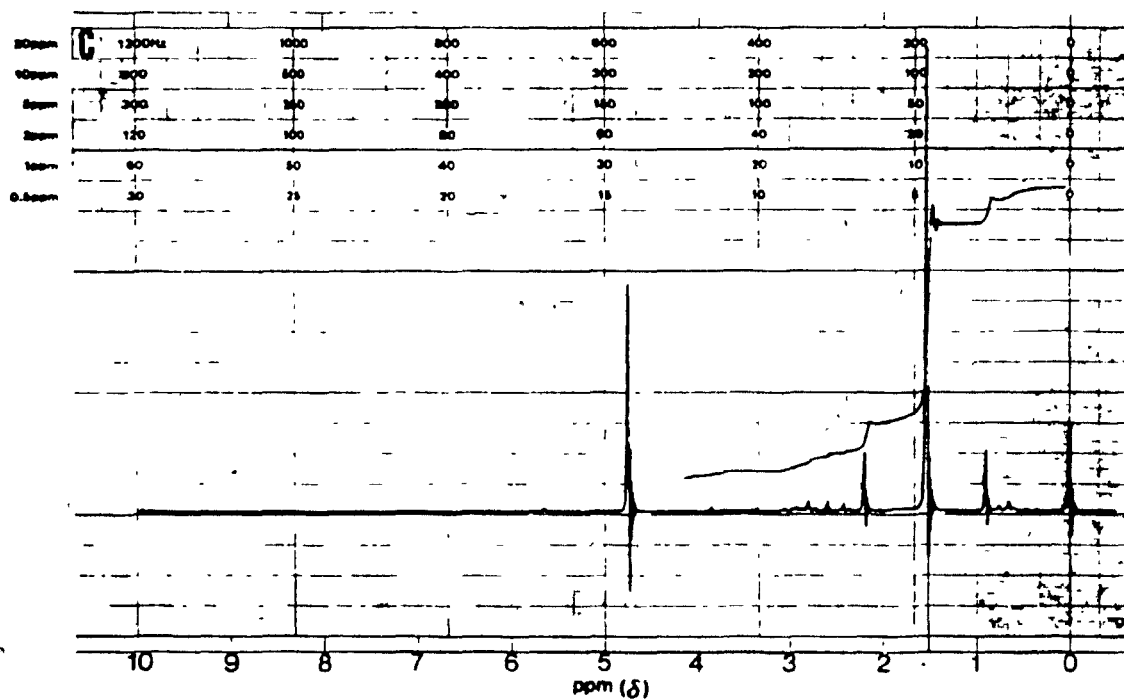
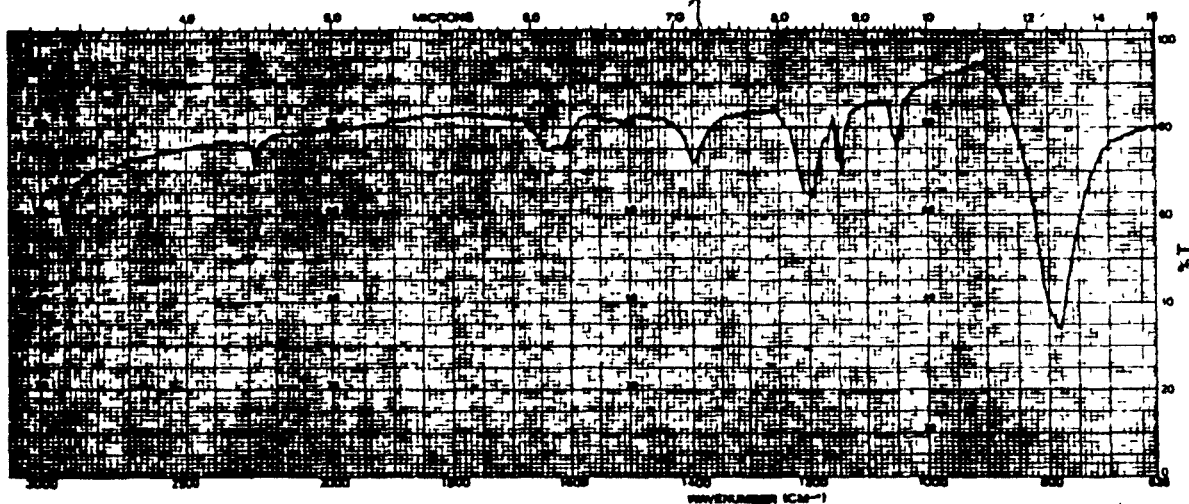
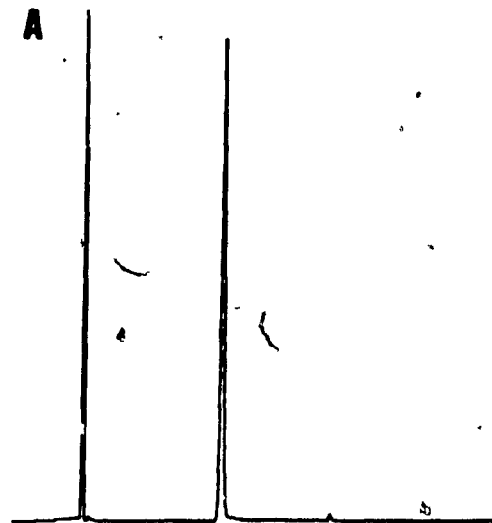


Figure 2. Chromatographic, elemental and spectroscopic analyses of dimethyllead compounds: (A) GC-AAS chromatogram of $\text{Me}_2\text{Bu}_2\text{Pb}$; (B) IR spectrum of Me_2PbCl_2 ; (C) NMR spectrum of Me_2PbCl_2 .

Elemental Analysis

Calculated: 7.79% C 1.96% H 23.01% Cl

Found: 7.35% C 1.91% H 23.83% Cl

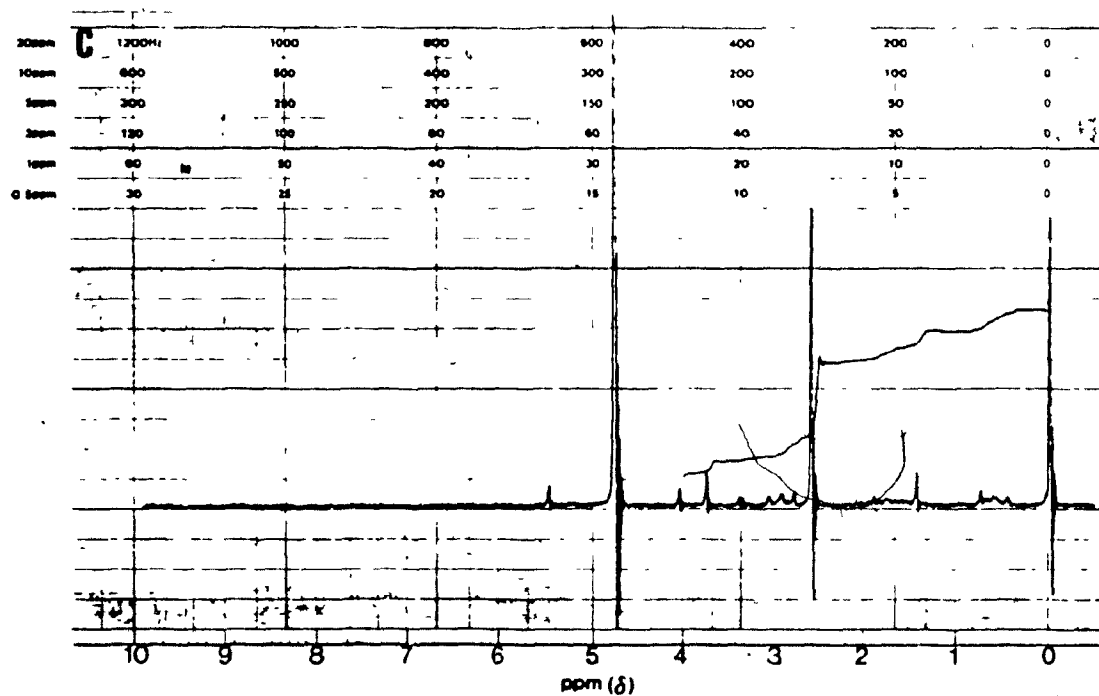
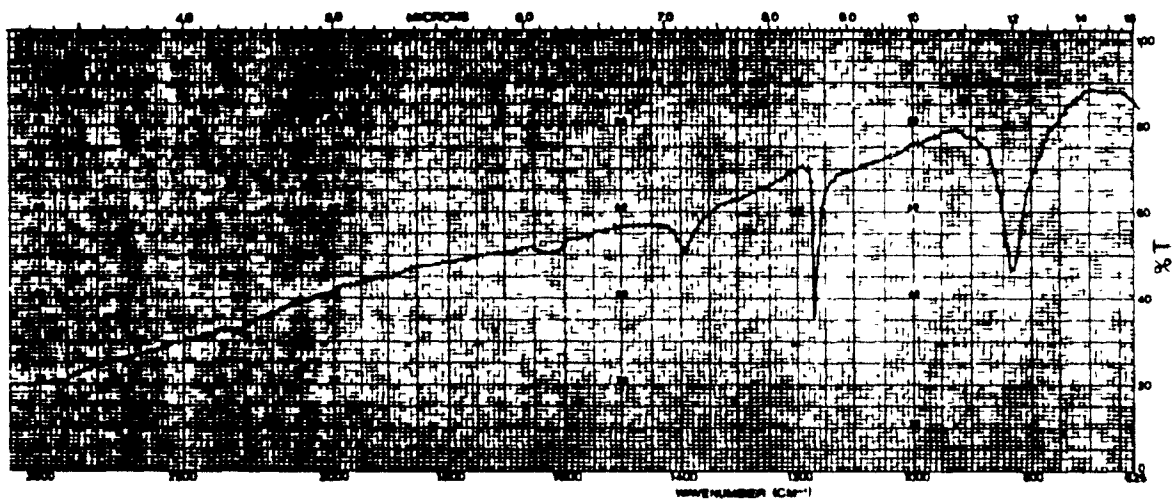
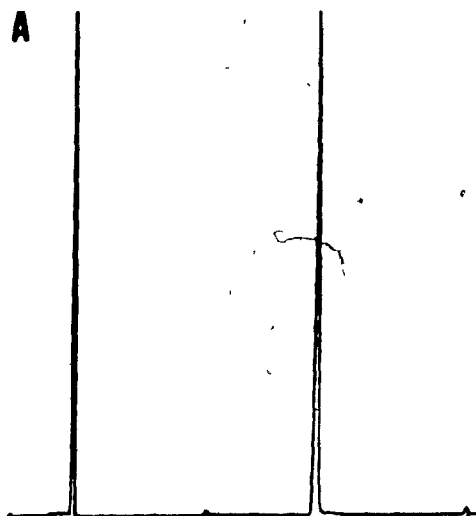


Figure 3. Chromatographic, elemental and spectroscopic analyses of triethyllead compounds: (A) GC-AAS chromatogram of Et_3BuPb ; (B) IR spectrum of Et_3PbCl ; (C) NMR spectrum of Et_3PbCl .

Elemental Analysis

Calculated: 21.85% C 4.58% H 10.75% Cl

Found: 21.98% C 4.87% H insufficient
sample for Cl

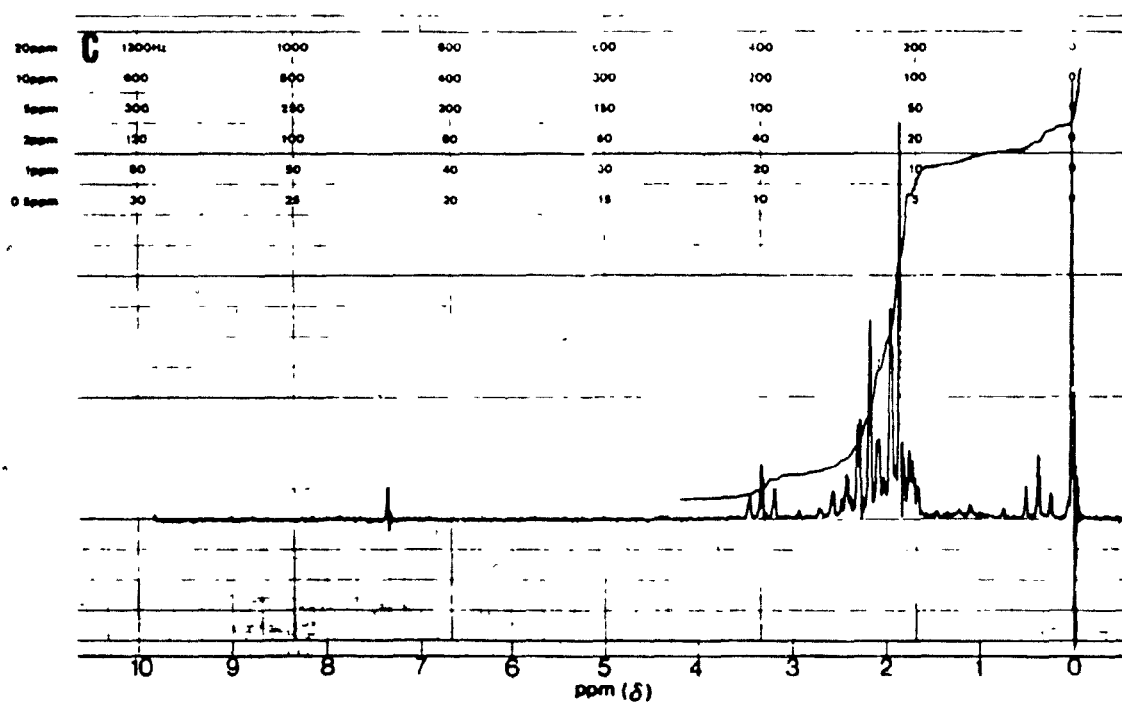
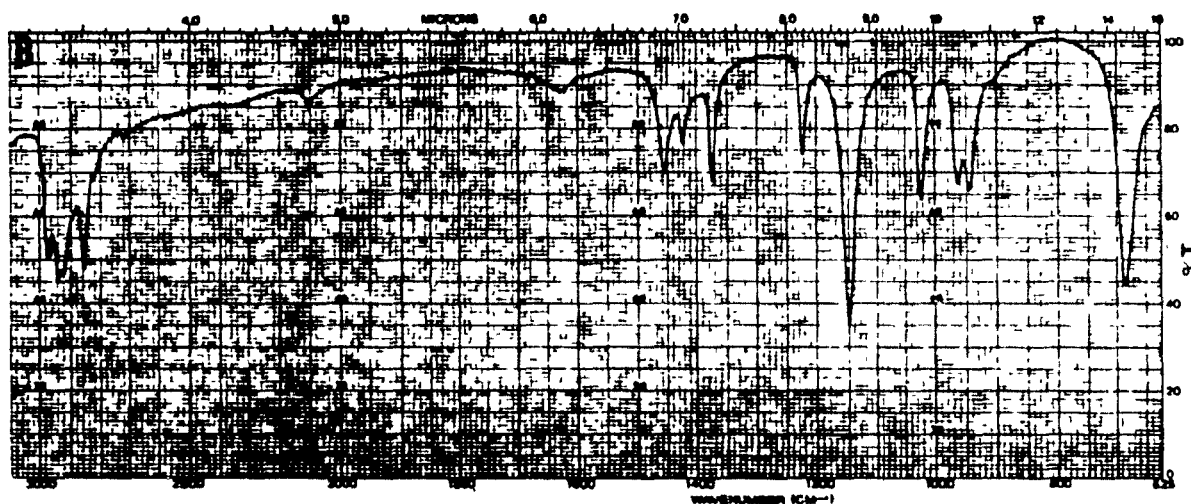
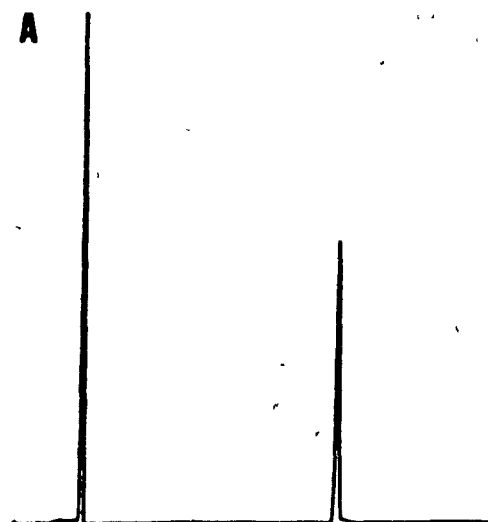
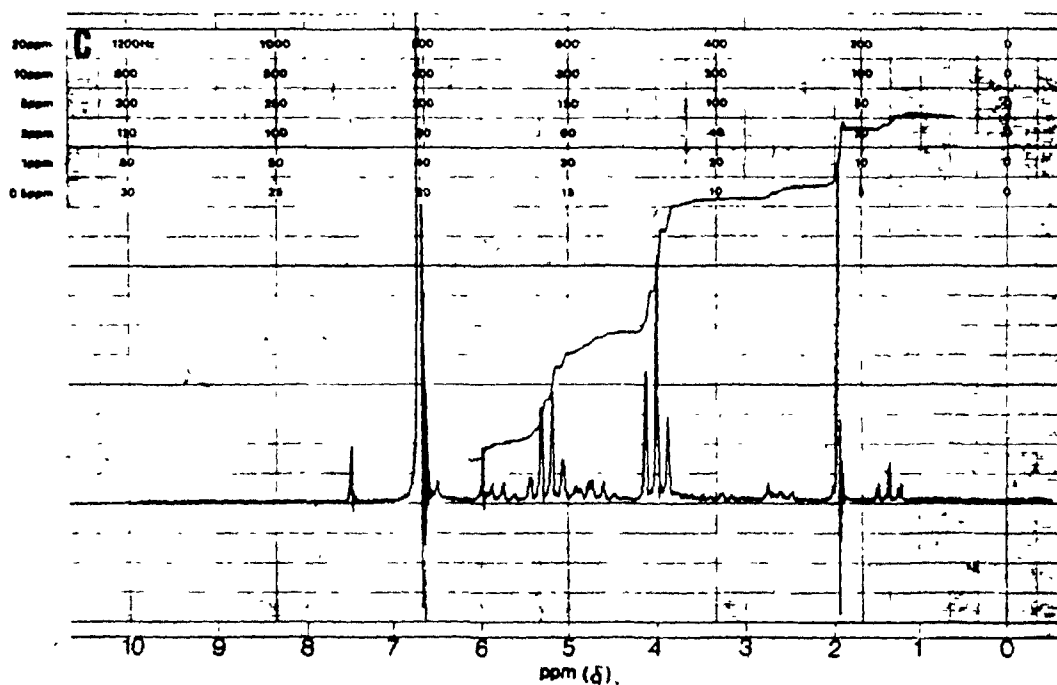
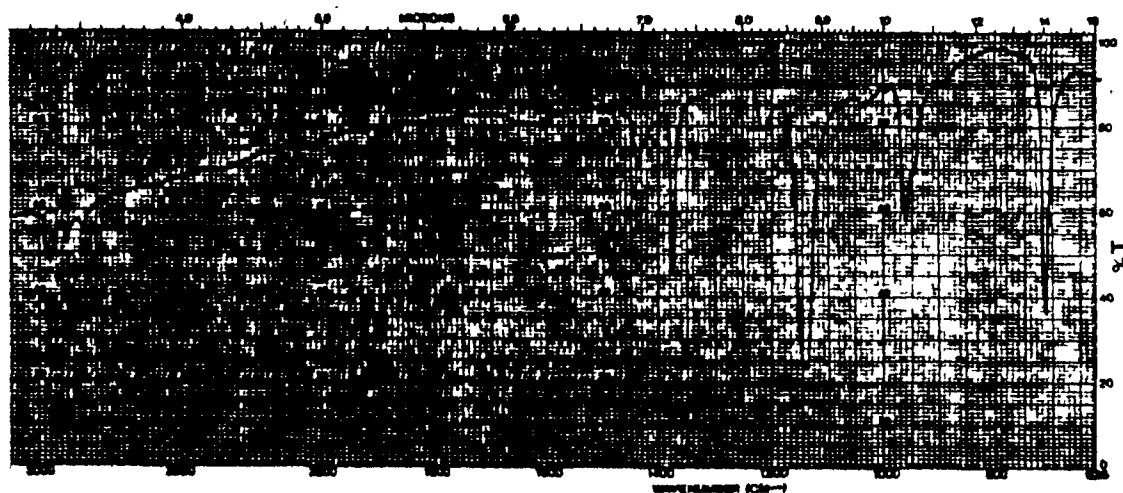
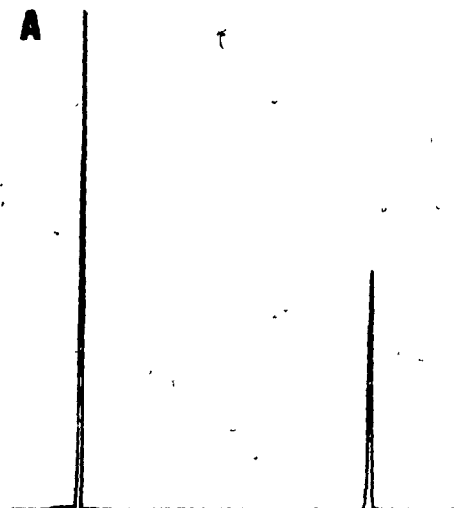


Figure 4. Chromatographic, elemental and spectroscopic analyses of diethyllead compounds: (A) GC-AAS chromatogram of $\text{Et}_2\text{Bu}_2\text{Pb}$; (B) IR spectrum of Et_2PbCl_2 ; (C) NMR spectrum of Et_2PbCl_2 .

Elemental Analysis

Calculated: 14.29% C 2.99% H 21.09% Cl

Found: 13.92% C 2.89% H 21.04% Cl



The IR spectrophotometer used gave consistently higher wavenumbers for polystyrene film standard peaks than the known values over the 3000 to 900 cm^{-1} range. The average \pm standard deviation of these differences was $3 \pm 2 \text{ cm}^{-1}$.

The nuclear magnetic resonance (NMR) spectra (Figs. 1C, 2C, 3C, 4C) also indicated the presence of only methyl and methylene groups in the organolead halide standards.

The trimethyllead and dimethyllead spectra (Figs. 1C and 2C) showed a singlet from the equivalent methyl protons at 1.55 ppm and 2.62 ppm respectively. Since one isotope of lead, ^{207}Pb (abundance 21%, $I=1/2$) has nuclear spin, the main resonance signal was split by $^{207}\text{PbCH}$ coupling, forming two satellites, located symmetrically on either side of the singlet (Fritz and Schwarzhans 1964). The satellites occurred at 0.90 ppm and 2.20 ppm in the trimethyllead spectrum, whereas in the dimethyllead spectrum, they occurred at 1.47 ppm and 3.77 ppm. The area under the satellites corresponded to the ^{207}Pb abundance. The lead-proton coupling constants, $J(^{207}\text{PbCH})$ of Me_3PbCl and Me_2PbCl_2 were 78 and 138 Hz respectively. These values are similar to those reported; 76 Hz for Me_3PbCl in CDCl_3 (Singh 1975) and 154.5 Hz for Me_2PbCl_2 in DMSO (Shier and Drago 1966). However, as coupling constants are affected by sample concentration (Singh 1975) and solvent (Shier and Drago 1966), direct comparisons cannot be made. The singlet at 4.75 ppm was caused by H_2O impurities in the deuterium oxide. Signals from the internal standard occurred in the 0.3-0.8 ppm, 1.5-2.0 ppm and 2.7-3.5 ppm regions.

The triethyl and diethyllead NMR spectra (Figs. 3C and 4C) indicated the presence of methyl and methylene protons. The methyl and methylene protons exhibited very similar chemical shifts in triethyllead. However, $^{207}\text{PbCCH}$

coupling produced clearly visible methyl proton satellites with a triplet split from coupling between the methyl and methylene protons centered at 0.38 ppm and 3.32 ppm, in the triethyllead spectrum (Fig. 3C) run in CDCl_3 , because of fewer solvent impurities. The main triplet split signal was centered at 1.84 ppm, whereas the methylene proton chemical shift was centered slightly downfield at -2.3 ppm. The diethyllead spectrum (Fig. 4C) showed a triplet and a quartet centered at 2.04 ppm and 3.29 ppm respectively, indicating mutually coupled methyl and methylene protons. Integration of the spectrum showed a 3:2 methyl:methylene proton ratio. Methylene proton satellites from $^{207}\text{PbCH}$ coupling were symmetrically centered on either side of the main quartet split at 2.71 ppm and 3.86 ppm. The methyl proton satellites were centered at -0.63 ppm and at -4.7 ppm (nearly covered by H_2O singlet).

The $J(^{207}\text{PbCCH})$ value for Et_3PbCl was 177 Hz whereas the $J(^{207}\text{PbCCH})$ and $J(^{207}\text{PbCH})$ values for Et_2PbCl_2 were 320 and 68 Hz respectively. No coupling constant values for Et_3PbCl and Et_2PbCl_2 were found in the literature although $J(^{207}\text{PbCH})$ is usually smaller than $J(^{207}\text{PbCCH})$ (Harris et al. 1978). However, Et_3PbOAc in CDCl_3 had a $J(^{207}\text{PbCCH})$ value of 177 Hz and $\text{Et}_2\text{PbOAc}_2$ in CDCl_3 had $J(^{207}\text{PbCCH})$ and $J(^{207}\text{PbCH})$ values of 305 and 81 Hz respectively (de Vos et al. 1980).

The lead content of various synthesized organolead standards (Table 4) indicated that derivatization of methyl or ethyllead salts with either phenylmagnesium chloride or n-butyilmagnesium chloride Grignard reagent was virtually quantitative. Quantitative derivatization of alkyllead halides with n-butyilmagnesium chloride has been previously reported (Chau et al. 1983, 1984, Estes et al. 1982). Trimethylbutyllead (Me_3BuPb), which has the lowest boiling point of the examined organolead compounds, had a slightly elevated percentage

Table 4. Lead content of synthesized organolead standards

Compound	--Pb Content (μg)--		% Derivatization ⁱⁱ +SD
	Mean+SD ⁱ		
	Measured ⁱⁱⁱ	Expected ^{iv}	
	(A)	(B)	
Me ₃ PhPb	132.9+ <u>1.7</u>	141.1	94.2+ <u>1.2</u>
Et ₃ PhPb	133.2+ <u>0.5</u>	139.5	95.5+ <u>0.4</u>
Me ₂ Ph ₂ Pb	162.5+ <u>2.0</u>	164.1	99.0+ <u>1.2</u>
Et ₂ Ph ₂ Pb	117.6+ <u>1.7</u>	112.2	104.8+ <u>1.5</u>
Me ₃ BuPb	187.6+ <u>5.7</u>	153.4	122.3+ <u>3.7</u>
Et ₃ BuPb	148.8+ <u>1.4</u>	149.5	99.5+ <u>0.9</u>
Me ₃ Bu ₂ Pb	175.5+ <u>2.6</u>	165.4	106.1+ <u>1.6</u>
Et ₂ Bu ₂ Pb	135.7+ <u>4.4</u>	134.3	101.0+ <u>3.3</u>

i- N=8 replicate determinations

ii- $A/B \times 100 + SD_{A/B} \times 100$

iii- determined from linear regression equations

iv- calculated Pb content of derivatized organolead halide

derivatization, probably caused by volatilization of the compound within the nebulizer chamber of the AAS burner.

Gas chromatographic-AAS analysis (Figs. 1A, 2A, 3A, 4A) of the butylated organolead standards found minimal product contamination. The Me_3BuPb standard (Fig. 1A) produced $98.2 \pm 0.2\%$ of the total lead signal (area), whereas the dimethyldibutyllead ($\text{Me}_2\text{Bu}_2\text{Pb}$) standard (Fig. 2A) produced $97.4 \pm 0.7\%$ of the total lead signal. The triethylbutyllead (Et_3BuPb) standard (Fig. 3A) did not contain any extraneous lead containing peaks, whereas the diethyldibutyllead ($\text{Et}_2\text{Bu}_2\text{Pb}$) standard (Fig. 4A) produced $97.8 \pm 0.9\%$ of the total lead signal. These GC-AAS analyses of the butylated organolead halides indicate a high degree of purity of the alkyllead halides as inorganic lead or organolead salt impurities would be butylated and observed.

The synthesized organolead compounds were used as standards for all subsequent studies.

4. EXTRACTION METHODOLOGY

4.1 Introduction

An extraction methodology for organolead salts from biological tissue involves several procedures. Initially, tissue sample modification is necessary to reduce or eliminate possible organolead interaction with the sample tissue and to minimize foaming or emulsion formation during extraction with organic solvents.

Most previous studies used methodologies that precipitate the proteins with acid (Cremer 1959) or salt (Bolanowska 1968, Nielsen et al. 1978, Johnson et al. 1982). However, any organoleads associated with the proteins were likely precipitated as well, limiting extraction efficiency. Other methods solubilize the sample tissue with tetramethylammonium hydroxide (TMAH) heated to 60°C (Chau et al. 1984) or enzymatic hydrolysis (Forsyth and Marshall 1983).

The organolead salts are then extracted from the sample. Ionic suppression by addition of NaCl followed by organic solvent extraction has been used until recently (Bolanowska 1968, Hayakawa 1971, Potter et al. 1977, Nielsen et al. 1978, Estes et al. 1981, Johnson et al. 1982). This has been a useful technique for metabolic studies, particularly of Et_3Pb^+ (Bolanowska 1968, Hayakawa 1972), but the more polar Me_3Pb^+ and R_2Pb^{2+} species were not efficiently recovered.

The use of a complexation agent overcomes the problems associated with ionic suppression. Diphenylthiocarbazone (dithizone) has been used to extract Et_3Pb^+ from rat tissue (Cremer 1959). Dithizone can complex with both R_3Pb^+ and

R_2Pb^{2+} species (Henderson and Snyder 1961, Aldridge and Street 1981) and successfully extracted these species from tissue samples (Forsyth and Marshall 1983). Other ionic alkyllead complexation agents include sodium diethyldithiocarbamate (NaDDTC) (Chau et al. 1983, 1984, Chakraborti et al. 1984), 3-hydroxyflavone (Aldridge and Street 1981), and ammonium pyrrolidine dithiocarbamate (APDC) (Appendix C). At present, dithizone and NaDDTC are the primary complexation agents used in environmental extraction methodologies.

Masking agents are employed to improve the selectivity of the complexation agent. Potassium cyanide has been used with dithizone (Forsyth and Marshall 1983), whereas ethylenediaminetetraacetic acid (EDTA) has been used with dithizone (De Jonghe et al. 1983) and NaDDTC (Chakraborti et al. 1984). Although a masking agent such as EDTA may be useful for experimental samples containing high levels of inorganic lead (soil, lake sediments), recent soft tissue methodologies do not employ a lead(II) masking agent (Forsyth and Marshall 1983, Chau et al. 1984).

Derivatization of the organolead salts prior to GC-AAS analysis is necessary because (1) although trialkyllead salts have been directly analyzed by gas chromatography with packed (Hayakawa 1971) and fused silica columns (Estes et al. 1981), analyte peak tailing occurred, indicating undesirable column interaction and (2) direct dialkyllead salt analysis by gas chromatography has not been reported. Derivatization of the organolead salts improves thermal stability, volatility and chromatographic performance without altering the original alkyl groups attached to the lead atom. Reaction with a Grignard reagent replaces the reactive Cl group with a hydrocarbon moiety, producing tetraorganolead, which has excellent chromatographic properties (Parker et al. 1961, Bonelli and Hartmann 1963, Dawson Jr. 1963, Chau et al.

1975, 1983, 1984, Chakraborti et al. 1984). Phenyl (Forsyth and Marshall 1983) and n-butyl (Estes et al. 1982, Chau et al. 1983, 1984, Chakraborti et al. 1984) derivatives of extracted ionic alkyllead compounds have been used in environmental studies.

The purpose of this study was to develop an extraction methodology capable of recovering environmentally relevant levels of ionic alkyllead species from avian tissues.

4.2 Materials and Methods

4.2.1 Enzyme Hydrolysis

Enzyme preparations and methyl cellosolve (2-methoxyethanol) were obtained from Sigma Chemical Co.. Other inorganic and organic reagents were ACS grade or better. Double distilled water was prepared as previously described (Section 3.2). Low ammonia content distilled water was prepared by passing distilled water through an activated charcoal-ion exchange system (Corning Water Purifier Model LD-5).

Egg, liver, kidney and brain tissue was collected from mature domestic chickens (Gallus domesticus) donated by the Poultry Unit at Macdonald College. Whole egg (minus shell) was homogenized using a Polytron homogenizer (Brinkmann Instruments) at low speed. The other tissues were homogenized with a teflon pestle tissue grinder. Homogenized tissue was pooled. Subsamples (2.50 g) were weighed using a Sartorius 1219 MP top loading electronic balance and stored in plastic vials at -20°C.

Sample tissue (2.50 g) was incubated in a 50 mL Nalgene screw cap centrifuge tube at 37°C for 48 h in 20 mL of 5% ethanol/0.5 M sodium dihydrogen

phosphate buffer (pH 7.5) containing 40 mg each of Lipase Type VII and Protease Type XIV (Sigma Chem. Co.). The ethanol (absolute) was added to the hydrolysis mixture to minimize bacterial growth during hydrolysis (Nomoto et al. 1960).

The course of enzymatic hydrolysis was monitored by the ninhydrin reaction using the procedure of Yemm and Cocking (1955) with the following modifications; the reaction time and temperature were changed to 45 min at 80-90°C respectively. Reagent and hydrolysis blanks (no tissue) were run and analyzed with the samples. Absorbances were read against the reagent blanks at 570 nm with a Perkin-Elmer Lambda 3 UV/VIS Spectrophotometer (Perkin-Elmer Corp.). The instrument was used in accordance with manufacturer's instructions. A sample calculation appears in Appendix D.

The acid hydrolysis procedure was adapted from Nomoto et al. (1960). Tissue (50-70 mg wet weight) was added to a glass test tube, weighed by analytical balance, and centrifuged momentarily (1550 rpm, Precision Chemical Centrifuge). Constant boiling HCl (1.0 mL) was added, and the tube recentrifuged. The mixture was frozen in liquid air, allowed to thaw under nitrogen, and then refrozen under nitrogen to remove dissolved oxygen. The sample tube was flame sealed and rotated while heated at 110°C for 24 h in a hydrolysis oven. The hydrolysates were made up to 10.0 mL with citrate buffer. Samples were then withdrawn for the ninhydrin procedure. Reagent (acid) blanks were run and analyzed with the samples. The amino nitrogen content was determined as for the hydrolysate. The extent of enzymatic hydrolysis was calculated by dividing the mean corrected amino nitrogen from enzymatic hydrolysis with the mean corrected amino nitrogen from an equivalent amount of acid hydrolyzed sample.

4.2.2 Extraction Methodology

Solvents were distilled in glass grade (Caledon Laboratories Ltd.) and inorganic reagents were ACS grade or better. The ammoniacal buffer consisted of diammonium citrate (22.6 g), potassium cyanide (4.0 g) and sodium sulfite (24.0 g) made up to 250 mL with double distilled water. The pH was adjusted to 10.0 with concentrated ammonium hydroxide.

The extraction methodologies were tested by recovery trials using tissue from adult domestic chickens (Gallus domesticus) donated by the Poultry Unit at Macdonald College. Four samples (2.50 g) of each tested tissue were used for each experiment. Each sample was dissolved in 20 mL of 5% ethanol/0.5 M sodium dihydrogen phosphate buffer (pH 7.5), and was spiked with a mixture of Me_3PbCl , Me_2PbCl_2 , Et_3PbCl and Et_2PbCl_2 before or after hydrolysis. The extraction and butylation procedures were performed and the resulting butylates analyzed by GC-AAS. The percentage recovery of each analyte was determined by dividing the mean peak area of the recovered butylate by the mean peak area of the butylate in the recovery "standards" (Appendix E). The butylated recovery "standards" were analyzed concurrently with the recovery samples by GC-AAS. Analysis of variance and the Newman-Keuls multiple range test was performed on coded and arcsine transformed percentage data.

Extraction method 1. Ammoniacal buffer (5 mL) was added to the hydrolysate. The sample was then extracted three times (5 min, mechanical shaker) with 0.01% (w/v) dithizone (10 mL) in 50% benzene/hexane, followed by centrifugation (4000 rpm, 5 min, IEC Centrifuge Model PR-1, International Equipment Co.) to hasten phase separation. The pooled organic extracts were centrifuged (10,000 rpm, IEC Model B-20 Centrifuge, International Equipment

Co.) for 10 min to facilitate removal of residual buffer. The organic layer was pipetted into a 50 mL plastic screw cap centrifuge tube and back extracted three times (2 min, mechanical shaker) with 0.15 M HNO_3 (10 mL). Centrifugation (4000 rpm, 2 min, IEC Model PR-1 Centrifuge) hastened phase separation after each extraction. The combined acidic washes were neutralized with 1 N NaOH (4.5 mL) and further basified with ammoniacal buffer (5 mL) prior to three extractions (1 min) with 0.01% (w/v) dithizone (5 mL) in 50% benzene/hexane. Centrifugation (1500 rpm, IEC Model PR-1 Centrifuge) followed each extraction. The combined organic extracts were centrifuged 5 min (1550 rpm, Precision Clinical Centrifuge, Precision Sci. Co.), residual buffer removed and the volume was reduced to 1-2 mL in a 15 mL graduated glass centrifuge tube under a stream of nitrogen at 30°C.

Extraction method 2. The following changes to extraction method 1 were made: (1) the initial pooled dithizone extracts were centrifuged at 4400 rpm for 10 min using an IEC PR-1 Centrifuge, (2) the final pooled dithizone extracts were centrifuged two times at 1550 rpm, and (3) the final volume prior to derivatization was adjusted to 1.0 mL.

- 4.2.3 Butylation

Solvents were distilled in glass or in the case of tetrahydrofuran (THF), anhydrous HPLC grade (Caledon Laboratories Ltd.). N-butylmagnesium chloride (BuMgCl) was obtained from Alfa Products, Ventron Corp.

Butylation method 1. Solvent (2 mL, THF in experiments A to C, benzene in experiment D, Table 5) and 500 μL of BuMgCl (2.5 M in experiments A to C, 2.27 M in experiment D) was added to the concentrated dithizone extracts under nitrogen. The solution was magnetically stirred for 10 min at ambient

temperature, then cooled in an ice bath. Hexane (3 mL) was added, the mixture was vortexed for 10 s (Vortex-Genie, Fisher Sci. Co.), recooled, 0.5 mL of double distilled water added, vortexed momentarily and the volume then adjusted to 13 mL with distilled water. The mixture was extracted with hexane (3 mL) for 0.5 min and then centrifuged for 2 min (1550 rpm). Two additional extractions (0.5 min) with hexane (3 mL) were performed followed by centrifugation. The pooled hexane extracts were:

(1) Experiment A (Table 5)--back extracted once with double distilled water (5 mL), adjusted to a 15 mL volume and then dried with anhydrous sodium sulfate.

(2) Experiment B and C (Table 5)--as (1), but 10 mL of the dried hexane was transferred to another 15 mL graduated glass centrifuge tube and reduced in volume to 2 mL under a stream of nitrogen at 30°C.

(3) Experiment D (Table 5)--back extracted once with double distilled water (5 mL), dried with anhydrous sodium sulfate, transferred to another 15 mL graduated glass centrifuge tube with three hexane washings (0.5 mL each) and then reduced in volume to 0.5 mL under a stream of nitrogen at 30°C.

Butylation method 2. Butylmagnesium chloride (0.5 mL, 2.27 M) was added to the dithizone extract under nitrogen. The solution was vortexed 10 s, magnetically stirred for 10 min at ambient temperature and then cooled in an ice bath. Several drops of water were added to the solution. The solution was vortexed momentarily, recooled and then the volume was adjusted to 11.5 mL. The mixture was shaken (0.5 min), centrifuged 5 min (1550 rpm, Precision Clinical Centrifuge), and the aqueous layer discarded by Pasteur pipette. Double distilled water (10 mL) was added to the organic phase, the mixture was

Table 5. Recovery procedures and mean recoveries of ionic alkyllead compounds from biological tissues

Exp't	Tissue	Spiking ¹ Level	Recovery Procedure				Mean ¹¹ Recovery ¹¹¹ +SD			
			Extraction Method		Butylation Method		Analyte ¹¹¹			
			1	2	1	2	Me ₃ PbCl ^{ns}	Et ₃ PbCl ^{ns}	Me ₂ PbCl ₂ [*]	Et ₂ PbCl ₂ [*]
A	Egg	130-210 ^{iv}	x		x		98 ₄	79 ₈	95 ₁₀	97 ₆
B	Egg	13-21 ^{iv}	x		x		89 ₄	81 ₁₇	115 ₂₅	100 ₂₀
C	Egg	13-21 ^v	x		x		93 ₇	82 ₄	96 ₉	112 ₁₂
D	Egg	3-4 ^v	x		x		63 ₃	56 ₅	33 ₉	67 ₁₅
	Liver	3-4 ^v	x		x		59 ₈	48 ₇	19 ₅	36 ₁₁
E ^{vi}	Egg	3-4 ^v		x		x	105 _{9a}	82 _{4a}	94 _{29a}	95 _{12a}
	Liver	3-4 ^v		x		x	99 _{18a}	74 _{7a}	26 _{7b}	66 _{9b}
	Kidney	3-4 ^v		x		x	94 _{15a}	74 _{9a}	25 _{7b}	71 _{10b}
	Brain	3-4 ^v		x		x	83 _{9a}	85 _{7a}	29 _{11b}	59 _{11b}

1- ppb Pb

11- N=4 replicate determinations

111- F-test * 0.05 significance
ns not significant

iv- spiked after hydrolysis

v- spiked prior to hydrolysis

vi- means with the same letter for Exp't E in
column are not significantly different
(p=0.05, Newman-Keuls multiple range test)

F-test takes precedence over Newman-Keuls
multiple range test

shaken (0.5 min), centrifuged (1550 rpm, 2 min) and the aqueous layer discarded. The sample was then centrifuged (1550 rpm, 5 min), transferred to another 15 mL graduated glass centrifuge tube and dried with anhydrous sodium sulfate.

4.3 Results and Discussion

4.3.1 Enzyme Hydrolysis

Each tissue is composed of a variety of complex macromolecules such as glycoproteins, lipoproteins, lipids and phospholipids. The relative proportion of these macromolecules is tissue dependent. As enzymatic hydrolysis proceeded, soluble and insoluble components were released. Generally, hydrolyzed tissues displayed noticeable physical changes during the initial 16 h of hydrolysis. Most fibril material was solubilized and foaming (when shaken) was suppressed. Some precipitation occurred indicating some insoluble components were present. The hydrolysate controls (no tissue) also had a precipitate caused by an insoluble enzyme fraction; this likely constituted some of the observed precipitate in the tissue hydrolysates.

Liver hydrolysates (Experiment A, Table 6) containing 20 or 40 mg each of lipase and protease preparations achieved 83% or 88% hydrolysis respectively after 24 hours. The release of amino nitrogen (Fig. 5) was enhanced during the initial 24 hours of hydrolysis with 40 mg each of lipase and protease. Therefore, to maximize the initial rate of hydrolysis, 40 mg each of the lipase and protease preparations were used in subsequent tissue hydrolysis.

The extent of hydrolysis after 24 h of the other tissues with 40 mg each of lipase and protease (egg, kidney and brain) was 39%, 72% and 48%

Table 6. Extent of tissue hydrolysis after 24 h enzymatic digestion relative to acid hydrolysis

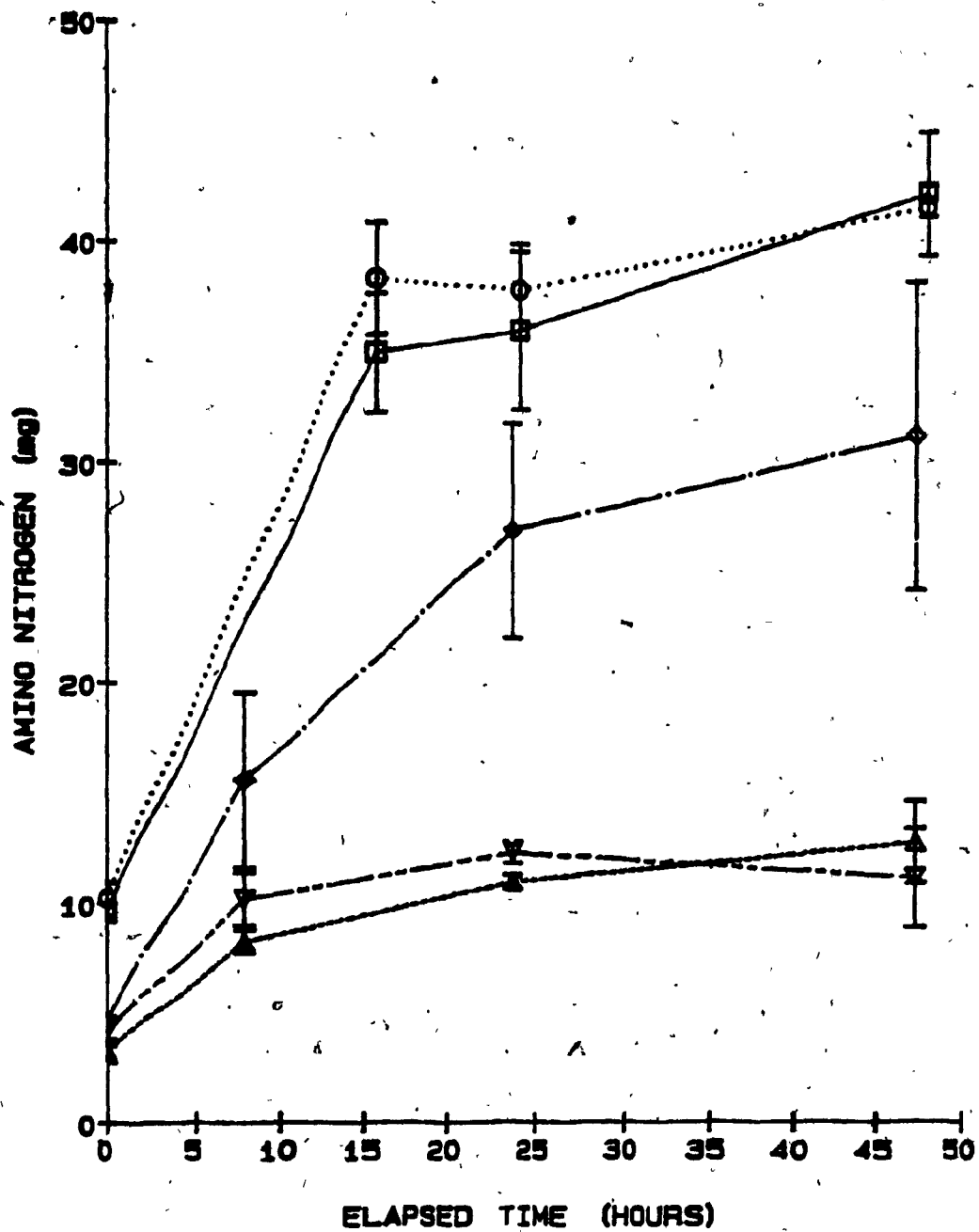
Tissue	Exp't	Protease/ Lipase added(mg)	Mean ⁱ ±SD Amino Nitrogen (mg) ⁱⁱ		% Hydrolysis X/Y*100±SD ⁱⁱⁱ
			Enzyme (X) Hydrolysis	Acid (Y) Hydrolysis	
Liver	A	20/20	35.9±3.6	43.1±0.1	83±8
Liver	A	40/40	37.7±2.1	43.1±0.1	88±5
Egg	B	40/40	11.0±0.3	28.4±2.5	39±4
Kidney	B	40/40	26.8±4.9	37.7±2.1	72±18
Brain	B	40/40	12.3±0.5	25.7±4.0	48±8

ⁱ- N=3 replicate determinations

ⁱⁱ- calculated from linear regression equations and corrected for background amino nitrogen by reagent and hydrolysis blanks

ⁱⁱⁱ- determined by $SD = [X/Y \sqrt{(SD_X/X)^2 + (SD_Y/Y)^2}] * 100$

Figure 5. Amino nitrogen released by: $\text{---}\square\text{---}$, liver hydrolyzed with 20 mg protease/20 mg lipase and $\text{---}\circ\text{---}$, liver; $\text{---}\triangle\text{---}$, egg; $\text{---}\diamond\text{---}$, kidney; $\text{---}\nabla\text{---}$, brain hydrolyzed with 40 mg protease/40 mg lipase during 48 h. Error bars represent \pm one standard deviation of three replicate determinations.



respectively (Experiment 8, Table 6). The increase in amino nitrogen between 24 and 48 h (Fig. 5) was not considered sufficient to adopt a 48 h hydrolysis period and the 24 h hydrolysis period was used for all subsequent environmental tissue analysis. The 24 h hydrolysis results (Table 6) extended into the range of enzymatic hydrolysis of pure protein solutions (60-90% relative to acid hydrolysis) reported by Nomoto et al. (1960). All hydrolyzed tissues were suitable for liquid-liquid extraction regardless of the extent of hydrolysis. Enzymatic hydrolysis modified the four different tissues sufficiently to allow liquid-liquid extraction without extensive precipitation or emulsification and may have reduced organolead-sample tissue association.

4.3.2 Extraction Recovery

An important criterion of the recovery procedures reported in Forsyth and Marshall (1983) and the present work was to isolate the ionic alkyllead species with a minimum of coextractives from biological tissues. Soft tissue contains numerous lipophilic components which would be extracted into the organic phase of a liquid-liquid extraction. Whole egg homogenate was used extensively as the recovery procedure sample tissue because it was easy to obtain, homogenize and is a well-documented tissue. Preliminary work using a single extraction procedure indicated that the final extracts contained sufficient levels of coextractives to rapidly contaminate a GC column.

A double extraction procedure was developed in which the ionic alkyllead species were initially partitioned into the organic phase as dithizonates, followed by an acidic back extraction that dissociated the organolead dithizone complex allowing extraction of the trialkyl- and dialkyllead species into the aqueous phase. Organic soluble coextractives, however, remained in

the organic phase. Basification of the aqueous extracts enabled repartitioning of the ionic trialkyllead and dialkyllead species as dithizonates into the organic phase for derivatization. This procedure, when coupled to butylation produced a relatively clean extract suitable for analysis without further cleanup.

An initial concern was whether hydrolysis lowered alkyllead salt recoveries. A 24 hour hydrolysis at 37°C had no discernable effect on recoveries (Experiments B and C, Table 5) of either the trialkyl- or dialkyllead species. At a spiking level of 13-21 ppb as Pb, recoveries were between 81-115% (Table 5) whether the samples were spiked prior to or after hydrolysis. These results indicated that; (a) heat induced decomposition of ionic alkyllead species was minimal under hydrolysis conditions, (b) the enzyme preparations had no direct detrimental effect, and (c) any binding sites in the egg hydrolysate did not compete successfully with dithizone for the alkylleads. The high recoveries (79-115%) of trialkyllead and dialkyllead from egg homogenate over a spiking range of 3-210 ppb Pb (Experiments A to C, Table 5) indicated that the recovery procedure would be adaptive to large variations of analyte concentrations within an environmental sample.

Recoveries of all four alkyllead compounds decreased when the sample volume was reduced to 0.5 mL just prior to GC-AAS analysis (Experiment D, Table 5). The butylation procedure was therefore modified (BUTYLATION Method 2, Section 4.2.3), resulting in greatly improved organolead recoveries (82-105%) from egg tissue (Experiment E, Table 5).

Trialkyllead recoveries did not vary significantly ($p=0.05$, Newman-Kéuls multiple range test) among the four tissues. However, the dialkyllead

recoveries were significantly less ($p=0.05$, Newman-Keuls multiple range test) from liver, brain and kidney tissue than the egg. The dimethyllead recoveries were particularly suppressed. Chau et al. (1984) noted large Pb(II) peaks in fish samples spiked with dimethyllead not seen in parallel controls (no tissue), suggesting sample induced decomposition of dimethyllead. However, the 3-4 ppb (as Pb) organolead spiking levels used in Experiments D and E (Table 5) were too low to determine whether additional Pb(II) occurred in the recovery tissue samples with the lowered dialkyllead recoveries.

Dialkyllead recoveries may have been lowered by tissue sample metabolic activity. Egg is composed primarily of storage proteins, whereas the other examined tissues have cellular metabolic activity known to dealkylate organolead compounds (Cremer 1959, Casida et al. 1971, Bolanowska and Wisniewska-knypl 1971), probably occurring in the microsomes (Cremer 1959, Casida et al. 1971). Microsomal dealkylation of the dialkylleads during liver, brain and kidney sample hydrolysis is possible, but unlikely as (1) liver has much greater microsomal dealkylation activity than kidney or brain (Bolanowska and Wisniewska-knypl 1971), yet the dialkyllead recoveries were not significantly different ($p=0.05$, Newman-Keuls multiple range test) among these tissues, (2) trialkyllead recoveries would probably have been lowered by dealkylation as well, but they were not significantly different ($p=0.05$, Newman-Keuls multiple range test) among the four tissues (Experiment E, Table 5), and (3) enzymatic hydrolysis should have rapidly suppressed microsomal activity.

The decrease in dialkyllead recoveries may have been caused by competitive binding in the sample hydrolysate or physical occlusion of the dialkylleads within insoluble hydrolysate products. However, the factor(s) involved in

suppression of dialkyllead recoveries were not eliminated by TMAH tissue solubilization or NaDDTC extraction as Chau et al. (1984) reported dimethyllead recoveries of 56-89% at spiking levels of 0.5-10 ppm (~150-3000 times greater than the present study). Generally, a suppressive effect becomes more apparent at lower spiking levels. Chau et al. (1984), therefore may have experienced similar dialkyllead recoveries from fish tissue if the spiking levels had been comparable to the present study.

The extraction methodology, as outlined above, produces reasonable recoveries of Me_3Pb^+ , Et_3Pb^+ and $\text{Et}_2\text{Pb}^{2+}$ from four different biological tissues at a spiking level (3-4 ppb as Pb) much lower than previously reported. Organolead recoveries from egg homogenate were consistently high over a spiking level range of 3-210 ppb (as Pb). Dimethyllead recoveries were lowered in liver, brain and kidney samples by unknown suppressive factor(s).

5. ANALYTICAL INSTRUMENTATION

5.1 Introduction

Analytical instrumentation for organolead analysis has continually improved as the need for enhanced selectivity and sensitivity arose from biochemical and environmental studies.

UV/Visible spectroscopy was an early method used to analyze organolead compounds. Ionic alkyllead species have been complexed with dithizone (Cremer 1959, Henderson and Snyder 1961, Bolanowska 1968), 3-hydroxyflavone (Aldridge and Street 1981) and 4-(2-pyridylazo)resorcinol (Noden 1980, Jarvie et al. 1981) for quantitation. Partial speciation was possible (R_3Pb^+ , R_2Pb^{2+}), but detection limits were only ~ 0.02 -2 μg (Table 7).

Gas chromatography (GC) has been used frequently for organolead speciation and is ideally suited for separating a complex mixture of compounds; sensitivity and specificity are detector dependent (Table 7).

Electron capture detection (ECD) of organoleads (Dawson Jr. 1963, Cantuti and Cartoni 1968, Potter et al. 1977, Jarvie et al. 1981, Forsyth and Marshall 1983) offers high sensitivity (Table 7), but coextractives, such as aromatic, oxygen or halogen containing compounds cause a response and could interfere if they have a similar retention time to those of the organoleads.

Flame ionization detection (FID) (Soulages 1966, Harrison and Laxen 1978b) has less sensitivity (Table 7) and selectivity than ECD. DuPuis and Hill Jr. (1979), however, reported a modified FID system which was sensitive and element selective (Table 7).

v

Table 7. Detection limit and precision of instrumentation used for organolead analysis

Equipment	Analyte	Detection Limit ⁱ	Precision ⁱⁱ (%)	Author
UV/VIS	R ₃ Pb ⁺	2 µg	6	Bolanowska (1968)
"	R ₂ Pb ²⁺	0.02 µg	- ⁱⁱⁱ	Noden (1980)
GC-Dz ^{iv}	R ₄ Pb	1 µg	1.3	Parker et al. (1961)
GC-ECD ^v	Me ₄ Pb	0.8 ng	-	Hayakawa (1971)
	Et ₄ Pb	6.4 pg	-	
GC-FID ^{vi}	Me ₄ Pb	0.1 ng	5	Harrison and Laxen (1978b)
	Et ₄ Pb	1 ng	5	
GC-HAFID ^{vii}	Me ₄ Pb	19 pg	-	DuPuis and Hill Jr. (1979)
GC-MS ^{viii}	Me ₄ Pb	47 pg	6	Nielsen et al. (1981)
	Et ₄ Pb	6.4 pg	-	
GC-MPD ^{ix}	R ₄ Pb	0.71 pg	-	Estes et al. (1982)
ABT-FAAS ^x	Et ₄ Pb	10-20 ng	-	Coker (1978)
	Me ₄ Pb	"	-	
GC-GFAAS ^{xi}	Me ₄ Pb	31 pg	2	Chakraborti et al. (1981)
	Et ₄ Pb	19 pg	2	
"	R ₄ Pb	0.12 ng	5.1	Bye et al. (1978)
	Et ₄ Pb	1.1 ng	4.7	
GC-QTAAS ^{xii}	R ₄ Pb	0.1 ng	-	Chau et al. (1975)
"	R ₄ Pb	0.05-0.1 ng	-	Chakraborti et al. (1984)

i- as Pb

ii- reported as relative standard deviation

iii- not reported

iv- dithizone

v- electron capture detection

vi- flame ionization detection

vii- hydrogen atmosphere flame ionization detection

viii- mass spectrometry

ix- microwave induced plasma detection

x- absorption tube flame atomic absorption spectrometer

xi- graphite furnace atomic absorption spectrometer

xii- quartz T-tube furnace equipped atomic absorption spectrometer

Mass spectrometry detection (MSD) (Laveskog 1971, Jarvie and Whitmore 1981, Nielsen et al. 1981) is selective (single ion monitoring) and sensitive (Table 7), but is an expensive system.

Microwave induced plasma detection (MPD) (Reamer et al. 1978, Estes et al. 1981) is sensitive and selective (Table 7), but plasma systems do not tolerate typical solvent volumes used in environmental analysis (>1 μ L) without solvent venting. This technique requires considerable technical expertise and initial equipment costs are expensive.

Atomic absorption spectrometry (AAS) detection offers several advantages over the previously discussed systems and has been used extensively to quantitate organolead compounds. Flame (Harrison et al. 1974, Coker 1978) and graphite furnace (Sirota and Uthe 1977, Beccaria et al. 1978, De Jonghe et al. 1983) atomizers have been used. Graphite furnaces are 100-500 times more sensitive than flame burners (Table 7). Although AAS is a sensitive, element specific system, organolead speciation requires compound separation prior to analysis. Modification costs are minimal, high selectivity and sensitivity (Table 7) are possible, and only modest technical expertise is necessary. Flame (Kolb et al. 1966, Ballinger and Whittmore 1968, Coker 1978), graphite furnace (Robinson and Kiesel 1977, Bye et al. 1978, Radzuik et al. 1979, Cruz et al. 1980) and quartz T-tube furnace (Chau et al. 1975, Ebdon et al. 1982, Chakraborti et al. 1984) atomizers have been used (Table 7). Flame AAS, although readily available and inexpensive, cannot provide the sensitivity of graphite furnace or quartz T-tube furnace atomizers.

High pressure liquid chromatography-atomic absorption spectrometry (LC-AAS) has been used to analyze tetraalkylleads (Botre et al. 1976, Koizumi

et al. 1979, Messman and Rains 1981), but was unsuitable for the trace analysis of ionic alkyllead compounds (Appendix F).

GC-AAS systems have become the preferred instrumentation for organolead analysis (Chau et al. 1975, Bye et al. 1978, Chakraborti et al. 1981), providing compound separation and Pb specific detection. The quartz T-tube furnace has become the principal atomizer system used in recent organolead studies (Chakraborti et al. 1984, Chau et al. 1984) as it is inexpensive, robust and sensitive.

5.1.1 Instrumentation Optimization and Characterization

Optimization and characterization of the instrumentation system prior to environmental analysis provide an overall appraisal of system analytical capability.

Univariate optimization, in which one system operating parameter is varied across a range of values while the remaining variables are held constant, has been the predominant method used (DuPuis and Hill Jr. 1979, Radzuik et al. 1979, Forsyth and Marshall 1983, Chakraborti et al. 1984). Operating parameters critical to system performance are identified, enabling the analyst to logically define each parameter value rather than relying on trial and error. The system should be optimized in terms of several instrumental characteristics, including sensitivity, reproducibility and resolution. Further characterization of instrumental performance, including limit of detection and range of linearity, under optimized operating parameters, completes system appraisal.

The reproducibility of the analyte response in an instrument is a measure

of precision. Various studies reported 2-10% variability (as relative standard deviation) in system response to organolead compounds (Table 7). Maximizing instrumentation reproducibility (precision) is an important step for minimizing error associated with quantitation of the environmental samples.

The instrumentation must isolate each analyte sufficiently to allow quantitation. When using gas chromatography to separate compounds, the GC column should have a minimum resolution (peak separation/peak width) of 1.5 for quantitative (99.9%) separation between two adjacent peaks (Schenk et al. 1981). Lower resolution (R) values between adjacent peaks indicates greater peak overlap, resulting in less accurate integration of peak area.

The limit of detection (LOD) is the smallest concentration or amount of analyte that can be determined to be statistically different from background noise (blank) (Keith et al. 1983, Foley and Dorsey 1984). The recommended LOD value, at three standard deviations above the mean background noise, permits a confidence level of 99.86% for measurements, assuming a normal distribution of background noise signals (Winefordner and Long 1983).

The range of linearity extends from the limit of detection and includes the region in which detection response is directly proportional to analyte concentration (Szepesy 1970). Sample quantitation within the range of linearity prevents excessive error from nonlinear analyte response. An upper limit of linearity in AAS systems is imposed by residual unabsorbed light reaching the photomultiplier tube (PMT). Unabsorbable light may occur from nonabsorbing lines originating from the source cathode material or the hollow cathode lamp fill gas passing within the spectral bandwidth of the monochromator (Price 1974).

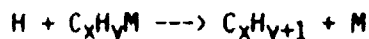
5.1.2 Atomization Processes

Further development of analytical instrumentation for organolead analysis, particularly quartz T-tube furnace atomizers for GC-AAS systems, would benefit from a better understanding of the atomic processes involved. However, research of organolead atomization processes in non-flame systems is limited.

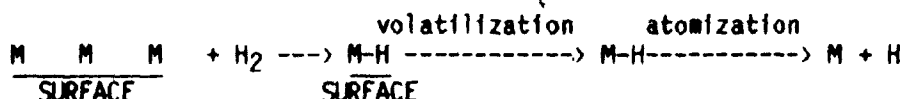
Quartz T-tube and graphite furnaces appear to atomize organolead compounds by different processes. Quartz T-tube furnaces effectively atomized organolead (Chau et al. 1975, Chakraborti et al. 1984) and organoselenide (Van Loon and Radzuik 1976) compounds at 900-1000°C, whereas graphite furnaces required much higher operating temperatures (1500-2000°C) for optimum organolead response (Robinson et al. 1977, Radzuik et al. 1979, Chakraborti et al. 1981). The lower effective operating temperature of quartz furnaces may result from quartz being less absorptive than carbon (at 1000°C) (Parris et al. 1977). However, the use of hydrogen with quartz furnace systems rather than the inert gases typically used with graphite furnaces is a more likely reason.

Hydrogen enhances the atomization of compounds in a variety of analytical instrumentation. The addition of hydrogen to carrier or furnace gases has improved the sensitivity and reproducibility of quartz furnace response to organoleads (Chau et al. 1975, Chakraborti et al. 1984, Forsyth and Marshall 1985), organoselenides (Van Loon and Radzuik 1976) and hydride forming elements (Welz and Melcher 1983). Organoleads gave virtually no response in a quartz furnace system in the absence of hydrogen (Chakraborti et al. 1984, Forsyth and Marshall 1985). Graphite furnace (Parris et al. 1977) and plasma (Reamer et al. 1978, Estes et al. 1982) system sensitivity and reproducibility to organoleads and hydride forming elements were also enhanced by hydrogen.

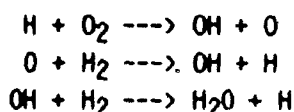
Hydrogen likely maintains a volatile lead population and mediates the atomization of lead compounds in the resonance radiation pathway of the quartz T-tube furnace. Parris et al. (1977) suggested that hydrogen radicals assisted in the decomposition reactions:



and may form hydrides with metal atoms deposited on the furnace tube surface, transporting the metal back into the resonance radiation pathway:



Hydrogen radicals were essential for the atomization of selenium hydride (Dedina and Rubeska 1980) and arsine (Weiz and Melcher 1983). Oxygen in the presence of excess hydrogen heated above 600°C was reported to promote hydrogen radical formation:



Hydrogen radicals were concluded to outnumber OH radicals by at least several orders of magnitude (Dedina and Rubeska 1980).

The purpose of this study was to develop an inexpensive quartz T-tube furnace which was sufficiently robust for prolonged usage in an automated GC-AAS system and capable of detecting environmental levels of organolead compounds. An automated GC-AAS system for organolead analysis has not been previously reported in the literature. Automation of sample introduction

(autosampler) and of quantitation (recording integrator) improves both reproducibility and through sample output. The GC-AAS operating parameters were optimized and the GC-AAS system characteristics examined to ensure reliable analytical performance. The atomic processes occurring within a quartz T-tube furnace were studied, particularly the role of hydrogen in organolead atomization. Possible improvements in the GC-AAS system were examined.

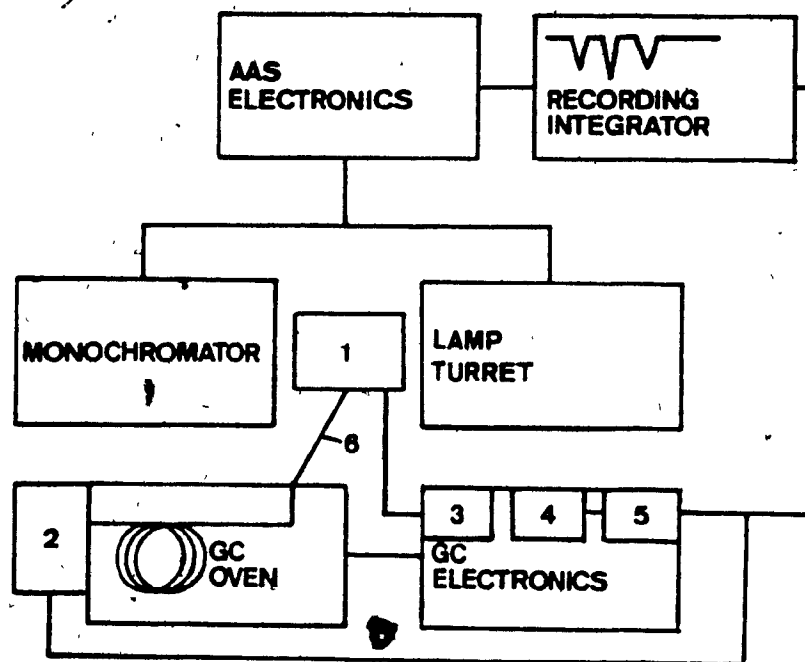
5.2 Materials and Methods

5.2.1 GC-AAS System

The GC-AAS system (Fig. 6) was assembled with a Hewlett Packard Model 5750 gas chromatograph equipped with an autosampler (Model 7670A, Hewlett Packard Co.) interfaced with a Zeiss FMD-3 atomic absorption spectrometer (Carl Zeiss, FRG).

The GC was fitted with a 1.8 m, 6.25 mm o.d., 2 mm i.d. glass column packed with 10% OV-101 in 80/100 mesh Supelcoport (Supelco Inc.). A transfer line between the GC column and the quartz T-tube furnace was made from a 1 m section of methyl silicone coated wide bore (i.d. 0.31 mm) fused silica capillary column (Hewlett Packard Co.). A zero dead volume 1/4 in (0.64 cm) to 1/16 in (0.16 cm) Swagelok reducing union connected the transfer line to the end of the GC column. The transfer line was enclosed in an insulated, heated 1/4 in (0.64 cm) o.d. copper tube. The temperature was maintained by heating tape (Cole Palmer Co.), controlled and monitored by the GC electronics. A temperature controller circuit removed from a Model 310 Hall Electrolytic Conductivity Detector (Tracor Inc.) was incorporated into the GC electronics to control the quartz furnace temperature. Furnace temperature was maintained

Figure 6. Block diagram of the flow system and electronics for the GC-QTAAS system: 1, quartz T-tube furnace; 2, autoinjector; 3, furnace temperature control circuit; 4, variable time delay solvent purge circuit; 5, autoinjector electronics; 6, heated transfer line.



within $\pm 2^{\circ}\text{C}$, and monitored by a calibrated digital temperature indicator (Model 199, Omega Engineering Inc.). A timed gas purge cycle circuit allowed automated gas switching to the furnace.

The AAS was equipped with a deuterium lamp background correction system. A recording integrator (Hewlett Packard Model 3390A) received the recorder output from the AAS electronics. All instrumentation were operated in accordance to manufacturer's recommendations.

Normal GC-AAS system operating conditions were:

(a) GC--carrier gas, He, 35 mL min^{-1} ; injector temperature, 200°C ; temperature program, 50°C (1 min) linear increase ($8^{\circ}\text{C min}^{-1}$) to 250°C (1 min); transfer line temperature, 250°C .

(b) AAS furnace--upper tube surface temperature, 900°C ; makeup gas H_2 ; makeup gas flow rate, 50 mL min^{-1} ; H_2 entry route, inlets F and K (Fig. 7); gas purge cycle, air (500 mL min^{-1} for initial 3 min of GC temperature program).

(c) AAS--hollow cathode lamp current, 10 ma; wavelength, 217 nm; slit width, 0.3 mm; bandwidth, 0.75 nm; photomultiplier tube amplifier, step 1 (lowest setting); deuterium lamp current, 200 ma.

5.2.1.1 Quartz T-tube furnace The quartz furnace (Fig. 8) consisted of a quartz T-tube (upper tube, 10 cm X 9 mm o.d., 7 mm i.d.; lower tube 6 cm X 6.25 mm o.d., 4 mm i.d.) which was heated by two wound heating elements, each formed from 1.8 m of 22 gauge Alloy 875 resistance wire. (Hoskins Alloys of Canada). A layer of Fiberfrax ceramic fiber (The Carborundum Co.) insulated and cushioned the quartz tube within two sections of shaped refractory brick (A.P. Green Fire Brick Co.). Four Swagelok 1/8 in. (0.32 cm) NPT (National Pipe

Figure 7. GC-AAS Interface: A, 6.25 mm o.d. lower tube of quartz T-tube; B, 1/4 in (0.64 cm) Swagelok nut; C, alumina tube; D, 1/4 in (0.64 cm) graphite ferrule; E, 1/4 in (0.64 cm) to 1/8 in (0.32 cm) Swagelok reducing union; F, H₂ inlet; G, air inlet; H, 1/8 in (0.32 cm) vespel/graphite ferrule; I, 1/8 in (0.32 cm) Swagelok nuts; J, 1/8 in (0.32 cm) to 1/16 in (0.16 cm) Swagelok reducing union; K, H₂ inlet; L, capillary graphite ferrule; M, 1/16 in (0.16 cm) Swagelok nut; N, fused silica capillary column (transfer line); O, P, longitudinal sections of reducing unions E and J respectively.

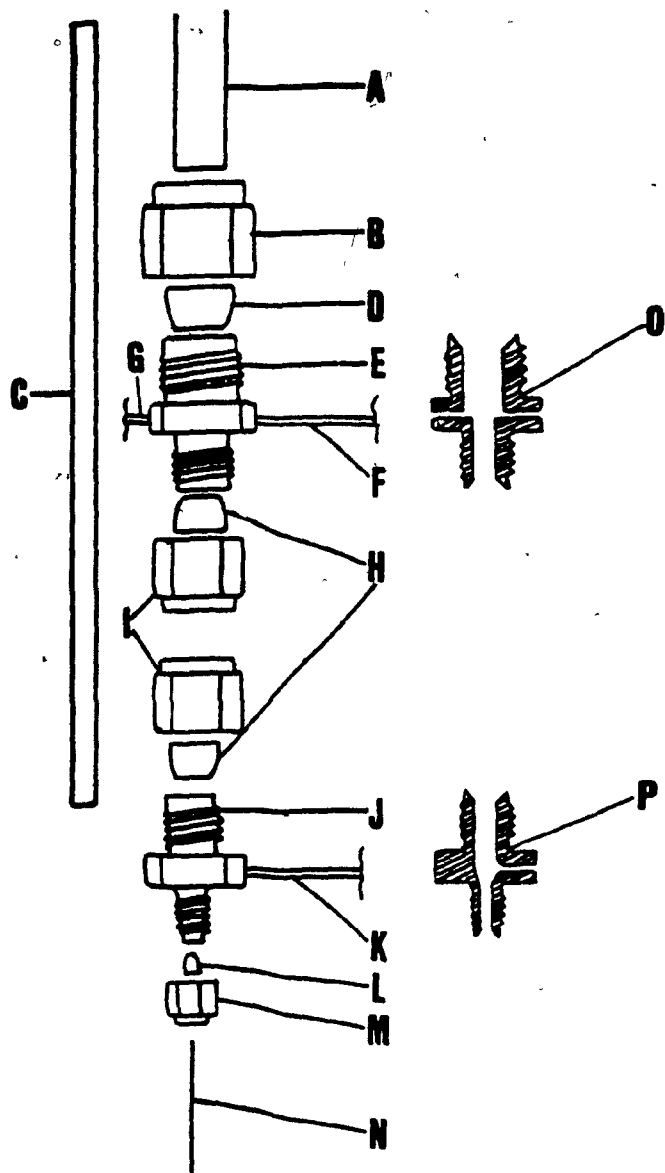
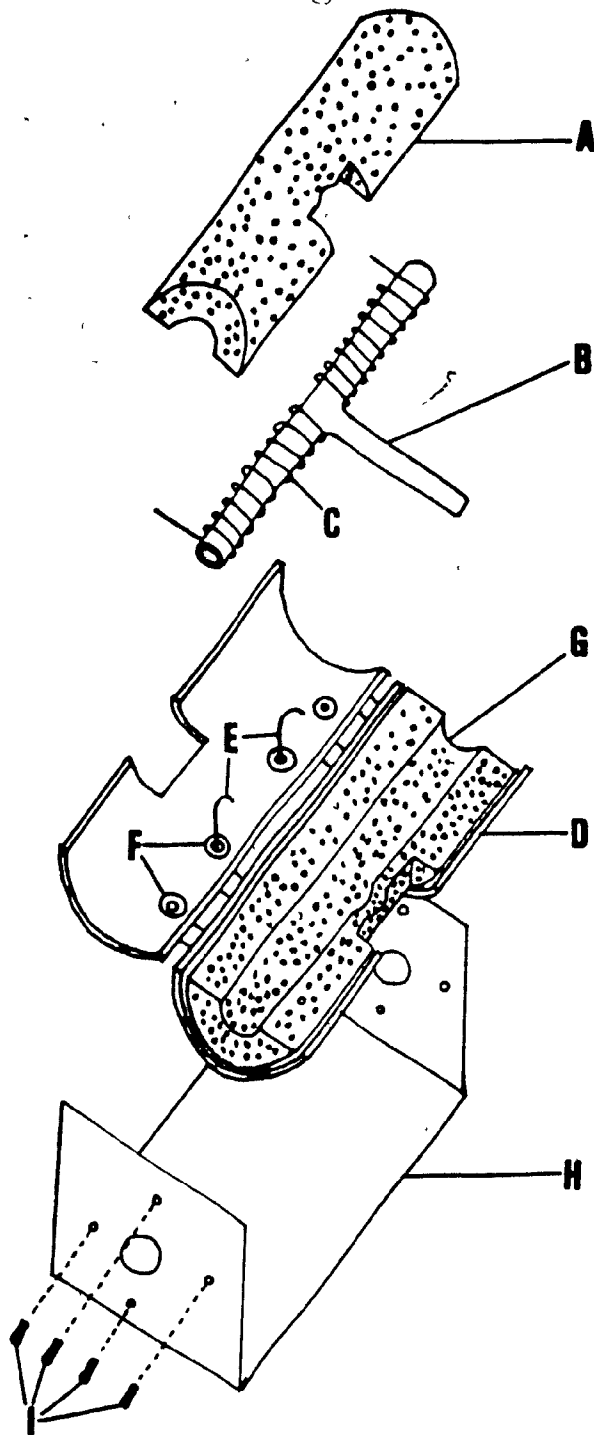


Figure 8. Exploded view of quartz T-tube furnace: A, shaped firebrick upper casing; B, quartz T-tube; C, Alloy 875 resistance heating wire; D, hinged aluminum casing; E, type K thermocouples; F, Swagelok connectors with ceramic tubing inserts; G, shaped firebrick, lower casing; H, aluminum mounting bracket; I, machine (6-32) screws.

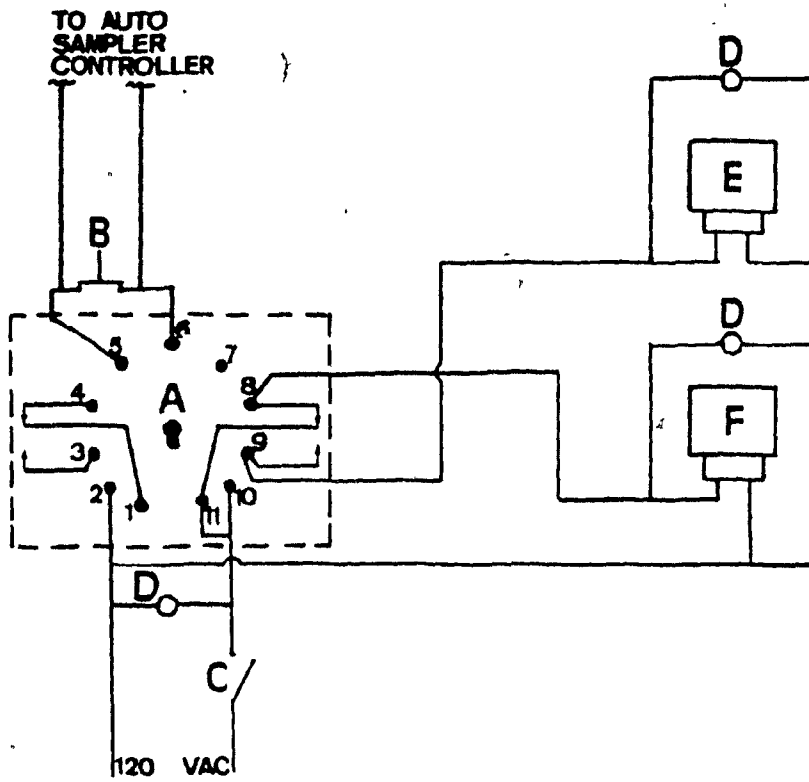


Thread) to 1/8 in (0.32 cm) tube connectors were mounted in the furnace casing (11 cm X 4.8 cm o.d., 4 cm i.d.) as entry ports for electrical connections to the heating elements and to position two type K (Chromel-Alumel) thermocouples (placed 1-2 mm from the quartz tube surface). Ceramic tubing (Omega Engineering Inc.) mounted within the Swagelok connectors was used as electrical and thermal insulation. The furnace casing was held together by an aluminum mounting bracket. The furnace was positioned within the optical path of the AAS by an adjustable ball joint affixed to the mounting bracket.

5.2.1.2 GC-AAS Interface The interface of the capillary column transfer line with the quartz furnace (Fig. 7) utilized readily available parts. A 1/4 in (0.64 cm) to 1/8 in (0.32 cm) Swagelok reducing union, modified with two attached 1/16 in (0.16 cm) stainless steel tubing gas inlets, positioned a section of alumina tubing (8.5 cm X 1/8 in (0.32 cm) o.d., 1/16 in (0.16 cm) i.d., Omega Engineering Inc.) within the lower tube of the quartz T-tube furnace. A 1/8 in (0.32 cm) to 1/16 in (0.16 cm) Swagelok reducing union, similarly modified with an attached 1/16 in (0.16 cm) stainless steel tubing gas inlet, was attached to the end of the alumina tube. The transfer line was passed through the 1/8 in (0.32 cm) to 1/16 in (0.16 cm) reducing union and alumina tube to the upper tube of the quartz T-tube. Graphite ferrules were used at all glass metal connections to avoid breakage when forming a gas tight seal.

5.2.1.3 Timed Gas Purge Circuit The gas purge timing circuit (Fig. 9) events were synchronized by a solid state delay relay (Model T2K-00300-461, National Controls Corp.) which was connected to two solenoid valves (Asco No. 8595C5) controlling the entry of furnace makeup gases. Both solenoid valves were normally closed types, so that only the energized valve was open. The

Figure 9. Variable time delay gas purge circuit: A, solid state adjustable time delay relay; B, momentary contact switch; C, SPST switch; D, neon indicator lights; E, air flow solenoid valve; F, H₂ solenoid valve.



normal system configuration is shown in figure 9; the H₂ solenoid was energized. During automated operation, the circuit was activated by a momentary contact across pins 5 and 6 of the relay, altering the power flow configuration for a preselected time (3-300 s), such that the air solenoid valve was energized (opened). The H₂ solenoid valve simultaneously deenergized (closed). The gas flow configuration was monitored by neon indicator lights.

5.2.2 Optimization and Characterization of GC-AAS System.

Compressed gases used were extra dry or prepurified grade (Medigaz Ltee) with the exception of ammonia (anhydrous) and methane (commercial grade). Gas flow rates were measured by precalibrated rotameter or soap bubble flowmeter.

A stock solution containing Me₃BuPb (3.07×10^{-6} g mL⁻¹ (as Pb)), Me₂Bu₂Pb (2.70×10^{-6} g mL⁻¹ (as Pb)), Et₃BuPb (1.49×10^{-6} g mL⁻¹ (as Pb)) and Et₂Bu₂Pb (1.34×10^{-6} g mL⁻¹ (as Pb)) in isooctane was used for the optimization studies. Serial dilution of this stock solution with isooctane provided working standards.

Triplicate sample injections (10 µL) were performed by the autosampler unless otherwise noted. Peak area response and area/height ratio were recorded.

Five operating parameters were each systematically varied to optimize the GC-AAS system performance: (a) transfer line position within the furnace, (b) GC column gas flow rate, (c) furnace temperature, (d) hydrogen furnace makeup gas flow rate and (e) furnace makeup gas. While one parameter was altered, the others were held constant: furnace makeup gas flow rate, 50 mL min⁻¹; transfer line position, junction of upper and lower quartz tube (0 mm); GC column flow

rate, 55 mL min⁻¹; furnace temperature, 900°C; furnace makeup gas, H₂.

Each parameter was varied over a wide range. The transfer line was positioned 0, 5, 10 and 20 mm back from the upper tube junction. The transfer line was always extended ~1 cm from the tip of the alumina tube (Fig. 7). The GC column gas flow rate was changed to 20, 35, 55 and 77 mL min⁻¹ during the optimization study. The furnace temperature was varied from 600°C to 1000°C in 100°C increments. The hydrogen makeup gas flow rate was varied from 0 to 150 mL min⁻¹. Five different gases (H₂, NH₃, CH₄, He and air) and a gas mixture (1:1 NH₃:H₂) were examined as furnace makeup gas. The furnace makeup gas was split after the H₂ solenoid valve (Fig. 9) and entered the GC-AAS furnace interface through inlets F and K (Fig. 7). The NH₃/H₂ mixture was produced by metering the two gases into a Swagelok tee union prior to entering the H₂ solenoid valve. Ammonia absorbed strongly at 217 nm, therefore ammonia peak area responses were measured at 283.3 nm, then converted to 217 nm peak area response using sensitivity ratios (217 nm:283.3 nm) observed in a linearity study.

The resolution between Me₂Bu₂Pb and Et₃BuPb (which have identical molecular weights) was determined from the retention times and peak area/height ratios recorded during the GC column flow rate parameter study.

A comparison of linearity (at 217 nm versus 283.3 nm) of the GC-AAS system response to serial dilutions of the alkylbutyllead stock solution (10⁻⁹ g mL⁻¹ to 10⁻⁶ g mL⁻¹) was performed under optimized operating conditions.

The linearity of the GC-AAS system response at 217 nm to serial dilutions of the alkylbutyllead stock solution (10^{-9} g ml $^{-1}$ to 10^{-7} g ml $^{-1}$) under normal (optimized) operating conditions (Section 5.2.1) was analyzed by linear regression. The significance of each regression equation was determined by analysis of variance. The significance of each equation parameter was examined by t-test.

The limit of detection for each alkylbutyllead standard was determined from GC-AAS system background noise and sensitivity measured as peak height counts (available directly from the Hewlett Packard 3390A recording integrator). Background noise was estimated by measuring all (a minimum of 20) peak to peak baseline noise perturbations along 2 min (run time) intervals centered on each alkylbutyllead standard retention time. The GC-AAS system sensitivity to each alkylbutyllead standard was measured by injection of serial dilutions of the alkylbutyllead standard stock solution (10^{-9} g ml $^{-1}$ to 10^{-7} g ml $^{-1}$) with the recording integrator reporting height counts rather than peak area.

5.2.3 Atomic Processes

Compressed gases used were extra dry or prepurified grade (Medigaz Ltee). Gas flow rates were measured by precalibrated rotameter or soap bubble flowmeter. Triplicate sample injections (10 μ L) were performed by the autosampler unless otherwise noted. Peak area response and area/height ratio were recorded.

5.2.3.1 Volatilization of Deposited Lead in Furnace Tetraethyllead (1.31×10^{-9} g) was injected into the GC-AAS system which had an isothermal

column temperature of 100°C and column flow rate of 55 mL min⁻¹. Other GC-AAS operating conditions were as described earlier (Section 5.2.1). Gas rotameters were configured to allow two gases (air/H₂ or N₂/H₂) to be metered into a Swagelok tee connector just prior to entering the H₂ solenoid (Fig. 9). Each gas rotameter could be turned on or off to allow rapid switching of the gas supplied to the H₂ solenoid.

The peak area response of the Et₄Pb was initially recorded under 50 mL min⁻¹ furnace H₂ makeup gas. Further sample injections were made with air or N₂ as the furnace makeup gas (50 mL min⁻¹). At either 1 or 5 min after the retention time of Et₄Pb (under the experimental conditions) the air or N₂ was switched to H₂ (50 mL min⁻¹). The resulting signal was recorded (Hewlett Packard 3390A) at both 217 nm and 283.3 nm. Solvent and gas switching (N₂ to H₂, air to H₂) blanks were run.

5.2.3.2 Lead Volatilization from Quartz Insert A 6 mm o.d., 4 mm i.d., 7 cm long quartz tube was fitted with Swagelok 1/4 in (0.64 cm) to 1/16 in (0.16 cm) reducing unions at both ends. The quartz tube assembly was charged with approximately 250 µL of Et₄Pb, flushed briefly with extra dry N₂ (Medigaz Ltée.), sealed with 1/16 in (0.16 cm) end caps, and then heated rapidly by a wound electrical heating element to 800°C. The temperature was measured with a Chromel-Alumel thermocouple. After 5 min, the assembly was allowed to cool, and purged with N₂ (100 mL min⁻¹) for several minutes. The lead coated quartz tube was then cut into two 3.5 cm sections. Each section was wiped externally, rinsed with acetone and hexane, oven dried, allowed to cool, and then weighed.

One section was placed in the AAS furnace (on one side of the upper tube) and heated to 900°C with H_2 (50 mL min^{-1}) as the furnace makeup gas. The gas purge circuit was disabled for these experiments. The section was periodically removed from the furnace, allowed to cool and then weighed. The other section was placed in a muffle furnace, heated to 900°C for 16 h, removed, allowed to cool and then weighed.

Another quartz tube (4 cm X 6 mm o.d., 4 mm i.d.) was charged with several drops of Et_4Pb , heated (by a wound electrical resistance heating element) to 800°C under air for several minutes, and allowed to cool. The procedure was repeated 2 times. The exterior was then wiped, rinsed with acetone and hexane, oven dried, allowed to cool, and then weighed. The entire quartz tube was placed in the AAS furnace (on one side of the upper tube) and heated to 900°C with H_2 (50 mL min^{-1}) as the furnace makeup gas. Periodic weighings were made as before.

5.2.3.3 Gas Mixtures at Two Furnace Temperatures GC-AAS system response to the $10^{-7} \text{ g mL}^{-1}$ dilution of the alkylbutyllead stock solution with various air/ H_2 or N_2/H_2 furnace makeup gas mixtures was examined at two furnace temperatures (600°C and 900°C). Normal GC-AAS operating conditions were used (Section 5.2.1) except that the air or N_2 entered the GC-AAS interface through inlet F (Fig. 7), and was thus entrained along the ceramic insert exterior (Fig. 8). The hydrogen entered through inlet K (Fig. 7), and was therefore contained within the ceramic insert interior until reaching the upper tube of the AAS furnace. The gas entry configuration prevented damage to the transfer line from combustion of air/ H_2 mixtures in the lower section of the GC-AAS interface. The furnace makeup gases (or mixtures) examined were H_2 , 4:1 H_2/air

or N_2 , 1:1 H_2 /air or N_2 , 1:4 H_2 /air or N_2 , air and N_2 . The furnace makeup gas flow rate was 50 mL min^{-1} . The gases were metered by precalibrated rotameters.

5.3 Results and Discussion

5.3.1 GC-AAS System

The quartz tube furnace was designed to: (a) permit its physical placement within the optical path of the AAS, (b) optically transmit the incident resonance radiation, (c) contain the atomic vapour within the optical pathway, (d) be compatible with readily available GC gas fittings (Swagelok), and (e) be sufficiently robust for prolonged usage.

Various flame tube adapters (Rubeska and Moldan 1968, Delves 1970) have improved sensitivity for lead by retaining the atoms in the optical path. The physical dimensions of the tube affect the sensitivity of the instrumentation. Ebdon et al. (1982) reported that decreasing the internal diameter (volume) of a flame heated ceramic tube atomizer enhanced organolead response, presumably by increasing the lead atom concentration and tubal area illuminated by the resonance radiation from the hollow cathode lamp.

The sensitivity of a tube atomizer would therefore likely be enhanced by using a long narrow tube configuration. The maximum tube length which could be mounted in the AAS optical path was 10 cm. A longer tube length was considered too near the optics associated with the monochromator. Preliminary experimentation with a series of apertures indicated that 7 mm was apparently the minimal diameter opening that would pass sufficient resonance radiation to allow a low gain PMT amplifier setting. A 7 mm internal diameter quartz tube

was therefore used as the upper tube of the furnace (Fig. 8). The silica acted as a light guide by internal surface reflection. The tube area was well illuminated by the resonance radiation. The outer diameter of the lower tube (6.25 mm) allowed the use of readily available Swagelok fittings in the GC-AAS interface.

Reliable electrical resistance heating elements were considered essential for prolonged use of the quartz furnace in an automated GC-AAS system. Preliminary studies showed that heating elements made from an iron-chromium-aluminum wire (Alloy 875) were superior to heating elements made from nickel-chromium wire (Chromel, Hoskins Alloys of Canada, Ltd.) under furnace operating conditions. Alloy 875 has a higher maximum continuous operating temperature (1290°C) than Chromel (1180°C) which would have allowed a higher furnace operating temperature if necessary. The Chromel wire corroded more than the Alloy 875 wire when installed in the furnace.

The GC-AAS interface (Fig. 7) was designed to: (a) minimize the thermal transition zone of the furnace, (b) introduce various furnace support gases, and (c) transport and preserve the organolead analytes to the atomization region of the furnace in a minimum gas volume.

An initial problem with the GC-AAS system was analyte decomposition outside the atomization region of the furnace. A thermal gradient between the upper and lower tube of the furnace allowed excessive heating of the transfer line. Thompson and Thomerson (1974) reported that the inlet tube of the quartz T-tube furnace used had to be cooled to prevent premature hydride decomposition.

Preliminary work was done with air cooled stainless steel tubing heat

exchangers mounted on the lower tube next to the heated region of the furnace. However, heat exchange was difficult to control, and system performance degraded. Removal of all surrounding insulation (Fig. 8) from the lower tube proved successful, allowing air circulation to reduce the thermal transition zone. The ceramic insert (Fig. 7) positioned and shielded the transfer line. The hydrogen gas was entrained inside and outside the ceramic insert (through inlets F and K, Fig. 7) for cooling, and swept the lower tube void volume. The fused silica transfer line was flexible and remained inert when treated periodically with dimethyldisilazane and Silyl-8 (Chromatographic Specialties Ltd.).

Metal transfer lines have been frequently used (Chau et al. 1975, Bye et al. 1978, Chakraborti et al. 1984) although glass (Chakraborti et al. 1981), quartz capillary (Reamer et al. 1978), and teflon-lined aluminum tubing (Radziuk et al. 1979) have also been reported. The continued use of metal transfer lines is surprising as the general trend in gas chromatography has been the replacement of metal columns with borosilicate and fused silica columns to minimize column surface-analyte interaction.

Initial work with the GC-AAS system showed that operation of the furnace under a hydrogen atmosphere resulted in carbon deposition from the injected solvent, inside and at the exits of the upper tube. Continued carbon deposition may have reduced resonance light transmittance through the furnace (by developing carbon plugs at the tube exits) and lowered AAS system response. Carbon (as graphite) lowered AAS response to arsine (Parris et al. 1977, Welz and Melcher 1983). Preliminary studies with air/hydrogen mixtures indicated that carbon deposition could not be prevented without analyte signal suppression. The automated gas purge circuit (Fig. 9) allows combustion of the

injection solvent under air to prevent carbon decomposition, and maximum GC-AAS sensitivity by switching back to H₂ for sample analysis.

5.3.2. Optimization and Characterization of GC-AAS System

The four alkylbutyllead standards behaved similarly during the optimization study. Results given are from Me₃BuPb (unless otherwise noted) for simplification. The other data are presented in Appendix G.

The transfer line was not a critical GC-AAS system parameter. Preliminary work indicated that variation of transfer line temperature from 200°C to 275°C had no observable effect on peak area response or area/height ratio. A temperature of 250°C was selected for subsequent use to permit any high molecular weight coextractives to elute during GC-AAS system operation. The position of the transfer line inside the furnace (Fig. 10) also had little effect on the peak area response although the peak shape (as measured by area/height ratio--an approximation of the half height peak width (min)) broadened as the transfer line was moved away from the upper tube of the furnace. The 0 mm position of the transfer line from the upper tube was selected as it minimized peak broadening and simplified positioning of the transfer line within the furnace assembly.

The GC-AAS system was sensitive to the total gas flow (GC column + furnace makeup gas flow rates) rate through the furnace and the quantity of hydrogen in the furnace makeup gas. The effects of total gas flow rate through the furnace were shown when the GC column flow rate (Fig. 11) or the furnace makeup gas flow rate (Fig. 12) was varied with the other held constant. The GC column flow rate (Fig. 11) affected peak area response, peak shape and column resolution. The peak area maxima and optimized peak shape (minimum area/height

Figure 10. Response of peak area and area/height ratio of 3.07 ng (as Pb) Me_3BuPb to changes in transfer line distance from upper tube. $\text{---}\square\text{---}$, peak area response; $\text{---}\diamond\text{---}$, area/height ratio. Error bars represent \pm one standard deviation of three replicate determinations.

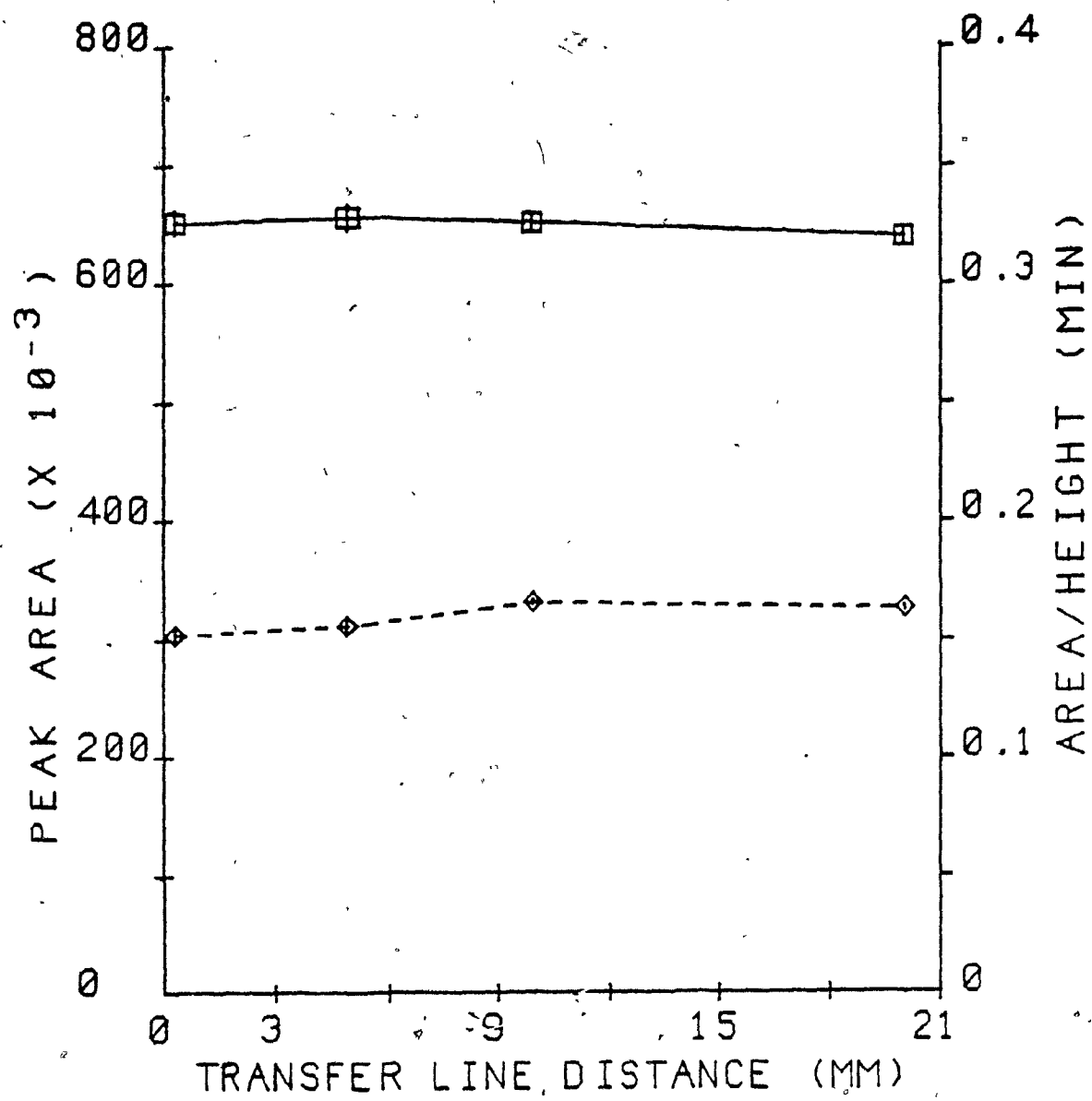


Figure 11. Response of peak area and area/height ratio of 3.07 ng (as Pb) Me₃BuPb to changes in GC column flow rate. —□—, peak area response; —◇—, area/height ratio. Error bars represent \pm one standard deviation of three replicate determinations.

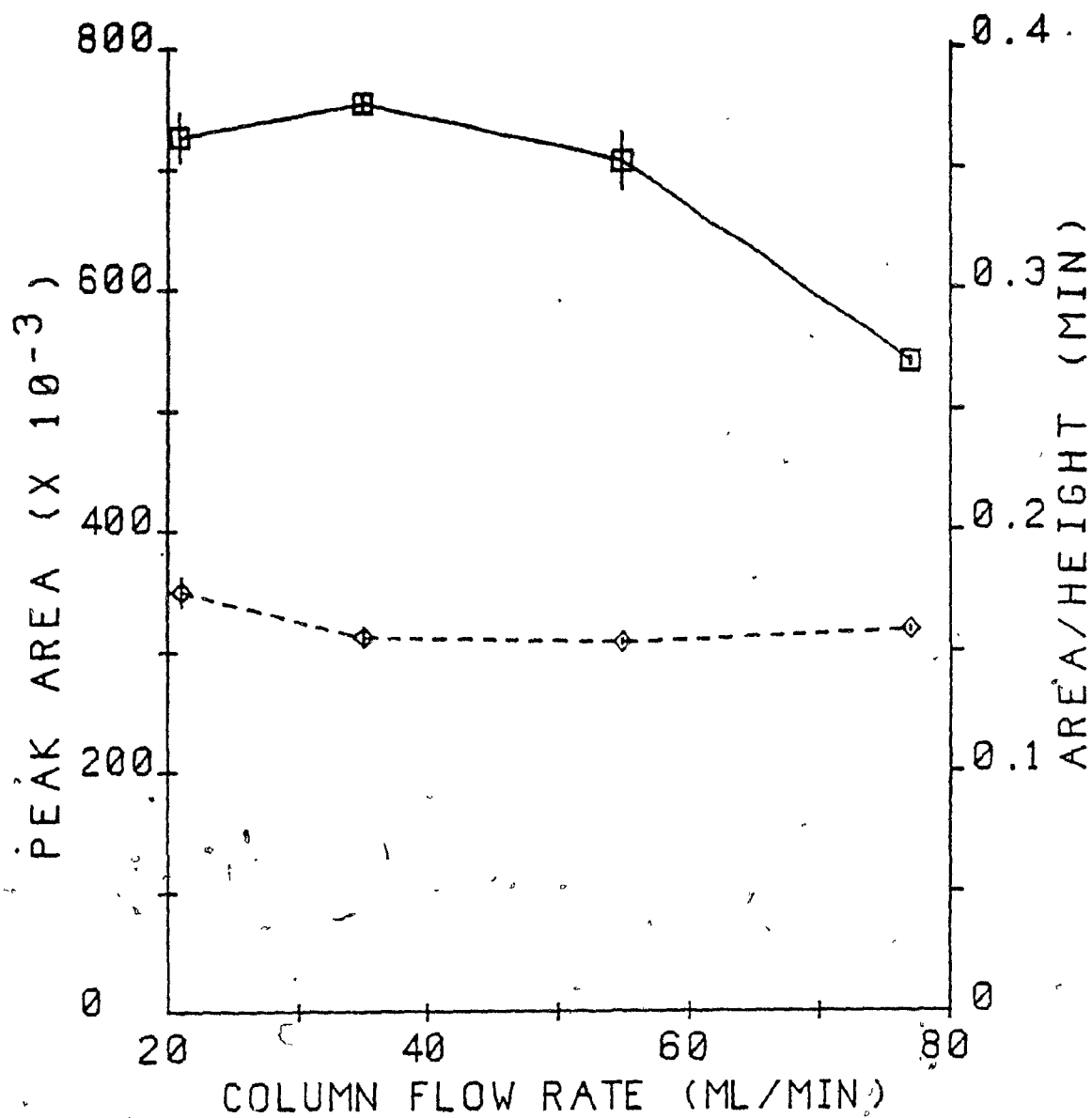
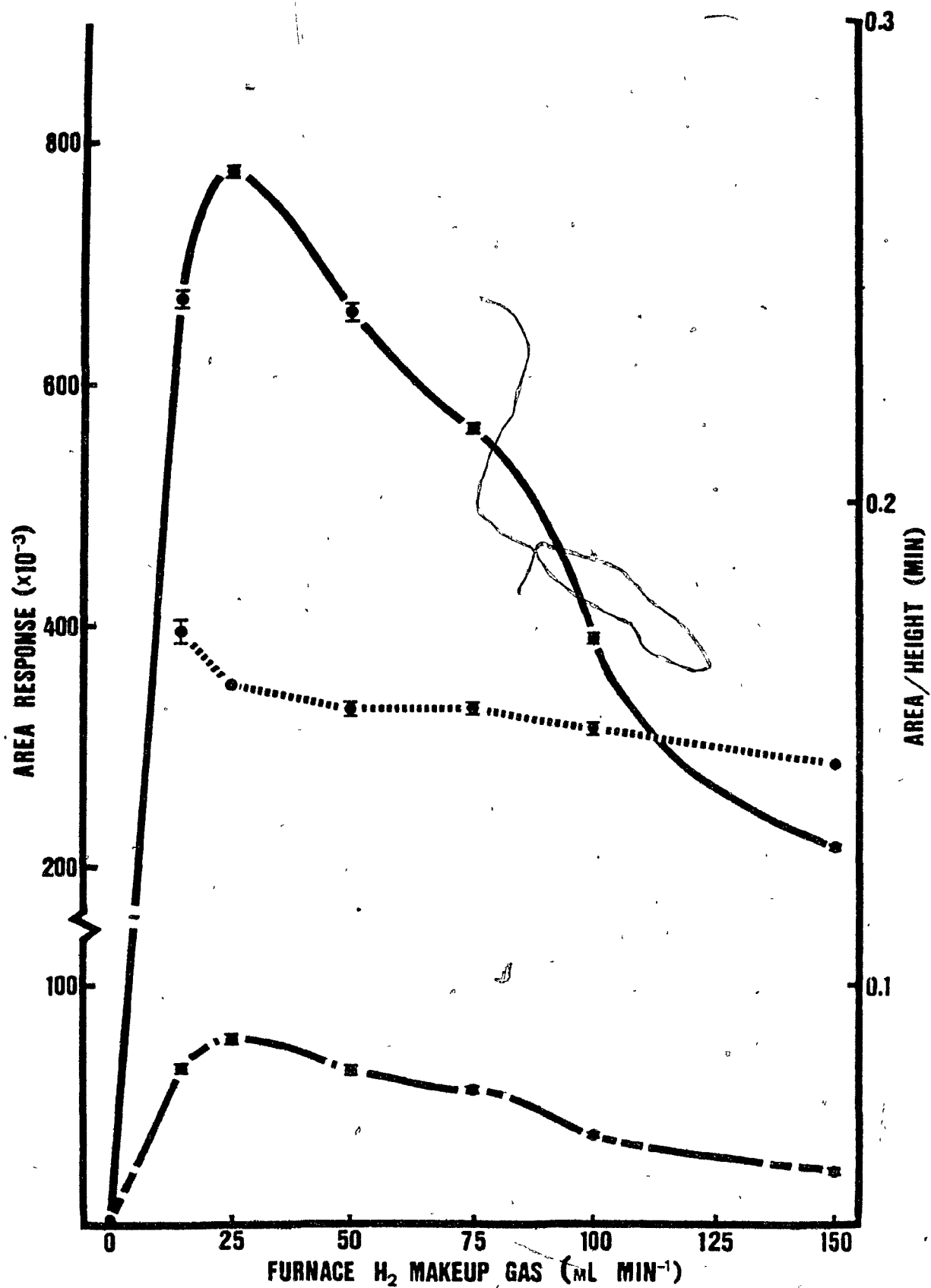


Figure 12. Response of peak area (—●—, 3.07 ng Pb ; -●-, 0.31 ng Pb); area/height ratio ■■■●■■■, of Me₃BuPb (3.07 ng Pb) to changes in furnace makeup gas flow rate. Error bars represent \pm one standard deviation of three replicate determinations.



ratio) occurred at 35 mL min^{-1} with the H_2 furnace makeup gas flow held constant at 50 mL min^{-1} (total gas flow through the furnace, 85 mL min^{-1}). The lowered response at column flow rates less than 35 mL min^{-1} may have been caused by thermal decomposition. The reduced peak area response at column flow rates above 35 mL min^{-1} was likely caused by a decreased residence time of the lead atoms in the light path of the resonance radiation. Resolution between $\text{Me}_2\text{Bu}_2\text{Pb}$ and Et_3BuPb always exceeded 1.5, but maximized at a column flow rate of 35 mL min^{-1} (Appendix H). The hydrogen furnace makeup gas flow rate exerted a large influence on system response (Fig. 12). In the absence of hydrogen virtually no peak area response occurred, however, the peak area response maxima for 3.07 and 0.31 ng (as Pb) Me_3BuPb occurred at only 25 mL min^{-1} (Fig. 12) with the column flow rate held constant at 55 mL min^{-1} (total gas flow through the furnace, 80 mL min^{-1}). Maximum peak area responses of four different concentrations (ranging from 13 pg to 31 ng) of the four alkyllead standards occurred at the same H_2 flow rate (25 mL min^{-1}) (Appendix G), indicating that the optimum H_2 flow rate was independent of the quantity of lead injected. The rapid increase in peak area response between 0 and 25 mL min^{-1} H_2 suggested that an optimum level of hydrogen in the furnace was quickly reached, above which the total gas flow rate through the furnace became the predominate factor, lowering the peak area response. The suppressive effect of increasing gas flow rate through the detector on peak area response was shown by the continuous decrease in peak area response at furnace hydrogen makeup gas flow rates above 25 mL min^{-1} (Fig. 12). The decreased peak area response again was likely caused by reduced residence time of the lead atoms in the light path of the resonance radiation. The optimum total gas flow rate through the furnace was $80\text{--}85 \text{ mL min}^{-1}$.

The 35 mL min⁻¹ helium column flow rate produced maximum peak area response and optimum peak shape. The H₂ makeup gas results (Fig. 12) indicated that a minimum of approximately 30% H₂ in helium was necessary for optimum peak area response. The GC performance was optimized by selecting a 35 mL min⁻¹ column flow rate, whereas 50 mL min⁻¹ furnace makeup gas was selected to ensure sufficient H₂ in the furnace without exceeding the determined 80-85 mL min⁻¹ total gas flow maxima.

Reproducibility of peak area response generally decreased at parameter values below the peak area response maxima and increased at parameter values above the peak area response maxima (Figs. 11 and 12). However, the trend was not consistent, and reproducibility at the optimum parameter value was usually better than at most other parameter values.

The identity of the furnace makeup gas had a pronounced effect on peak area response and peak shape (Fig. 13). Hydrogen produced the largest peak area response. The 1:1 (v/v) ammonia and hydrogen mixture produced the second largest peak area response, but was only 56% as effective as hydrogen. Further discussion of these results is included in Section 5.3.3. Hydrogen was selected as the optimum furnace makeup gas.

The upper tube surface temperature affected peak area response and area/height ratio (Fig. 14). The peak area response and peak shape were relatively insensitive to furnace temperature changes above 800°C, although the reproducibility improved with increasing temperature. Below 800°C, peak area response dropped considerably, and peak broadening occurred. At lower furnace temperatures a slightly increased residence time of the lead atoms in the optical path would likely occur because of the lower thermal expansion of the

Figure 13. Response of peak area and area/height ratio of 3.07 ng (as Pb) Me_3BuPb to different furnace makeup gases. —, peak area response; ■■■■■, area/height ratio. Error bars represent \pm one standard deviation of three replicate determinations.

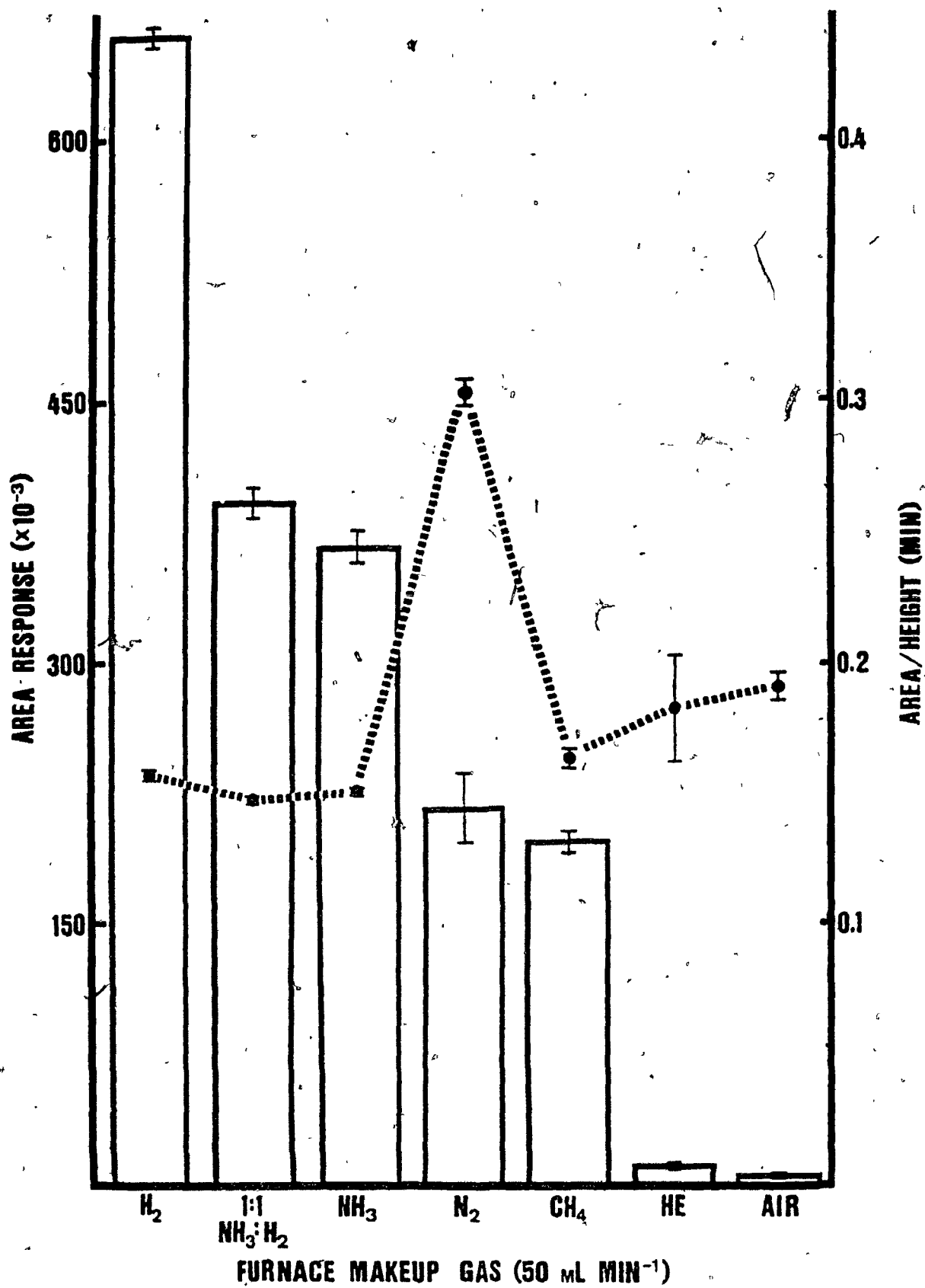
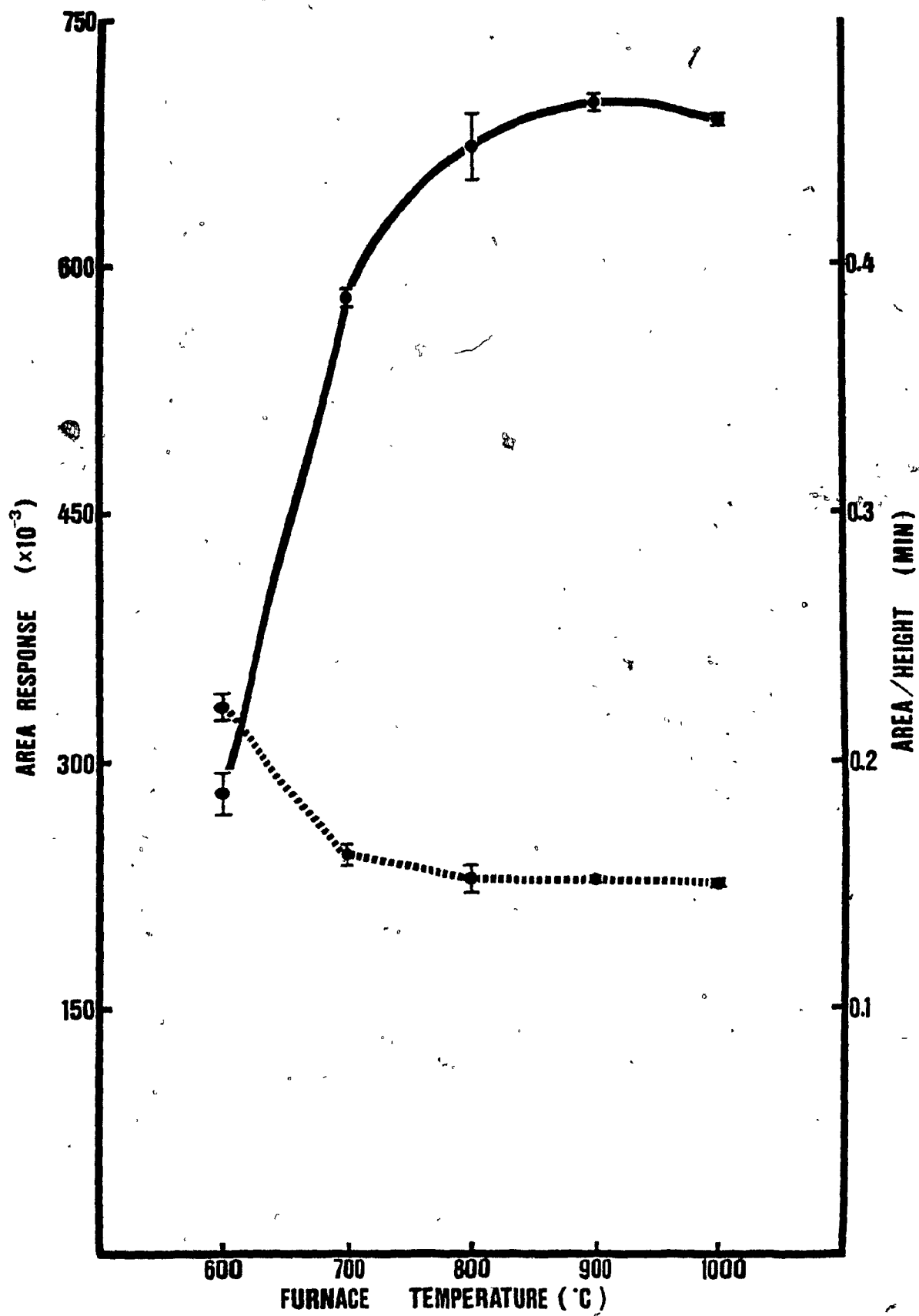


Figure 14. Response of peak area and area/height ratio of 3.07 ng (as Pb) Me₃BuPb to furnace temperature. —, peak area response; •••••, area/height ratio. Error bars represent \pm one standard deviation of three replicate determinations.





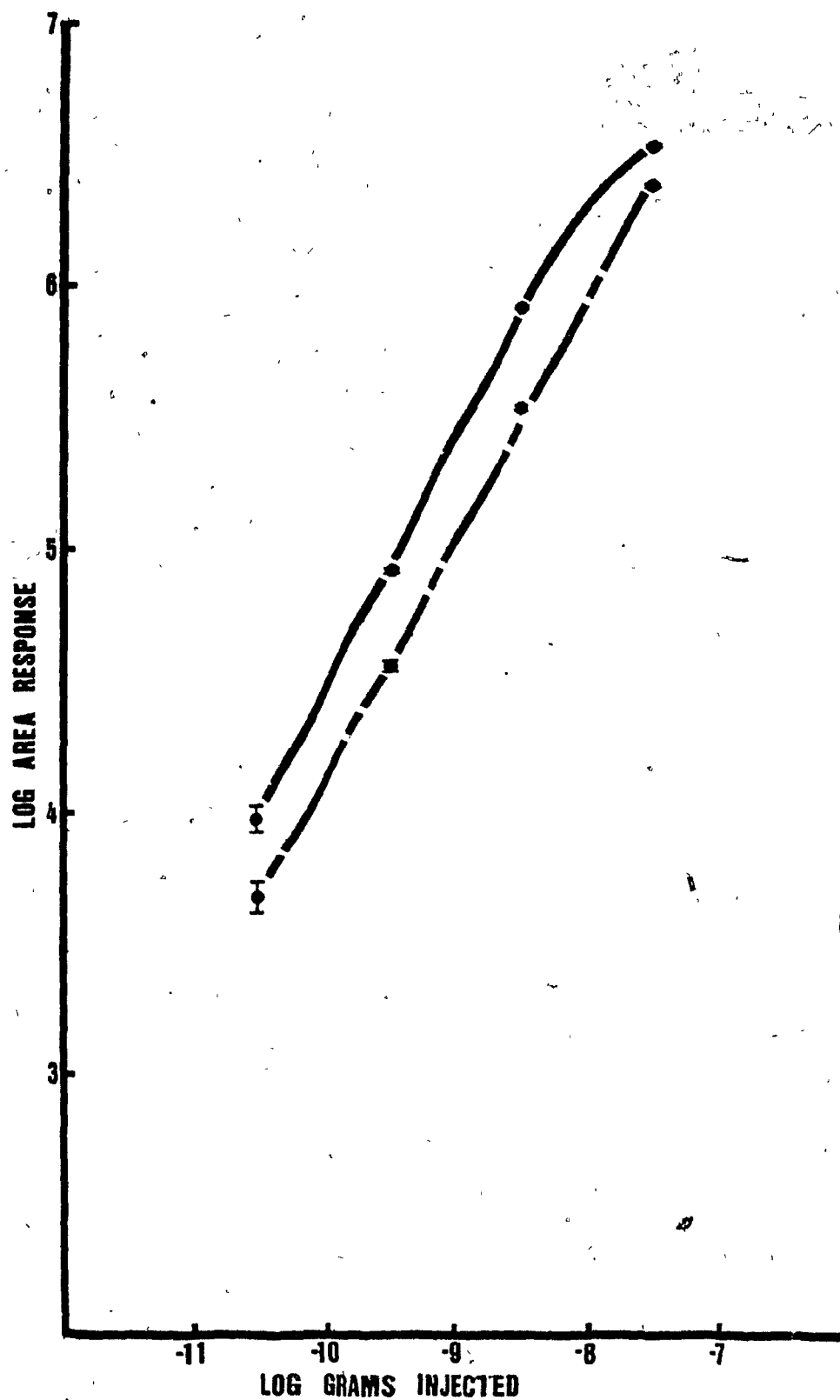
gases within the furnace. This effect should have produced an increase in peak area response. The decline in peak area response below 800°C was therefore probably caused by reduced furnace atomization efficiency. A furnace operating temperature of 900°C was selected as the peak area maxima occurred at that temperature. In addition, it was considered that a lower operating temperature would extend the lifespan of the electrical resistance heating elements.

Based on the optimization studies, the standard operating conditions for the GC-AAS system were: furnace makeup gas, H_2 ; furnace makeup gas flow rate, 50 mL min^{-1} ; furnace temperature, 900°C; GC column flow rate, 35 mL min^{-1} ; transfer line position in the furnace, at the junction of the upper and lower tubes.

The atomization efficiency of the quartz furnace did not decrease within the linearity limitations of the AAS. A log-log plot of the GC-AAS peak area response to the different Me_3BuPb concentrations at 217 and 283.3 nm (Fig. 15) showed that linearity was extended at 283.3 nm because of lowered absorbance, whereas at 217 nm, the increased absorbance became curvilinear above 3.07 ng Pb (as Me_3BuPb) injected, because of residual, unabsorbable light reaching the AAS photomultiplier tube. The range of linearity could be extended by operating the GC-AAS system at 283.3 nm, but with a loss of sensitivity.

The GC-AAS peak area response was linear from 13 pg to 3.07 ng Pb (as alkylbutyllead standards) at 217 nm. Analysis of variance (Appendix I) indicated that the response of each alkylbutyllead standard significantly ($p=0.01$) fitted the simple linear regression model. The Y intercept of each regression equation was not significantly different from zero ($p=0.01$, t-test, Appendix I), indicating that within experimental error, the linear regression

Figure 15. Peak area response of 31 pg-30.7 ng (as Pb) Me₃BuPb at:  ,
217 nm;  , 283.3 nm. Error bars represent \pm one standard
deviation of three replicate determinations.



line would pass through the origin.

The limit of detection (LOD) ranged from 4.8 to 6.7 pg Pb. The LOD was calculated by multiplying the mean peak to peak noise (N_{p-p}) plus three standard deviations ($3N_{SD}$) by the response factor of each alkylbutyllead (Table 8). Actual GC-AAS response (Fig. 16) with 13 pg Pb injected (as Et_2Bu_2Pb) was easily discerned from the baseline. These limits of detection are lower than any previously reported for a GC-AAS system (Table 7). Other authors reporting low picogram limits of detection (Reamer et al. 1978, Chakraborti et al. 1981, Nielsen et al. 1981) used more expensive (graphite furnace, mass spectrometer, microwave induced plasma) detector systems.

The reproducibility of analyte response to the GC-AAS system is superior to previously reported values. The mean peak area response of the alkylbutylleads from six replicate injections varied only 0.2-1.4% (relative standard deviation) at the nanogram Pb level (Table 9). At comparable levels, other authors have reported 2-5.1% reproducibility (Table 7). The GC-AAS system reproducibility was likely enhanced by the use of an autoinjector.

The automated GC-AAS system developed for this study has the lowest limit of detection reported for a GC-AAS system. The range of linearity at 217 nm extended from the limits of detection to approximately 3 ng Pb. The linear range could be extended by the use of the 283.3 nm Pb resonance line, but with a loss of sensitivity. The system reproducibility was enhanced by the use of an autoinjector. GC column resolution was sufficient for quantitative integration of all alkylbutyllead analytes.

Table 8. Limits of detection (LOD).

Compound	Mean ⁱ N _{p-p} ⁱⁱ --(Height Count)--	NSD ⁱⁱⁱ	Response Factor ^{iv}	LOD ^v (pg Pb)
Me ₃ BuPb	70.7	30.1	0.03976	6.4
Me ₂ Bu ₂ Pb	68.7	32.2	0.04031	6.7
Et ₃ BuPb	68.7	32.2	0.03986	6.6
Et ₂ Bu ₂ Pb	61.0	21.6	0.03811	4.8

i- N=6 replicate determinations

ii- mean peak to peak baseline noise

iii- standard deviation of N_{p-p}

iv- inverse of slope from linear regression analysis (pg Pb height count⁻¹)

v- (mean N_{p-p} + 3NSD)* response factor

Figure 16. Typical GC-AAS chromatograms of: (1) Me_3BuPb , (2) $\text{Me}_2\text{Bu}_2\text{Pb}$, (3), Et_3BuPb and (4) $\text{Et}_2\text{Bu}_2\text{Pb}$. Chromatogram A contains 0.27-0.31 ng (as Pb); B, 27-31 pg (as Pb); C, 13-31 pg (as Pb); D, solvent blank.

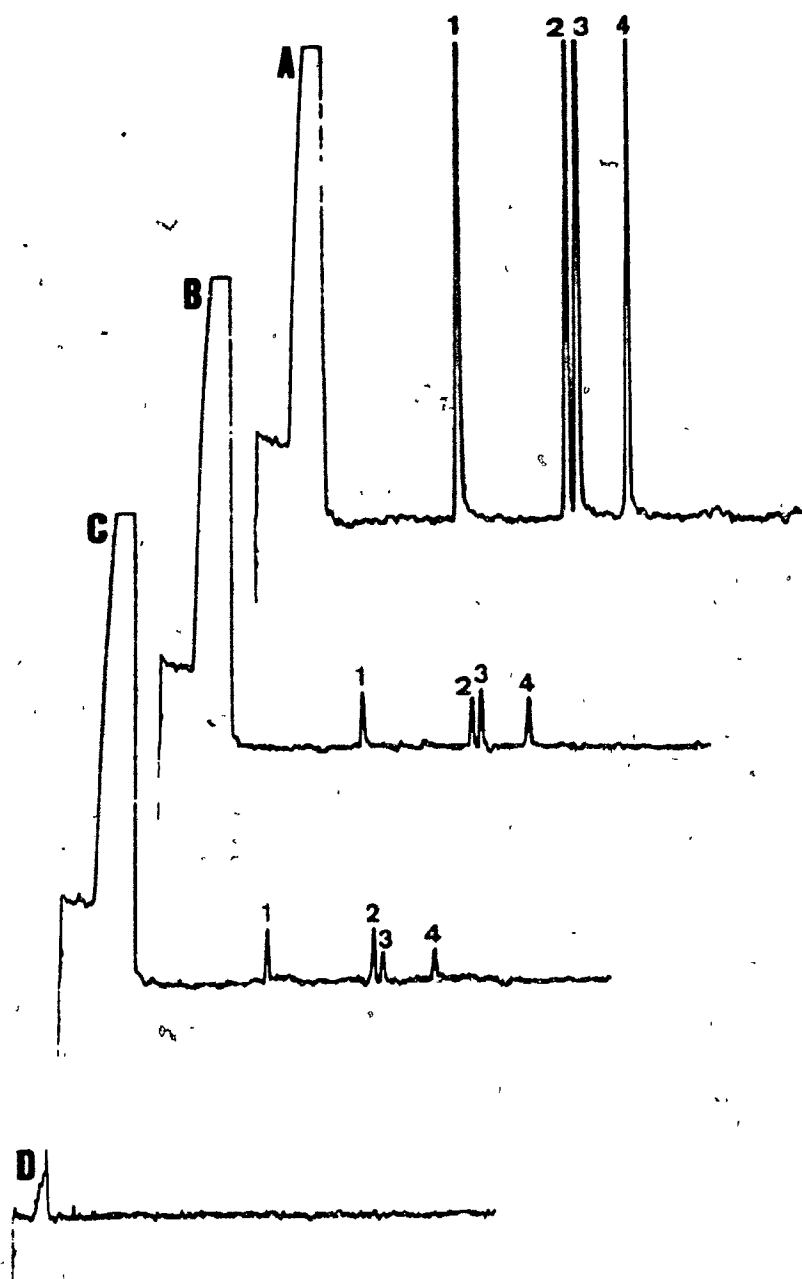


Table 9. GC-AAS system reproducibility

Compound	Quantity (ng Pb)	Mean ⁱ Peak Area _{±SD}	Reproducibility ⁱⁱ %
Me ₃ BuPb	3.07	832261.7 _{±1471.3}	_{±0.2}
Me ₂ Bu ₂ Pb	2.70	742703.3 _{±9461.4}	_{±1.3}
Et ₃ BuPb	1.49	446263.3 _{±6220.8}	_{±1.4}
Et ₃ Bu ₂ Pb	1.34	379296.7 _{±3142.1}	_{±0.8}

ⁱ- N=6 replicate determinations

ⁱⁱ- as relative standard deviation

5.3.3 Atomization Processes

Lead atomization in the quartz furnace was most efficient in the presence of hydrogen (Fig. 13). Other gases containing structural hydrogen (NH_3 , CH_4) also supported lead atomization, but not as efficiently as elemental hydrogen. Ammonia and methane were 56 and 30% as effective as hydrogen. The 1:1 (v/v) mixture of hydrogen and ammonia was not appreciably more effective (59 versus 56%) than pure ammonia, suggesting that ammonia had a direct suppressive effect on atomization. Because bond dissociation energies for ammonia, methane and hydrogen are not appreciably different (460, 435, and 432 kJ mol^{-1} respectively), all three gases might act as a hydrogen atom source. The lower atomization efficiency of methane and ammonia may be caused by CH_3 or NH_2 radicals scavenging free H radicals or lead metal. Nitrogen was 33% as efficient as hydrogen, but produced a much broader peak shape than any other tested furnace makeup gas, suggesting that a different atomization mechanism occurred. Helium was only 1.4% as efficient as H_2 , indicating that, in the absence of N_2 or a hydrogen atom source, virtually no lead atomization occurred. Air was the least efficient furnace makeup gas (0.4%) despite an approximate 78% N_2 content. Oxygen, the other major component of air (~21%) likely suppressed lead atomization below that which occurred under pure N_2 , by forming refractory lead oxides.

Hydrogen rapidly volatilized lead which had been deposited on the quartz surface of the furnace under an air or nitrogen atmosphere. Although lead metal has a boiling point 844°C above the surface temperature of the furnace, the deposited lead was volatilized in approximately 1-2 s when exposed to hydrogen at 900°C (Fig. 17, Tables 10 and 11), indicating that a volatile lead

hydride formed, and transported the lead back into the pathway of the resonance radiation with subsequent atomization.

When air was the furnace makeup gas, no peak area response occurred at the normal retention time of the injected organolead analyte (Et_4Pb) (Figs. 17B and 17C). Approximately 57% of the peak area response observed for Et_4Pb in a hydrogen atmosphere (Fig. 17A) occurred when the air was switched to H_2 , 1 or 5 min after the normal retention time of Et_4Pb (Figs. 17B and 17C). The deposited lead did not volatilize under oxidizing conditions as there was no significant difference ($p=0.05$, t-test) between the total peak area response at 1 or 5 min post retention time of Et_4Pb (Table 10).

A nitrogen furnace makeup gas did support atomization of the Et_4Pb (Figs. 17D and 17E), with a peak area response (~46% of the peak area response under H_2) occurring at the normal retention time of Et_4Pb . However, further lead was volatilized (28-39% of the peak area response under H_2) from the quartz surface when the N_2 was switched to H_2 , 1 or 5 min after the normal retention time of Et_4Pb (Figs. 17D and 17E), indicating incomplete atomization. The deposited lead continued to slowly volatilize under N_2 , as the total peak area response with 1 min post retention time N_2 to H_2 switching was significantly more ($p=0.05$, t-test) than the total peak area response with 5 min post retention time N_2 to H_2 switching (Table 11).

The peak area response which occurred when switching from air or N_2 to H_2 was measured at two lead resonance wavelengths, 217 and 283.3 nm to determine the response ratio. The Et_4Pb response ratio was not significantly different ($p=0.05$, t-test) from the response ratio of the signal occurring during gas switching. Air to H_2 switching controls produced a very small peak area

Figure 17. Peak area response of: (1) 1.31 ng Et₄Pb and (2) revolatilized lead under: A, H₂; B, air then air → H₂ switching 1 min post retention time; C, air then air → H₂ switching 5 min post retention time; D, N₂ then N₂ → H₂ switching 1 min post retention time; E, N₂ then N₂ → H₂ switching 5 min post retention time.

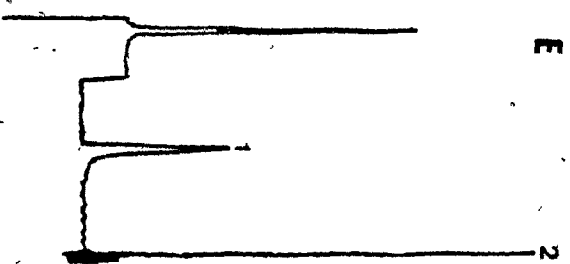
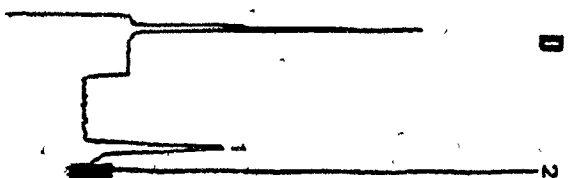
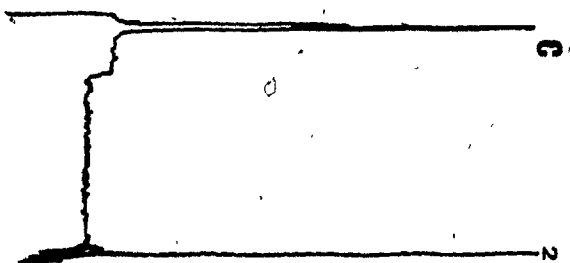
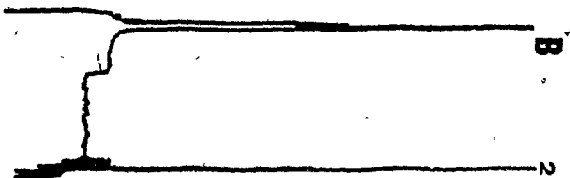
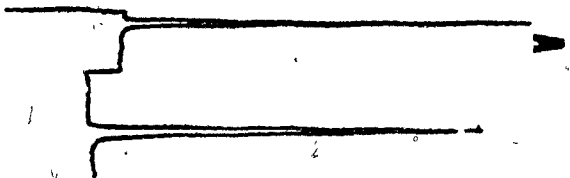


Table 10. Volatilization and atomization of lead in furnace with air to H₂ switching

Parameter Gas, Time	Mean ⁱ Peak Area+SD (Mean Area/Height+SD)	Total Response ^{ii, iv}		Response Ratio ^{iii, iv}
	-----Wavelength(nm)----- 217 283.3			
H ₂ , retention	196327+1902	80118+1013		2.45+0.04 ^{ns}
Air, retention	-	-		
Air -> H ₂ , 1 min post retention	112223+2708 ^v (0.013+0.001)	45094+1297 ^v	112223+2708 ^{ns}	2.49+0.09 ^{ns}
Air -> H ₂ , 5 min post retention	111217+6159 ^v (0.013+0.001)	-	111217+6159 ^{ns}	

i- N=3 replicate determinations

ii- peak area response under air at retention time + peak area response under air → H₂ switching 1 or 5 min post retention time

iii- peak area response at 217 nm/peak area response at 283.3 nm

iv- t-test ns- not significantly different, p=0.05

v- corrected for air → H₂ blank control

Table 11. Volatilization and atomization of lead in furnace
with N₂ to H₂ switching

Parameter Gas, Time	Mean ⁱ Peak Area±SD (Mean Area/Height±SD)	Wavelength(nm)----- 217 283.3	Total Response ^{ii,iv}	Response Ratio ^{iii,iv}
H ₂ , retention	190793±925 (0.266±0.002)	76489±1841		2.49±0.06 ^{ns}
N ₂ , retention	85005±3150 (0.330±0.008)			
N ₂ -> H ₂ 1 min post retention	53512±330 (0.015±0)	21644±2808	138517±3167*	2.47±0.32 ^{ns}
N ₂ , retention	90268±2011 (0.350±0.028)			
N ₂ -> H ₂ 5 min post retention	35869±2808 (0.019±0.002)		126137±3454*	

ⁱ- N=3 replicate determinations

ⁱⁱ- peak area response under N₂ at retention time + peak area
response under N₂ -> H₂ switching 1 or 5 min post retention time

ⁱⁱⁱ- peak area response at 217nm/peak area response at 283.3 nm

^{iv}- t-test ns- not significantly different, p=0.05

*- 0.05 significance

response, whereas N_2 to H_2 switching controls produced no peak area response. Solvent blanks (isooctane) also produced no peak area response. It is concluded that the observed peaks are caused by volatilized lead.

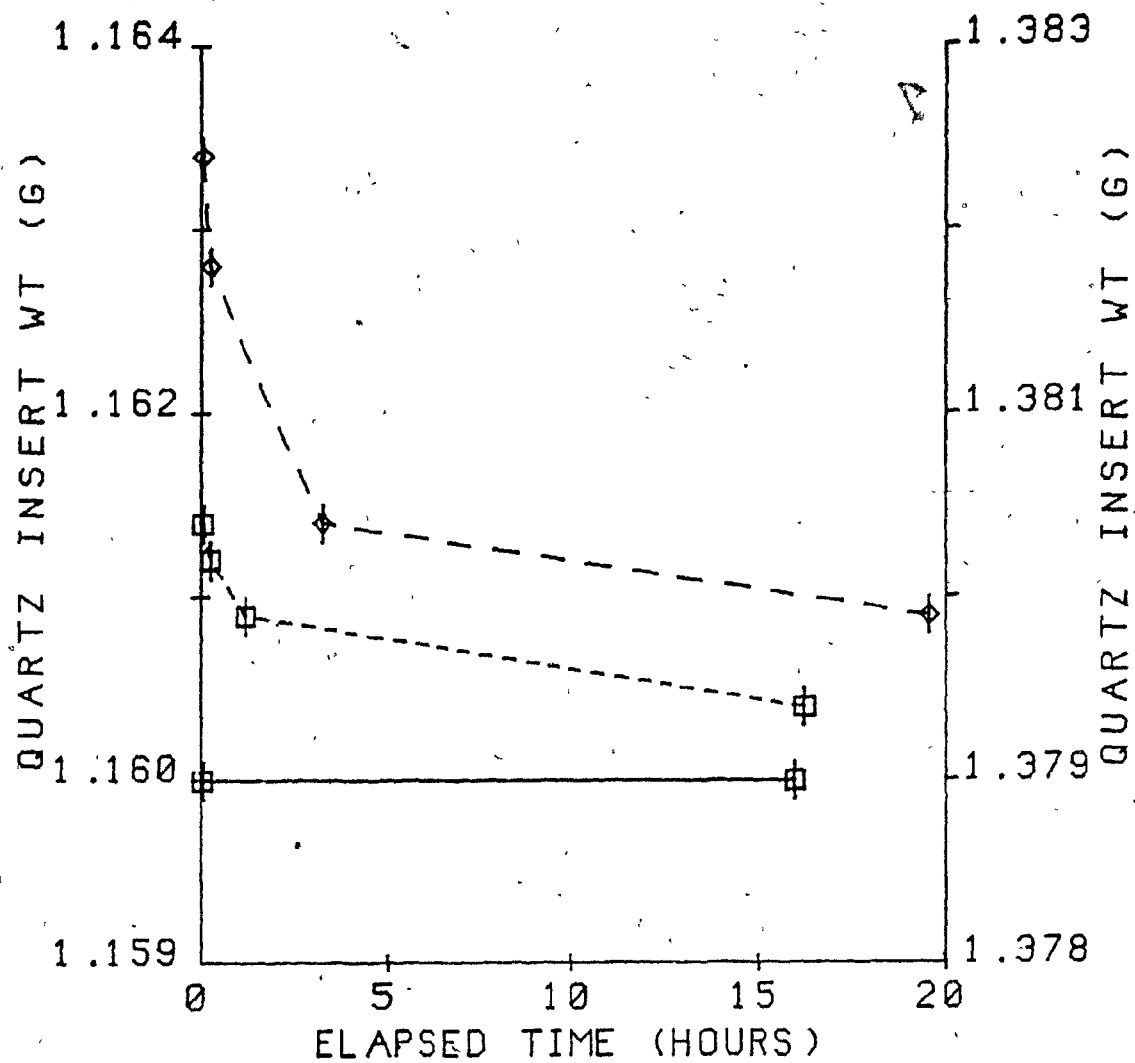
Hydrogen volatilized measurable amounts of lead from quartz inserts (lead coated quartz tubes) heated at $900^\circ C$ under hydrogen (Fig. 18). An insert, used as a control, lost no measurable weight after 16 h at $900^\circ C$ under air (Fig. 18), showing that lead was not volatilized under oxidizing conditions.

Lead oxides formed under an air atmosphere were reduced and volatilized under H_2 in the furnace, as seen in the Et_4Pb deposition/revolatilization study (Figs. 17B and 17C). A lead oxide coated insert lost weight over the entire heating period at $900^\circ C$ under H_2 (Fig. 18). The lead oxide coating was rapidly reduced (<15 min) to lead metal.

Absorbance signal saturation occurred at both 217 and 283.3 nm when the inserts were heated above $500^\circ C$ under H_2 , similar to the dependence of organolead peak area response on furnace temperature determined earlier (Fig. 14). A lead oxide deposit formed on the detector casing above the quartz tube opening in which the inserts were placed providing visual confirmation that lead was being removed from the quartz surface and transported out the upper quartz tube opening.

Several studies (Dedina and Rubeska 1980, Welz and Melcher 1983) found that low levels of oxygen in H_2 enhanced system response to various hydride forming elements. However, in the present study, air or nitrogen in hydrogen furnace makeup gas mixtures were generally detrimental to organolead response in the quartz T-tube furnace. The effects were dependent on the furnace temperature. At $900^\circ C$, the optimum peak area response occurred with pure H_2 .

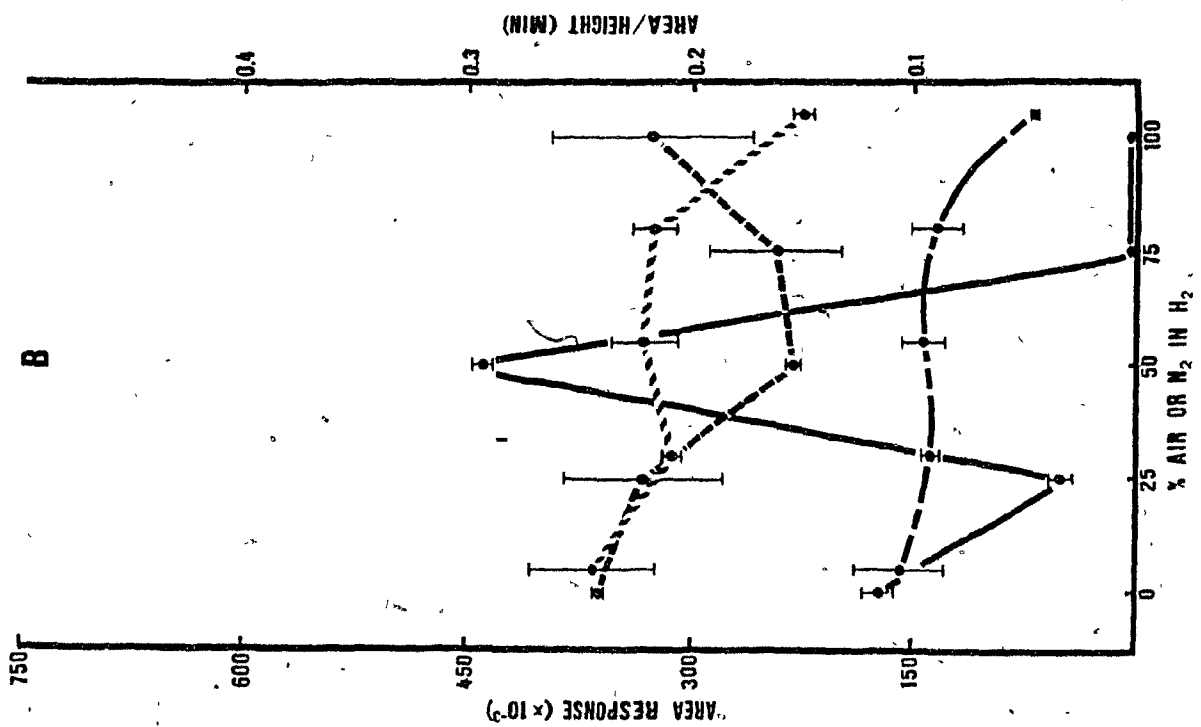
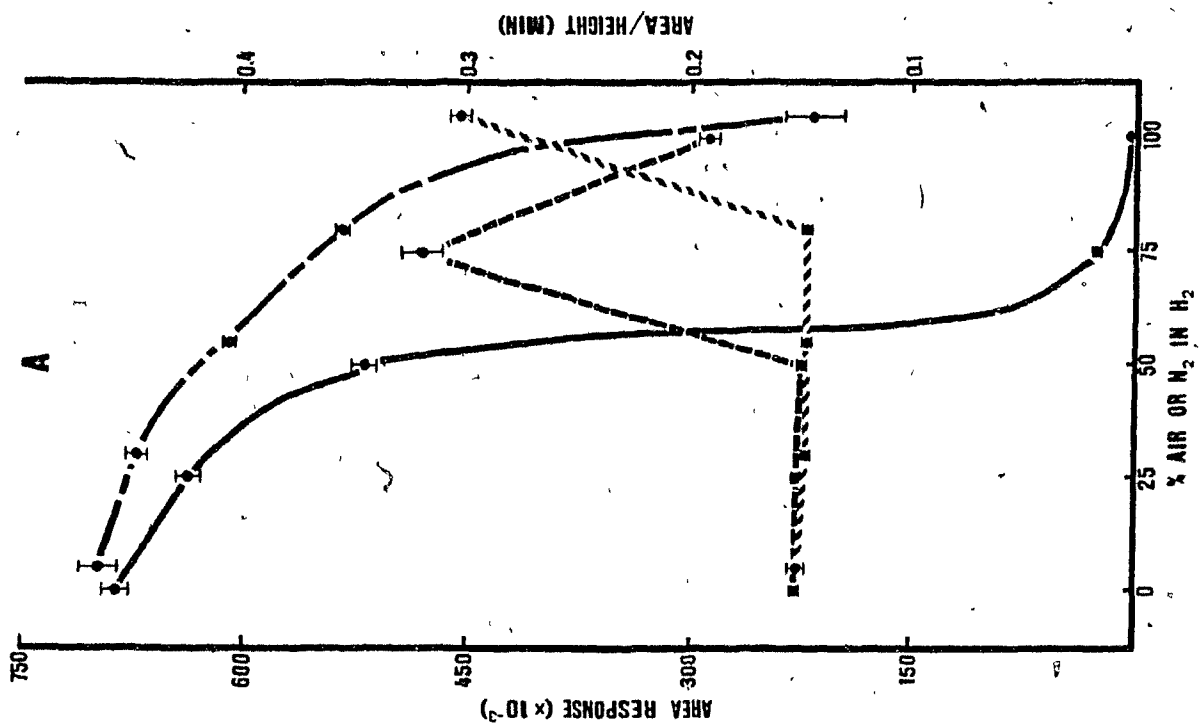
Figure 18. Weight loss of lead coated quartz inserts during heating at 900°C. —□—, under air; --□--, under H₂ (weight read from left Y axis); —◇—, under H₂ (weight read from right Y axis). Error bars represent the absolute uncertainty of single weighings on a standard analytical balance.



Peak area response decreased as the percentage of air or N_2 in H_2 increased, until reaching pure air or N_2 peak area response values (Fig. 19A). However, with a furnace temperature of $600^\circ C$, a 50% air/ H_2 mixture produced a 250% increase in response relative to pure hydrogen, whereas a 50% N_2/H_2 mixture caused a 10% reduction in response (Fig. 19B). The response enhancement may be caused by H radicals formed by the same reactions with oxygen proposed by Dedina and Rubeska (1980) for a fuel rich hydrogen-oxygen flame. The response enhancement occurred at $600^\circ C$ because the H radical concentration was insufficient for optimum lead atomization; increased H radical formation from the small flame inside the quartz furnace increased the H radical concentration, enhancing lead atomization and thus peak area response. At $900^\circ C$, no response enhancement occurred as a sufficient H radical concentration existed under pure H_2 . Nitrogen/ H_2 mixtures caused less severe response suppression, suggesting that the oxygen component of the air/ H_2 mixtures caused the increased suppression of peak area response. The nitrogen and oxygen likely interferes with the hydrogen radical mediated atomization of the organoleads by scavenging H radicals or forming less volatile products with lead.

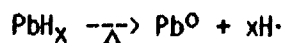
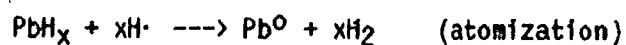
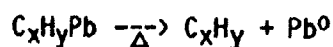
Experimental evidence suggests that a hydrogen radical mediated atomization of lead occurs in the quartz furnace. The small changes in peak area response to changes in furnace temperature above $800^\circ C$ suggested that an excess of H radicals existed at these temperatures, yet the operating temperature of the furnace was too low to produce any appreciable gas phase dissociation of H_2 molecules. Quartz has a strong catalytic effect at temperatures near $1000^\circ C$ (Welz and Melcher 1983) and was likely catalyzing H radical formation. Unsaturated oxygen atoms on the quartz surface may bind

Figure 19. Response of peak area (—●— , air; —●— , N₂) and area/height ratio(—■— , air, —■— , N₂) to changes in the percentage of air or nitrogen in the furnace makeup gas with 3.07 ng (as Pb) Me₃BuPb. The furnace was maintained at 900°C (A) or 600°C (B). Error bars represent \pm one standard deviation of three replicate determinations.



molecular hydrogen, resulting in surface hydroxyls and H radicals.

Since pyrolysis of organoleads at 900°C under an inert (helium) atmosphere produced virtually no atomization, the hydrogen radicals are necessary to (a) maintain a volatile lead population in the resonance radiation pathway and (b) mediate lead atomization:



The lead hydrides, although not characterized, are likely PbH_2 and/or PbH_4 .

6. ORGANOLEAD EGG INTERACTION

6.1 Introduction

Interaction with components of biological tissues reduces alkyllead extraction efficiency. Diethyllead, but not Et_3Pb^+ had an affinity for thiol compounds (Cremer 1959). Bolanowska (1968) found that some Et_3Pb^+ (4.3%) and $\text{Et}_2\text{Pb}^{2+}$ (7.3%) was removed from tissue homogenates with the protein fraction. Triethyllead chloride was bound to the globin moiety of rat hemoglobin, but had little affinity for human hemoglobin (Byington et al. 1980).

Forsyth and Marshall (1983) found that recoveries of alkyllead salts were lowered in the presence of egg homogenate. Enzymatic hydrolysis of the egg homogenate with a mixture of lipase and protease increased alkyllead salt recoveries, suggesting a reversible organolead binding to undetermined egg components.

Liquid whole egg consists of 64% egg albumin and 36% yolk (Parkinson 1966) which differ substantially in composition. Egg albumin has low lipid (0.02%) and inorganic ion (0.5%) content and consists primarily of water (88.5%) and proteins (10.5%), many of which are glycoproteins (Osuga and Feeney 1977). A major protein component (12%) of egg albumin is ovotransferrin, a typical transferrin capable of binding metallic cations. Ovotransferrin can tightly bind ($K_D=10^{-29}$ M) two Fe^{3+} per molecule (Aisen et al. 1970).

Egg yolk has a higher lipid (33.7%) and inorganic ion (1.1%) content than egg albumin (Powerie 1973). Most of the lipid is associated with protein (Parkinson 1966). Egg yolk proteins are composed of a number of conjugated proteins; glycoproteins, phosphoglycoproteins, lipoproteins and

phospholipoproteins (Osuga and Feeney 1977).

The purpose of this study was to determine if organolead egg binding was associated with a specific egg component; egg albumin, yolk or the transferrin protein, ovotransferrin. Ferric ion was to be tested for its capacity to dislodge bound organolead from egg homogenate and ovotransferrin.

6.2 Materials and Methods

Solvents were distilled in glass grade (Caledon Laboratories Ltd.) and inorganic reagents were ACS grade or better. The ammoniacal buffer consisted of diammonium citrate (9.04 g), potassium cyanide (1.6 g) and sodium sulfite (9.6 g) made up to 100 mL with double distilled water. The pH (10.0) was adjusted with concentrated ammonium hydroxide. Double distilled water was prepared as previously described (Section 3.2).

Whole egg homogenate (minus shell) was prepared from freshly laid eggs (obtained from the Poultry Unit at Macdonald College) using a Polytron homogenizer (Brinkmann Instruments). The egg homogenate was stored at 4°C. Egg yolk and albumin were separated with a commercial yolk separator. The yolk was gently rolled on a premoistened paper towel to remove residual albumin. Egg albumin was homogenized using a Polytron homogenizer, whereas the egg yolk was stirred with a glass rod until homogenous. Both egg components were stored at 4°C.

6.2.1 Analytical Methods.

Each egg component sample (egg homogenate, yolk, ovotransferrin) was made up to 49.5 mL with 0.1 M phosphate buffer (pH 7.5). An aqueous alkyllead solution (0.5 mL) containing the four ionic alkyllead standards (each 30-50 µg

as Pb) was added and the mixture immediately transferred to an Amicon Model 52 ultrafiltration cell (Amicon Corp.) fitted with a YM-10 membrane (Amicon Corp.), which has an exclusion limit of 10,000 daltons. The mixture was stirred slowly by magnetic stirrer in the ultrafiltration cell. The cell was pressurized to 55 psi (380 kPa) with N₂ and ultrafiltrate fractions collected at 0, 1, 6 and 24 h for recovery controls and egg homogenate and at 0 and 1 h only for the other treatments. The first milliliter of each 8 mL fraction was discarded and three 2 mL samples taken from the remaining ultrafiltrate. Ultrafiltration and fraction collections were performed at 40°C.

Ammoniacal buffer (0.2 mL) and 1 mL of 0.05% (w/v) dithizone in benzene were added to each 2 mL ultrafiltrate sample. The mixture was shaken by mechanical shaker in a 10 mL screw cap centrifuge tube for 5 min and then centrifuged (1550 rpm, Precision Clinical Centrifuge, Precision Sci. Co.) for several minutes. Double distilled water (4 mL) was added and the sample was centrifuged (1550 rpm) for several minutes. A 0.5 mL aliquot of the benzene layer was removed for derivatization. Anhydrous HPLC grade THF (2 mL) (Caledon Laboratories Ltd.) was added to the benzene extract of alkyllead dithizonates in a 15 mL calibrated centrifuge tube. Butylmagnesium chloride (0.5 mL, 2.27 M, Alfa Products, Ventron Corp.) was added under N₂ and the tube was sealed with a teflon lined screw cap. Each tube was vortexed (Vortex Genie, Fisher Sci Co.) for 20 s, and then magnetically stirred for 10 min at room temperature. The samples were cooled in ice water, diluted with 3 mL hexane, recooled, and excess Grignard reagent was destroyed by dropwise addition of 0.5 mL water. The samples were then recooled and made up to 13 mL with double distilled water. The hexane was removed after the mixture had been shaken (0.5 min) and then centrifuged. Two additional extractions with hexane (3 mL) were

performed. The combined hexane extracts were back extracted once with double distilled water (5 mL), diluted to 15 mL with hexane and dried over anhydrous sodium sulfate.

All analyses were performed with the GC-AAS system using normal operating conditions (Section 5.2.1).

6.2.2 Organolead Egg Interaction Studies

The organolead egg component interaction studies consisted of the following treatments:

(a) recovery controls--No egg component was added to the phosphate buffer.

(b) egg homogenate--Egg homogenate (2.00 g) was added to the phosphate buffer.

(c) egg albumin--Egg albumin (1.28 g, 64% of the 2.00 g whole egg homogenate weight, corresponding to percentage composition of whole egg) was added to the phosphate buffer.

(d) egg yolk--Yolk (0.72 g, 36% of the 2.00 g whole egg homogenate weight, corresponding to percentage composition of whole egg) was added to the phosphate buffer.

(e) ovotransferrin--Type IV (iron free) Conalbumin (Sigma Chemical Co.) (20 mg) was added to the phosphate buffer.

(f) Fe^{3+} + egg homogenate-- Fe^{3+} (31 μg as ferric ammonium sulfate) was added to the organolead-egg homogenate-phosphate buffer mixture after 1 min of

stirring in the ultrafiltration cell.

(g) Fe^{3+} + ovotransferrin-- Fe^{3+} (31 μg as ferric ammonium sulfate) was added to the organolead-ovotransferrin (20 mg)-phosphate buffer mixture after 1 min of stirring in the ultrafiltration cell.

(h) ultrafiltration control--A 0 h ultrafiltration fraction from unspiked egg homogenate was spiked with ionic alkyllead to produce a concentration equivalent to the organolead concentration in the ultrafiltration cell. Four 2 mL samples were taken and extracted as previously described.

The percentage recovery of each organolead analyte was determined by dividing the mean peak area response of the recovered butylate by the mean peak area response of the butylates in "recovery standards". Four replicate "recovery standards" were made from an appropriate amount of butylated organolead spiking solution diluted to the expected (assuming 100% recovery) recovery sample concentration.

Analysis of variance and Duncan's multiple range tests were performed on the analyte recoveries. The percentage recoveries were arcsine transformed prior to statistical analysis.

6.3 Results and Discussion

The interaction of ionic alkylleads with egg components was rapid. Initial studies with egg homogenate showed that analyte recoveries from the 24 h ultrafiltrate fraction were no less than recoveries from the 0 h ultrafiltrate fraction. However, collection of both the 0 and 1 h ultrafiltrate fractions were continued to monitor possible time dependent reductions of analyte recoveries during all experimental treatments. Analyte

recoveries less than those obtained from the recovery controls (buffer only) were assumed to be caused by interaction of the organoleads with the egg component.

The variances of the analyte recoveries at 0 and 1 h were not significantly different ($p=0.05$, f -test); therefore the data were pooled for analysis of variance (Appendices J and K) and Duncan's multiple range test. As percentages or proportions form a binomial rather than a normal distribution (Zar 1974), an arcsine transformation of the percentage recoveries was used to normalize the data prior to statistical analysis.

The alkylleads interacted more with egg homogenate/yolk than the other egg components. Alkyllead recoveries from egg homogenate were significantly less ($p=0.05$, Duncan's multiple range test) than from other egg components (except egg yolk) and the recovery controls (Table 12). The components of egg homogenate involved with alkyllead interaction have molecular weights exceeding 10,000 daltons, as the recoveries of alkylleads added to ultrafiltrate (collected from egg homogenate) were not significantly less ($p=0.05$, t -test) than the recovery controls.

The egg albumin lowered alkyllead recoveries significantly more than the recovery control or ovotransferrin treatments ($p=0.05$, Duncan's multiple range test), but significantly less than the egg homogenate (Table 12). The amount of egg albumin (1.28 g) used in the binding studies was equivalent to that in the whole egg homogenate, allowing direct comparison of alkyllead recoveries. Egg albumin, therefore contains some, but not the majority of binding sites in the whole egg homogenate.

Table 12. Effect of egg components on alkyllead recoveries

Alkyllead ⁱ	Cont. ⁱⁱ	Egg Homo.	Egg Album.	Egg Yolk	OT ⁱⁱⁱ	Fe ³⁺ +Egg Homo.	Fe ³⁺ +OT
-----Mean ^{iv} Percentage Recovery ^v , vi _{SD} -----							
Me ₃ Pb ⁺⁺⁺	95+7a	75+4d	88+5c	76+3d	90+2bc	74+3d	93+3ab
Me ₂ Pb ²⁺⁺⁺	100+5a	59+6d	81+3c	58+3d	92+3b	59+3d	94+3b
Et ₃ Pb ⁺⁺⁺	89+5a	36+4d	78+3c	32+3e	85+2b	36+3d	88+4ab
Et ₂ Pb ²⁺⁺⁺	93+7a	45+8d	77+6c	45+2d	87+2b	49+7d	90+9ab

i- F-test **= 0.01 significance

ii- Recovery from buffer in the absence of egg component

iii- Ovotransferrin

iv- Mean of 6 replicates at time 0 and 6 replicates at time 1 h

v- % Recovery= (peak area of recovered ionic alkyllead
(as alkylbutyllead)/peak area of alkyllead butylates in
recovery "standards") * 100

vi- Means with the same letter in each row are not significantly
different (p=0.05, Duncan's multiple range test)

Egg yolk has the majority of binding sites in the whole egg homogenate. Alkyllead recoveries from egg yolk (Table 12) were either not significantly different ($p=0.05$, Duncan's multiple range test) or in the case of Et_3Pb^+ , significantly less than from egg homogenate. The amount of egg yolk (0.72 g) used in the binding studies was equivalent to that in the whole egg homogenate, allowing direct comparison of alkyllead recoveries.

Triethyllead binds to myelin (Lock and Aldridge 1975) and interacts with cellular membranes (Aldridge 1978) which both contain phospholipids associated with proteins (Konat and Clausen 1974, Lehninger 1975). Egg yolk contains lipo- and phospholipoproteins (Osuga and Feeney 1977), whereas egg albumin has virtually none. The lowest alkyllead recovery (32%) occurred with the least polar alkyllead (Et_3Pb^+) in egg yolk, the egg component containing the most lipid. These results suggest that alkyllead (particularly ethylleads) interaction with egg yolk (or whole egg homogenate) is with the lipo- and phospholipoproteins.

Alkyllead recoveries from ovotransferrin were generally significantly more ($p=0.05$, Duncan's multiple range test) than from egg albumin (Table 12), although there was no significant difference between Me_3Pb^+ recoveries from ovotransferrin and egg albumin (Table 12). Alkyllead recoveries from ovotransferrin were, however, significantly less than the recovery controls (Table 12), indicating that ovotransferrin caused some, but not all of the observed alkyllead interaction with egg albumin.

The addition of ferric ion to egg homogenate or ovotransferrin (Table 12) did not significantly increase ($p=0.05$, Duncan's multiple range test) alkyllead recoveries, although all four analyte recoveries from Fe^{3+} + ovotransferrin

were greater than from ovotransferrin alone (Table 12), suggesting that some alkyllead may have been displaced by the ferric ion.

Alkyllead recoveries were significantly different ($p=0.05$, Duncan's multiple range test) within most of the egg components (Table 13). Trimethyllead recoveries were significantly greater than all the other analytes in all egg component treatments in which there were significant differences among the analytes (Table 13). Dimethyllead recoveries were generally significantly greater than either of the ethyllead salts (Table 13). The methyllead compounds therefore, interacted less with the various egg components than the ethyllead compounds. Triethyllead recoveries were generally significantly less than the other analytes (Table 13), although $\text{Et}_2\text{Pb}^{2+}$ recovery from egg albumin was significantly less than the Et_3Pb^+ recovery (Table 13).

In summary it may be concluded that all the tested egg components interact with the alkylleads and lower recoveries. The alkyllead interaction with whole egg homogenate is primarily from the yolk component, although egg albumin did interact with the alkylleads as well. Ovotransferrin lowered alkyllead recoveries less than egg albumin, suggesting that additional binding sites are present in the egg albumin. Methyllead salts interacted less with egg components than the ethyllead compounds. Alkyllead binding is likely associated with the lipid content of the egg yolk. Ferric ion addition did not displace significant amounts of alkylleads from egg homogenate or ovotransferrin binding sites. These results reflect the interaction of egg components with 15-25 ppm (as Pb) of each alkyllead present. However, the interaction behaviour of the egg components may vary with the alkyllead levels.

Table 13. Effect of analyte on alkyllead recoveries from egg components

Egg Component ⁱ	Me ₃ Pb ⁺	Me ₂ Pb ²⁺	Et ₃ Pb ⁺	Et ₂ Pb ²⁺
---Mean ⁱⁱ Percentage Recovery ⁱⁱⁱ , 1v _{SD} ---				
Egg homogenate ^{**}	79 _{4a}	59 _{6b}	41 _{4d}	48 _{8c}
Egg albumin ^{**}	93 _{5a}	81 _{3c}	87 _{3b}	83 _{6c}
Egg yolk ^{**}	80 _{3a}	58 _{3b}	35 _{4d}	48 _{2c}
Ovotransferrin ^{ns}	95 _{2a}	92 _{3a}	95 _{3a}	93 _{3a}
Fe ³⁺ + Egg homogenate ^{**}	78 _{3a}	59 _{3b}	41 _{4d}	53 _{7c}
Fe ³⁺ + Ovotransferrin ^{ns}	98 _{3a}	95 _{4a}	98 _{4a}	97 _{10a}

i- F-test

**- 0.01 significance
 ns- not significant

Note: F-test takes precedence
 over Duncan's multiple
 test

ii- mean of 6 replicates at time 0 and 6 replicates at time 1 h

iii- % Recovery= (% recovery from egg component/% recovery
 from buffer in the absence of egg component) * 100

iv- means with the same letter in each row are not significantly
 different (p=0.05, Duncan's multiple range test)

7. ENVIRONMENTAL SAMPLE ANALYSIS

7.1 Introduction

Organolead compounds are ubiquitous in the environment (Table 14) and have been isolated from rain water (Chakraborti et al. 1984), air (Table 1), fish (Sirota and Uthe 1977, Chau et al. 1979, 1980, 1984, Cruz et al. 1980) and human brains (Nielsen et al. 1978). Lake or river sediment (Cruz et al. 1980, Chau et al. 1984) and macrophytes (Chau et al. 1984) also contain organolead compounds (Table 14).

Organolead compounds can bioaccumulate in the environment. Organolead concentrations in organisms exceed the levels found in rain water (Table 14). Fish rapidly accumulate up to 700 times the Me_4Pb concentration of the surrounding water (Wong et al. 1981).

Avian populations contain organolead compounds which can produce lethal and sublethal effects. Pigeon populations contained ionic alkyllead compounds (Johnson et al. 1982). Ionic alkyllead compounds were found in dead and dying waders, wildfowl and gulls (Bull et al. 1983). An avian toxicity study found that lethal dosages of trialkylleads produced behavioural and morphological symptoms similar to the birds collected by Bull et al. (1983) (Osborn et al. 1983). Sublethal dosages of Me_3Pb^+ reduced protein reserves (muscle mass loss) and altered organ weights, whereas both Me_3Pb^+ and Et_3Pb^+ sublethal dosages altered feeding behaviour (Osborn et al. 1983).

Canadian avian populations have not been previously studied for the presence of organolead compounds. The herring gull (Larus argentatus) is used as the monitor species for toxic contaminants in the Great Lakes by Environment

Table 14. Concentrations of organolead compounds in environmental samples

Sample, Location	-----Organolead Compound-----			Reference
	R ₃ Pb ⁺	R ₂ Pb ²⁺	R ₄ Pb	
--Range(Mean±SD) ng Pb/g wet wt--				
Rain water, Antwerp, Belgium	N.D.-0.047 ⁱ	N.D.-0.068 ⁱ	- ⁱⁱ	Chakraborti et al. (1984)
River sediment	N.D.-660	N.D.-275	N.D.-1152	Chau et al. (1984)
Macrophytes	132-558	N.D.-113	68-16515	
Carp	906-2735	362-707	137-780	
Pike, St. Lawrence River Near Maitland Ont.	N.D.-215	N.D.	169-1018	
Fish, Ont. Lakes	-	-	3-16	Cruz et. al. (1980)
Cod	-	-	10-125	Sirota and Uthe (1977)
Mackerel	-	-	(54±0.5)	
Lobster, Halifax, N.S.	-	-	(162±0.4)	
Human brain Copenhagen, Denmark	N.D.-50	-	-	Nielsen et al. (1978)
Pigeon, Liverpool U.K.	N.D.-310 ⁱ	N.D.	N.D.	Johnson et al. (1982)
Wildfowl Mersey Estuary, U.K.	(550±260) ⁱⁱⁱ	-	-	Bull et al. (1983)

i- ng Organolead Compound/g wet wt

ii- not analyzed

iii- R₃Pb⁺ and R₂Pb²⁺

N.D.- Not detected

Canada. The herring gull is a top predator in the food web of the Great Lakes region. Although the herring gull is an opportunistic feeder, with a varied diet including insects, birds, small mammals and refuse, fish are the primary diet item (Mineau et al. 1984). Great Lakes adult breeding populations tend to remain in the region of the colony and are therefore considered a valuable environmental contamination indicator of the region near the colony (Gilbertson 1975).

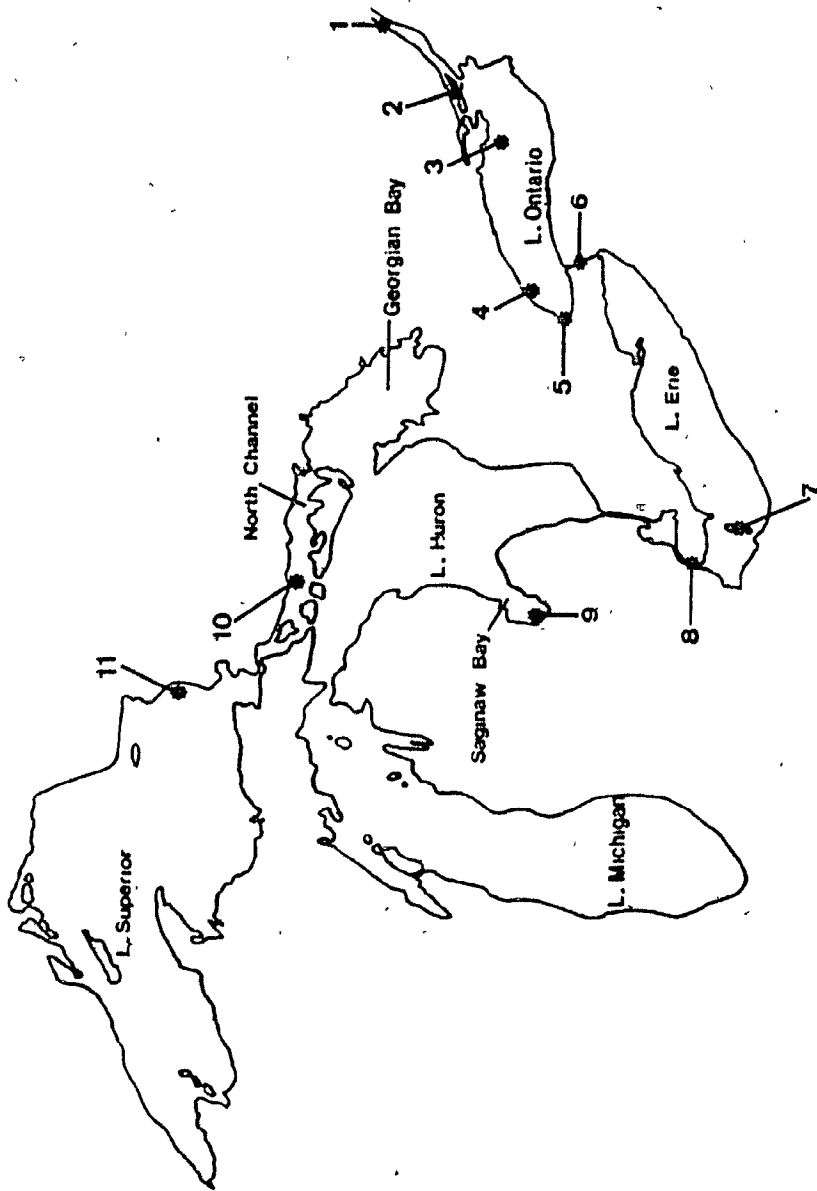
The mallard duck (Anas platyrhynchos) is the most abundant and widely distributed duck species in the Northern Hemisphere, making it a suitable monitor species for organolead contaminants in wildfowl populations. The mallard is primarily a herbivorous surface feeder which migrates annually (Bellrose 1976).

The purpose of this study was to determine the relative ionic alkyllead levels in various regions of the Great Lakes by analyzing herring gull tissue sampled from different herring gull breeding colonies in the Great Lakes. Analysis of mallard duck tissue provided estimates of wildfowl alkyllead tissue burdens.

7.2 Materials and Methods

Herring gull (Larus argentatus) and mallard (Anas platyrhynchos) tissues were sampled from various collection sites (Fig. 20) by the Canadian Wildlife Service. Further sample collection data are given in Appendix L. The tissue samples were received frozen and were stored at -20°C until analysis. The samples were thawed at room temperature, thoroughly mixed and then subsampled (2.50 g) for each determination. Subsamples were immediately analyzed using the optimized hydrolysis (Section 4.2.1) and recovery (Section 4.2.2).

Figure 20. Map of the Great Lakes region indicating the location of the herring gull colonies and mallard duck sampling sites used in this study as follows: 1, Upper Canada Migratory Bird Sanctuary; 2, Snake Island; 3, Scotch Bonnet Island; 4, Muggs Island; 5, Hamilton Harbour; 6, Niagara River; 7, Middle Island; 8, Fighting Island; 9, Channel Shelter Islands; 10, Double Island; 11, Agawa Rocks.



methodologies previously described.

The GC-AAS system was used with the optimized operating parameters (Section 5.2.1) and deuterium lamp background correction. Seven analytes were determined in each sample (four trialkyllead and three dialkyllead compounds). Each butylated extract was quantitated three times. The reported standard deviations estimate variability associated only with quantitation.

External standards containing Me_3BuPb , $\text{Me}_2\text{Bu}_2\text{Pb}$, Et_3BuPb and $\text{Et}_2\text{Bu}_2\text{Pb}$ were injected after every four environmental sample analyses to calibrate the GC-AAS system. Environmental sample quantitation was by linear interpolation between calibration (organolead standard peak area response) points. Methyl ethyllead compounds were identified by prediction of retention time using Kovats retention index (Table 15) developed from retention times of alkylbutyllead standards. Actual retention times of methyl ethyllead compounds were determined from transalkylation reaction products (Appendix M). Quantitation of the methyl ethyllead compounds was by comparison with a similar analyte for which standards were available; quantitation for Me_2EtPb^+ was based on peak area response and recoveries for Me_3Pb^+ . A sample calculation for a gull kidney sample appears in Appendix N.

To prevent spurious or non-Pb containing peaks from being identified as an organolead analyte, the following precautions were taken: (a) the deuterium lamp background correction was used during all analyses, (b) results were rejected if the GC retention time of an AAS absorbance was variable or if the signal was not integrated by the recording integrator during one or more of the three quantitations, and (c) some butylated extracts were analyzed at 217 nm and 283.3 nm (Fig. 21) to verify the GC-AAS selectivity for lead containing

Table 15. Absolute retention times and retention indices of mixed methylethylleads (based on retention times) relative to alkylbutyllead standards

Analyte	N	Absolute Retention Time (RT) (min)	Retention ⁱ Index (I)
Me ₃ BuPb	7	9.21	700
Me ₂ EtBuPb	8	11.22	800(805) ⁱⁱ
MeEt ₂ BuPb	9	13.04	900(906) ⁱⁱ
Me ₂ Bu ₂ Pb	10	14.23	1000
Et ₃ BuPb	10	14.65	1000
EtMeBu ₂ Pb	11	15.77	1100(1090) ⁱⁱ
Et ₂ Bu ₂ Pb	12	17.15	1200
Bu ₄ Pb	16	21.09	1600

ⁱ- predicted retention index (Kovats 1965)

ⁱⁱ- $I = 100N + 100n[(RT(A) - RT_R(N)) / (RT_R(N+n) - RT_R(N))]$

N- number of carbons in analyte

n- carbon number difference between R(N) and R(N+n)

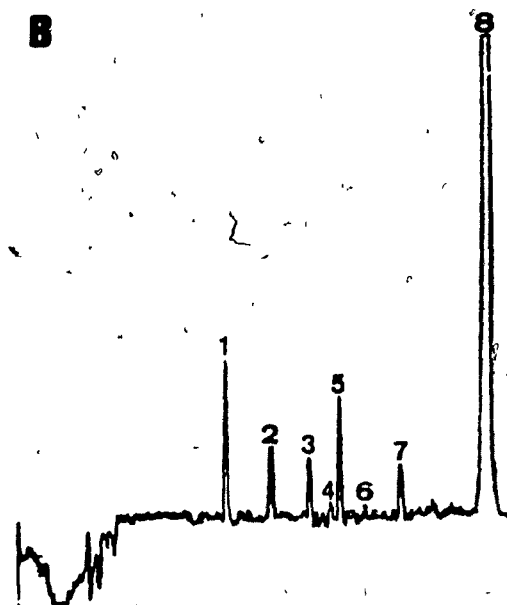
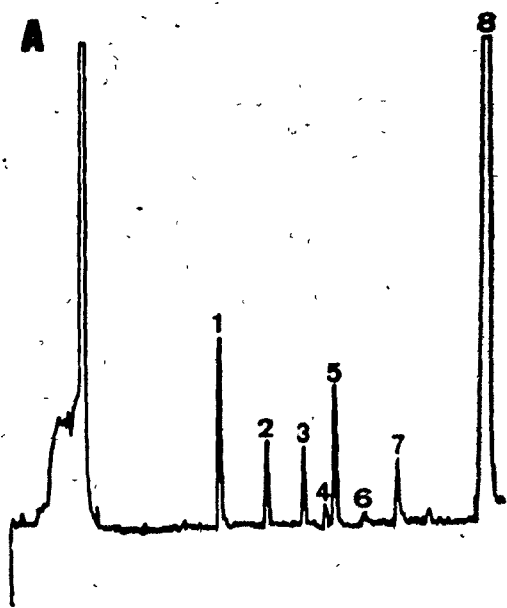
A- analyte for which retention index was calculated

R(N)- analyte containing N carbons

R(N+n)- analyte containing (N+n) carbons

Figure 21. GC-AAS chromatogram of male mallard kidney pool sample at: (A) 217 nm and (B) 283.3 nm containing 1, Me₃BuPb; 2, Me₂EtBuPb; 3, MeEt₂BuPb; 4, Me₂Bu₂Pb; 5, Et₃BuPb; 6, MeEtBu₂Pb; 7, Et₂Bu₂Pb and 8, Bu₄Pb. The sample was concentrated approximately two fold prior to analysis at 283.3 nm.

5



compounds.

Analysis of variance and Duncan's multiple range tests were performed on gull tissue analyte levels. Pearson correlation coefficients were determined between various gull tissue analytes.

7.3 Results and Discussion

Regional trends in alkyllead concentration occurred in the herring gull samples (Table 16). The methyllead concentration trend; Lake Ontario > Lake Huron < Lake Erie > Lake Superior was opposite to the ethyllead concentration trend; Lake Superior > Lake Huron > Lake Erie < Lake Ontario. Analysis of variance (Appendix 0) found significant differences in the regional trends (Table 17). Trimethyllead levels in kidney samples from Hamilton Harbour were significantly greater ($p=0.05$, Duncan's multiple range test) than the other collected tissues. Liver samples from Agawa Rock, Double Island, Middle Island and Agawa Rock kidney samples had significantly less ($p=0.05$, Duncan's multiple range test) Me_3Pb^+ than the other tissues (Table 17). Similarly, $\text{Me}_2\text{Pb}^{2+}$ levels in kidney tissue from Hamilton Harbour gulls were significantly greater ($p=0.05$, Duncan's multiple range test) than $\text{Me}_2\text{Pb}^{2+}$ levels from other sites. Liver samples from Double Island gulls had significantly less ($p=0.05$, Duncan's multiple range test) $\text{Me}_2\text{Pb}^{2+}$ than the other tissue samples (Table 17). Triethyllead levels, however, were significantly greater ($p=0.05$, Duncan's multiple range test) in gull kidney samples collected from Agawa Rock than in other gull tissues. The diethyllead levels were not significantly different ($p=0.05$, Duncan's multiple range test) among collected tissue (Table 17).

The herring gull does not appear to bioaccumulate ionic alkylleads as mature and immature bird analyte levels were not significantly different

Table 16. Ionic alkyllead levels (as alkylbutylleads) in herring gull liver and kidney samples collected from various Great Lakes colonies

Source	-----Me ₃ Pb ⁺ -----		-----Me ₂ EtPb ⁺ -----		-----Me ₂ Pb ²⁺ -----		-----Et ₃ Pb ⁺ -----		-----Et ₂ Pb ²⁺ -----	
	Liver	Kidney	Liver	Kidney	Liver	Kidney	Liver	Kidney	Liver	Kidney
Lake Superior	-----Mean ⁱ Alkyllead ⁱⁱ Concentration ⁱⁱⁱ SD (ng/g wet wt)-----									
Agawa Rocks										
Mature	2.3±0.1	4.5±0.2	N.D.	N.D.	1.7±0.3	1.2±0.5	7.3±0.2	8.8±0.4	2.2±0.6	1.6±0.2
Immature	1.3±0.1	2.3±0.1	N.D.	N.D.	1.6±0.4	1.4±1.1	2.2±0.3	6.3±0.6	0.8±0.1	1.4±0.2
Lake Huron										
Double Island										
Mature	3.0±0.1	5.5±0.3	N.D.	N.D.	N.D.	2.4±0.2	3.1±0.4	4.5±0.1	0.9±0.3	0.8±0.3
Immature	3.3±0.1	5.5±0.3	N.D.	N.D.	1.8±0.6	3.0±0.5	1.1±0.1	2.5±0.1	0.3±0.1	N.D.
Lake Erie										
Middle Island										
Mature	3.5±0.1	4.5±0.3	N.D.	0.3±0.1	2.6±0.3	2.0±0.3	1.2±0.1	1.0±0.1	0.3±0.2	0.4±0.2
Immature	1.7±0.3	4.3±0.1	0.3±0.2	0.6±0.1	1.6±0.4	1.9±0.4	0.8±0.1	1.1±0.1	0.4±0.2	N.D.
Lake Ontario										
Hamilton Harbour										
Mature	7.9±0.1	15.3±0.1	0.3±0.1	0.6±0.1	3.2±0.3	4.4±1.0	0.8±0.1	0.8±0.1	0.8±0.1	0.6±0.2
Immature	6.7±0.1	18.7±1.1	0.4±0.1	1.2±0.1	4.2±0.9	5.8±0.3	0.9±0.1	1.6±0.1	N.D.	N.D.

i- calculated from three replicate injections into the gas chromatograph

ii- no MeEtPb²⁺ was detected in any of the samples and Et₂MePb⁺ was detected in only one sample (0.3±0.1 ng/g, immature, Hamilton Harbour)

iii- corrected for recovery

N.D.- not detected

Table 17. Effect on gull tissue ionic alkyllead levels
(as alkylbutylleads) by sampling site.

Analyte ⁱ	-----Site-----							
	-Hamilton Har.-		--Agawa Rock--		--Double I.--		--Middle I.--	
	-----Tissue-----							
	Liver	Kidney	Liver	Kidney	Liver	kidney	Liver	Kidney
	-----Mean ^{ii,iii} Concentration ^{iv} (ng/g wet wt)-----							
Me ₃ Pb ⁺⁺⁺	7.3b	17.0a	1.8c	3.4c	3.2c	7.2b	2.6c	4.4bc
Me ₂ Pb ²⁺⁺⁺	3.7ab	5.1a	1.6cd	1.3cd	0.9d	2.7bc	2.1bcd	1.9cd
Et ₃ Pb ⁺⁺	0.9b	1.2b	4.8ab	7.6a	2.1b	3.5b	1.0b	1.1b
Et ₂ Pb ^{2+ns}	0.4a	0.3a	1.5a	1.5a	0.6a	0.4a	0.4a	0.2a.

ⁱ- F-test **- 0.01 significance
*- 0.05 significance
ns- not significant

Note: F-test takes precedence
over Duncan's multiple range
test.

ⁱⁱ- mature and immature values averaged

ⁱⁱⁱ- means with the same letter in each row are not significantly
different (0.05 level, Duncan's multiple range test)

^{iv}- corrected for recovery

($p=0.05$, paired comparison t-test, Appendix P) except $\text{Et}_2\text{Pb}^{2+}$ kidney levels, a data set containing several zero values. This indicates that the mature and immature bird alkyllead levels resulted from equilibration to environmental levels of alkyllead which were characteristic of the area surrounding the sampling site. The mature and immature bird analyte levels were therefore pooled for analysis of variance.

The presence of Me_3Pb^+ in all gull tissue samples was unexpected because Et_4Pb is the predominant organolead gasoline additive used in North America. Canadian leaded gasoline contains only Et_4Pb (Appendix Q, Chau et al. 1976, Radzuik et al. 1979), whereas American leaded gasoline contains either Et_4Pb or methylethyllead mixtures with Me_4Pb constituting a minor fraction of the total lead content (Robinson and Kiesel 1977, Robinson et al. 1977, DuPuis and Hill Jr. 1979, Estes et al. 1982). Domestic chickens (Gallus domesticus) also contained more methyllead than ethyllead (Table 18) indicating that the presence and ubiquitousness of Me_3Pb^+ was not limited to gulls in the Great Lakes region.

Although environmental or biological methylation of inorganic lead remains controversial (Section 2.1.2), it is a possible source of methyllead. Correlation (Pearson correlation coefficients) between alkyllead tissue concentrations of combined (mature and immature) birds and lake sediment lead levels (from Hodson et al. 1984) were generally significant ($p=0.01$, Table 19) for the methylleads, but not the ethylleads, indicating possible methylation, but not ethylation of inorganic lead. Trimethyllead levels in gull egg homogenate samples (Table 23) also correlated significantly ($r=0.86788$, $p=0.01$) with lake sediment lead levels (from Hodson et al. 1984). Host biomethylation of ingested inorganic lead, although unresearched, is also a possible

Table 18. Ionic alkyllead (as alkylbutyllead) levels in domestic chickens

Source	Analytes ⁱ			
	Me ₃ Pb ⁺	Me ₂ Pb ²⁺	Et ₃ Pb ⁺	Et ₂ Pb ²⁺
	-----Mean ⁱⁱ Concentration±SD (ng/g wet wt)-----			
Egg Homogenate	N.D.	N.D.	N.D.	0.6±0.6
Kidney	2.5±0.2	1.7±0.1	0.2±0.1	0.8±0.1
Brain	1.0±0.1	N.D.	N.D.	N.D.
Liver	1.8±0.1	0.7±0.1	0.2±0.3	0.3±0.3

ⁱ- no Me₂EtPb⁺, MeEt₂Pb⁺, or MeEtPb²⁺ was detected in any of the samples

ⁱⁱ- N=4 replicate determinations

N.D. - not detected

methyllead source.

The consumption of fish by herring gulls is a likely source of alkylleads as alkyllead compounds have been found in fish from the St. Lawrence River (Chau et al. 1984) and Me_4Pb rapidly accumulates in fish (Wong et al. 1981).

Avian alkyllead metabolism studies have not been reported although pigeon populations with measurable levels of tri- and dialkylleads did not contain tetraalkylleads (Johnson et al. 1982) suggesting rapid dealkylation of tetraalkylleads.

Correlation of the alkyllead levels in gull tissue also suggests that sequential dealkylation occurred. Trimethyllead and $\text{Me}_2\text{Pb}^{2+}$ levels in liver and kidney samples of combined (mature and immature) birds (Table 19) were significantly correlated ($p=0.05$, Pearson correlation coefficient). This correlation was independent of the tissue type or of the methyllead species. Triethyllead and $\text{Et}_2\text{Pb}^{2+}$ concentrations were similarly correlated (Table 19). Thus both the $\text{Me}_3\text{Pb}^+-\text{Me}_2\text{Pb}^{2+}$ and $\text{Et}_3\text{Pb}^+-\text{Et}_2\text{Pb}^{2+}$ levels were independent of the sampling site. However, there were no significant ($p=0.05$) correlations between any of the combinations of ethyllead levels with methyllead levels in any of the tissues. Similar trends, with fewer significant ($p=0.05$) correlations occurred when mature (Table 20) and immature (Table 21) bird tissue levels were examined separately. Sequential dealkylation of alkylleads would tend to produce correlated $\text{Me}_3\text{Pb}^+-\text{Me}_2\text{Pb}^{2+}$ and $\text{Et}_3\text{Pb}^+-\text{Et}_2\text{Pb}^{2+}$ body burdens. The absence of significant correlations between ethyl- and methyllead tissue levels suggests independent ethyl- and methyllead input sources to the gull populations.

Table 19. Correlations between alkyllead concentrations of gull tissue from combined birdⁱ
and lake sediment lead levelsⁱⁱ

	Me3Liver	Me3Kidney	Me2Liver	Me2Kidney	Et3Liver	Et3Kidney	Et2Liver	Et2Kidney
Me3Kidney Prob > r	0.93012 0.0008**							
Me2Liver Prob > r	0.73750 0.0368*	0.76956 0.0255*						
Me2Kidney Prob > r	0.89512 0.0027**	0.98128 0.0001**	0.72785 0.0407*					
Et3Liver Prob > r	-0.38201 0.3504	-0.39185 0.3370	-0.38704 0.3435	-0.50458 0.2022				
Et3Kidney Prob > r	-0.54102 0.1662	-0.49304 0.2144	-0.48147 0.2271	-0.56719 0.1426	0.89496 0.0027**			
Et2Liver Prob > r	-0.33288 0.4204	-0.42325 0.2961	-0.42332 0.2960	-0.55426 0.1540	0.93971 0.0005**	0.85025 0.0025**		
Et2Kidney Prob > r	-0.38403 0.3476	-0.48811 0.2198	-0.38222 0.3501	-0.56752 0.1423	0.77227 0.0247*	0.88009 0.0039**	0.84901 0.0077**	
PbSediment Prob > r	0.8984 0.0024**	0.9277 0.0009**	0.5081 0.1386	0.9348 0.0007**	-0.4226 0.2969	-0.4862 0.2218	-0.4123 0.3101	-0.4641 0.2467

i- N=8

ii- values taken from Hodson et al. 1984

*- 0.05 significance

** - 0.01 significance

Table 20. Correlations between alkyllead concentrations of gull tissue from mature birds¹

	Me3Liver	Me3Kid.	Me2Liver	Me2Kid.	Et3Liver	Et3Kid.	Et2Liver
Me3Kidney	0.98003						
Prob> r	0.0200*						
Me2Liver	0.65753	0.57426					
Prob> r	0.3425	0.4257					
Me2Kidney	0.96407	0.95437	0.44304				
Prob> r	0.0359*	0.0456*	0.5570				
Et3Liver	-0.67404	-0.53429	-0.41603	-0.71789			
Prob> r	0.3260	0.4657	0.5840	0.2821			
Et3Kidney	-0.68088	-0.53055	-0.52228	-0.68930	0.99078		
Prob> r	0.3191	0.4694	0.4777	0.3107	0.0092**		
Et2Liver	-0.43698	-0.27108	-0.28028	-0.49549	0.95848	0.94929	
Prob> r	0.5630	0.7289	0.7197	0.5045	0.0415*	0.0507	
Et2Kidney	-0.50572	-0.34437	-0.32986	-0.55736	0.97751	0.97002	0.99695
Prob> r	0.4943	0.6556	0.6701	0.4426	0.0225*	0.0300*	0.0031**

¹- N=4

** - 0.01 significance

* - 0.05 significance

Me3Kid. - Me₃BuPb levels in gull kidney

Me2Kid. - Me₂Bu₂Pb levels in gull kidney

Et3Kid. - Et₃BuPb levels in gull kidney

Table 21. Correlations between alkyllead concentrations of gull tissue from immature birds¹

	Me3Liver	Me3Kid.	Me2Liver	Me2Kid.	Et3Liver	Et3Kid.	Et2Liver
Me3Kidney	0.99918						
Prob> r	0.0008**						
Me2Liver	0.96291	0.95425					
Prob> r	0.0371*	0.0458*					
Me2Kidney	0.99918	0.99880	0.96734				
Prob> r	0.0008**	0.0012**	0.0327*				
Et3Liver	-0.47329	-0.50507	-0.37146	-0.49609			
Prob> r	0.5267	0.4949	0.6285	0.5039			
Et3Kidney	-0.48774	-0.51899	-0.38951	-0.51073	0.99977		
Prob> r	0.5123	0.4810	0.6105	0.4893	0.0002**		
Et2Liver	-0.87475	-0.89306	-0.77225	-0.88354	0.83211	0.83965	
Prob> r	0.1253	0.1069	0.2278	0.1165	0.1679	0.1604	
Et2Kidney	-0.53351	-0.56673	-0.37975	-0.54778	0.97156	0.96978	0.87575
Prob> r	0.4465	0.4333	0.6202	0.4522	0.0284*	0.0302*	0.1242

¹- N=4

** - 0.01 significance

* - 0.05 significance

Me3Kid. - Me₃BuPb levels in gull kidney

Me2Kid. - Me₂Bu₂Pb levels in gull kidney

Et3Kid. - Et₃BuPb levels in gull kidney

Methylleads may not only originate from a different source than ethylleads, but may also have a suppressive effect on ethyllead tissue levels. Although correlations between ethyl- and methyllead tissue levels were not significant ($p=0.05$), a negative correlation occurred in each case (Tables 19-21), reflecting the regional trends in alkyllead tissue concentrations (Table 16).

Gull egg homogenate (Table 22) samples contained primarily Me_3Pb^+ (9 out of 10 samples) at lower levels than those of other gull tissues. Correlation (Pearson correlation coefficients) of Me_3Pb^+ levels between combined or mature birds tissue and egg samples from the same sampling sites were significant ($p=0.05$) (Table 23A-B). Immature bird tissue and egg sample Me_3Pb^+ levels were not significantly ($p=0.05$) correlated (Table 23C). Only mature birds produce egg clutches, so a high degree of correlation between adult tissue and egg levels is not unexpected.

Mallard duck tissues (Table 24) contained lower levels of organolead salts than gull tissues. Generally, males contained higher levels of alkyllead salts than females in the sampled tissues (liver, kidney, brain and breast muscle) although a paired comparison t-test (Appendix R) indicated that only Et_3Pb^+ appeared to be significantly ($p=0.05$) different. The mallards were collected during fall migrations and could have originated from northern or southern Ontario breeding grounds. The tissue levels suggested that the mallard habitat was less polluted than that of the gull. Trimethyllead salt concentrations in the various tissues were similar or slightly greater than Et_3Pb^+ tissue levels and were prevalent, again suggesting a source of Me_3Pb^+ separate from industrial sources.

Table 22. Ionic alkyllead (as alkylbutyllead) levels in herring gull whole egg homogenate from Great Lakes colonies

Source	Analytes ⁱ			
	Me ₃ Pb ⁺	Me ₂ Pb ²⁺	Et ₃ Pb ⁺	Et ₂ Pb ²⁺
	-----Mean Concentration ⁱⁱ ± SD ⁱⁱⁱ (ng/g wet wt)-----			
<u>Lake Superior</u>				
Agawa Rock	0.2 ± 0.1	N.D.	N.D.	N.D.
<u>Lake Huron</u>				
Channel Shelter I.	N.D.	N.D.	N.D.	N.D.
Double Island	0.2 ± 0.1	N.D.	N.D.	N.D.
<u>Lake Erie</u>				
Middle Island	0.3 ± 0.1	N.D.	N.D.	N.D.
<u>Lake Ontario</u>				
Scotch Bonnet I.	0.5 ± 0.3	N.D.	0.3 ± 0.2	0.2 ± 0.1
Snake I.	0.5 ± 0.1	0.6 ± 0.2	N.D.	N.D.
Muggs I.	0.8 ± 0.3	0.7 ± 0.2	0.3 ± 0.1	0.3 ± 0.1
Hamilton Harbour	0.5 ± 0.1	N.D.	N.D.	N.D.
Niagara River	0.6 ± 0.3	N.D.	N.D.	0.2 ± 0.4
Fighting I.,	0.5 ± 0.1	N.D.	N.D.	N.D.
Detroit River				

ⁱ- no Me₂EtPb⁺, MeEt₂Pb⁺, or MeEtPb²⁺ was detected in any of the samples

ⁱⁱ- corrected for recovery

ⁱⁱⁱ- calculated from three replicate injections into the gas chromatograph

N.D. - not detected

Table 23. Correlations between trimethyllead concentrations of gull egg homogenate and other tissues

A. Combined Birds (N=8)

	Liver	Kidney
Egg	0.94444	0.92759
Prob> r	0.0004**	0.0009**

B. Mature Birds (N=4)

	Liver	Kidney
Egg	0.99773	0.96447
Prob> r	0.0023**	0.0355*

C. Immature Birds (N=4)

	Liver	Kidney
Egg	0.93149	0.93024
Prob> r	0.0685	0.0698

**-- 0.01 significance

*-- 0.05 significance

Table 24. Ionic alkyllead (as alkylbutyllead) levels in separate tissues from mallard ducks

Source		Me ₃ Pb ⁺	Me ₂ EtPb ⁺	MeEt ₂ Pb ⁺	Me ₂ Pb ²⁺	Et ₃ Pb ⁺	Et ₂ Pb ²⁺	MeEtPb ²⁺
-----Mean Concentration ¹ ± SD ¹¹ (ng/g wet wt)-----								
LIVER								
Female	1	0.4±0.2	N.D.	N.D.	N.D.	N.D.	5.5±0.8	N.D.
	2	0.6±0.1	N.D.	N.D.	N.D.	N.D.	N.D.	N.D.
	3	1.3±0.1	N.D.	N.D.	N.D.	0.5±0.2	0.3±0.1	N.D.
	4	0.7±0.2	N.D.	N.D.	N.D.	N.D.	0.3±0.3	N.D.
	5	0.4±0.1	N.D.	N.D.	1.7±0.4	0.3±0.1	0.8±0.3	N.D.
	(P)	0.6±0.1	N.D.	N.D.	N.D.	N.D.	N.D.	N.D.
Male	1	0.9±0.2	0.2±0.1	N.D.	0.8±0.5	0.5±0.1	0.7±0.3	N.D.
	2	4.3±0.2	1.2±0.2	1.3±0.2	2.2±0.5	2.0±0.5	1.5±0.4	0.6±0.1
	3	0.8±0.1	N.D.	0.6±0.1	N.D.	0.8±0.4	0.7±0.1	N.D.
	4	0.5±0.2	N.D.	N.D.	N.D.	0.6±0.3	0.8±0.3	N.D.
	5	0.6±0.1	0.2±0.1	N.D.	N.D.	0.7±0.1	1.3±0.2	N.D.
	(P)	1.4±0.1	0.5±0.2	0.7±0.1	N.D.	1.3±0.2	1.0±0.2	N.D.
KIDNEY								
Female(P)	A	1.4±0.1	0.4±0.2	0.3±0.1	N.D.	0.6±0.1	0.4±0.4	N.D.
	B	1.4±0.1	0.3±0.1	0.4±0.1	N.D.	0.7±0.1	1.0±0.2	N.D.
Male (P)	A	4.0±0.3	1.7±0.1	1.7±0.1	1.9±0.7	3.5±0.5	3.0±0.3	0.7±0.1
	B	4.3±0.2	1.8±0.2	1.8±0.2	2.0±0.4	3.3±0.1	1.3±0.5	N.D.
BRAIN								
Female(P)		0.6±0.1	N.D.	N.D.	N.D.	0.3±0.2	0.7±0.1	N.D.
Male (P)		1.1±0.1	0.5±0.1	0.8±0.2	1.4±0.2	1.2±0.3	0.5±0.5	N.D.
BREAST MUSCLE								
Female(P)		0.4±0.2	N.D.	0.4±0.2	N.D.	N.D.	0.5±0.4	N.D.
Male (P)		1.6±0.1	0.6±0.1	0.9±0.1	1.7±0.2	1.4±0.3	0.8±0.4	N.D.

1- corrected for recovery

11- calculated from three replicate injections

(P)- pooled sample from five individuals

N.D.- not detected

Trimethyllead is ubiquitous, being found in three avian species (herring gull, mallard duck and domestic chicken) and all examined tissue types. Significant correlation between alkyllead tissue levels in sampled herring gulls and lake sediment lead levels suggest possible methylation of inorganic lead. The ethyllead and methyllead tissue levels in the gull colonies were inversely related. Hamilton Harbour birds contained much higher levels of Me_3Pb^+ than Et_3Pb^+ , with no known automotive source of Me_3Pb^+ . Triethyllead tissue levels were greatest in Agawa Rock gull tissues, a relatively undeveloped region with fewer potential automotive sources of ethyllead salts than the region surrounding Hamilton Harbour. The correlation studies suggest that methyllead salts may have a suppressive effect on ethyllead levels in gulls.

8. CLAIMS OF ORIGINAL WORK

This study is an organized and concerted effort to develop extraction methodology and analytical instrumentation suitable for the trace analysis of ionic alkyllead compounds in environmental samples. The original discoveries are listed below under subject groups.

1. Organolead Synthesis

a) The first reported use of saline solution to extract dialkyllead salt impurities from trialkyllead standards.

b) The first reported synthesis of alkylphenyllead compounds from lead(II), using a one step synthesis method.

c) The first reported IR, NMR and MS spectra of Me_3PhPb , $\text{Me}_2\text{Ph}_2\text{Pb}$, Et_3PhPb and $\text{Et}_2\text{Ph}_2\text{Pb}$.

d) The first reported mass spectra of alkyllead-pyrrolidine dithiocarbamate complexes.

2. Extraction Methodology

a) The first use of enzymatic hydrolysis to prepare biological tissue for liquid-liquid extraction of ionic alkyllead compounds.

b) The first reported double extraction technique with dithizone to separate ionic alkylleads from coextractives, producing a clean extract with no further sample cleanup required.

c) The first reported extraction methodology for ionic alkylleads in avian

tissues.

3. Analytical Instrumentation

a) The first reported usage of an automated GC-AAS system for organolead analysis.

b) Original advancements in quartz T-tube furnace atomizer and GC-AAS interface design.

c) The first reported HPLC-QTAAS system, utilizing a HPLC-AAS interface design for solvent delivery to the quartz T-tube furnace atomizer.

d) The first reported comprehensive univariate optimization of GC-ECD and GC-AAS operating conditions for the analysis of alkylphenylleads and alkylbutylleads respectively.

e) The first examination of alkyllead atomization processes in a heated quartz T-tube furnace.

4. Organolead Interaction With Egg

a) The first reported evidence of ionic alkyllead binding with avian egg components.

5. Environmental Sample Analysis

a) The first determination of ionic alkyllead levels in Canadian avian populations.

b) The first evidence of environmental methylation of inorganic lead from biological tissue analysis.

9. RECOMMENDATIONS FOR FUTURE WORK

1. It is recommended that the extraction of $\text{Me}_2\text{Pb}^{2+}$ from biological tissue be improved by further extraction methodology development.

2. Further studies should be made into the interaction of ionic alkyllead with tissue matrices.

3. Development of a capillary column GC-AAS system (with H_2 as the column carrier gas) should be done to enhance analyte separation and permit a lower total system gas flow through the quartz T-tube furnace.

4. The atomic processes should be studied further to determine molecular species formed.

5. Further studies into a usable HPLC-AAS system should be made, particularly for the analysis of underivatized alkyllead salts.

6. The continued monitoring of ionic alkyllead levels in herring gull populations should be done to determine long term trends in alkyllead levels in the environment.

7. The ionic alkyllead levels of fish and water samples from the Great Lakes region should be analyzed to determine the aquatic pathways of alkyllead uptake in the herring gull.

10. APPENDICES

Appendix A. GC-ECD analysis of alkyllead compounds

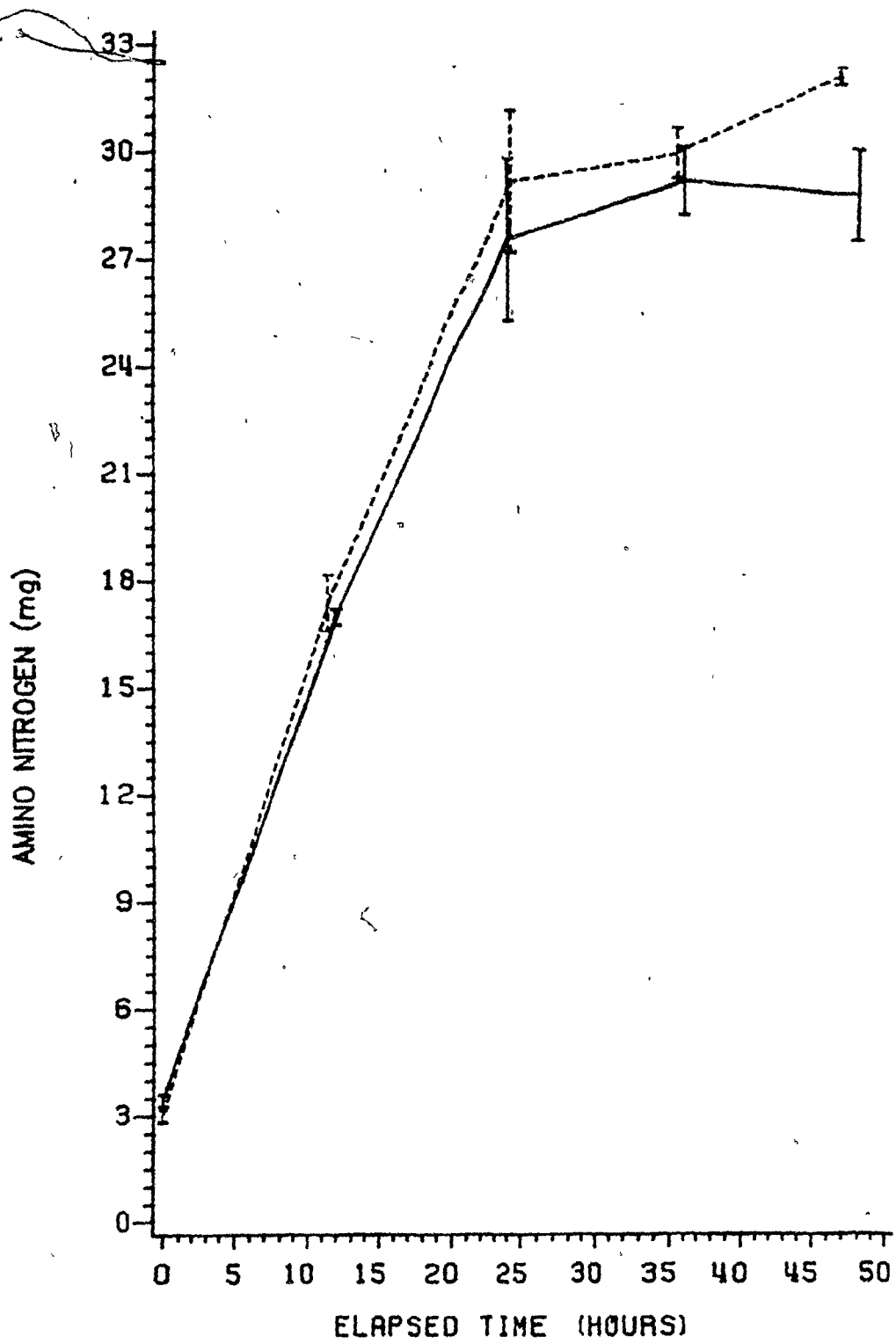
A Varian 3700 gas chromatograph equipped with a ^{63}Ni electron capture detector, a 30 m X 0.327 mm DB-1 fused silica capillary column and a splitless injector was used in this investigation. Operating conditions were as follows: carrier gas, helium, 3 mL min⁻¹; detector makeup gas, nitrogen, 30 mL min⁻¹; detector temperature, 300°C; injector temperature, 200°C; temperature program, isothermal at 50°C for 2 min followed by linear ramping to 200°C at 4°C min⁻¹. Quantitation was performed by external standards using a Shimadzu C-RIB data processor.

Solvents were distilled in glass grade from Caledon Laboratories Ltd. Inorganic reagents including diphenylthiocarbazone (dithizone) were ACS reagent grade or better. The ammoniacal buffer comprised 11.3 g diammonium citrate, 2.0 g potassium cyanide and 12.0 g sodium sulfite in 250 mL H₂O. The pH was adjusted with concentrated ammonium hydroxide.

Enzymatic Hydrolysis

Whole egg homogenate was incubated at 37°C for 24 h in 60 mL of 5% ethanol/0.1 M phosphate buffer (pH 7.5) containing 30 mg Lipase Type VII and 30 mg Protease Type XIV. Enzyme preparations were obtained from Sigma Chemical Co. The course of the enzymatic hydrolysis of whole egg homogenate was monitored by the ninhydrin reaction (Yemm and Cocking 1955) (Fig. A1). Three replicate trials were run on each of two separate days. Within experimental error, no differences were observed between 24 h and 36 h. The enzymatic hydrolysis was 72±9% effective after 24 h and 78±9% effective after 48 h relative to classical acid hydrolysis. Relative to the protease alone, a combination of protease and

Figure A1. The release of amino nitrogen from egg homogenate during enzymatic hydrolysis: —, trial 1; - - - - -, trial 2. Error bars represent \pm one standard deviation of three replicate determinations.



lipase resulted in a more homogeneous hydrolysate, with less tendency to emulsify when extracted with organic solvents.

Extraction

Two extraction procedures were developed; the single complexometric extraction was suitable for water samples, whereas the double extraction procedure provided additional cleanup for the more complex whole egg homogenate. Residual droplets of aqueous phase in organic centrifugates were conveniently removed by placing the capped centrifuge tube in a freezer (-20°C) for one-half hour. After this time, the organic phase was decanted leaving a pellet of ice behind.

Method 1 (used for water samples) Ammoniacal buffer (pH 8.5, 10 mL) was added to the sample (60 mL) which was then extracted three times with 0.005% (w/v) dithizone (10 mL) in 50% benzene/hexane. The organic extracts were combined, reduced in volume to 0.5 mL and derivatized directly.

Method 2 (used for egg homogenate) Absolute ethanol (15 mL for Experiments B and D or 22 mL for Experiments E and F), and ammoniacal buffer (pH 9.5, 10 mL) were added to the sample. The mixture was extracted three times with 0.05% (w/v) dithizone (10 mL) in 50% benzene/hexane. The organic extracts were combined, centrifuged and back extracted three times with 10 mL HNO_3 (0.15 M). The aqueous washes were combined, neutralized with NaOH and further basified with 5 mL ammoniacal buffer (pH 9.5). The alkyllead salts were recovered by extracting the aqueous phase three times with 0.01% dithizone (10 mL) in 50% benzene/hexane. These washes were combined, centrifuged and the organic layer reduced in volume to 0.5 mL.

Derivatization

Anhydrous THF (2 mL) and 0.5 mL phenylmagnesium bromide (3 M, Aldrich Chem. Co.) were added to the concentrated extracts under nitrogen. The solution was stirred for 30 min at room temperature then transferred quantitatively to a centrifuge tube (15 mL). The volume was adjusted to 10 mL with water, then extracted three times with hexane. Centrifugation followed each extraction to hasten phase separation. For Experiments A-D, the combined hexane extracts were washed once with water (5 mL), twice with 30% H₂O/CH₃CN (2 mL) then diluted to 15 mL with hexane. For Experiments E and F, the hexane extracts were washed once with water (5 mL), diluted to 15 mL with hexane, then washed three times with CH₃CN (1 mL). The hexane was readjusted to 15 mL and analyzed directly.

The derivatization sequence was performed directly on the dithizonates because of small but persistent losses of the free alkyllead salts during solvent removal. It was imperative that the extracts not be taken to dryness (freeze drying of the lead salts or of their corresponding dithizonates resulted in appreciable loss). Phenylation yields were also consistently better on the dithizonates than on the free salts. It is postulated that the dithizone acts as a keeper in this system.

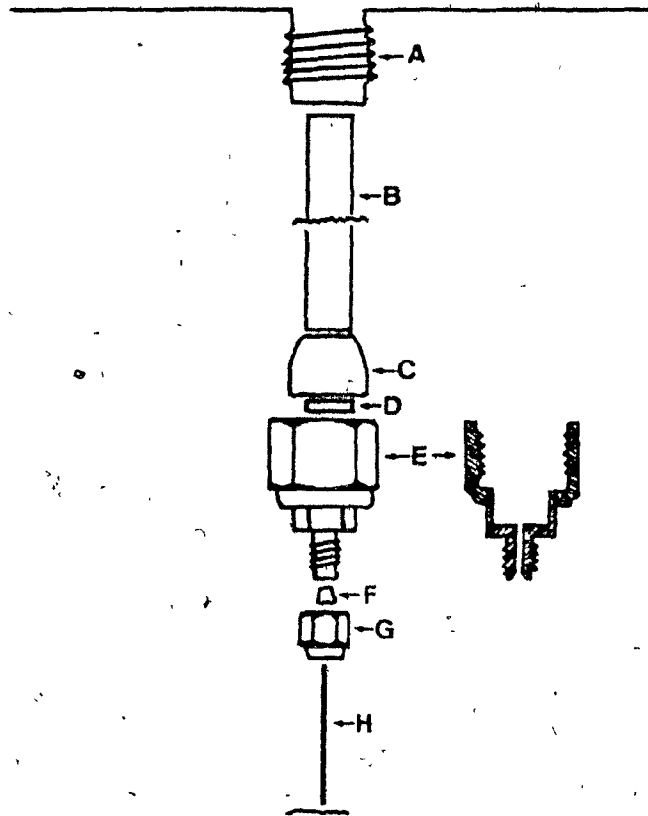
Chromatography

The commercial splitless injector system was unsuitable for these analyses because of persistent sample decomposition despite exhaustive silylation of the inserts and of the injector body with dimethyldichlorosilane in boiling xylene. On-column silylating agents (Silyl-8 or hexamethyldisilazane) were not appreciably better. The problem was overcome by using an all glass insert and

other injector modifications (Fig. A2). The salient features of the modified system were an increased internal volume and a decreased metal surface area. The major modification consisted of an adaptor, a 1/4 in (0.64 cm) stainless steel Swagelok nut that was silver soldered to a 1/16 in (0.16 cm) SSI male connector. The interior of the adaptor was drilled out to accept a 6.25 mm o.d. borosilicate glass insert (2 mm i.d. X 82 mm). A 1/4 in (0.64 cm) diameter disk of lead foil (2 mm thickness) provided a gas tight seal between this insert and the adaptor. The borosilicate insert was held in place by tightening the adaptor onto the bulkhead fitting in the roof of the chromatographic oven, which slightly deformed the vespel/graphite ferrule (C) and the lead foil (D).

Three capillary columns were examined for separation, bleed and inertness characteristics. A thirty meter borosilicate column coated dynamically with SE-30 (Canadian Capillary Co.) developed significantly more bleed and produced more peak tailing of organoleads during programming than did a 25 m methyl silicone fused silica column (Hewlett Packard Co.). A 30 m fused silica DB-1 column (J and W Scientific Co.), however, improved separation of the alkyllead standards from coextractives and was employed in all subsequent studies. Helium was chosen as carrier gas over nitrogen because it increased resolution of the mixture and nitrogen was chosen over 5% argon/methane as makeup gas because it resulted in more stable detector operation. Nitrogen doped with 10 ppm oxygen caused increased detector response to coextractives, but did not enhance analyte response appreciably. Five operating parameters were varied systematically to optimize the detector response (a combination of sensitivity and reproducibility) to each of the four analytes. Detector response to approximately equimolar alkylphenyllead standard was plotted as a function of:

Figure A2. Splitless injector composed of: A, injector heater block fitting; B, 1/4 in (0.64 cm) o.d. borosilicate insert; C, 1/4 in (0.64 cm) vespel/graphite ferrule; D, lead foil pierced by a pinhole; E, 1/4 in (0.64 cm) Swagelok nut silver soldered to a 1/16 in (0.16 cm) SSI male connector; F, 0.4 mm graphite ferrule; G, 1/16 in (0.16 cm) Swagelok nut; H, fused silica capillary column.



(a) injector temperature, (b) carrier gas flow rate, (c) column depth inside injector and (d) detector makeup gas flow rate. Each data point was the average of three replicate determinations and the standard deviation was recorded as an error bar. Each parameter was varied separately while the other four parameters were maintained constant: makeup gas, 30 mL min⁻¹; injector temperature, 200°C; 2.0 cm column depth; 2.0 min initial hold. Based on sensitivity and reproducibility, a carrier gas flow rate of 3.0 mL min⁻¹ and a makeup gas flow rate of 30 mL min⁻¹ nitrogen were judged optimal (Fig. A3). At column flow rates above 3.0 mL min⁻¹, the resolution of analytes from coextractives rapidly deteriorated. More importantly, there was a pronounced deterioration in the analyte peak shape. Although increased sensitivity was observed using lower makeup gas flow rates, the poorer reproducibility and the increased susceptibility to contamination of the detector (particularly by metal deposits) did not warrant this modest improvement. When determinations of egg homogenate were attempted using 20.0 mL min⁻¹ makeup gas, frequent decontamination of the detector (high temperature baking) was necessary. An isothermal hold time between one and three minutes did not alter response or reproducibility. No septum purging was found to be necessary during chromatographic runs. Under these conditions the observed retention times for the four alkylphenyllead standards and their corresponding retention indices relative to a series of n-bromoalkanes were determined (Pacholec and Poole 1982) (Table A1). Under the programming conditions the log of the adjusted retention time versus carbon number was distinctly curvilinear ($r=0.965$) and a better correlation was obtained using the actual retention time ($r=0.997$). These data were used to predict retention indices (Kovats 1965) of EtMe₂PhPb, Et₂MePhPb and EtMePh₂Pb (Table A1). Calibration curves were generated for each of the alkylphenyllead standards using chromatographic conditions described

Figure A3. Detector response for equimolar alkylphenyllead standards to changes in: A, injector temperature,; B, column flow rate; C, column depth inside injector and D, detector makeup gas flow rate. Error bars represent \pm one standard deviation of three replicate determinations.

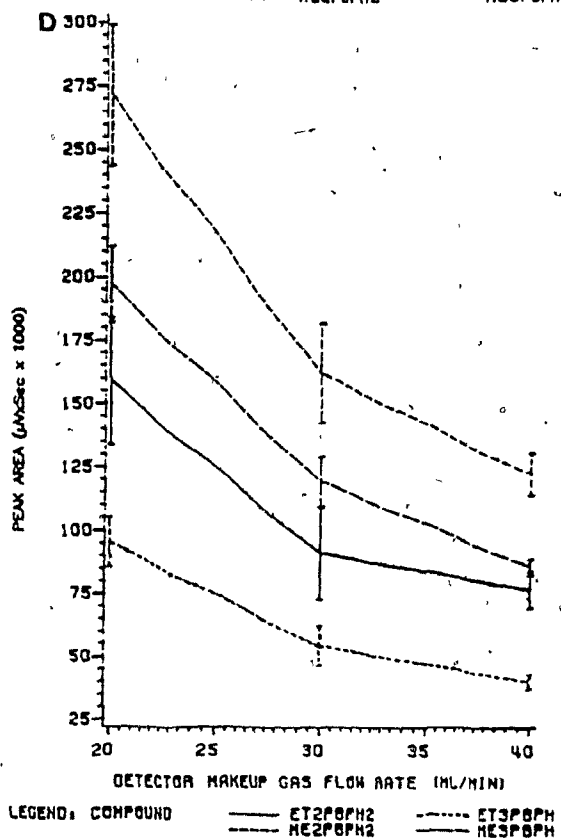
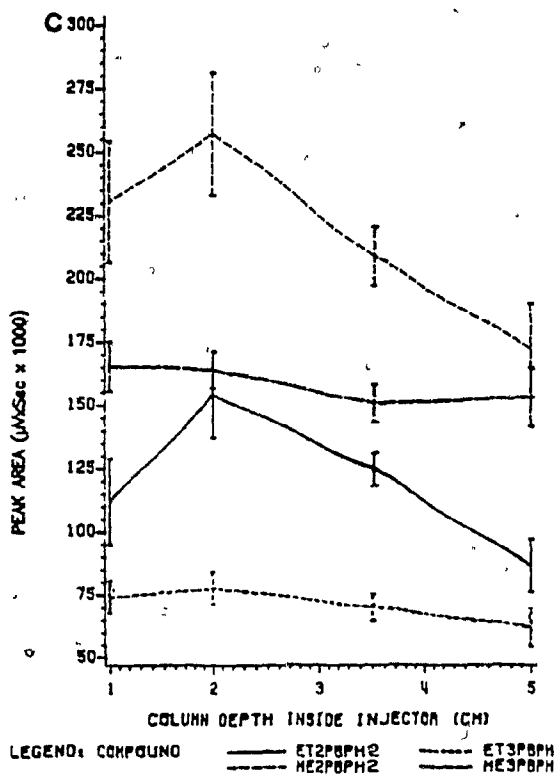
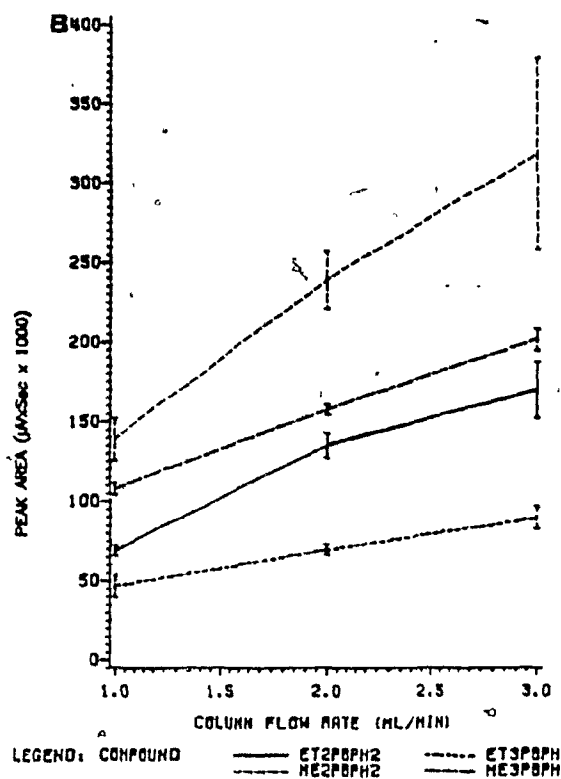
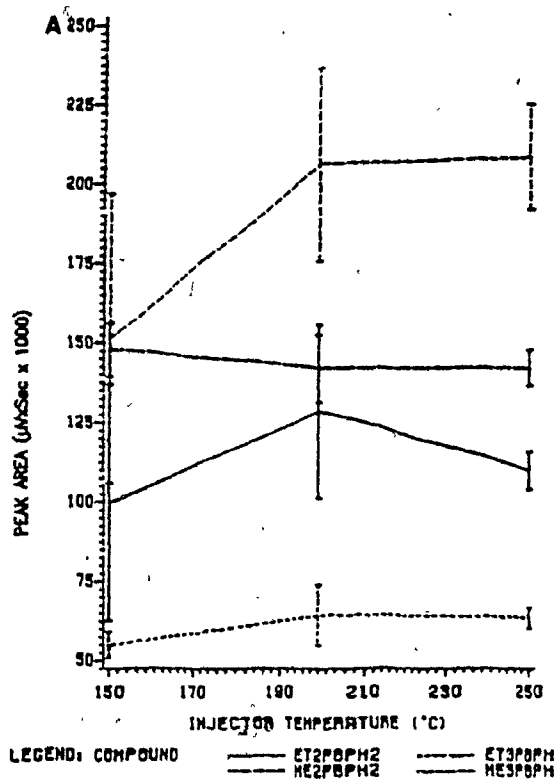


Table A1. Absolute retention times and retention indices (based on retention times) of alkylphenylleads relative to a homologous series of n-bromoalkanes

Analyte	Absolute Retention Time(min)	Retention Index ⁱ (I)	Analyte	Absolute Retention Time(min)	Retention Index ⁱ (I)
n-C ₈ H ₁₇ Br	11.47	800	Et ₃ PhPb	24.76	1217 ⁱⁱ
Me ₃ PhPb	16.15	941 ⁱⁱ	n-C ₁₄ H ₂₉ Br	29.84	1400
n-C ₁₀ H ₂₁ Br	18.13	1000	Me ₂ Ph ₂ Pb	30.87	1443 ⁱⁱ
EtMe ₂ PhPb	19.25	1033(1036) ⁱⁱ	EtMePh ₂ Pb	33.11	1532(1536) ⁱⁱ
Et ₂ MePhPb	22.11	1125(1129) ⁱⁱ	Et ₂ Ph ₂ Pb	35.14	1620 ⁱⁱ
n-C ₁₂ H ₂₅ Br	24.26	1200	n-C ₁₈ H ₃₇ Br	39.47	1800

ⁱ- Predicted retention index (Kovats 1965)

$$ii - I = 100N + 100n[(RT(A) - RT_{R(N)}) / (RT_{R(N+n)} - RT_{R(N)})]$$

N- number of carbons in analyte

n- carbon number difference between R(N) and R(N+n)

A- analyte for which retention index was calculated

R(N)- analyte containing N carbons

R(N+n)- analyte containing (N+n) carbons

above. A linear increase in detector response was observed with increasing analyte concentrations (range 4 pg to 500 pg) of each of the four alkylphenyllead standards (Table A2).

Recoveries

Table A3 summarizes the results of six recovery trials. Using the simplified extraction procedure (Method 1) or the double extraction technique (Method 2), recoveries from distilled water or from phosphate buffer (spiked at 1-20 ppb Pb) were consistently high. No consistent differences in recoveries from the two methods were detected.

Only Method 2 was attempted for samples of whole egg homogenate. The hydrolysis when incorporated into the determination sequence had no substantial effect on the mean recovery of ethyllead salts, however, precision was considerably improved (Experiment E versus Experiment F, Table A3). In contrast, the mean recovery of methyllead salts was dramatically improved, indicating that the methyllead salts were rapidly bound up by the egg matrix. The determinations were commenced 15 min after each sample was spiked. The enzymatic pretreatment apparently releases the bound analytes.

The possibility that transalkylation of one lead salt by another might occur during the isolation procedures or upon chromatography of the derivatives was investigated in the following studies.

Gas chromatography-mass spectrometry identified the following mixed alkylphenyl leads; EtMe_2PhPb , Et_2MePhPb and EtMePh_2Pb , as well as biphenyl and terphenyls in the crude reequilibration reaction mixtures. None of these "mixed" alkylleads have been detected during recovery trials of alkylphenyllead

Table A2. Linear regression analysis of calibration curves for alkylphenylleads

Analyte	Linear Regression Equation ¹	Correlation Coefficient	Data Points
Me ₃ PhPb	$Y = 415.9x + 1843$	0.9998	15
Et ₃ PhPb	$Y = 238.9x + 494.4$	0.9997	15
Me ₂ Ph ₂ Pb	$Y = 662.5x + 3163.0$	0.9996	15
Et ₂ Ph ₂ Pb	$Y = 547.1x + 778.7$	0.9988	15

¹ - Y = peak area ($\mu\text{V}\cdot\text{s}$) and x = pg Pb

Table A3. Mean recoveries of ionic alkylleads from water, buffer and whole egg homogenate using different extraction procedures.

Exp't	Matrix	Spiked at ¹ (ppb)	Procedure		-----Alkylphenyllead-----				Number of Replicates
			Hydrolysis	Method 1 2	Me ₃ PbCl	Et ₃ PbCl	Me ₂ PbCl ₂	Et ₂ PbCl ₂	
-----Mean Percent Recovery+SD-----									
A	Distilled ¹¹ water	14-19		x	93 ₊₃	103 ₊₇	72 ₊₄	90 ₊₅	6
B	Distilled ¹¹ water	0.9-1.5		x	92 ₊₅	85 ₊₃	60 ₊₃	99 ₊₁₃	3
C	Phosphate ¹¹ buffer	14-19		x	89 ₊₃	100 ₊₆	70 ₊₂	86 ₊₅	3
D	Whole egg ¹¹¹ homogenate	400-525	x	x	90 ₊₃	85 ₊₄	62 ₊₂	78 ₊₄	3
E	Whole egg ¹¹¹ homogenate	30-50		x	35 ₊₆	83 ₊₂₆	23 ₊₁₅	115 ₊₂₂	5
F	Whole egg ¹¹¹	30-50	x	x	80 ₊₁₂	79 ₊₄	76 ₊₁₅	117 ₊₁₅	6

i- reported as ppb Pb

ii- volume 60 mL

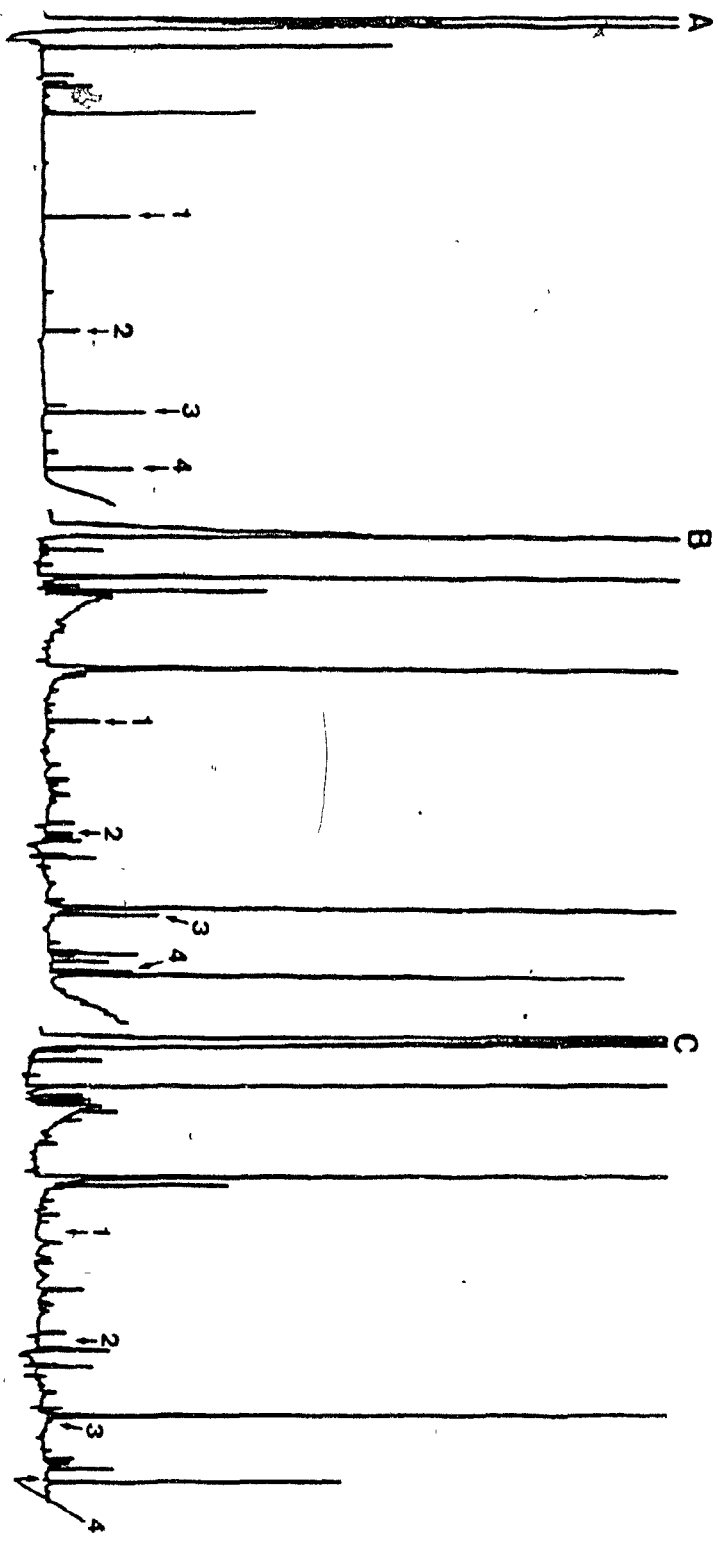
iii-weight 2.5 g

standards or during recovery trials using trialkyllead chlorides or dialkyllead chlorides.

Figure A4 records chromatograms of (A) synthetic mixture of alkylphenyllead standards, (B) one of the replicate recovery trials from experiment F (equivalent to 30-50 ppb Pb in whole egg homogenate) and (C) a control recovery trial from whole egg homogenate. Because recoveries from water, phosphate buffer and from hydrolyzed egg homogenate were consistently high and as there were no significant peaks in the chromatograms which could have been attributed to transalkylation products, it is concluded that transalkylation was not a major source of loss.

The application of the method to herring gull whole egg homogenate was tested by analyzing three samples. The procedures followed were exactly those for Experiment F of the recovery trials. No practical difficulties were encountered, indicating that chicken egg homogenate was a suitable substitute matrix for these samples. No indication of the presence of lead salts in these samples was obtained and it is concluded that, at the time of analysis, these analytes were present at less than 1-4 ppb in herring gull egg samples. Recovery trials directly from herring gull egg homogenate were not attempted for lack of suitable samples; thus binding to this matrix may be different from those interactions observed in the case of chicken egg homogenate.

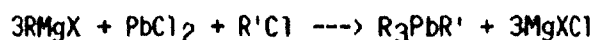
Figure A4. GC-ECD chromatograms of: A, synthetic mixture of 15.0 pg Me_3PhPb (1), 15.0 pg Et_3PhPb (2), 15.9 pg $\text{Me}_2\text{Ph}_2\text{Pb}$ (3), and 17.1 pg $\text{Et}_2\text{Ph}_2\text{Pb}$ (4); B, recovery sample from whole egg homogenate (spiked with 30-50 ppb alkyllead salts); C, recovery trial from control whole egg homogenate.



Appendix B. Alkylphenyllead synthesis

Tetraalkyleads can be synthesized from lead(II) chloride by reaction with a Grignard reagent and alkyl halide.

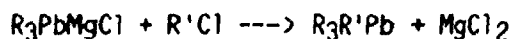
Gorsich and Robbins (1969) reported a one step method for the synthesis of tetraalkylleads from a Grignard reagent, lead(II) chloride and alkyl chloride:



The reaction proceeded by initially forming a trialkylplumbylmagnesium chloride complex:



The trialkylplumbylmagnesium chloride was then reacted with an alkyl halide:



The R_3PbMgCl intermediate formed readily in THF, but not in diethyl ether. The lead(II) salt must be added to the Grignard to prevent lead metal formation (Williams 1970), which was likely caused by disproportionation of the R_2Pb intermediate when excess Grignard was not available to react to form the R_3PbMgCl complex (Williams 1970).

The purpose of the study was to synthesize unsymmetrical alkylphenyllead compounds for use as analytical standards.

Solvents (except THF) were distilled in glass grade from Caledon Laboratories Ltd. The tetrahydrofuran was HPLC anhydrous grade (Caledon

Laboratories Ltd.). Inorganic reagents were ACS grade or better. Alkyl- and phenylmagnesium chloride were obtained from Alfa Products, Ventron Corp. The compressed nitrogen was extra dry grade from Medigaz Ltee, Montreal.

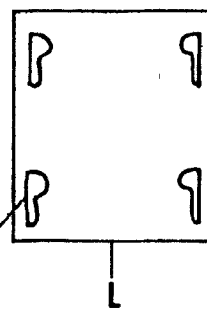
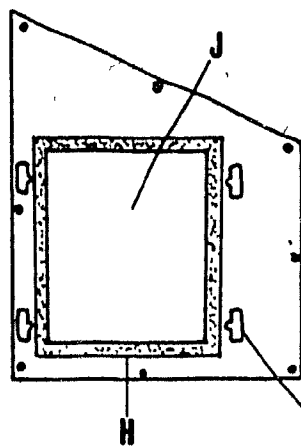
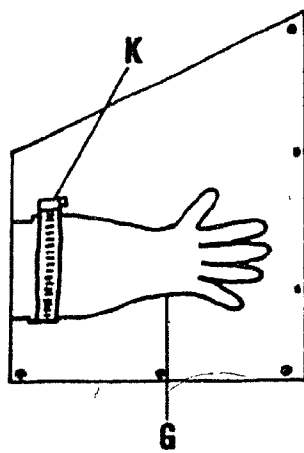
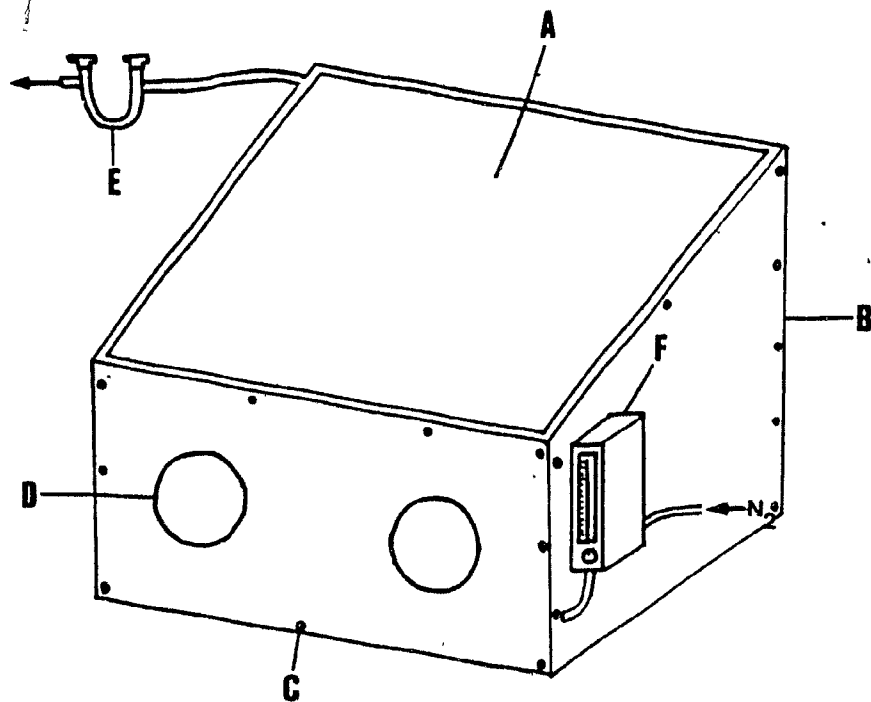
The handling of oxygen and moisture sensitive reagents, anhydrous solvents and organolead synthesis was simplified by the use of a home made glove box (Fig. A5).

Ethylphenyllead Synthesis.

Lead(II) chloride (PbCl_2) was reacted with phenylmagnesium chloride (PhMgCl), ethylmagnesium chloride (EtMgCl) and ethyl bromide (EtBr). The molar ratio of $\text{EtBr}:\text{PbCl}_2$ was 4:1, whereas the molar ratio of $\text{PhMgCl}:\text{EtMgCl}:\text{PbCl}_2$ was varied to optimize the yield of the desired product(s); for the synthesis of tetraethyllead and triethylphenyllead, a molar ratio of 1:3:1 was used, and a molar ratio of 2:2:1 was optimum for the synthesis of diethylphenyllead and ethyltriphenyllead.

The phenylmagnesium chloride (1.95 M in THF), ethylmagnesium chloride (2.08 M in THF) and ethyl bromide were added in appropriate quantities to a 300 mL three-necked round bottom flask under nitrogen (glove box). Tetrahydrofuran (100 mL) was added; the flask was stoppered and transferred to a crushed ice bath in a fume hood. A water cooled Liebig condenser fitted with an air lock (oil filled U trap) was attached to the central joint of the round bottom flask. The reaction mixture was stirred vigorously and the temperature monitored with a thermocouple. When the solution temperature reached 0-3°C, 10 g of finely crushed PbCl_2 was added through the other side arm over approximately 10 minutes. The PbCl_2 dispenser, a bent sealed glass tube with a ground glass joint, was removed and the nitrogen connected. The mixture was

Figure A5. Controlled atmosphere glove box consisting of: A, plexiglass sheet, 48.3 cm X 43.2 cm X 0.32 cm; B, masonite side section, 30.5 cm (front) X 38.1 cm X 48.3 cm (back); C, masonite front section, 61 cm X 30.5 cm X 0.5 cm; D, glove port, PVC tubing, 11.4 cm i.d., 12.7 o.d.; E, glass U-tube, oil filled; F, gas rotameter; G, neoprene gloves; H, foam rubber seal; I, door mounting hardware; J, door opening, left side, 20.3 cm X 25.4 cm; K, 12.7 cm hose clamp; L, masonite door, 25.4 cm X 30.5 cm.



reacted at ice bath temperature for approximately 10 minutes, and then allowed to warm to room temperature over one hour. The flask contents were transferred to a 500 mL separatory funnel with several washings of hexane (total volume-100 mL) and then partitioned three times with double distilled water (50 mL). The organic layer was filtered, dried with sodium sulfate and reduced to a constant volume under vacuum (rotary evaporation at 35°C).

Distillation The distillation apparatus (Ace Glass Inc., Vineland, N.Y.) consisted of; (a) 10 mL round bottom flask used as the distillation flask, (b) Vigreux column, indent section either 60 or 130 mm in length (glass blown at Macdonald College) heated with electric cord (Cole Parmer Co.) and wrapped with aluminum foil, (c) integral still head condenser unit and (d) cow receiver with four 5 mL receiver flasks.

The distillation flask was heated in an oil bath, with both the bath and column temperature monitored by thermocouples. The vacuum was maintained by a mechanical high vacuum pump (Model D25, Precision Sci.) and monitored by a mercury manometer. A liquid air cold trap was placed before the pump in the vacuum line to prevent possible contamination.

The reaction products were transferred to the 10 mL distillation flask, the distillation apparatus assembled and the vacuum slowly applied to about 3 mm Hg. The flask contents were magnetically stirred with a teflon coated stir bar. The oil bath and Vigreux column temperatures were slowly increased, with the column temperature being maintained at least 5°C cooler than the heating bath. The temperatures were stabilized as soon as condensate was observed in the still head and the fraction collected (Table A4). The fractions were analyzed by gas chromatography for purity.

Table A4. Distillation conditions for R_xPh_4-xPb compounds

Oil Bath Temperature (°C)	Column Height (cm)	Column ¹ Temp (°C)	Distillate
Ambient-92	130	62-65	Et_4Pb
149-154	60	130-133	Et_3PhPb
204-207	130	182-184	Et_2Ph_2Pb
103-107	130	89-93	Me_3PhPb
177-179	130	168-172	Me_2Ph_2Pb

¹- 3 mm Hg

Biphenyl, a byproduct of the synthesis could not be separated from triethylphenyllead with the available distillation apparatus. Accordingly, the following synthetic route to triethylphenyllead was used.

Triethyllead chloride (4.5 g, 0.014 moles) was added to 50 mL tetrahydrofuran in a 100 mL three-necked round bottom flask. Phenyllithium (0.028 moles, 1.9 M, Aldrich Chem Co.) was held in a pressure equalized cylindrical separatory funnel under nitrogen. The flask was placed in an ice bath with the separatory funnel attached to the center joint. Nitrogen (prepurified grade, Medigaz) was introduced into the top of the separatory funnel, passed into the flask and exited through a water cooled condenser with an oil filled U-trap attached. The temperature of the reaction mixture was monitored with a thermocouple inside a glass insert.

The mixture was magnetically stirred and cooled to 3°C. The phenyllithium was added dropwise over 30 minutes; the ice bath was removed and the reaction mixture was allowed to warm to room temperature.

The flask contents were transferred to a 500 mL separatory funnel with a hexane rinse (100 mL); then partitioned three times with double distilled water (50 mL). The pooled aqueous extracts were back extracted three times with hexane (25 mL), which was then added to the separatory funnel.

The combined mixture was then filtered and dried with anhydrous sodium sulfate. The solvent was removed under vacuum (rotary evaporation at 40°C). The residue was fractionally distilled under vacuum using a 60 mm Vigreux column (Table A4).

Methylphenyllead Synthesis

Lead(II) chloride was reacted with phenylmagnesium chloride, methylmagnesium chloride and methyl bromide. The molar ratio of $\text{MeBr}:\text{PbCl}_2$ was 4:1. The molar ratio $\text{PhMgCl}:\text{MeMgCl}:\text{PbCl}_2$ was 1:3:1 to obtain trimethylphenyllead, whereas a 3:1:1 molar ratio optimized the synthesis of dimethylphenyllead.

The reaction apparatus, conditions and isolation of the reaction products was as described for ethylphenyllead synthesis. Vacuum fractional distillation was carried out as reported in Table A4.

Compound Characterization.

Elemental Analysis (C,H)

Samples were analyzed by C.B.R.I Technological Services Unit, Research Branch, Agriculture Canada, Ottawa, Ontario, Canada.

Infrared (IR) Spectroscopy

The alkylphenylleads were run as neat liquids in a demountable sodium chloride window assembly with a 0.025 mm metal foil spacer (Perkin-Elmer Corp.). Spectra were recorded from 4000 to 635 cm^{-1} on a Model 257 Perkin-Elmer Spectrophotometer.

Nuclear Magnetic Resonance (NMR) Spectroscopy

The alkylphenylleads were run in spectrophotometer grade carbon tetrachloride (Aldrich Chem Co.) with 1% tetramethylsilane as the internal reference compound. Spectra were recorded over a 600 Hz sweep width on a

Varian EM360 NMR Spectrometer (Varian Associates Inc.) at ambient temperature.

Gas Chromatography

The alkylphenylleads and reaction mixtures were analyzed with a Varian 3700 gas chromatograph (Varian Associates Inc.) equipped with a ^{63}Ni electron capture detector. Operating conditions were as given in Forsyth and Marshall (1983). Analysis of the reaction products by GC-AAS was also performed under conditions described in Section 5.2.1.

Gas Chromatography-Mass Spectrometry

Samples were analyzed by the Canadian Wildlife Service, Wildlife Toxicology Division, Hull, Quebec, Canada.

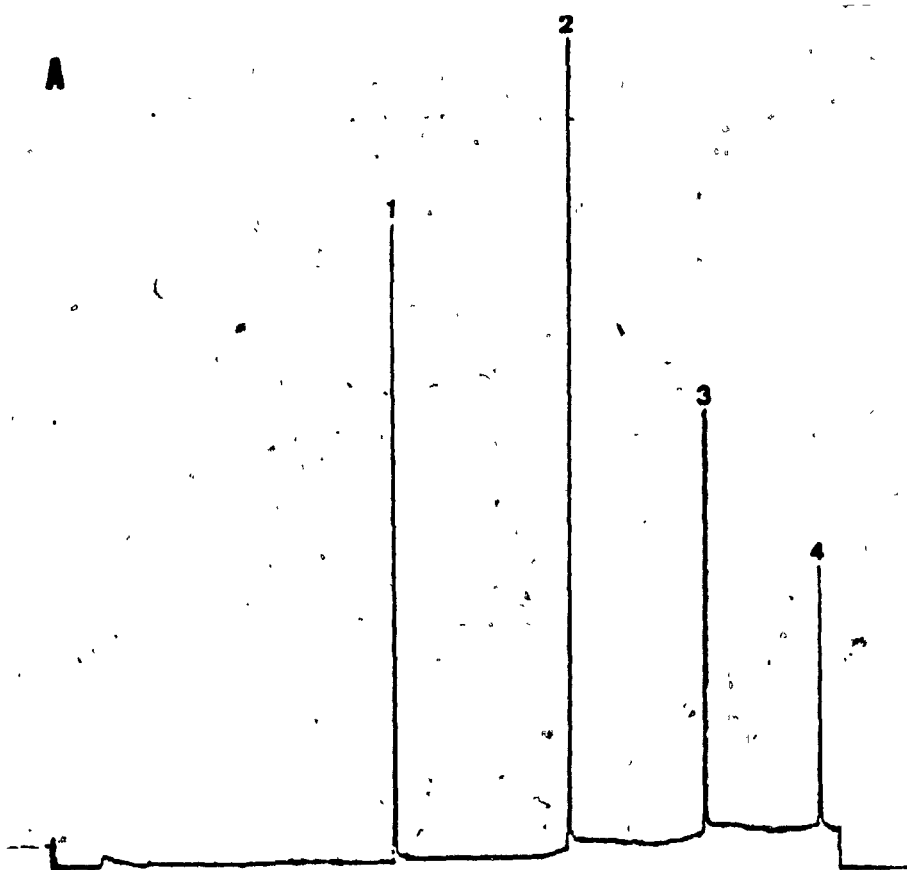
Results and Discussion

The alkylphenyllead reaction mixtures contained 3-4 products (Fig. A6A and A6B) although Me_4Pb , absent from the methylphenyllead reaction products (Fig. A6B), was likely removed during rotary evaporation of the mixture prior to analysis. Fractional distillation of the reaction mixture isolated the desired alkylphenylleads with a high degree of purity (Fig. A7A-D). Further compound characterization by elemental analysis, IR, NMR and mass spectroscopy confirmed compound identities (Figs. A8-A11).

Alkyllead phenylates were initially chosen to minimize loss of derivatized alkylleads during solvent reduction in the recovery procedure. Also, it was felt that phenyl groups would enhance electron capture detection. Chromatography of the alkyllead phenylates was excellent (Fig. A6A). Phenylation of the extracted ionic alkylleads initially produced sufficiently

Figure A6. GC-ECD chromatograms of: (A) ethylphenyllead reaction mixture containing 1, Et_4Pb ; 2, Et_3PhPb ; 3, $\text{Et}_2\text{Ph}_2\text{Pb}$; 4, EtPh_3Pb and (B) a methylphenyllead reaction mixture containing 1, Me_3PhPb ; 2, $\text{Me}_2\text{Ph}_2\text{Pb}$; 3, MePh_3Pb .

A



B

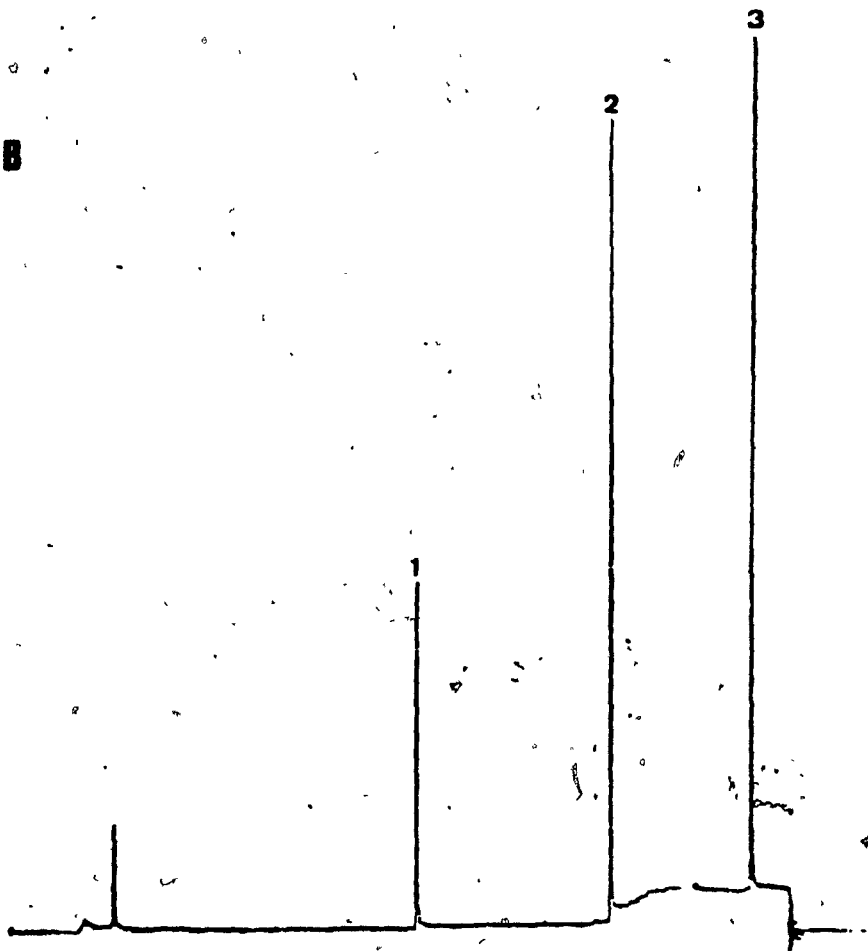


Figure A7. GC-AAS chromatograms of: (A) Me_3PbPb ; (B) Et_3PbPb ; (C) $\text{Me}_2\text{Ph}_2\text{Pb}$; (D) $\text{Et}_2\text{Ph}_2\text{Pb}$.

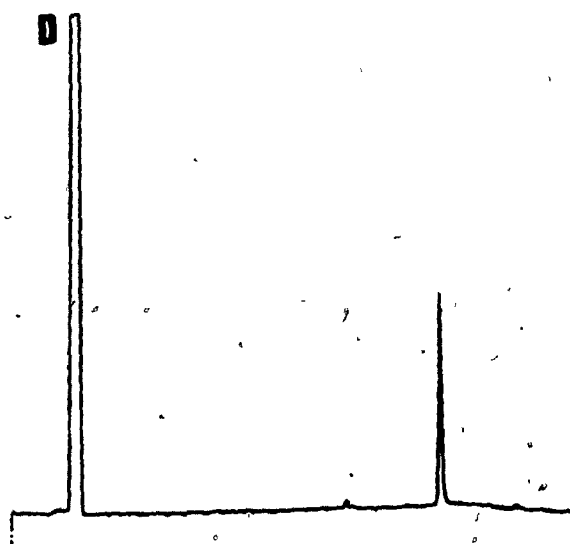
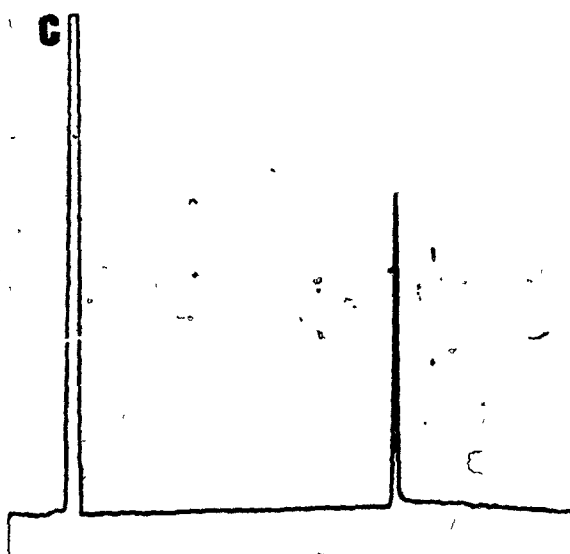
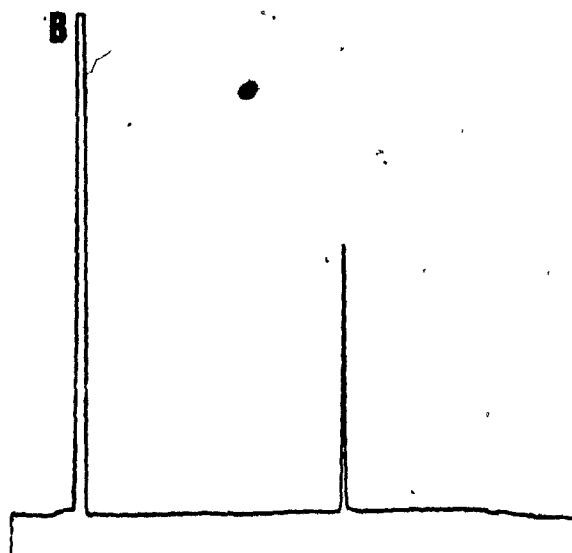
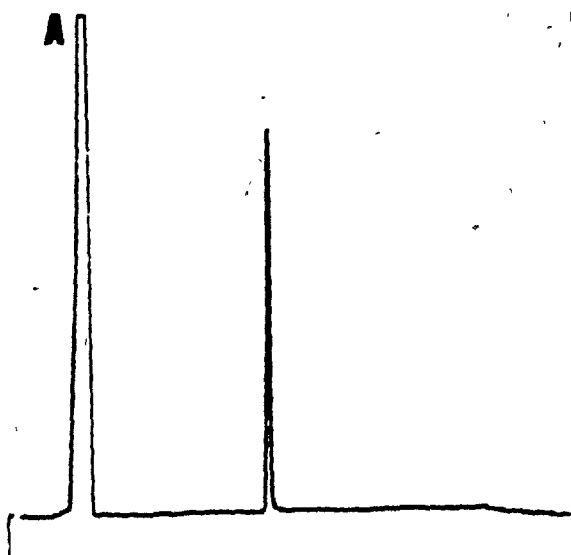


Figure A8. Elemental analysis, (A) mass spectrum, (B) IR spectrum and (C) NMR spectrum of Et_3PbPb .

Elemental Analysis:

Calculated: 38.80% C 5.43% H

Found: 38.64% C 6.00% H

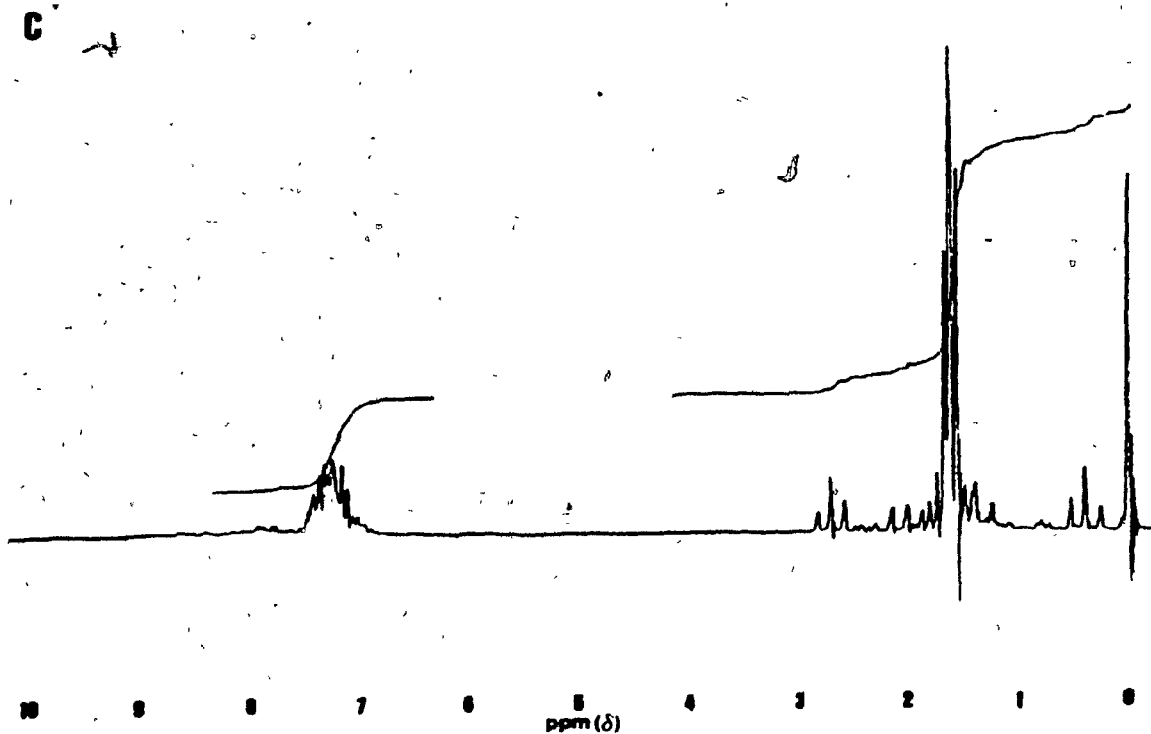
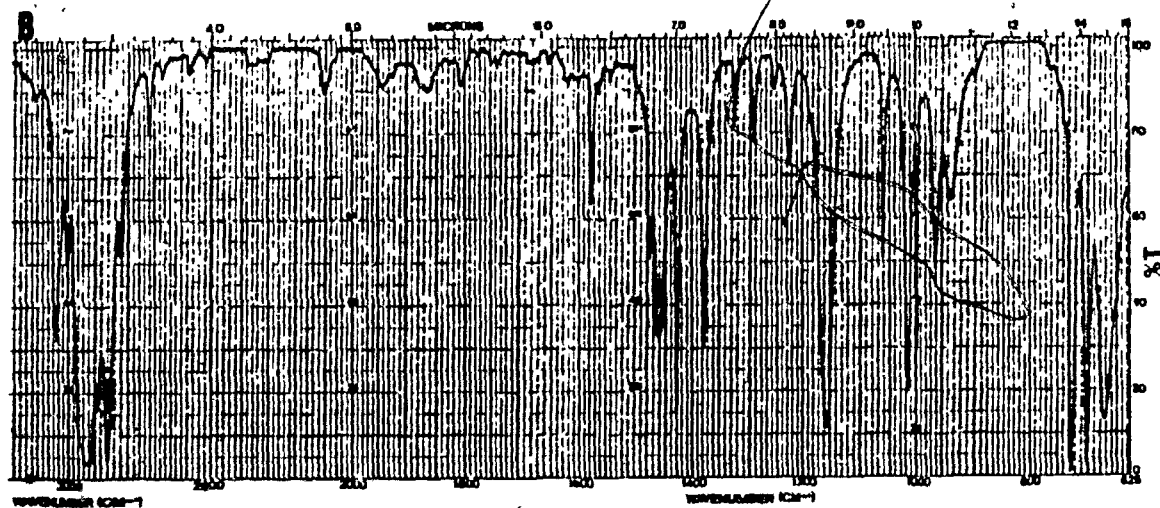
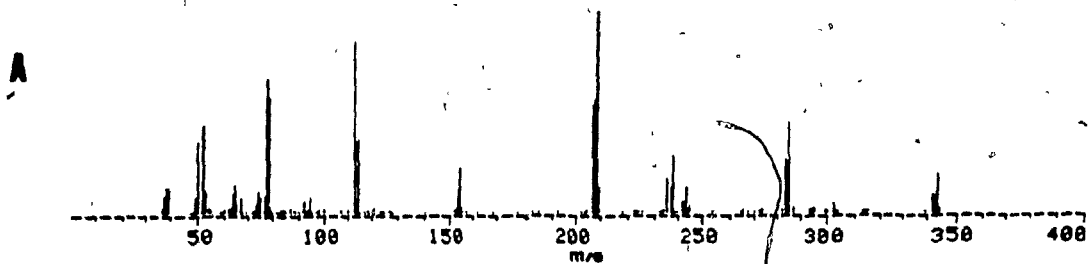


Figure A9. Elemental analysis, (A) mass spectrum, (B) IR spectrum and (C) NMR spectrum of Me_3PhPb .

Elemental Analysis

Calculated: 32.82% C 4.28% H

Found: 32.82% C 3.76% H

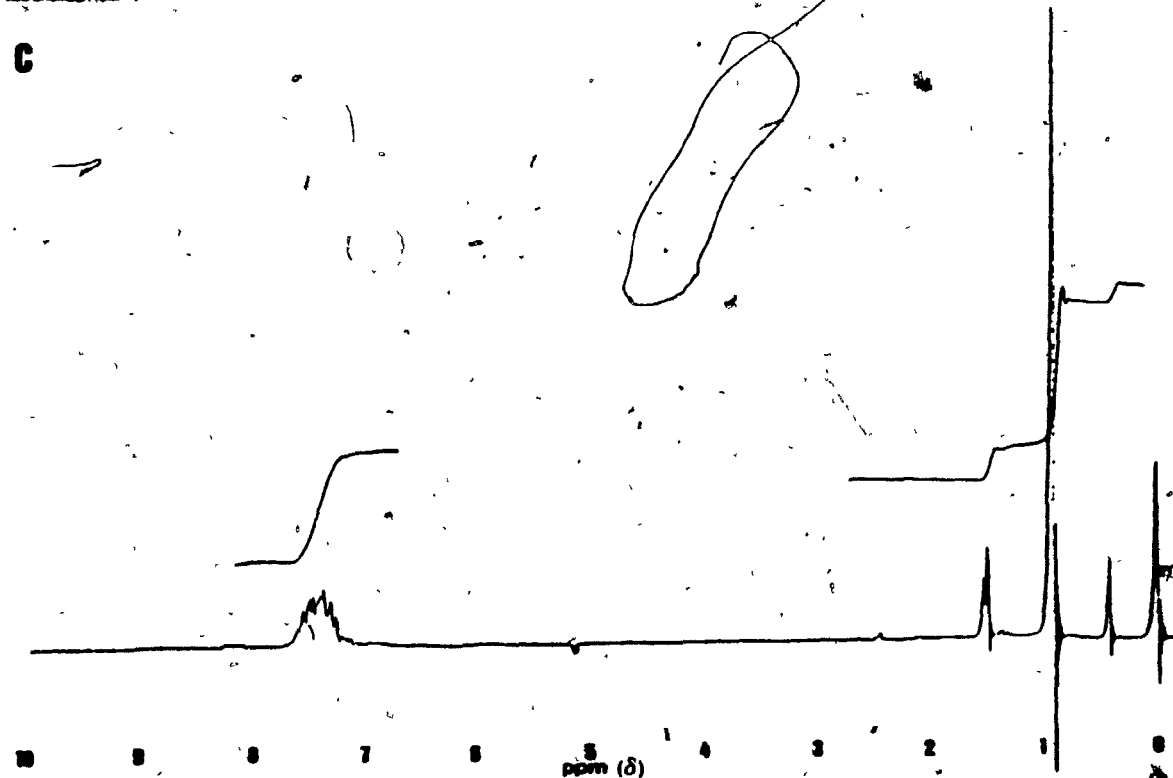
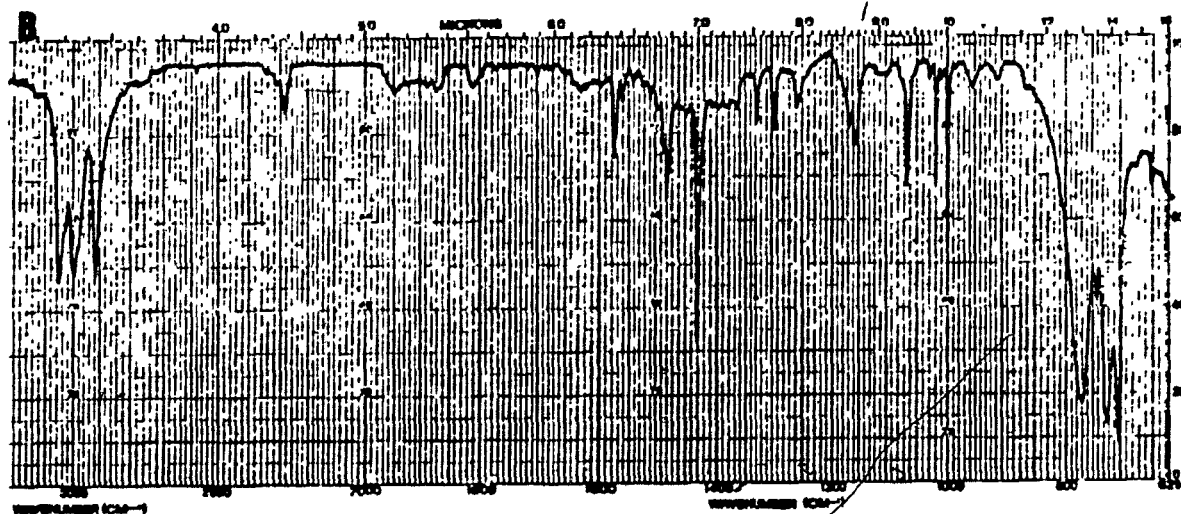
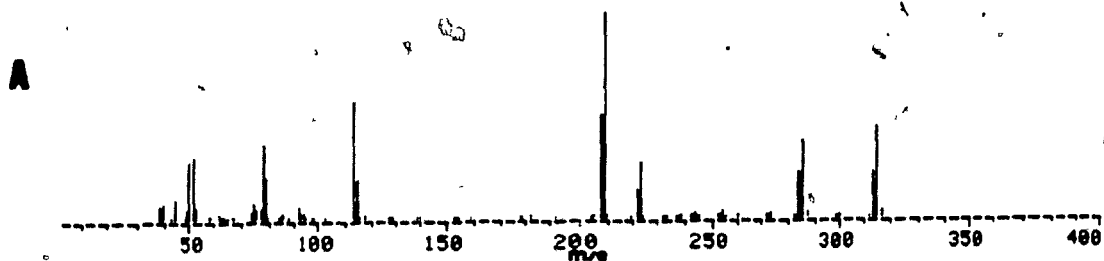


Figure A10. Elemental analysis, (A) mass spectrum, (B) IR spectrum and (C) NMR spectrum of $\text{Me}_2\text{Ph}_2\text{Pb}$.

Elemental Analysis

Calculated: 42.95% C 4.12% H

Found: 42.59% C 3.86% H

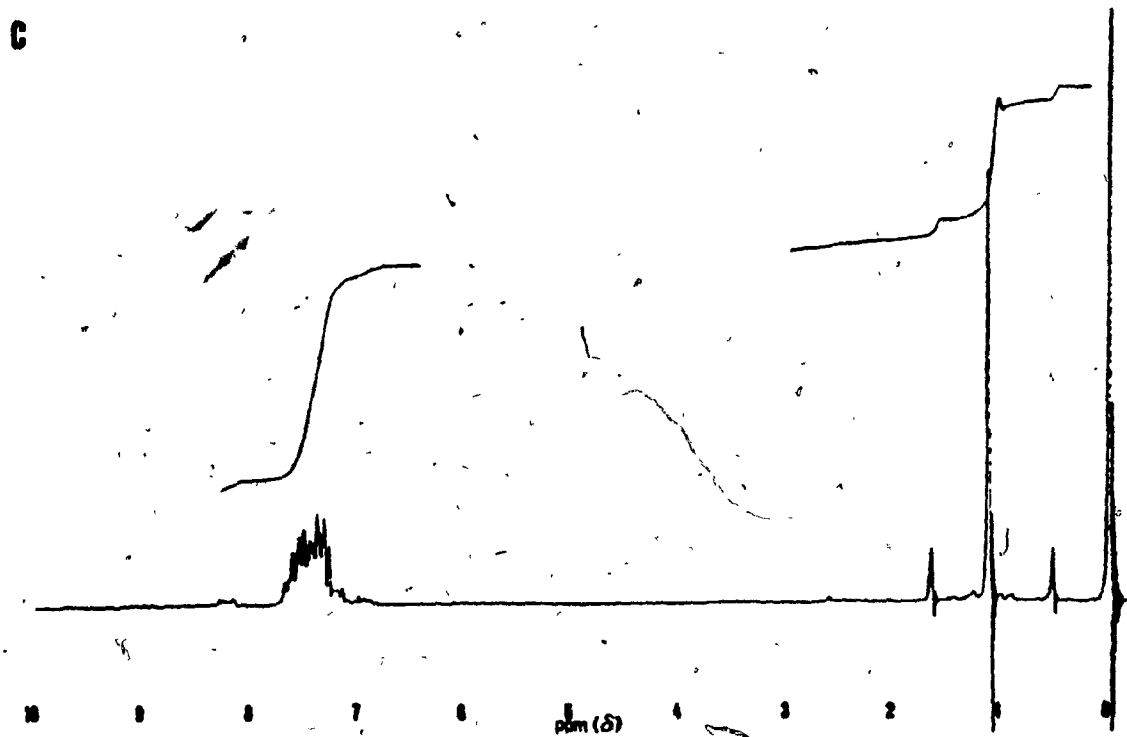
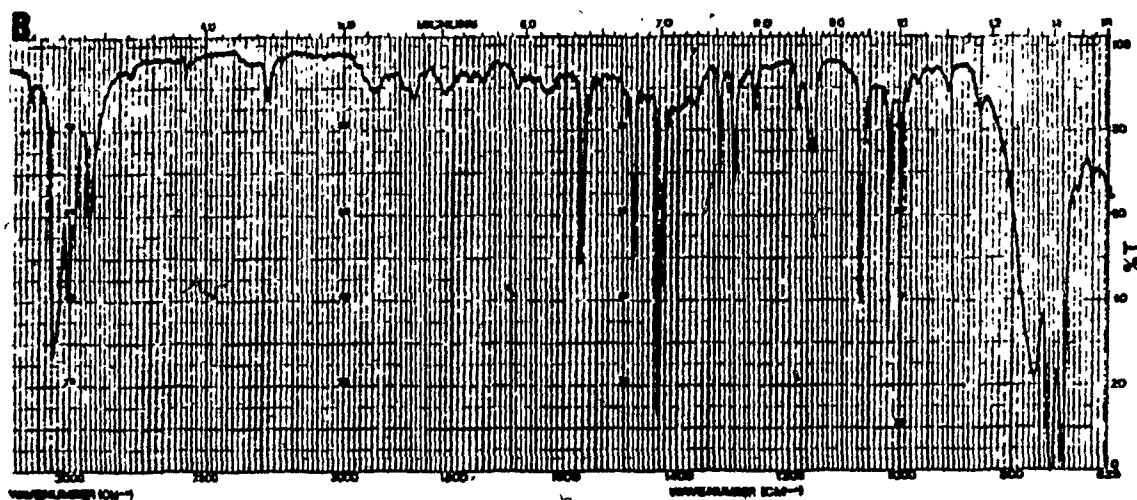
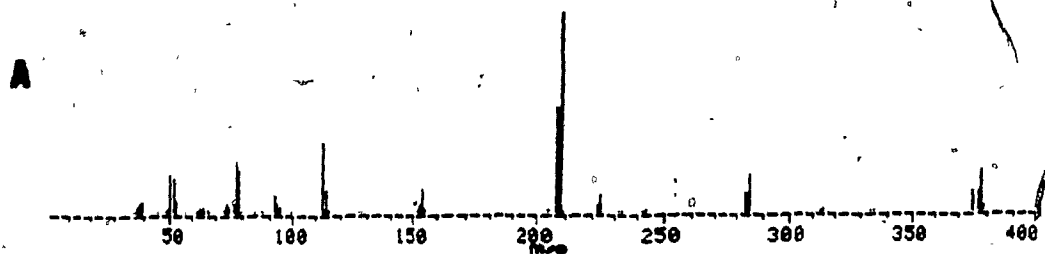
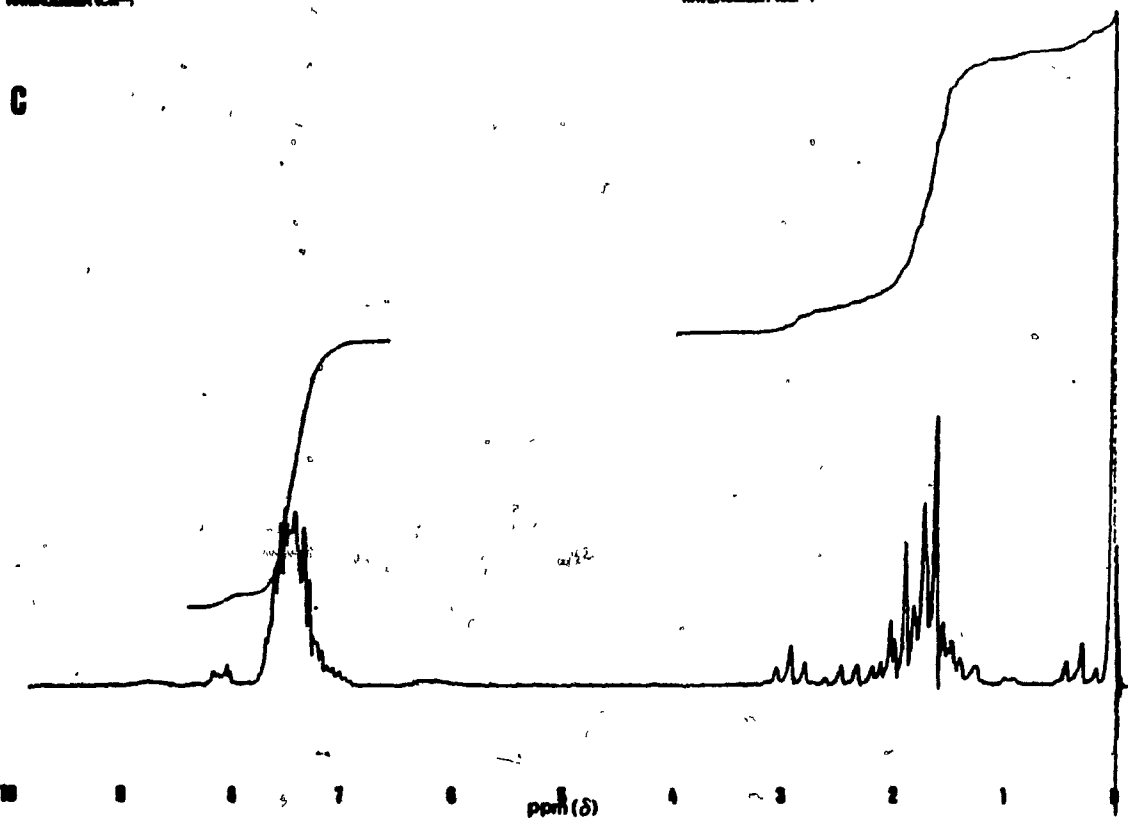
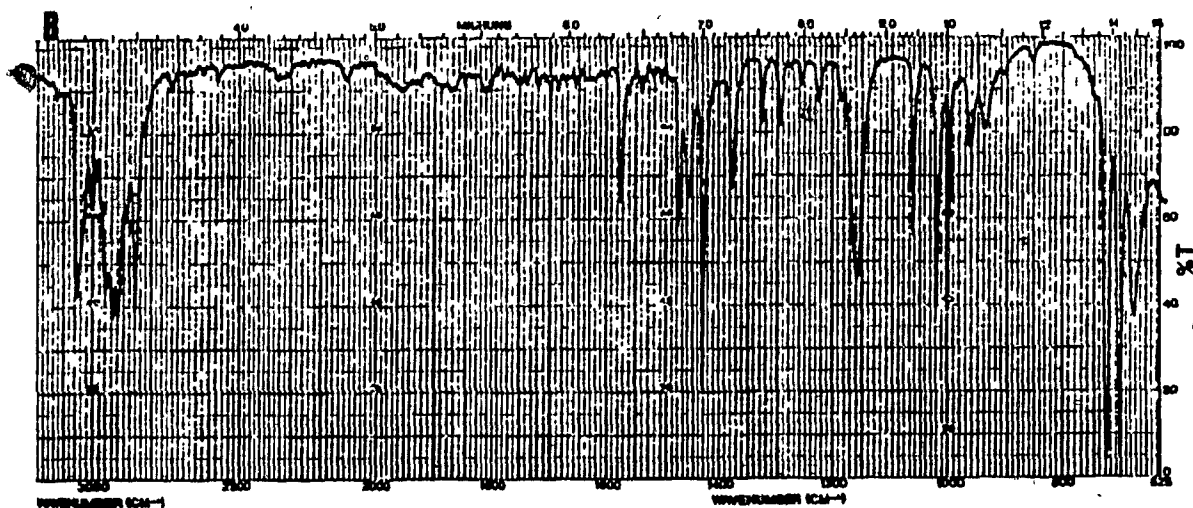
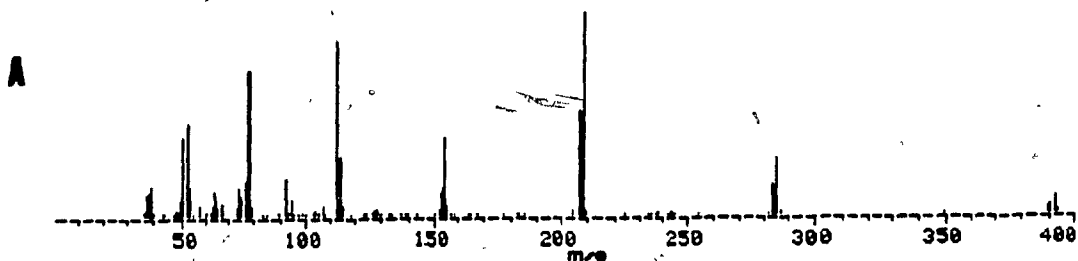


Figure A11. Elemental analysis, (A) mass spectrum, (B) IR spectrum and (C) NMR spectrum of $\text{Et}_2\text{Ph}_2\text{Pb}$.

Elemental Analysis

Calculated: 45.81% C 4.80% H

Found: 45.87% C 4.58% H



clean extracts (Forsyth and Marshall 1983), however, it was found that the phenyl Grignard reagent used was atypically clean, as later lots of Grignard reagent from the same and other sources produced extracts containing interfering peaks when analyzed by GC-ECD or GC-AAS. Although an extract cleanup procedure could have been used, further steps in the analytical procedure were considered undesirable. Butylation, therefore, was selected and found to produce clean extracts suitable for use with the GC-AAS system.

Appendix C. Complexation of organoleads with ammonium pyrrolidine dithiocarbamate (APDC)

Alkyllead and inorganic lead halides were dissolved in distilled water (1 mL). Several drops of 2% (w/v) ammonium pyrrolidine dithiocarbamate (APDC) were added and the resulting lead-PDC complexes extracted with methyl isobutyl ketone.

The complexes were analyzed by Dr. D.B. Maclean, Chemistry Dep't, McMaster University using a VG 7070 mass spectrometer under the following conditions: accelerating voltage, 4 kV; ionization voltage, 70 eV; emission current, 200 μ A; ion source temperature, 180°C.

The mass spectra (Figs. A12A and B, A13A and B, A14) indicated that R_3Pb^+ formed a 1:1 lead:PDC complex, whereas R_2Pb^{2+} and Pb^{2+} formed 1:2 lead:PDC complexes.

Figure A12. Mass spectra of: A, Et_3PbPDC complex; B, $\text{Et}_2\text{Pb}(\text{PDC})_2$ complex.

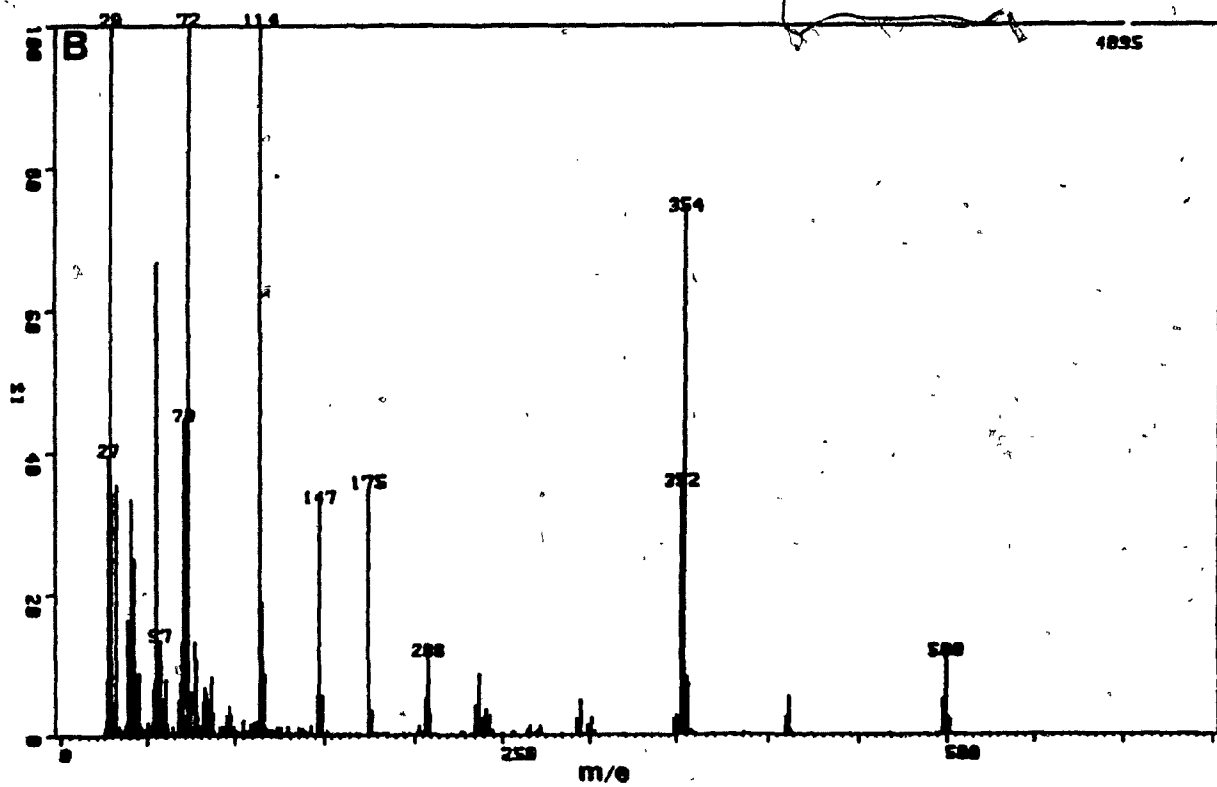
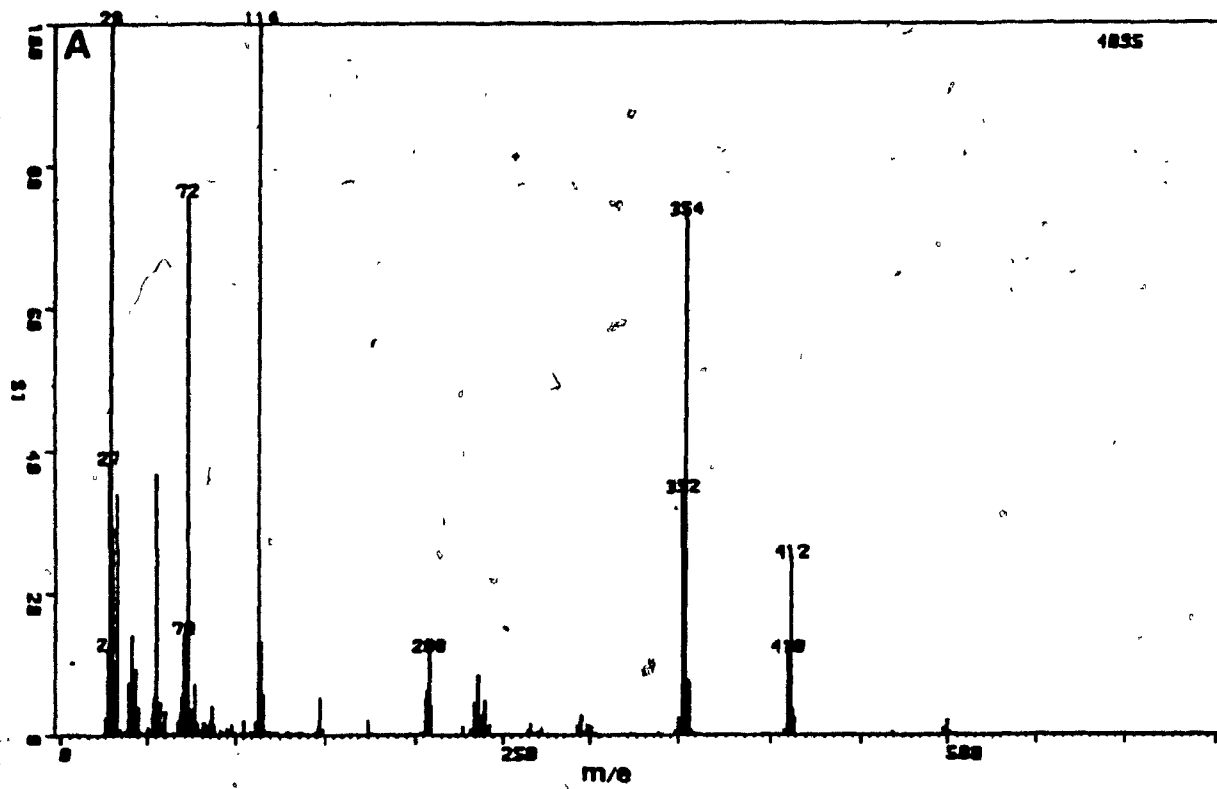


Figure A13. Mass spectra of: A, Me_3PbPDC complex; B, $\text{Me}_2\text{Pb}(\text{PDC})_2$ complex.

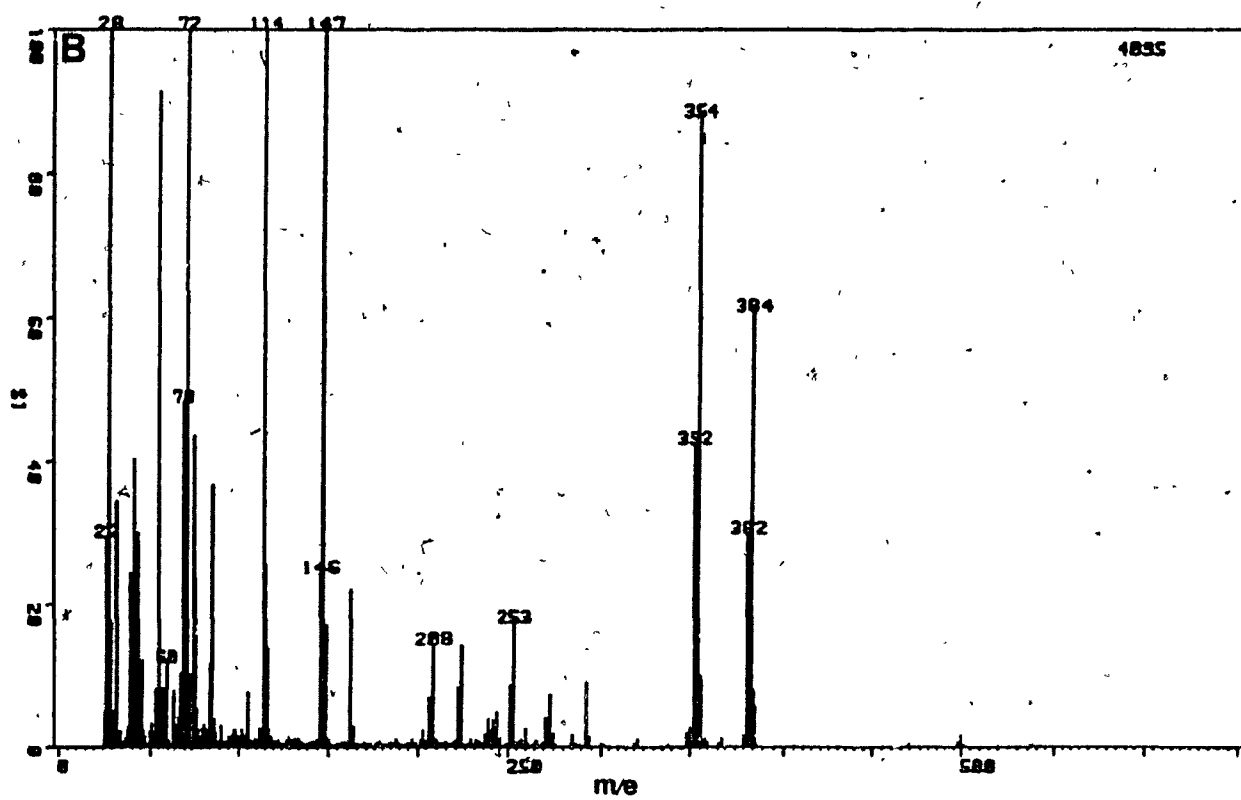
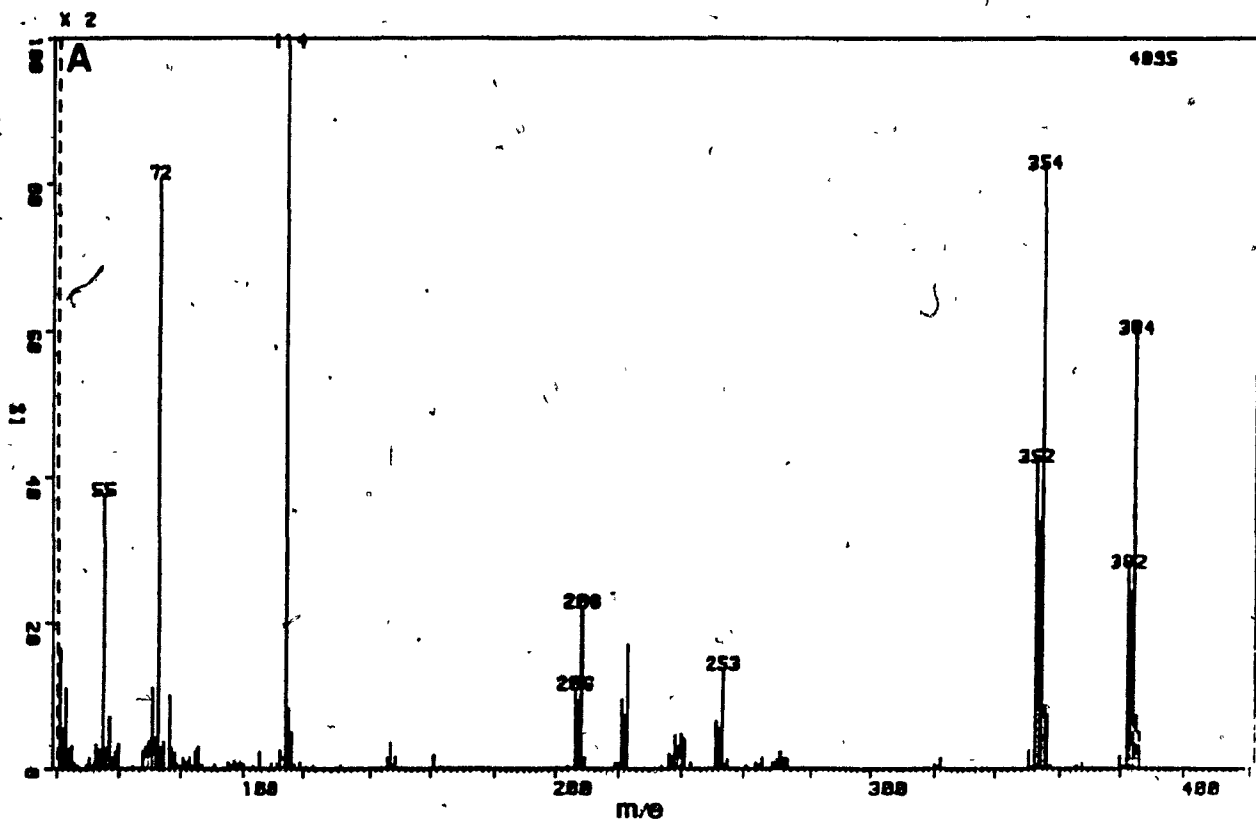
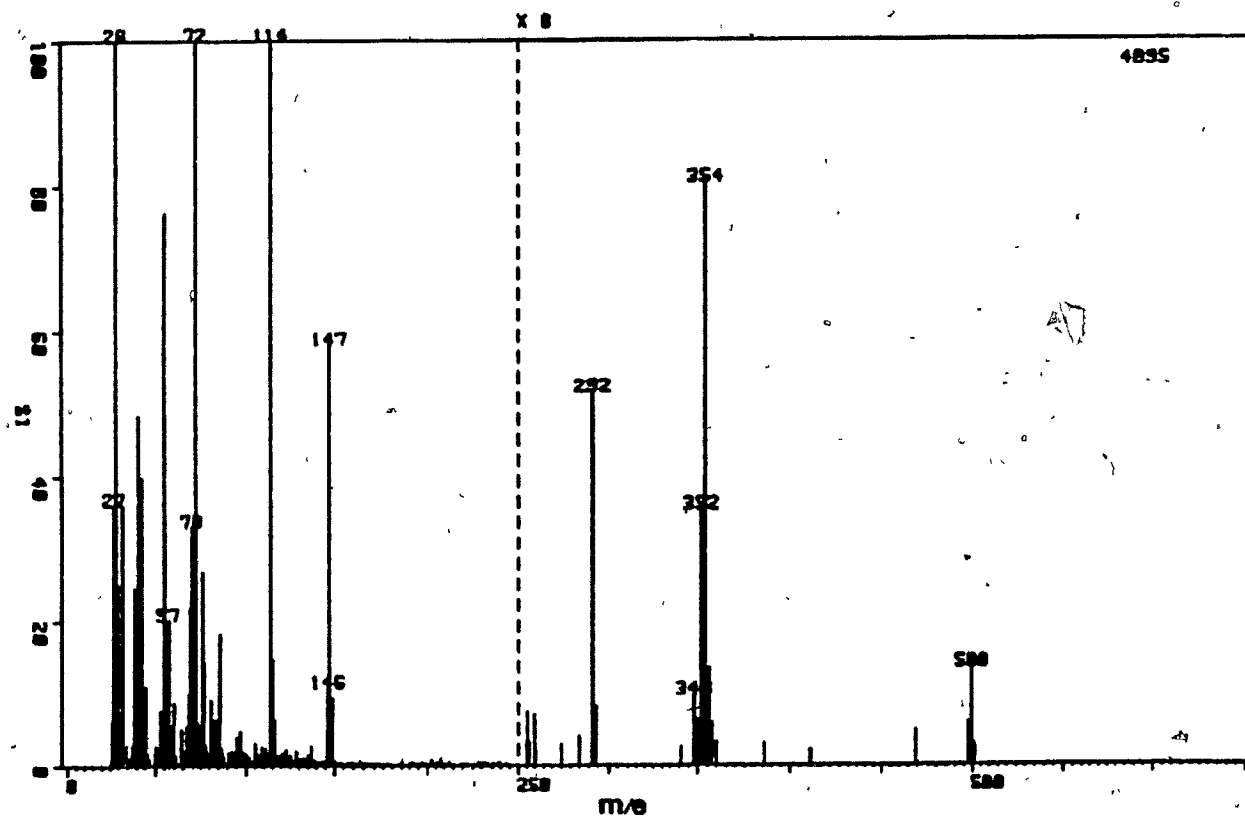


Figure A14. Mass spectrum of $\text{Pb}(\text{PDC})_2$ complex.



Appendix D. Calculations of amino nitrogen

Three replicates of each sample were analyzed using the ninhydrin reaction. Every sample was read against a reagent blank run concurrently with the samples. L-alanine (Calbiochem) standards were run with each group of samples. The amino nitrogen content of the samples was determined by linear regression equations produced from the L-alanine standards. The enzyme or acid hydrolysate amino nitrogen content was corrected for background amino nitrogen by subtraction of the mean hydrolysis (no tissue) blank or acid blank amino nitrogen value respectively.

Sample Calculation: Liver at 24 hours of enzymatic hydrolysis with 40 mg each of protease and lipase added.

The mean (N=3) absorbance of the three replicates were 0.409, 0.442 and 0.403.

The calculated linear regression equation was:

$$\begin{aligned} \text{Absorbance} &= 0.0261 + 0.220x & r &= 0.9989 & N &= 12 \\ x &= \text{amino nitrogen } (\mu\text{g}) \end{aligned}$$

The obtained amino nitrogen values (μg) were 1.74, 1.89 and 1.71.

To determine amino nitrogen (mg), the total hydrolysate volume (22 mL) divided by the sampling volume (5 μL) was multiplied by the amino nitrogen value expressed in milligrams.

$$\begin{aligned}\text{total amino nitrogen (mg)} &= 1.74/1000 * (22000/5) = 7.66 \\ &8.32/1000 * (22000/5) = 8.32 \\ &1.71/1000 * (22000/5) = 7.52\end{aligned}$$

However, each of these samples had been diluted 1:4 prior to absorbance reading, therefore these values were multiplied by 5, resulting in 38.3, 41.6 and 37.6 mg respectively. The mean amino nitrogen value of the hydrolysate (no tissue) blank at 24 h was similarly determined to be 1.5 mg. The background corrected hydrolysate amino nitrogen values were therefore:

$$\begin{aligned}\text{Background corrected} &= 38.3 - 1.5 = 36.8 \\ \text{Amino nitrogen (mg)} &= 41.6 - 1.5 = 40.1 \\ &= 37.6 - 1.5 = 36.1\end{aligned}$$

The mean corrected amino nitrogen value \pm SD was 37.7 ± 2.1 mg.

Appendix E. Calculations for organolead recoveries from biological tissue

A. Calculation for background correction

It was found that unspiked tissue hydrolysates contained organolead compounds. Correction for these background levels of analyte was necessary to prevent heightened recoveries in trace level recovery experiments (Exp'ts D and E, Table 5). Three replicates of unspiked tissue hydrolysate were analyzed by GC-AAS. The organolead analyte peak areas were integrated by a recording integrator (Hewlett Packard 3390A). To correct for slight changes in the sensitivity of the GC-AAS system, the mean peak area of the background organolead was converted to the mean background organolead quantity by interpolation from methyl and ethylbutyllead standards run during the unspiked tissue analysis. This mean background organolead quantity was then converted back to the equivalent background peak area by interpolation from methyl and ethylbutyllead standards run during the analysis of the recovery experiment.

Example Calculation: Me_3Pb^+ recovery from liver (Exp't E, Table 5).

Recovery Sample	Uncorrected Recovery Peak Area		Mean Background Peak Area	=	Corrected Recovery Peak Area
Liver #1	28087	-	8616	=	19471
Liver #2	33023	-	8616	=	24407
Liver #3	25592	-	8616	=	16976
Liver #4	32725	-	8616	=	24109

Mean corrected recovery peak area \pm SD = 21241 \pm 3632 (N=4).

B. Calculation for percentage recovery

The percentage recovery of each analyte was determined by dividing the mean peak area of the recovered butylate by the mean peak area of the butylate

in the recovery "standards". Four replicate "standards" were made by butylating an appropriate amount of organolead spiking solution, which was diluted to the expected (assuming 100% recovery) sample concentration.

Sample Calculation: Me_3Pb^+ from liver (Exp't E, Table 5).

The mean peak area \pm SD of Me_3BuPb in the recovery "standards" was 213932 ± 1399 (N=4).

Mean recovery = $21241 \pm 3632 / 21392 \pm 1399$

The quotient error was calculated by the equation:

$$\text{SD}_{\text{quotient}} = A/B \sqrt{(\text{SD}_A/A)^2 + (\text{SD}_B/B)^2}$$

where A = mean recovered peak area

B = mean recovery "standard" peak area

SD_A = standard deviation of A

SD_B = standard deviation of B

$$\begin{aligned} \text{Mean recovery } \pm \text{SD} &= 21241/21392 \pm 21241/21392 \sqrt{(3632/21241)^2 + (1399/21392)^2} \\ &= 0.993 \pm 0.182 \end{aligned}$$

$$\begin{aligned} \text{Mean \%recovery } \pm \text{SD} &= 0.993 \times 100 \pm 0.182 \times 100 \\ &= 99 \pm 18\% \end{aligned}$$

Appendix F. High pressure liquid chromatography-atomic absorption spectroscopy.

A high pressure liquid chromatography (HPLC) system consisting of a HPLC pump (Altex Model 110, Altex Scientific Inc.), syringe loading injector (Rheodyne Model 7125, Rheodyne Inc.) and HPLC column was interfaced with a Zeiss FMD-3 atomic absorption spectrophotometer (AAS) (Carl Zeiss, FRG) (Fig. A15). The solvent flow from the injector was connected to an AAS quartz T-tube furnace (Fig. A16) by a HPLC-AAS interface (Fig. A17).

Normal HPLC-AAS system operating conditions were:

- (a) HPLC- solvent flow rate, 1 mL min^{-1}
- (b) AAS furnace- upper and lower tube temperature, $950\text{--}1000^\circ\text{C}$; air flow rate, 400 mL min^{-1} ; H_2 flow rate, 320 mL min^{-1} .
- (c) AAS-hollow cathode lamp current 7 ma; wavelength, 283.3 nm; slit width, 0.3 mm; band width 0.75 nm; photomultiplier tube amplifier, step 1 (lowest setting); deuterium lamp current, 200 ma.

Quartz T-tube furnace

The furnace design (Fig. A16) was modified from Chau et al. (1975). The quartz T-tube was heated by two independent coiled nickel-chromium resistance alloy wire elements (Chromel A, Hoskins Manufacturing Co.). Power to the heating elements was supplied by two Variac variable transformers and the current monitored by ampere meters. Two type K (Chromel-Alumel) thermocouples were positioned near the lower element for temperature monitoring, with a third inserted in the upper quartz tube during furnace warmup. The quartz T-tube was

Figure A15. HPLC-AAS system: A, Variac variable voltage transformers; B, electronic temperature monitor; C, Altex model 110 HPLC pump; D, HPLC column (used as a pulse dampener in this configuration); E, Rheodyne model 7125 syringe loading sample injector; F, monochromator; G, ampere meters; H, quartz furnace assembly; I, type K thermocouple; J, furnace position adjuster; K, gas rotameter; L, lamp turret; M, amplifier, AAS electronics.

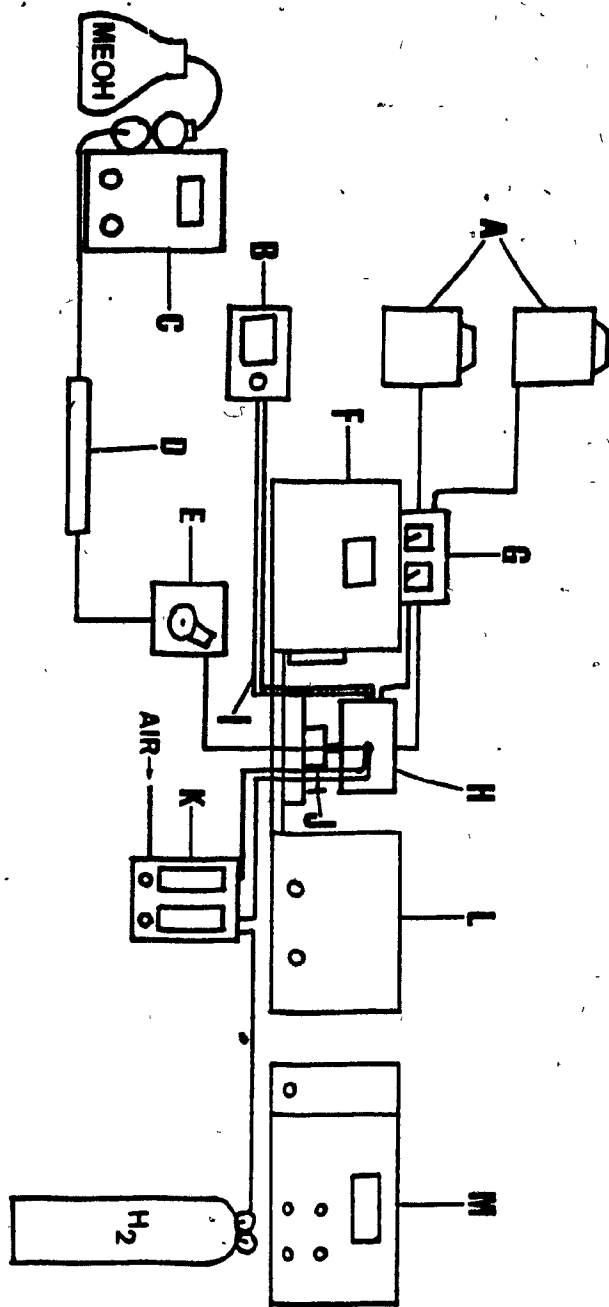
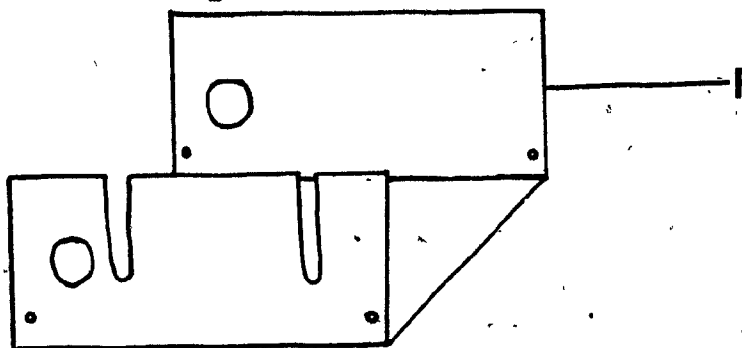
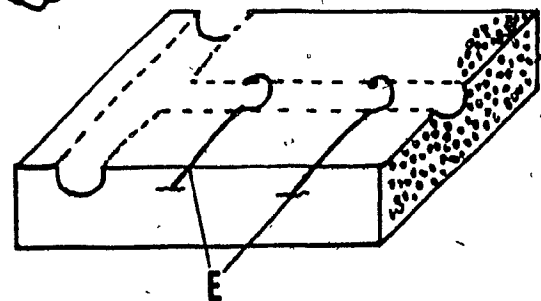
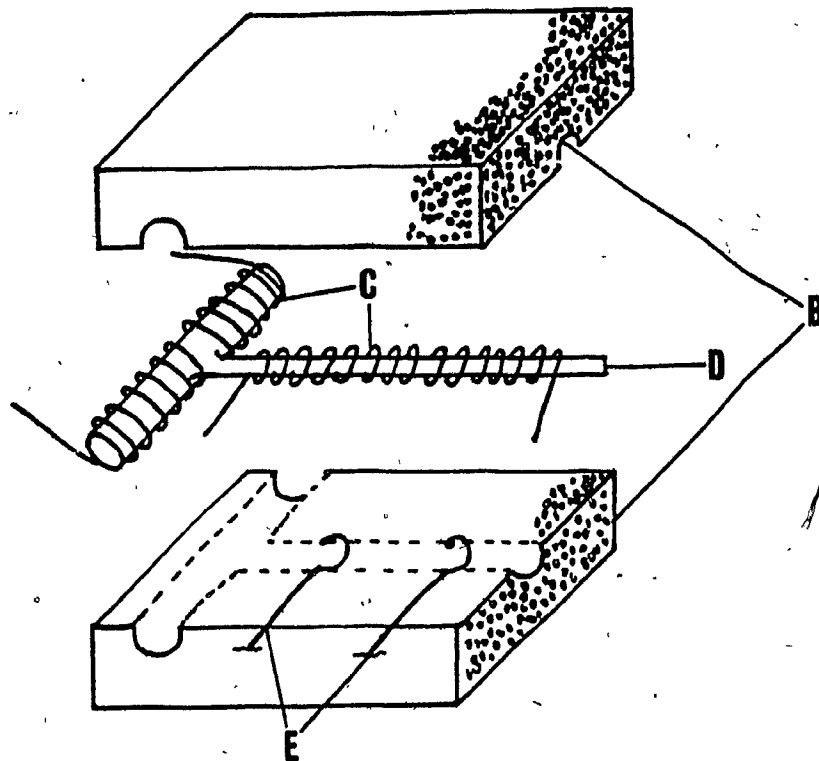
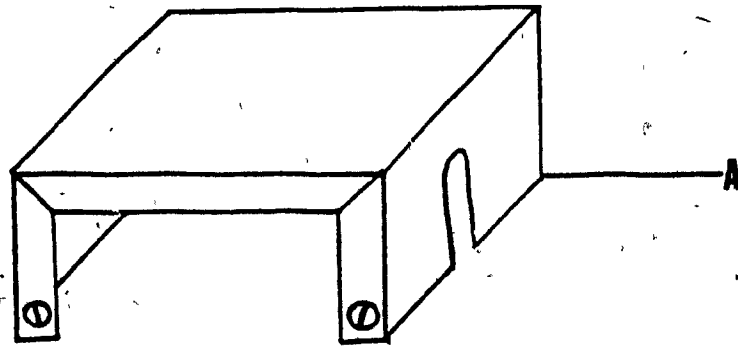


Figure A16. Exploded view of quartz T-tube furnace: A, aluminum casing, upper section, 105 cm X 6.9 cm X 5.2 cm; B, refractory brick; C, heating elements, upper element coiled from 152 cm of Chromel A electrical resistance wire, gauge 24, lower element coiled from 122 cm of same material; D, quartz T-tube, upper tube 6 cm X 9 mm i.d., 11 mm o.d., lower tube 10 cm X 4 mm i.d., 6.15 mm o.d.; E, type K (Chromel-Alumel) thermocouples; F, aluminum casing, lower section, 10 cm X 6.6 cm X 5.0 cm.



covered with Fiberfrax ceramic cloth (The Carborundum Co.) and two shaped sections of refractory brick (A.P. Green Fire Brick Co.) held together by an aluminum enclosure.

HPLC-AAS Interface

The nebulizer design (Fig. A17) utilized readily available parts, which required little modification. The Swagelok 1/4 in (0.64 cm) to 1/8 in (0.32 cm) reducing union was drilled out to 1/8 in (0.32 cm) to allow a 1/8 in (0.32 cm) stainless steel (S.S.) tube to pass through to the Swagelok 1/8 in (0.32 cm) tee union. Air was introduced through inlet K (Fig. A17) (1/16 in (0.16 cm) S.S. tubing silver soldered into the reducing union), whereas, hydrogen entered through inlet L (Fig. A17) and was entrained between parts A (Fig. A17) and E (Fig. A17). The HPLC solvent passed through a 0.01 in (0.025 mm) i.d., 1/16 in (0.16 cm) o.d. S.S. tube into the furnace. A flame ignited directly in front of the nebulizer tip, where the entrained H_2 and air came in contact. Flameless operation allowed the formation of solvent droplets, excessive signal noise and poor detector response to the organolead compounds.

Various concentrations of Et_3PbCl were injected (10 μ L volume) into the quartz T-tube furnace to examine AAS system sensitivity and linearity. The HPLC separation of alkyllead halides was examined using a 4.6 X 250 mm Altex Ultrasphere (5 μ m) SI column (Altex Scientific Inc.) with various tetrahydrofuran:hexane:organic acid (propionic and acetic) mobile phases.

The AAS system responded linearly to the amount of organic lead injected (Fig. A18). The detection limit was estimated to be approximately 1-5 ng Pb.

Tetrahydrofuran was substituted for acetone (used in thin-layer

Figure A17. Exploded view of HPLC-AAS interface: A, stainless steel tubing, 13 cm X 1/16 in (0.16 cm) o.d., 0.01 in (0.025 cm) i.d.; B, Swagelok 1/8 in (0.32 cm) tee union; C, 1/8 in (0.32 cm) to 1/16 in (0.16 cm) teflon reducing ferrules; D, 1/8 in (0.32 cm) Swagelok nuts; E, stainless steel tubing, 7.9 cm X 1/8 in (0.32 cm) o.d., 3/32 in (0.24 cm) i.d.; F, 1/8 in (0.32 cm) Vespel ferrules; G, Swagelok 1/4 in (0.64 cm) to 1/8 (0.32 cm) reducing union; H, 1/4 in (0.64 cm) graphite ferrule; I, 1/4 in (0.64 cm) Swagelok nut; J, lower tube of quartz furnace, 6.15 mm o.d.; K, H₂ inlet; L, air inlet.

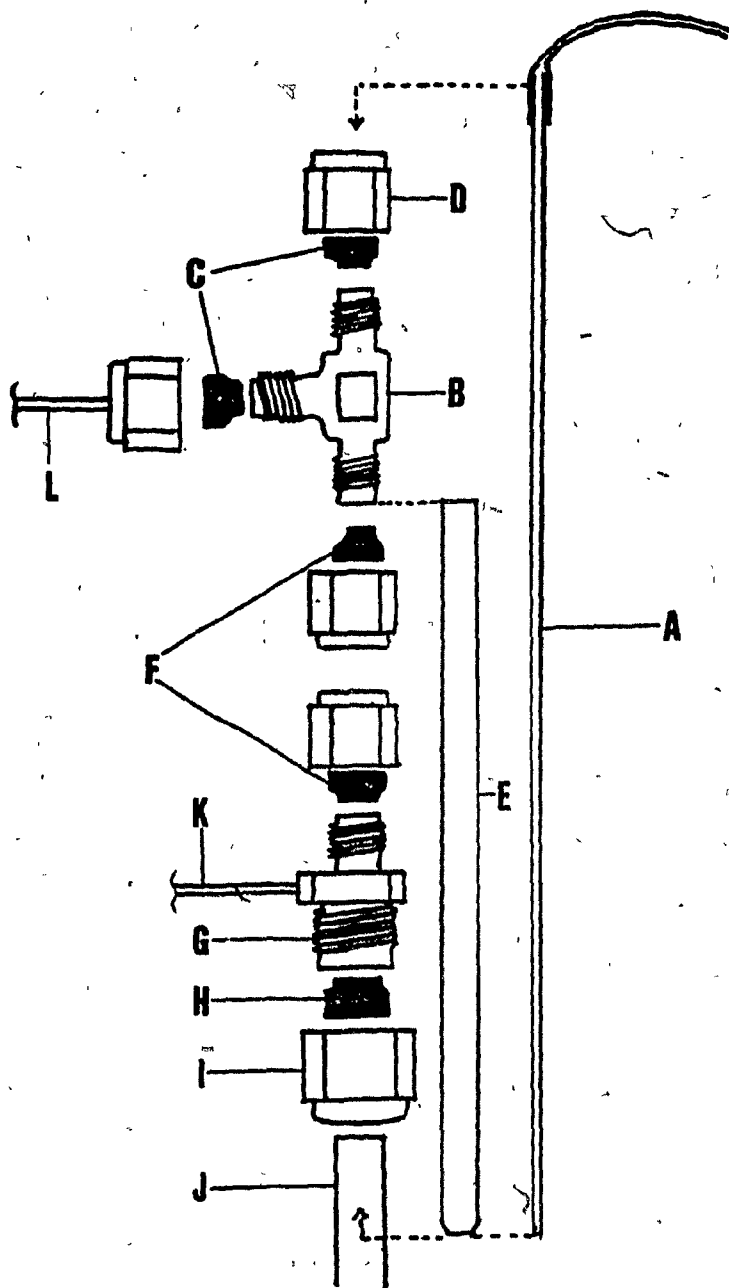
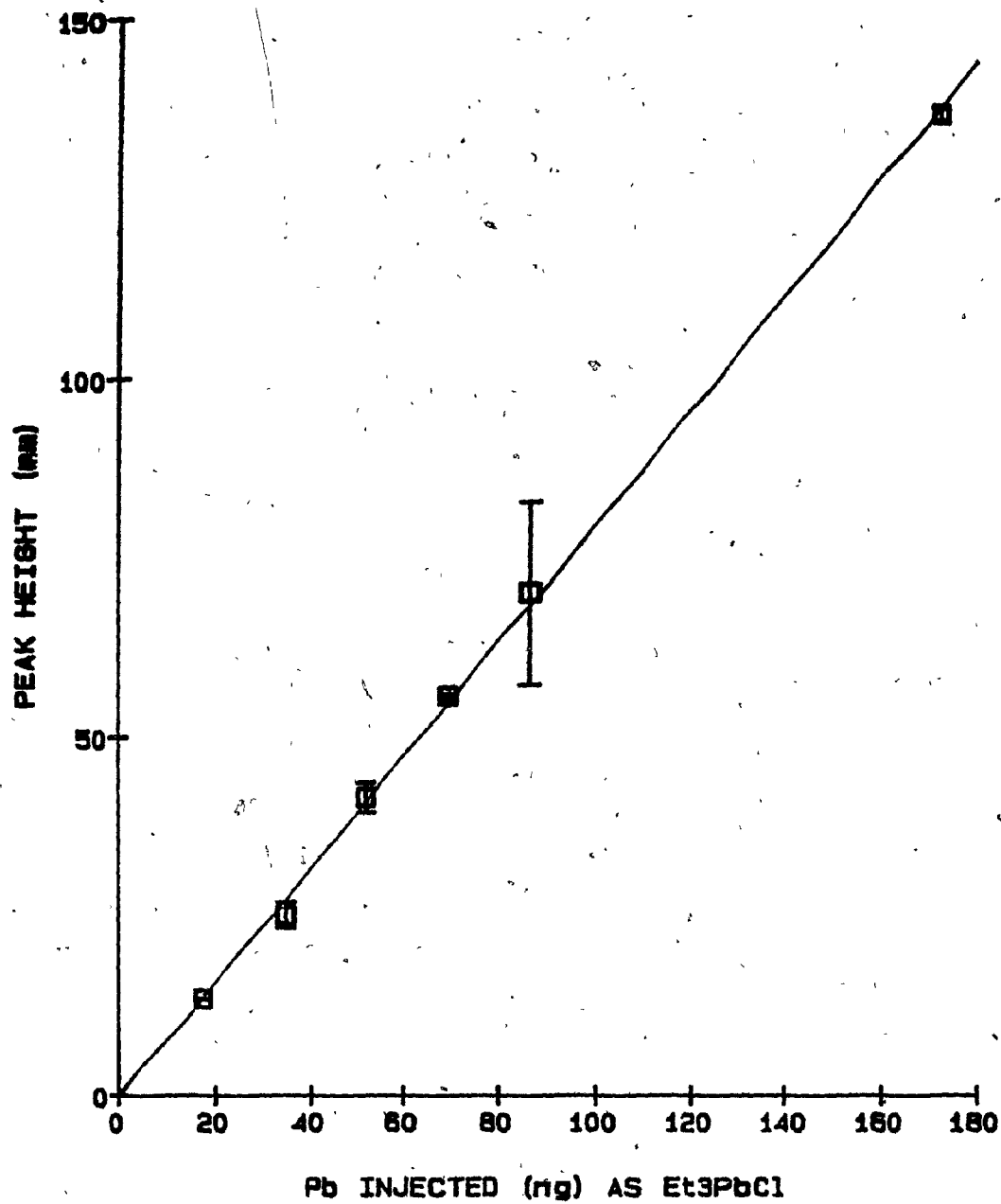


Figure A18. Response of HPLC-AAS to 17.2-172 ng Pb as Et_3PbCl . Error bars represent \pm one standard deviation of three replicate determinations.



chromatography) because of cleaner burning in the quartz T-tube furnace. The organic acids were added to the mobile phase to reduce solute tailing by blocking hydrogen bonding sites on the silica surface (Lawrence and Leduc 1978). Propionic and formic acid, (10% (v/v)) in the mobile phase reduced tailing of Et_3PbCl but Me_3PbCl tailed extensively. Acetic acid (10% (v/v)), was not as effective on the peak shape of Et_3PbCl but did improve the peak shape of Me_3PbCl . Although baseline separation of Et_3PbCl and Me_3PbCl was possible (with 1:7:3 propionic:THF:hexane) the dialkyllead dichlorides chromatographed very poorly under all tested conditions. It was considered that HPLC separation was likely possible with ion pairing or reverse chromatography of complexed alkylleads (Appendix C) but the dilution factor imposed by conventional analytical columns would exclude trace analysis. The recent introduction of microbore HPLC columns, may permit the direct trace analysis of underivatized ionic alkyllead compounds.

Appendix G. Effects of parameters on GC-AAS system
sensitivity and analyte peak shape

1. H₂ furnace makeup gas flow rate

Analyte H ₂		-----Analyte Concentration (g/mL)-----			
flow rate		10 ⁻⁹	10 ⁻⁸	10 ⁻⁷	10 ⁻⁶
(mL/min)					
		-----Mean Peak Height Response+SD-----			
		----- (Mean Area/Height Ratio+SD) -----			
Me3	0	-	-	-	3164+1935 (.0160+0.006)
Me2		-	-	-	25221+666 (0.151+0.002)
Et3		-	-	-	18599+642 (0.174+0.007)
Et2		-	-	-	14711+2200 (0.161+0.015)
Me3	15	9848+1851 (0.269+0.019)	65997+1667 (0.186+0.005)	671333+6613 (0.174+0.002)	3746167+29267 (0.275+0.002)
Me2		6736+266 (0.200+0.002)	61788+1193 (0.189+0.003)	617947+4863 (0.178+0.001)	3219500+22990 (0.240+0.001)
Et3		5585+558 (0.247+0.016)	43138+2350 (0.213+0.012)	421910+2144 (0.200+0.003)	2942500+10770 (.0235+0.001)
Et2		6104+974 (0.286+0.002)	32289+673 (0.195+0.006)	313080+1809 (0.180+0.001)	2546300+12836 (0.206+0.001)
Me3	25	8902+339 (0.178+0.002)	78957+1128 (0.164+0.003)	779823+838 (0.163+0)	3583500+27487 (0.260+0.002)
Me2		8999+554 (0.193+0.008)	71182+686 (0.166+0.001)	703577+3306 (0.163+0.001)	3194333+36094 (.0234+0.002)
Et3		5580+472 (0.200+0.005)	44481+1936 (0.174+0.004)	445090+4422 (0.173+0.002)	2789800+45230 (0.217+0.003)
Et2		4764+1061 (0.197+0.036)	36160+1028 (0.166+0.002)	363453+3960 (0.166+0.001)	2516067+23974 (0.197+0.001)
Me3	50	7941+910 (0.185+0.017)	65792+746 (0.164+0.001)	659667+5863 (0.158+0.001)	3187467+28719 (0.230+0.003)
Me2		6654+765 (0.183+0.012)	60648+662 (0.167+0.002)	590833+4258 (0.158+0.001)	2975700+14052 (0.216+0.001)
Et3		4254+870 (0.189+0.037)	36913+1342 (0.173+0.005)	363670+3192 (0.166+0.002)	2500733+10762 (0.195+0.001)
Et2		3811+753 (0.187+0.038)	32191+759 (0.176+0.002)	300233+1802 (0.162+0.002)	2272033+13670 (0.182+0)

Appendix G cont'd

Analyte H ₂		Analyte Concentration (g/mL)			
flow rate		10 ⁻⁹	10 ⁻⁸	10 ⁻⁷	10 ⁻⁶
(mL/min)					
		-----Mean Peak Height Response+SD----- ----- (Mean Area/Height Ratio+SD) -----			
Me3	75	6508+992 (0.173+0.016)	57294+619 (0.165+0.002)	563120+2967 (0.158+0.001)	300900+22853 (0.219+0.001)
Me2		6068+2131 (0.188+0.044)	51065+951 (0.165+0.003)	500890+1434 (0.156+0)	2798133+5928 (0.205+0)
Et3		3888+1160 (0.222+0.052)	30959+352 (0.170+0.002)	306046+593 (0.163+0)	2266433+5530 (0.184+0.001)
Et2		3959+669 (0.219+0.039)	26305+670 (0.169+0.004)	253380+1662 (0.161+0.002)	2047100+5981 (0.174+0.001)
Me3	100	5133+315 (0.206+0.021)	39302+468 (0.169+0.001)	390293+4316 (0.154+0.001)	2565867+4234 (0.192+0)
Me2		4339+627 (0.181+0.022)	35800+1047 (0.172+0.004)	248040+2296 (0.155+0.001)	2394967+2627 (0.183+0)
Et3		2901+584 (0.204+0.043)	20709+1683 (0.173+0.011)	208437+997 (0.162+0)	1767522+4508 (0.166+0.001)
Et2		3238+1290 (0.248+0.083)	18422+1142 (0.176+0.007)	177743+1148 (0.161+0.001)	1561900+624 (0.161+0)
Me3	150	3107+573 (0.196+0.032)	23697+544 (0.156+0.002)	217907+1163 (0.146+0)	1775900+2390 (0.161+0.001)
Me2		2944+973 (0.183+0.049)	20761+1193 (0.155+0.009)	194287+1075 (0.147+0)	1627033+2001 (0.160+0.001)
Et3		2451+539 (0.219+0.055)	11278+534 (0.148+0.003)	113497+290 (0.149+0.001)	1044833+4130 (0.154+0.001)
Et2		1120+19 (0.156+0.004)	10566+329 (0.158+0.005)	98454+979 (0.150+0.002)	919490+1690 (0.153+0.001)

Me3- Me₃BuPbMe2- Me₂Bu₂PbEt3- Et₃BuPbEt2- Et₂Bu₂Pb

Appendix G cont'd.

2. Furnace temperature

Furnace Temp. (°C)	Analyte (10^{-7} g/mL)			
	Me ₃ BuPb	Me ₂ Bu ₂ Pb	Et ₃ BuPb	Et ₂ Bu ₂ Pb
	-----Mean Peak Area Response+SD----- ----- (Mean Area/Height Ratio+SD) -----			
600	284620+8647 (0.222+0.004)	280790+4166 (0.212+0.004)	271247+1795 (0.288+0.003)	182733+3260 (0.216+0.002)
700	582483+16130 (0.163+0.004)	552477+674 (0.164+0.001)	348243+1050 (0.173+0.001)	285437+1532 (0.160+0.001)
800	670940+20152 (0.153+0.006)	618227+7297 (0.154+0.001)	375627+3018 (0.158+0.001)	318910+1991 (0.156+0.001)
900	697863+6421 (0.153+0.001)	622370+571 (0.153+0.001)	373347+708 (0.155+0)	320247+55 (0.155+0)
1000	688653+1498 (0.151+0.001)	613270+1278 (0.151+0)	365440+643 (0.152+0)	316677+280 (0.152+0.001)

3. Furnace makeup gas

Makeup Gas	Analyte (10^{-7} g/mL)			
	Me ₃ BuPb	Me ₂ Bu ₂ Pb	Et ₃ BuPb	Et ₂ Bu ₂ Pb
	-----Mean Peak Area Response+SD----- ----- (Mean Area/Height Ratio+SD) -----			
H ₂	659667+5863 (0.158+0.001)	590833+4258 (0.158+0.001)	363670+3192 (0.166+0.002)	300233+1802 (0.162+0.002)
NH ₃	366993+8248 (0.151+0.001)	328419+9353 (0.153+0.001)	197429+6462 (0.156+0.002)	169068+4012 (0.156+0.001)
1:1 H ₂ :NH ₃	390886+9371 (0.149+0.001)	347578+10095 (0.151+0.001)	208828+5679 (0.153+0.001)	179747+5601 (0.154+0.004)
N ₂	216817+19223 (0.304+0.005)	154937+7406 (0.236+0.010)	173427+24627 (0.349+0.037)	93972+13089 (0.303+0.023)
CH ₄	197060+5957 (0.164+0.003)	187693+2982 (0.165+0.001)	114207+4529 (0.176+0.004)	89090+1771 (0.162+0.002)
He	9176+984 (0.183+0.020)	8426+849 (0.193+0.014)	5648+1477 (0.189+0.041)	6077+2962 (0.254+0.071)
Air	2887+266 (0.191+0.005)	1870+306 (0.158+0.023)	-	-

4. Transfer line position from upper tube of AAS furnace

Position (mm)	Analyte (10^{-7} g/mL)			
	Me ₃ BuPb	Me ₂ Bu ₂ Pb	Et ₃ BuPb	Et ₂ Bu ₂ Pb
	-----Mean Peak Area Response+SD-----			
	----- (Mean Area/Height Ratio+SD) -----			
0	652137+10352 (0.152+0.002)	576156+5572 (0.153+0.002)	342810+3232 (0.158+0.002)	293050+4958 (0.155+0.003)
5	656127+11417 (0.156+0.002)	587833+4975 (0.156+0.002)	349853+10067 (0.160+0.001)	299467+1528 (0.157+0.001)
10	651447+7447 (0.166+0.001)	543000+4163 (0.168+0.001)	317347+1727 (0.183+0.001)	249237+4515 (0.175+0.001)
20	637867+6515 (0.163+0.001)	545063+3275 (0.169+0.001)	319900+2694 (0.183+0.001)	257430+2389 (0.178+0.002)

5. GC column flow rate

Flow Rate (mL/min)	Analyte (10^{-7} g/mL)			
	Me ₃ BuPb	Me ₂ Bu ₂ Pb	Et ₃ BuPb	Et ₂ Bu ₂ Pb
	-----Mean Peak Area Response+SD-----			
	----- (Mean Area/Height Ratio+SD) -----			
20	726797+20385 (0.175+0.006)	635137+19230 (0.172+0.010)	406943+15574 (0.178+0.001)	317863+14950 (0.170+0.004)
35	753850+5981 (0.156+0.002)	652357+21349 (0.161+0.006)	413153+16375 (0.161+0.002)	351140+1629 (0.154+0.001)
55	705580+23033 (0.154+0.001)	633170+8403 (0.154+0.002)	375870+5086 (0.156+0.003)	326627+2034 (0.155+0.005)
77	539020+3036 (0.159+0.001)	480927+2291 (0.158+0)	286780+239 (0.160+0.001)	243637+1074 (0.161+0.001)

Appendix H. GC column resolution of $\text{Me}_2\text{Bu}_2\text{Pb}$ and Et_3BuPb (10^{-7} g/mL)

GC Column	T_{r1}	T_{r2}	$W_{h/21}$	$W_{h/22}$	W_{b1}	W_{b2}	R
Gas Flow Rate ($\mu\text{L min}^{-1}$)	(min)	(min)	(min)	(min)	(min)	(min)	
20	14.91	15.34	0.162	0.167	0.275	0.284	1.54
35	14.21	14.63	0.151	0.151	0.257	0.257	1.63
55	13.62	14.02	0.145	0.146	0.246	0.248	1.62
77	12.48	12.88	0.148	0.150	0.251	0.255	1.58

T_{r1} - retention time of $\text{Me}_2\text{Bu}_2\text{Pb}$

T_{r2} - retention time of Et_3BuPb

$W_{h/21}$ - half height peak width of $\text{Me}_2\text{Bu}_2\text{Pb}$,
calculated by $0.939 \cdot \text{AR} / \text{HT}$

$W_{h/22}$ - half height peak width of Et_3BuPb ,
calculated by $0.939 \cdot \text{AR} / \text{HT}$

W_{b1} - baseline peak width of $\text{Me}_2\text{Bu}_2\text{Pb}$,
calculated by $W_{h/21} \cdot (4/2.354)$ (from Simpson 1976)

W_{b2} - baseline peak width of Et_3BuPb ,
calculated by $W_{h/22} \cdot (4/2.354)$

R= $2[(T_{r1} - T_{r2}) / (W_{b1} + W_{b2})]$ (from Simpson 1976)

Appendix I. Analysis of variance and t-tests of linear regression equations

Me₃BuPb Y=1624.3 + 266.3X N=9

Source	SS	df	MS	F	Prob>F	r ²	SD _{reg}
Regression	1.202e+12	1	1.202e+12	213698	0.0001	0.9999	2371.4
Residual	39364106.7	7	5623443.8				

Parameter	Value	SD	t	Prob>t
Intercept	1624.3	1026.1	1.58	0.157
Slope	266.3	0.576	462.3	0.0001

Me₂Bu₂Pb Y=2019.6 + 268.3X N=9

Source	SS	df	MS	F	Prob>F	r ²	SD _{reg}
Regression	9.438e+12	1	9.438e+12	35276	0.0001	0.9999	5172.4
Residual	1.873e+08	7	26754221.9				

Parameter	Value	SD	t	Prob>t
Intercept	2019.6	2238.2	0.902	0.3968
Slope	268.3	1.43	187.8	0.0001

Et₃BuPb Y=363.2 + 295.4X N=9

Source	SS	df	MS	F	Prob>F	r ²	SD _{reg}
Regression	3.484e+11	1	3.484e+11	115387	0.001	0.9999	1737.6
Residual	21134932.3	7	3019276.0				

Parameter	Value	SD	t	Prob>t
Intercept	363.2	751.9	0.483	0.644
Slope	295.4	0.869	339.7	0.0001

Et₂Bu₂Pb Y=332.1 + 278.9X N=9

Source	SS	df	MS	F	Prob>F	r ²	SD _{reg}
Regression	2.511e+11	1	2.511e+11	247382	0.0001	0.9999	1007.4
Residual	7104571.4	7	1014938.8				

Parameter	Value	SD	t	Prob>t
Intercept	332.1	435.9	0.762	0.471
Slope	278.9	0.561	497.4	0.0001

Appendix J. Analysis of variance¹Me₃BuPb

Source	SS	df	MS	F	Pr>F
Total	587.15	82			
Model	482.75	6	80.46	58.60	0.0001
Error	104.40	76	1.37		

Me₂Bu₂Pb

Source	SS	df	MS	F	Pr>F
Total	2291.90	82			
Model	2185.96	6	364.33	261.40	0.0001
Error	105.94	76	1.39		

Et₃BuPb

Source	SS	df	MS	F	Pr>F
Total	5450.62	82			
Model	5341.19	6	890.20	618.30	0.0001
Error	109.42	76	1.44		

Et₂Bu₂Pb

Source	SS	df	MS	F	Pr>F
Total	3608.25	82			
Model	3323.99	6	553.99	148.12	0.0001
Error	284.26	76	3.74		

¹- N=83 (one observation missing)

Appendix K. Analysis of variance

Whole Egg Homogenate

Source	SS	df	MS	F	Pr>F
Total	1170.23	47			
Model	1012.48	3	337.49	94.10	0.0001
Error	157.75	44	3.59		

Egg Albumin

Source	SS	df	MS	F	Pr>F
Total	160.55	47			
Model	79.97	3	26.66	14.60	0.0001
Error	80.59	44	1.83		

Egg Yolk

Source	SS	df	MS	F	Pr>F
Total	1350.92	47			
Model	1305.92	3	435.31	425.60	0.0001
Error	45.00	44	1.02		

Ovotransferrin

Source	SS	df	MS	F	Pr>F
Total	29.43	47			
Model	4.07	3	1.36	2.36	0.0848
Error	25.36	44	0.58		

Fe³⁺+Egg Homogenate

Source	SS	df	MS	F	Pr>F
Total	984.10	47			
Model	885.67	3	295.22	132.00	0.0001
Error	98.43	44	2.24		

Fe³⁺+Ovotransferrin

Source	SS	df	MS	F	Pr>F
Total	120.58	43			
Model	115.81	3	1.59	0.55	0.6516
Error	4.77	40	2.90		

Appendix L. Environmental sample collection data.

Herring gull and mallard duck tissue samples were collected by the Canadian Wildlife Service. Samples were received coded and no further identification was provided until all analyses were completed to prevent any experimental bias.

A. Herring gull

All herring gull liver and kidney samples were from tissue pools of 10 mixed sex mature or immature birds from each colony with the exception of Middle Island, Lake Erie mature bird liver, which consisted of 7 pooled livers. Samples were collected during the summer of 1983.

Herring gull whole egg homogenate samples were from:

- (1) Agawa Rock, Lake Superior--13 eggs pooled, collected in May, 1983.
- (2) Channel Shelter Island, Lake Huron--10 eggs pooled, collected in April, 1982.
- (3) Double Island, Lake Huron--13 eggs pooled, collected in May, 1983.
- (4) Fighting Island, Detroit River--11 eggs pooled, collected in April, 1982.
- (5) Hamilton Harbour--13 eggs pooled, collected in May, 1982.
- (6) Middle Island, Lake Erie--13 eggs pooled, collected in April, 1983.
- (7) Mugs Island, Lake Ontario--9 eggs pooled, collected in April, 1982.
- (8) Niagara River--12 eggs pooled, collected in May, 1982.
- (9) Scotch Bonnet Island, Lake Ontario--13 eggs pooled, collected in May, 1982.
- (10) Snake Island, Lake Ontario--13 eggs pooled, collected in April, 1982.

B. Mallard duck

All collected mallards were immature birds. Kidney, liver, brain and breast muscle samples were taken from tissue pools of 5 females or 5 males. Kidney and liver samples from individual birds were examined as well. The

samples were collected from a wildlife sanctuary east of Morrisburg, Ontario in September, 1983.

C. Domestic chicken

Brain, kidney and liver tissue samples were collected from mixed sex mature birds donated by the Poultry Unit at Macdonald College in May, 1984. Tissue pools, consisting of 15 brains, 3 kidneys and 2 livers were used for analyses.

Appendix M. Transalkylation reaction

The continual use of mixtures of methylethylleads in gasoline marketed in the United States made the ability to detect and identify the possible ionic alkylleads resulting from these methylethylleads desirable. Dealkylation of MeEt_3Pb , $\text{Me}_2\text{Et}_2\text{Pb}$ and Me_3EtPb would produce the mixed ionic methylethylleads MeEt_2Pb^+ , Me_2EtPb^+ and MeEtPb^{2+} . Although the retention times for these mixed methylethylbutyllead compounds were predicted using Kovat's (Kovats 1965) retention index, the synthesis of mixed methylethylbutyllead compounds allowed direct measurement of retention times. Tetraorganolead compounds will exchange organic groups with other organolead compounds, producing unsymmetrical tetraalkylleads.

Equimolar amounts of $\text{Me}_2\text{Bu}_2\text{Pb}$ and $\text{Et}_2\text{Bu}_2\text{Pb}$ standards (in isooctane) were added to a 5° mL Reactivial, which was sealed and heated to 150°C for 21 h. A GC-AAS chromatogram of the reaction mixture (Fig. A19) indicated that extensive exchange of organic groups occurred, resulting in various unsymmetrical tetraalkylleads, including MeEt_2BuPb , Me_2EtBuPb and MeEtBu_2Pb , with retention times between the retention times of known standards.


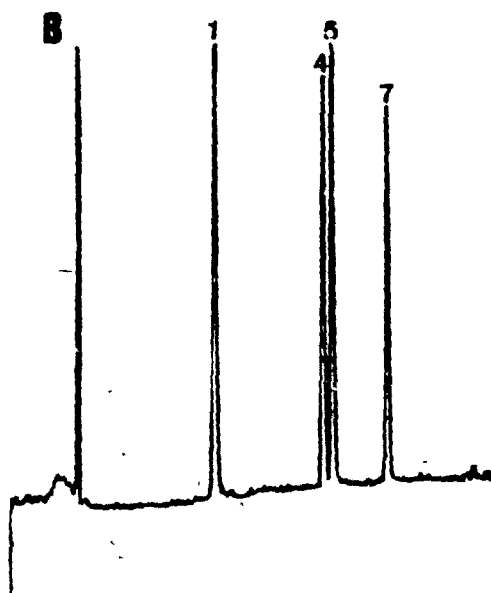
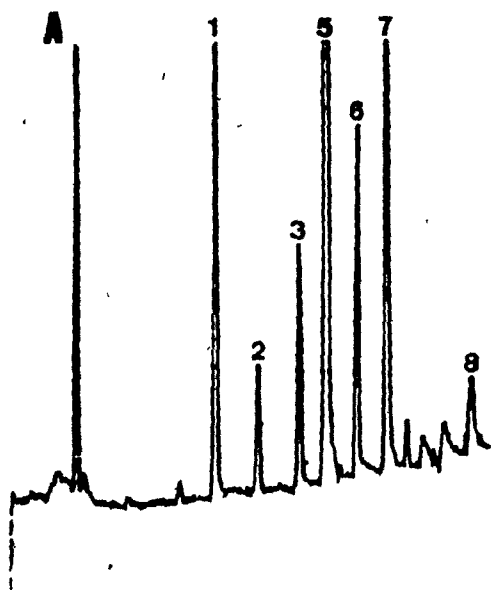


Figure A19. GC-AAS chromatograms of: (A) reaction mixture and (B) alkylbutyllead standard mixture containing 1, Me_3BuPb ; 2, Me_2EtBuPb ; 3, MeEt_2BuPb ; 4, $\text{Me}_2\text{Bu}_2\text{Pb}$; 5, Et_3BuPb ; 6, EtMeBu_2Pb ; 7, $\text{Et}_2\text{Bu}_2\text{Pb}$; 8, Bu_4Pb .



Appendix N. Calculation of alkylbutyllead levels in environmental samples

Example A. Calculation for Me_3Pb^+ (as Me_3BuPb) in gull kidney

The Me_3BuPb peak area responses from three replicate injections were 29936, 26422 and 27284. Interpolation between two bracketing concentrations of Me_3BuPb standards (from series of alkylbutyllead standards run periodically during sample analysis) by linear regression gave 0.201, 0.175 and 0.181 ng Me_3BuPb .

To determine total Me_3BuPb (ng), the total butylate volume (1000 μL) divided by the injection volume (22.5 μL) was multiplied by the Me_3BuPb values:

$$\begin{aligned}\text{total } \text{Me}_3\text{BuPb (ng)} &= 0.201 \times (1000/22.5) = 8.93 \\ &0.175 \times (1000/22.5) = 7.78 \\ &0.181 \times (1000/22.5) = 8.04\end{aligned}$$

Division by the sample weight (2.5 g) yielded ng/g wet wt.

$$\begin{aligned}\text{Me}_3\text{BuPb (ng/g wet wt)} &= 8.93/2.50 = 3.57 \\ &= 7.78/2.50 = 3.11 \\ &= 8.04/2.50 = 3.22\end{aligned}$$

The mean Me_3BuPb (ng/g wet wt) $\pm \text{SD} = 3.30 \pm 0.24$

Me_3BuPb recovery from kidney was 83%, therefore to correct for recovery, the mean and standard deviation were multiplied by the inverse of analyte recovery.

$$\begin{aligned}\text{Me}_3\text{BuPb (ng/g wet wt)} &= (3.30 \times 0.83^{-1}) \pm (0.24 \times 0.83^{-1}) \\ \text{(corrected for recovery)} &= 3.97 \pm 0.29 \\ &= 4.0 \pm 0.3\end{aligned}$$

Example B. Calculation for $\text{Et}_2\text{Pb}^{2+}$ (as $\text{Et}_2\text{Bu}_2\text{Pb}$)

The $\text{Et}_2\text{Bu}_2\text{Pb}$ peak area responses from three replicate injections were 12505, 13241 and 14543. Interpolation between two bracketing concentrations of $\text{Et}_2\text{Bu}_2\text{Pb}$ standards (from series of alkylbutyllead standards run periodically during sample analysis) by linear regression gave 0.097, 0.104 and 0.116 ng $\text{Et}_2\text{Bu}_2\text{Pb}$.

Total $\text{Et}_2\text{Bu}_2\text{Pb}$ was calculated as for Me_3BuPb :

$$\begin{aligned}\text{Total } \text{Et}_2\text{Bu}_2\text{Pb (ng)} &= 0.0973 \times (1000/22.5) = 4.33 \\ &0.104 \times (1000/22.5) = 4.62 \\ &0.116 \times (1000/22.5) = 5.16\end{aligned}$$

However, a mean value of 0.26 ng $\text{Et}_2\text{Bu}_2\text{Pb}$ was determined in blank hydrolysate controls. This value was therefore subtracted from the total $\text{Et}_2\text{Bu}_2\text{Pb}$.

$$\begin{aligned}\text{Corrected total } \text{Et}_2\text{Bu}_2\text{Pb (ng)} &= 4.33 - 0.26 = 4.07 \\ &4.62 - 0.26 = 4.36 \\ &5.16 - 0.26 = 4.90\end{aligned}$$

Division by sample weight (2.50 g) yielded ng/g wet wt

$$\begin{aligned}\text{Et}_2\text{Bu}_2\text{Pb (ng/g wet wt)} &= 4.07/2.50 = 1.63 \\ &4.36/2.50 = 1.74 \\ &4.90/2.50 = 1.96\end{aligned}$$

The mean $\text{Et}_2\text{Bu}_2\text{Pb}$ (ng/g wet wt) $\pm \text{SD} = 1.78 \pm 0.17$

$\text{Et}_2\text{Bu}_2\text{Pb}$ recovery from kidney was 59%, therefore:

$$\begin{aligned}\text{Et}_2\text{Bu}_2\text{Pb (ng/g wet wt)} &= (1.78 \times 0.58^{-1}) + (0.17 \times 0.59^{-1}) \\ \text{(corrected for recovery)} &= 2.97 \pm 0.29 \\ &= 3.0 \pm 0.3\end{aligned}$$

Example C. Calculation for Me_2EtPb^+ (as Me_2EtBuPb) from gull kidney

The Me_2EtBuPb peak area responses from three replicate injections were 12739, 12599 and 13406. Interpolation between two bracketing concentrations of Me_3BuPb (expressed as Pb) standards by linear regression gave 0.0494, 0.0487 and 0.0527 ng Pb.

To determine total Pb (ng):

$$\begin{aligned}\text{Total Pb (ng)} &= 0.0494 \times (1000/22.5) = 2.20 \\ &0.0487 \times (1000/22.5) = 2.16 \\ &0.0527 \times (1000/22.5) = 2.34\end{aligned}$$

To convert from Pb to Me_2EtBuPb the total Pb was multiplied by the molecular weight of Me_2EtBuPb divided by the atomic weight of Pb:

$$\begin{aligned}\text{Me}_2\text{EtBuPb (ng)} &= 2.20 \times (323.446/207.2) = 3.43 \\ &2.16 \times (323.446/207.2) = 3.37 \\ &2.34 \times (323.446/207.2) = 3.65\end{aligned}$$

Division by the sample weight (2.50 g) gave ng/g wet wt Me_2EtBuPb .

$$\begin{aligned}\text{Me}_2\text{EtBuPb (ng/g wet wt)} &= 3.43/2.50 = 1.37 \\ &3.37/2.50 = 1.35 \\ &3.65/2.50 = 1.46\end{aligned}$$

The mean Me_2EtBuPb (ng/g wet wt) $\pm \text{SD} = 1.39 \pm 0.06$

The Me_3Pb^+ recovery from kidney (83%) was used to correct Me_2EtBuPb :

$$\begin{aligned}\text{Me}_2\text{EtBuPb (ng/g wet wt)} &= (1.39 \times 0.83^{-1}) + (0.06 \times 0.83^{-1}) \\ \text{(corrected for recovery)} &= 1.67 \pm 0.07 \\ &= 1.7 \pm 0.1\end{aligned}$$

Similarly, for MeEt_2BuPb , Et_3BuPb calibration and Et_3Pb^+ recovery values were used and for MeEtBu_2Pb , $\text{Et}_2\text{Bu}_2\text{Pb}$ calibration and $\text{Et}_2\text{Pb}^{2+}$ recovery values were used.

Appendix 0. Analysis of variance

Analyte	Source	SS	df	MS	F	Prob>F
Me ₃ Pb ⁺	Total	357.9670	15			
	Model	341.5793	7	48.7970	23.82	0.0001
	Error	16.3877	8	2.0485		
Me ₂ Pb ²⁺	Total	30.5631	15			
	Model	26.8803	7	3.8400	8.34	0.0038
	Error	3.6828	8	0.4603		
Et ₃ Pb ⁺	Total	100.9391	15			
	Model	80.2728	7	11.4675	4.44	0.0264
	Error	20.6663	8	2.5833		
Et ₂ Pb ²⁺	Total	5.9427	15			
	Model	4.0408	7	0.5773	2.43	0.1186
	Error	1.9019	8	0.2377		

Appendix P. Paired-observation t-test between ionic alkyllead
(as alkylbutyllead) concentrations of immature and
mature gull tissues

Comparison	Mean	Standard Error of Mean	t	Pr> t
A. Liver (N=4)				
MATMe3-IMMe3	0.9125	0.4167	2.19	0.1163
MATMe2-IMMe2	-0.3900	0.6099	-0.64	0.5680
MATet3-IMet3	1.8675	1.1741	1.59	0.2099
MATet2-IMet2	0.6675	0.2834	2.36	0.0998
B. Kidney (N=4)				
MATMe3-IMMe3	-1.0875	1.3733	-0.79	0.4863
MATMe2-IMMe2	-0.5175	0.3190	-1.62	0.2032
MATet3-IMet3	0.8850	0.8014	1.10	0.3501
MATet2-IMet2	0.4550	0.1384	3.29	0.0461*

*- 0.05 significance

MAT- mature gull

IM- immature gull

Me3- Me₃BuPb

Me2- Me₂Bu₂Pb

Et3- Et₃BuPb

Et2- Et₂Bu₂Pb

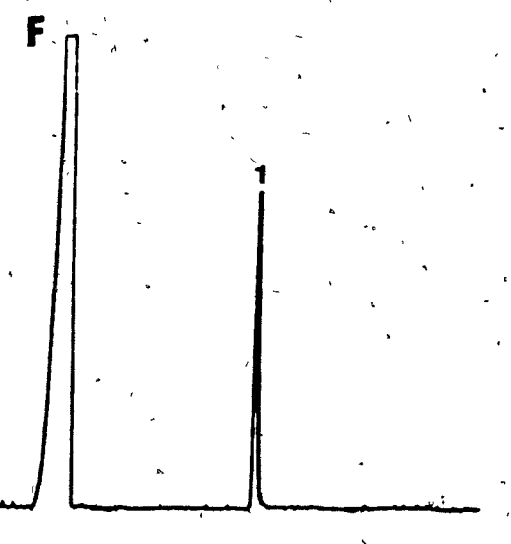
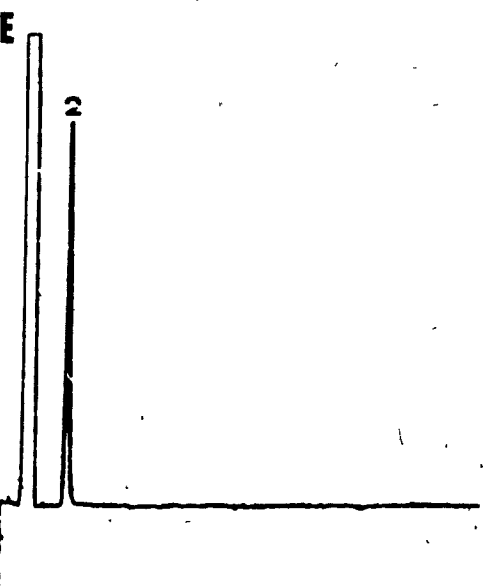
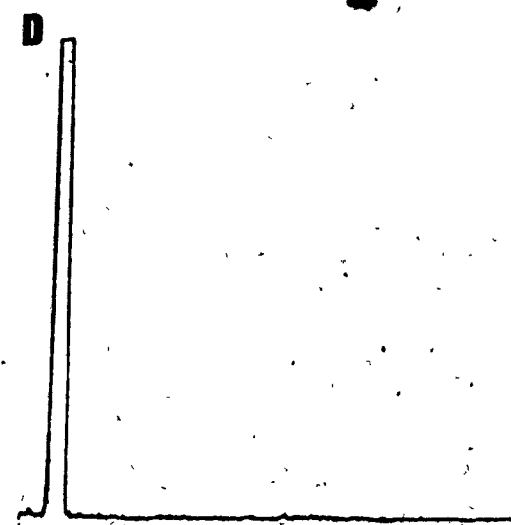
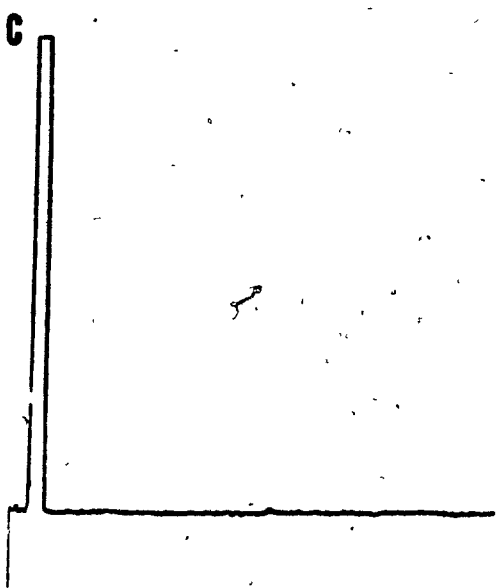
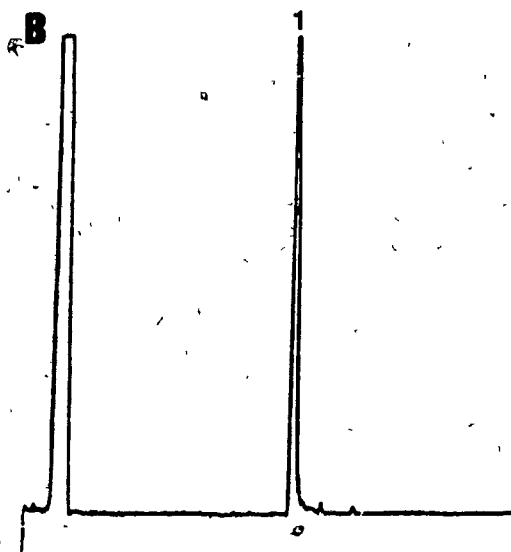
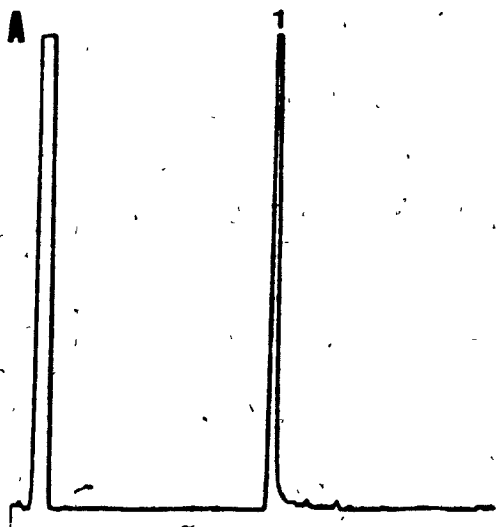
Appendix Q. Analysis of canadian gasolines for alkyllead content.

As it became evident that there was an appreciable source of methylleads into the environment, it was necessary to check if Canadian gasolines contained tetraalkyllead other than Et_4Pb .

Gasoline samples were collected from two suppliers, Esso and Shell in the Montreal area. The samples were diluted approximately 1000 fold with hexane and analyzed with GC-AAS operating under normal operating conditions (Section 5.2.1) with the exception that the air purge cycle was only 20 s long, allowing analysis of Me_4Pb .

The GC-AAS chromatograms (Fig. A20) indicated that the leaded⁰ gasolines contained only Et_4Pb , with no Me_4Pb or mixed methylethylleads present.

Figure A20. GC-AAS chromatograms of gasolines and standards containing 1- Et_4Pb or 2- Me_4Pb . (A) Esso regular leaded; (B) Shell regular leaded; (C) Esso regular unleaded; (D) Esso super unleaded; (E) Me_4Pb and (F) Et_4Pb .



Appendix R. Paired-observation t-test between ionic alkyllead
(as alkylbutyllead) concentrations of male and
female mallard ducks

Comparison	Mean	Standard Error of Mean	t	Pr> t
N=4				
MMe3-FMe3	1.2950	0.4956	2.61	0.0795
MMe2-FMe2	1.1350	0.3844	2.95	0.0599
MEt3-FEt3	1.5600	0.3833	4.07	0.0268*
MEt2-FEt2	0.6575	0.3476	1.89	0.1550

*- 0.05 significance

M- male mallard

F- female mallard

Me3- Me₃BuPb

Me2- Me₂Bu₂Pb

Et3- Et₃BuPb

Et2- Et₂Bu₂Pb

11. LITERATURE CITED

Ahlberg, J., C. Ramel, and C.A. Wachtmeister. 1972. Organolead compounds shown to be genetically active. *Ambio* 1:29-31.

Ahmad, I., Y.K. Chau, P.T.S. Wong, A.J. Carty, and L. Taylor. 1980. Chemical alkylation of lead (II) salts to tetraalkyllead (IV) in aqueous solution. *Nature* 287:716-717.

Ahotupa, M., K. Hartiala, and A. Aitio. 1979. Effects of tetraethyl lead on the activities of drug metabolizing enzymes in different tissues of the rat. *Acta. Pharmacol. Toxicol.* 44:359-363.

Aisen, P., S.H. Koenig, W.E. Schillinger, I.H. Scheinberg, K.G. Mann, and W. Fisk. 1970. Absence of dimers and nature of iron binding in transferrin solutions. *Nature* 226:859-861.

Aldridge, W.N. 1978. The biological properties of organo- germanium, -tin, and -lead compounds. Pages 9-31. In Gielen, M. and P.G. Harrison (eds.) *The organometallic and coordination chemistry of germanium, tin and lead.* Freund Publishing House Ltd., Israel.

Aldridge, W.N. and B.W. Street. 1981. Spectrophotometric and fluorimetric determination of tri- and di-organotin and -organolead compounds using dithizone and 3-hydroxyflavone. *Analyst* 106:60-68.

Aldridge, W.N., J.E. Cremer, and C.J. Threlfall. 1962. Trialkylleads and oxidative phosphorylation: a study of the action of trialkylleads upon rat liver mitochondria and rat brain cortex slices. *Biochem. Pharmacol.* 11:835-846.

- Aldridge, W.N., B.W. Street, and D.N. Skilleter. 1977. Oxidative phosphorylation. Halide dependent and halide independent effects of triorganotin and triorganolead on mitochondrial functions. *Biochem. J.* 168:353-364.
- Amberger, E. and R. Honigschmid-Grössich. 1965. Synthese und IR spectren der methoxide des zwei und vierwertigen bleis. *Chem. Ber.* 98:3795-3803.
- Ballinger, P.R. and I.M. Whittemore. 1968. Quantitative determination of lead alkyl distribution in gasoline by gas chromatography and atomic absorption spectrophotometry. *Am. Chem. Soc., Div. Petrol. Chem., Prepr.* 13:133-138.
- Beattie, A.D., M.R. Moore, and A. Goldberg. 1972. Tetraethyl lead poisoning. *Lancet* 2:12-15.
- Beccaria, A.M., E.D. Mor, and G. Poggi. 1978. A method for the analysis of traces of inorganic and organic lead compounds in marine sediments. *Ann. Chim.* 68:607-617.
- Bellrose, F.C. 1976. Ducks, geese and swans of North America. Stackpole Books, Pa.
- Birch, J., R.M. Harrison, and D.P.H. Laxen. 1980. A specific method for 24-48 hour analysis of tetraalkyl lead in air. *Sci. Total Environ.* 14:31-42.
- Bjerrum, P. 1978. Private communication. Cited by Grandjean, P. and T. Nielsen. 1979. Organolead compounds: Environmental health aspects. *Residue Rev.* 72:97-154.

Bolanowska, W. 1968. Distribution and excretion of triethyllead in rats. Br. J. Ind. Med. 25:203-208.

Bolanowska, W. and J.M. Wisniewska-knypl. 1971. Dealkylation of tetraethyl lead in the homogenates of rat and rabbit tissues. Biochem. Pharmacol. 20:2108-2110.

Bolanowska, W., J. Piotrowski, H. Garczynski. 1967. Triethyllead in the biological material in cases of acute tetraethyllead poisoning. Arch. Toxikol. 22:278-282.

Bondy, S.C., M.E. Harrington, C.L. Anderson, and K.N. Prasad. 1979. The effect of low concentrations of an organic lead compound on the transport and release of putative neurotransmitters. Toxicol. Lett. 3:35-41.

Bonelli, E.J. and H. Hartmann. 1963. Determination of lead alkyls by gas chromatography with electron capture detector. Anal. Chem. 35:1980-1981.

Booth, R.J., S.A. Fieldhouse, H.C. Starkie, and M.C.R. Symons. 1976. Unstable intermediates. Part 165. Radicals in irradiated organolead compounds: An electron spin resonance study. J. Chem. Soc. Dalton Trans. 1506-1515.

Botre, C., F. Caçace, and R. Cozzani. 1976. Direct combination of high-pressure liquid chromatography and atomic absorption for the analysis of metallorganic compounds. Anal. Lett. 9:825-830.

Bull, K.R., W.J. Every, P. Freestone, J.R. Hall, D. Osborn, A.S. Cooke, and T. Stowe. 1983. Alkyl lead pollution and bird mortalities on the Mersey Estuary, UK, 1979-1981. Environ. Pollut. Ser. A Ecol. Biol. 31:239-259.

Bye, R. and P.E. Paus, R. Solberg, and Y. Thomassen. 1978. Atomic absorption spectroscopy used as a specific gas chromatography detector. Comparison of flame and graphite furnace techniques in the determination of tetraalkyllead compounds. *At. Absorpt. Newsl.* 17:131-133.

Byington, K.H., D.A. Yates, and W.A. Mullins. 1980. Binding of triethyllead chloride by hemoglobin. *Toxicol. Appl. Pharmacol.* 52:379-385.

Calingaert, G., F.J. Dykstra, and H. Shapiro. 1945. The preparation of alkyllead salts. *J. Am. Chem. Soc.* 67:190-192.

Cantuti, V. and G.P. Carboni. 1968. The gas chromatographic determination of tetraethyllead in air. *J. Chromatogr.* 32:641-647.

Casida, J.E., E.C. Kimmel, B. Holm, and G. Widmark. 1971. Oxidative dealkylation of tetra-, tri-, and dialkyltins and tetra- and trialkylleads by liver microsomes. *Acta. Chem. Scand.* 25:1497-1499.

Chakraborti, D., W.R.A. De Jonghe, W.E. Van Mol, R.J.A. Van Cleuvenbergen, and F.C. Adams. 1984. Determination of ionic alkyllead compounds in water by gas chromatography/atomic absorption spectrometry. *Anal. Chem.* 56:2692-2697.

Chakraborti, D., S.G. Jiang, P. Surkijn, W. De Jonghe, and F. Adams. 1981. Determination of tetraalkyllead compounds in environmental samples by gas chromatography-graphite furnace atomic-absorption spectrometry. *Anal. Proc.* 18:347-351.

Chau, Y.K. and P.T.S. Wong. 1978. Occurrence of biological methylation of elements in the environment. Pages 39-53. In Brinckman, F.E. and J.M. Bellama (eds.). Organometals and organometalloids occurrence and fate in the environment, ACS Symposium Series No. 82.

Chau, Y.K., P.T.S. Wong, and P.D. Goulden. 1975. A gas chromatograph-atomic absorption spectrophotometer system for the determination of volatile alkyl lead and selenium compounds. Pages 295-302. Proc. Int. Conf. Heavy metals in the environment, 1975, Vol. 1, Toronto.

Chau, Y.K., P.T.S. Wong, and O. Kramar. 1983. The determination of dialkyllead, trialkyllead, tetraalkyllead and lead (II) ions in water by chelation/extraction and gas chromatography/atomic absorption spectrometry. Anal. Chim. Acta. 146:211-217.

Chau, Y.K., P.T.S. Wong, and H. Saitoh. 1976. Determination of tetraalkyl lead compounds in the atmosphere. J. Chromatogr. Sci. 14:162-164.

Chau, Y.K., P.T.S. Wong, G.A. Bengert, and J.L. Dunn. 1984. Determination of dialkyllead, trialkyllead, tetraalkyllead and lead (II) compounds in sediment and biological samples. Anal. Chem. 56:271-274.

Chau, Y.K., P.T.S. Wong, G.A. Bengert, and O. Kramar. 1979. Determination of tetraalkyllead compounds in water, sediment and fish samples. Anal. Chem. 51:186-188.

Chau, Y.K., P.T.S. Wong, O. Kramar, G.A. Bengert, R.B. Cruz, J.O. Kinnrade, J. Lye, and J.C. Van Loon. 1980. Occurrence of tetraalkyllead compounds in the aquatic environment. Bull. Environ. Contam. Toxicol. 24:265-269.

Clark, R.J.H., A.G. Davies, and R.J. Puddephatt. 1968. Vibrational spectra and structures of organolead compounds I. Methyllead halides. J. Am. Chem. Soc. 90:6923-6927.

Coker, D.T. 1978. A simple, sensitive technique for personal and environmental sampling and analysis of lead alkyl vapours in air. Ann. Occup. Hyg. 21:33-38.

Cooper, C.L., A. Hudson, and R.A. Jackson. 1973. An electron spin resonance study of the reactivity of organotin and organolead radicals. J. Chem. Soc. Perkin Trans. 2. 1056-1060.

Craig, P.J. 1980. Methylation of trimethyl lead species in the environment: An abiotic process? Environ. Technol. Lett. 1:17-20.

Cremer, J.E. 1959. Biochemical studies on the toxicity of tetraethyl lead and other organolead compounds. Br. J. Ind. Med. 16:191-199.

Cremer, J.E. 1961. Toxicity of tetraethyllead and related alkyl metallic compounds. Ann. Occup. Hyg. 3:226-30.

Cremer, J.E. 1962. The action of triethyl tin, triethyl lead, ethyl mercury and other inhibitors on the metabolism of brain and kidney slices in vitro using compounds labelled with ^{14}C . J. Neurochem. 9:289-298.

Cremer, J.E. and S. Callaway. 1961. Further studies on the toxicity of some tetra and trialkyl lead compounds. Br. J. Ind. Med. 18:277-282.

Cruz, R.B., C. Lorouso, S. George, Y. Thomassen, J.D. Kinrade, L.R.P. Butler, J. Lye, and J.C. Van Loon. 1980. Determination of total, organic solvent extractable, volatile and tetraalkyllead in fish, vegetation, sediment and water samples. *Spectrochim. Acta., Part B* 35:775-783.

Davies, A.G. and R.J. Puddephatt. 1967. Organometallic reactions. Part IX. The preparation and reaction of trialkyllead alkoxides. *J. Chem. Soc. Sect. C Org. Chem.* 2663-2669.

Davis, R.K., A.W. Horton, E.E. Larson, and K.L. Stemmer. 1963. Inhalation of tetraethyllead and tetraethyllead. *Arch. Environ. Health.* 6:473-479.

Dawson Jr., H.J. 1963. Determination of methyl ethyl lead alkyls in gasoline by gas chromatography with an electron capture detector. *Anal. Chem.* 35:542-545.

Dedina, J. and I. Rubeska. 1980. Hydride atomization in a cool hydrogen-oxygen flame burning in a quartz tube atomizer. *Spectrochim. Acta., Part B* 35:119-128.

De Jonghe, W.R.A. and F.C. Adams. 1980. Organic and inorganic lead concentrations in environmental air in Antwerp, Belgium. *Atmos. Environ.* 14:1177-1180.

De Jonghe, W.R.A., W.E. Van Mol, and F.C. Adams. 1983. Determination of trialkyllead compounds in water by extraction and graphite furnace atomic absorption spectrometry. *Anal. Chem.* 55:1050-1054.

Delves, H.T. 1970. A micro-sampling method for the rapid determination of lead in blood by atomic absorption spectrophotometry. *Analyst* 95:431-438.

de Vos, D., D.C. Van Beelen, and J. Wolters. 1980. ^1H and ^{13}C NMR investigations on alkyllead (IV) compounds. Bull. Soc. Chim. Belg. 89:791-796.

DuPuis, M.D. and H.H. Hill, Jr. 1979. Analysis of gasoline for antiknock agents with a hydrogen atmosphere flame ionization detector. Anal. Chem. 51:292-295.

Ebdon, L., R.W. Ward, and D.A. Leathard. 1982. Development and optimisation of atom cells for sensitive coupled gas chromatography-flame atomic-absorption spectrometry. Analyst 107:195-199.

Ember, L. 1984. EPA study backs cut in lead use in gas. Chem. Eng. News. April:18

Environment Canada. 1985. Personal communication.

Epstein, S.S. and N. Mantel. 1968. Carcinogenicity of tetraethyl lead. Experientia 24:580-581.

Estes, S.A., P.C. Uden, and R.M. Barnes. 1981. High-resolution gas chromatography of trialkyllead chlorides with an inert solvent interface for microwave excited helium plasma detection. Anal. Chem. 53:1336-1340.

Estes, S.A., P.C. Uden, and R.M. Barnes. 1982. Plasma emission spectral detection for high-resolution gas chromatographic study of group IV organometallic compounds. J. Chromatogr. 239:181-189.

Foley, J.P. and J.G. Dorsey. 1984. Clarification of the limit of detection in chromatography. Chromatographia 18:503-511.

Forsyth, D.S. and W.D. Marshall. 1983. Determination of alkyllead salts in water and whole eggs by capillary column gas chromatography with electron capture detection. Anal. Chem. 55:2132-2137.

Forsyth, D.S. and W.D. Marshall. 1985. Performance of an automated gas chromatograph-silica furnace-atomic absorption spectrometer for the determination of alkyllead compounds. Anal. Chem. 57:1299-1305.

Fritz, H.P. and K.E. Schwarzhans. 1964. IR und $^1\text{H-NMR}$ -spectren von alkyl-blei-cyclopentadienylen. Chem. Ber. 97:1390-1397

Galzigna, L., G.C. Corsi, B. Sala, and A.A. Rizzoli. 1969. Inhibitory effect of triethyl lead on serum cholinesterase in vitro. Clin. Chim. Acta. 26:391-393.

Gilbertson, M. 1975. A great lakes tragedy. Nat. Can. (Ottawa) 4:22-25.

Gilman, H. and J.D. Robinson. 1930. The preparation of diethyl lead dichloride and triethyl lead chloride. J. Am. Chem. Soc. 52:1975-1978.

Gilroy, K.M., S.J. Price, and N.J. Webster. 1972. Determination of $\text{D}[(\text{CH}_3)_3\text{Pb}-\text{CH}_3]$ by the toluene carrier method. Can. J. Chem. 50:2639-2641.

Gorsich, R.D. and R.O. Robbins. 1969. A synthesis of unsymmetrical organolead compounds. J. Organometal. Chem. 19:444-446.

Grandjean, P. 1983. Health significance of organo-lead compounds. Pages 179-190. In Rutter, M. and R.R. Jones (eds.). Lead versus health. Sources and effects of low level lead exposure, John Wiley and Sons, New York.

Grandjean, P. and T. Nielsen. 1979. Organolead compounds: Environmental health aspects. *Residue Rev.* 72:97-154.

Grove, J.R. 1980. Investigations into the formation and behaviour of aqueous solutions of lead alkyls. Pages 45-52. In Branica, M. and Z. Konrad (eds.). *Proc. International Experts Discuss. on Lead Occurrence, Fate and Pollution in the Marine Environment*, Rovinj, Yugoslavia, Oct. 18-22, 1977, Pergamon Press, New York.

Harris, R.K., J.D. Kennedy, and W. McFarlane. 1978. Group IV-Silicon, Germanium, Tin and Lead. Pages 309-377. In Harris, R.K. and B.E. Mann. (eds.). *NMR and the Periodic Table*, Academic Press, New York.

Harrison, R.M. and D.P.H. Laxen. 1978a. Natural source of tetraalkyllead in air. *Nature* 275:738-740.

Harrison, R.M. and D.P.H. Laxen. 1978b. Sink processes for tetraalkyllead compounds in the atmosphere. *Environ. Sci. Technol.* 12:1384-1391.

Harrison, R.M., R. Perry, and D.H. Slater. 1974. An adsorption technique for the determination of organic lead in street air. *Atmos. Environ.* 8:1187-1194.

Hayakawa, K. 1971. Microdetermination and dynamic aspects of in vivo alkyl lead compounds part I. Analytical methods. *Jpn. J. Hyg.* 26:377-385.

Hayakawa, K. 1972. Microdetermination and dynamic aspects of in vivo alkyl lead compounds. Part II. Studies on the dynamic aspects of alkyl lead compounds in vivo. *Jpn. J. Hyg.* 26:526-535.

- Henderson, S.R. and L.J. Snyder. 1961. Rapid spectrophotometric determination of triethyllead, diethyllead, and inorganic lead ions, and application to the determination of tetraorganolead compounds. *Anal. Chem.* 33:1172-1175.
- Heywood, R., R.W. James, R.J. Sortwell, D.E. Prentice, and P.S.I. Barry. 1978. The intravenous toxicity of tetraalkyllead compounds in Rhesus monkeys. *Toxicol. Lett.* 2:187-197.
- Heywood, R., R.W. James, A.H. Pulseford, R.J. Sortwell, and P.S.I. Barry. 1979. Chronic oral administration of alkyl lead solutions to the Rhesus monkey. *Toxicol. Lett.* 4:119-125.
- Hodson, P.V., D.M. Whittle, P.T.S. Wong, U. Borgmann, R.L. Thomas, Y.K. Chau, J.O. Nriagu, and D.J. Hallett. 1984. Lead contamination of the Great Lakes and its potential effects on aquatic biota. Pages 335-369. In Nriagu, J.O. and M.S. Simmons (eds.). *Toxic contaminants in the Great Lakes*, John Wiley and Sons, New York.
- Huntzicker, J.J., S.K. Friedlander, and C.I. Davidson. 1975. Material balance for automobile emitted lead in Los Angeles basin. *Environ. Sci. Technol.* 9:448-457.
- Jarvie, A.W.P. and A.P. Whitmore. 1981. Methylation of elemental lead and lead (II) salts in aqueous solution. *Environ. Technol. Lett.* 2:197-204.
- Jarvie, A.W.P., R.N. Markall, and H.R. Potter. 1981. Decomposition of organolead compounds in aqueous systems. *Environ. Res.* 25:241-249.
- Jarvie, A.W.P., R.N. Marshall, and H.R. Potter. 1975. Chemical alkylation of lead. *Nature* 255:217-218.

- Jarvie, A.W.P., A.P. Whitmore, R.N. Markall, and H.R. Potter. 1983. Lead biomethylation, an elusive goal. *Environ. Pollut. Ser. B. Chem. Phys.* 6:81-94.
- Jaworski, J.F. 1979. Effects of lead in the environment-1978. Quantitative aspects. National Research Council Canada, NRCC Association Committee on Scientific Criteria for Environmental Quality. Publication No. NRCC 16736.
- Johnson, M.S., H. Pluck, M. Hutton, and G. Moore. 1982. Accumulation and renal effects of lead in urban populations of feral pigeons, Columbia livia. *Arch. Environ. Contam. Toxicol.* 11:761-767.
- Kehoe, R.A. and F. Thammann. 1931. The behaviour of lead in the animal organism. II. Tetraethyllead. *Am. J. Hyg.* 13:478-489.
- Keith, L.H., W. Crummett, J. Deegan, Jr., R.A. Libby, J.K. Taylor, and G. Wentler. 1983. Principles of environmental analysis. *Anal. Chem.* 55:2210-2218.
- Kennedy, G.L., D.W. Arnold, and J.C. Calandra. 1975. Teratogenic evaluation of lead compounds in mice and rats. *Food Cosmet. Toxicol.* 13:629. Cited by Grandjean, P. and T. Nielsen. 1979. Organolead compounds: Environmental health aspects. *Residue Rev.* 72:97-154.
- Koizumi, H., R.D. McLaughlin, and T. Hadeishi. 1979. High gas temperature furnace for species determination of organometallic compounds with a high pressure liquid chromatograph and a zeeman atomic absorption spectrometer. *Anal. Chem.* 51:387-392.

- Kolb, B., G. Kemmer, F.H. Schleser, and E. Wiedeking. 1966. Elementspezifische anzeige gaschromatographische getrennter metallverbindungen mittels atom-absorptions-spektroskopie (AAS). Z. Anal. Chem. 221:166-175.
- Konat, G. and J. Clausen. 1974. The effect of long term administration of triethyllead on the developing rat brain. Environ. Physiol. Biochem. 4:236-242.
- Konat, G. and J. Clausen. 1980. Suppressive effect of triethyllead on entry of proteins into the CNS myelin sheath in vitro. J. Neurochem. 35:382-387.
- Konat, G., H. Offner, and J. Clausen. 1976. Triethyllead restrained myelin deposition and protein synthesis in the developing rat forebrain. Exp. Neurol. 52:58-65.
- Konat, G., H. Offner, and J. Clausen. 1979. The effect of triethyllead on total and myelin protein synthesis in rat forebrain slices. J. Neurochem. 32:187-190.
- Kovats, E. 1965. Gas chromatographic characterization of organic substances in the retention index system. Pages 229-247. In Giddings, J.C. and R.A. Keller (eds.). Advances in Chromatography, Vol. 1, Marcel Dekker Inc., New York.
- Laveskog, A. 1971. A method for determination of tetramethyl lead (TML) and tetraethyl lead (TEL) in air. Pages 549-557. In Englund, H.M. and W.T. Beery (eds.). Proc. Second International Clean Air Congress, Academic Press, New York.

- Lawrence, J.F. and R. Leduc. 1978. High performance liquid chromatography of some acidic and basic organic compounds on silica gel with mobile phases containing organic acids. *Anal. Chem.* 50:1161-1163.
- Leeper, R.W., L. Summers, and H. Gilman. 1954. Organolead compounds. *Chem. Rev.* 54:101-167.
- Lehninger, A.L. 1975. *Biochemistry*. Worth Publishers, Inc., New York.
- Lock, E.A. and W.N. Aldridge. 1975. The binding of triethyltin to rat brain myelin. *J. Neurochem.* 25:871-876.
- Lovelock, J.E. and R.J. Maggs. 1973. Halogenated hydrocarbons in and over the Atlantic. *Nature* 241:194-196.
- McClain, R.M. and B.A. Becker. 1972. Effects of organolead compounds on rat embryonic and fetal development. *Toxicol. Appl. Pharmacol.* 21:265-274.
- Messman, J.D. and T.C. Rains. 1981. Determination of tetraalkyllead compounds in gasoline by liquid chromatography-atomic absorption spectrometry. *Anal. Chem.* 53:1632-1636.
- Mineau, P., G.A. Fox, R.J. Norstrom, D.V. Weseloh, D.J. Hallett, and J.A. Ellenton. 1984. Using the herring gull to monitor levels and effects of organochlorine contamination in the Canadian Great Lakes. Pages 425-452. In Nriagu, J.O. and M.S. Simmons (eds.). *Toxic Contaminants in the Great Lakes*, John Wiley and Sons, New York.

Neshkov, N.S. 1971. Effects of chronic poisoning with ethylated gasoline on spermatogenesis and sexual functions in males. *Gig. Truda. i Prof. Zabol.* 15:45. Cited by Grandjean, P. and T. Nielsen. 1979. Organolead compounds: Environmental health aspects. *Residue Rev.* 72:97-154.

Nielsen, T., H. Egsgaard, and E. Larsen. 1981. Determination of tetramethyllead and tetraethyllead in the atmosphere by a two step enrichment method and gas chromatographic-mass spectrometric isotope dilution analysis. *Anal. Chim. Acta.* 124:1-13.

Nielsen, T., K.A. Jensen, and P. Grandjean. 1978. Organic lead in normal human brains. *Nature* 274: 602-603.

Noden, F.G. 1980. The determination of tetraalkyllead compounds and their degradation products in natural water. Pages 83-91. In Branica, M. and Z. Konrad (eds.). *Proc. International Experts Discuss. on Lead Occurrence, Fate and Pollution in the Marine Environment*, Rovinj, Yugoslavia, Oct. 18-22, 1977, Pergamon Press, New York.

Nomoto, M., Y. Narahashi, and M. Murakami. 1960. A proteolytic enzyme of Streptomyces griseus VI. Hydrolysis of protein by Streptomyces griseus protease. *J. Biochem.* 48:593-602.

Odenbro, A. and J.E. Kihlstrom. 1977. Frequency of pregnancy and ova implantation in triethyllead treated mice. *Toxicol. Appl. Pharmacol.* 39: 359-363.

Osborn, D., W.J. Every, and K.R. Bull. 1983. The toxicity of trialkyl lead compounds to birds. *Environ. Pollut. (Series A)* 31:261-275.

- Osuga, D.T. and R.E. Feeney. 1977. Egg proteins. Pages 209-255. In Whitaker, J.R. and S.R. Tannenbaum (eds.). Food Proteins, Avi Publishing Co., Westport, Conn.
- Pacholec, F. and C.F. Poole. 1982. Retention index scheme and calibration method for gas chromatography with electron capture detection. Anal. Chem. 54:1019-1021.
- Paneth, F.A., W. Hofeditz, and A. Wunsch. 1935. Free organic radicals in the gaseous state part V. The reaction products of free methyl in hydrogen and helium. J. Chem. Soc. 372-379.
- Parker, W.W., G.Z. Smith, and R.L. Hudson. 1961. Determination of mixed lead alkyls in gasoline by combined gas chromatographic and spectrophotometric techniques. Anal. Chem. 33:1170-1171.
- Parkinson, T.L. 1966. The chemical composition of eggs. J. Sci. Fd. Agric. 17:101-107.
- Parris, G.E., W.R. Blair, and F.E. Brinckmann. 1977. Chemical and physical considerations in the use of atomic absorption detectors coupled with a gas chromatograph for determination of trace organometallic gases. Anal. Chem. 49:378-386.
- Potter, H.R., W.P. Jarvie, and R.N. Markall. 1977. Detection and determination of alkyl lead compounds in natural waters. Wat. Pollut. Control 76:123-128.

- Powerie, W.D. 1973. Chemistry of eggs and egg products. Pages 61-90. In Stadelman, W.J. (ed.). Egg Science and Technology, Avi Publishing Co., Westport, Conn.
- Pratt, G.L. and J.H. Purnell. 1964. Gas-phase reactions of ethyl radicals with nitric oxide. J. Chem. Soc., Faraday Trans. 60:371-377.
- Price, W.J. 1974. Analytical atomic absorption spectrometry. Heyden and Sons Ltd., London.
- Purdue, L.J., R.G. Enrione, R.J. Thompson, and B.A. Bonfield. 1973. Determination of organic and total lead in the atmosphere by atomic absorption spectrometry. Anal. Chem. 45:527-530.
- Radziuk, B., Y. Thomassen, J.C. Van Loon, and Y.K. Chau. 1979. Determination of alkyl lead compounds in air by gas chromatography and atomic absorption spectrometry. Anal. Chim. Acta. 105:255-262.
- Reamer, D.C., W.H. Zoller, and T.C. O'Haver. 1978. Use of a gas chromatograph-microwave plasma detector for the determination of tetraalkyl lead species in the atmosphere. Anal. Chem. 50:1449-1453.
- Reisinger, K., M. Stoeppler, and H.W. Nurnberg. 1981. Evidence for the absence of biological methylation of lead in the environment. Nature 291:228-230.
- Rifkin, E.B. and C. Walcutt. 1956. Decomposition of TEL in an engine. Ind. Eng. Chem. 48:1532-1539.
- Robinson, J.W. 1961. Determination of lead in gasoline by atomic absorption spectroscopy. Anal. Chim. Acta. 24:451-455.

- Robinson, J.W. and E.L. Kiesel. 1977. Concentrations of molecular and organic lead in the atmosphere. J. Environ. Sci. Health. Part A. Environ. Sci. Eng. 12:411-422.
- Robinson, J.W., E.L. Kiesel, J.F. Goodbread, R. Bliss, and R. Marshall. 1977. The development of a gas chromatography-furnace atomic absorption combination for the determination of organic lead compounds, atomization processes in furnace atomizers. Anal. Chim. Acta. 92:321-328.
- Roderer, G. 1976. Induction of giant multinucleate cells with tetraethyl lead. Naturwissenschaften 63:248.
- Roderer, G. 1979. Hemmung der cytokinese und bildung von risenzellen bei Poterioochromonas malhamensis durch organische bleiverbindungen und andere agenzien. Protoplasma 99:39-51.
- Rohbock, E., H.W. Georgii, and J. Muller. 1980. Measurements of gaseous lead alkyls in polluted atmospheres. Atmos. Environ. 14:89-98.
- Rubeska, I. and B. Moldan. 1968. Investigations on long-path absorption tubes in atomic-absorption spectroscopy. Analyst 93:148-152.
- Sanders, L.W. 1964. Tetraethyllead intoxication. Arch. Environ. Health. 8:270-277.
- Schenk, G.H., R.B. Hahn, and A.V. Hartkopf. 1981. Introduction to analytical chemistry. Allyn and Bacon Inc., Toronto.
- Schepers, G.W.H. 1964. Tetraethyl and tetramethyllead. Comparative experimental pathology: part I. Lead absorption and pathology. Arch. Environ. Health. 8:277-295.

- Schmidt, U. and F. Huber. 1976. Methylation of organolead and lead(II) compounds to $(CH_3)_4Pb$ by microorganisms. *Nature* 259:157-158.
- Schroeder, T., D.D. Avery, and H.A. Cross. 1972. The LD_{50} value of tetraethyl lead. *Experientia* 28:425-426.
- Shapiro, H. and F.W. Frey. 1968. The organic compounds of lead. John Wiley and Sons, New York.
- Slier, G.D. and R.S. Drago. 1966. Solvates of some methyllead compounds and their $^{207}Pb-CH_3$ coupling constants. *J. Organometal. Chem.* 6:359-363.
- Simpson, C.F. (ed.) 1976. Practical high pressure liquid chromatography. Heyden and Sons Ltd., New York.
- Singh, G. 1975. Proton and carbon-13 NMR study of group IVB ($^{117}, ^{119}Sn, Pb$) and mercury (^{199}Hg) organometallics. *J. Organomet. Chem.* 99:251-262.
- Sirota, G.R. and J.F. Uthe. 1977. Determination of tetraalkyllead compounds in biological materials. *Anal. Chem.* 49:823-825.
- Soulages, N.L. 1966. Determination of methyl ethyl lead alkyls and halide scavengers in gasoline by gas chromatography and flame ionization detection. *Anal. Chem.* 39:1340-1341.
- Springman, F., E. Bingham, and K.L. Stemmer. 1963. The acute effects of lead alkyls. *Arch. Environ. Health.* 6:469-472.
- Summers, A.O. and S. Silver. 1978. Microbial transformations of metals. *Annu. Rev. Microbiol.* 32:637-672.

Szepesy, L. 1970. Gas chromatography. CRC Press, Cleveland, Ohio.

Thayer, J.S. 1978. Demethylation of methylcobalamin: Some comparative rate studies. Pages 188-204. In Brinkman, F.E. and J.M. Bellama (eds.). Organometals and organometalloids occurrence and fate in the environment, ACS Symposium Series, No. 82.

Thayer, J.S. 1983. The reaction between lead dioxide and methylcobalamin. J. Environ. Sci. Health. A18:471-481.

Thompson, K.C. and D.R. Thomerson. 1974. Atomic-absorption studies on the determination of antimony, arsenic, bismuth, germanium, lead, selenium, tellurium and tin by utilising the generation of covalent hydrides. Analyst 99:595-601.

Van Loon, J.C. and B. Radziuk. 1976. A quartz "T" tube furnace atomic absorption spectroscopy system for metal speciation studies. Can. J. Spectrosc. 21:46-49.

Venugopal, B. and I.D. Luckey. 1978. Metal toxicity in mammals. Vol. 2. Plenum Press, New York.

Welz, B. and M. Melcher. 1983. Investigations on atomisation mechanisms of volatile hydride-forming elements in a heated quartz cell. Analyst 108:213-224.

Widmaier, O. 1953. Reaktionzerfalle von bleizin. Brennstoff-Chem. 34:83 Cited by Grandjean, P. and T. Nielsen. 1978. Organolead compounds: environmental health aspects. Residue Rev. 72:97-154.

- Williams, K.C. 1970. Synthesis of organolead compounds III. Preparation and reactions of trialkylplumbylmagnesium chlorides. *J. Organomet. Chem.* 22:141-148.
- Winefordner, J.D. and G.L. Long. 1983. Limit of detection. A closer look at the IUPAC definition. *Anal. Chem.* 55:712A-724A.
- Wong, P.T.S., Y.K. Chau, and P.L. Luxon. 1975. Methylation of lead in the environment. *Nature* 253:263-264.
- Wong, P.T.S., Y.K. Chau, O. Kramar, and G.A. Bengert. 1981. Accumulation and depuration of tetramethyllead by rainbow trout. *Water Res.* 15:621-626.
- Wood, J.M. and H.-K. Wang. 1983. Microbial resistance to heavy metals. *Environ. Sci. Technol.* 17:582A-590A.
- Yemm, E.W. and E.C. Cocking. 1955. The determination of amino acids with ninhydrin. *Analyst* 80:209-213.
- Zar, J.H. 1974. Biostatistical analysis. Prentice-Hall Inc., Englewood Cliffs, New Jersey.